National Library
of Canada

Bibliothèque nationale
du Canada

Acquisitions and
Bibliographic Services Branch

Direction des acquisitions et
des services bibliographiques

395 Wellington Street
Ottawa, Ontario
K1A 0N4

395, rue Wellington
Ottawa (Ontario)
K1A 0N4

Your file Votre référence

Our file Notre référence

NOTICE

The quality of this microform is heavily dependent upon the quality of the original thesis submitted for microfilming. Every effort has been made to ensure the highest quality of reproduction possible.

If pages are missing, contact the university which granted the degree.

Some pages may have indistinct print especially if the original pages were typed with a poor typewriter ribbon or if the university sent us an inferior photocopy.

Reproduction in full or in part of this microform is governed by the Canadian Copyright Act, R.S.C. 1970, c. C-30, and subsequent amendments.

AVIS

La qualité de cette microforme dépend grandement de la qualité de la thèse soumise au microfilmage. Nous avons tout fait pour assurer une qualité supérieure de reproduction.

S'il manque des pages, veuillez communiquer avec l'université qui a conféré le grade.

La qualité d'impression de certaines pages peut laisser à désirer, surtout si les pages originales ont été dactylographiées à l'aide d'un ruban usé ou si l'université nous a fait parvenir une photocopie de qualité inférieure.

La reproduction, même partielle, de cette microforme est soumise à la Loi canadienne sur le droit d'auteur, SRC 1970, c. C-30, et ses amendements subséquents.

Canada

UNIVERSITY OF ALBERTA

ABSOLUTE INFRARED ABSORPTION INTENSITIES OF LIQUID CHLOROBENZENE AND TOLUENE

BY

YORAM APELBLAT ©

A thesis submitted to the Faculty of Graduate Studies and Research in partial fulfillment of the requirements for the degree of DOCTOR OF PHILOSOPHY.

DEPARTMENT OF CHEMISTRY

Edmonton, Alberta

Spring 1996

National Library of Canada

Acquisitions and Bibliographic Services Branch

395 Wellington Street
Ottawa, Ontario
K1A 0N4

Bibliothèque nationale du Canada

Direction des acquisitions et des services bibliographiques

395, rue Wellington
Ottawa (Ontario)
K1A 0N4

Your file Votre référence

Our file Notre référence

The author has granted an irrevocable non-exclusive licence allowing the National Library of Canada to reproduce, loan, distribute or sell copies of his/her thesis by any means and in any form or format, making this thesis available to interested persons.

L'auteur a accordé une licence irrévocable et non exclusive permettant à la Bibliothèque nationale du Canada de reproduire, prêter, distribuer ou vendre des copies de sa thèse de quelque manière et sous quelque forme que ce soit pour mettre des exemplaires de cette thèse à la disposition des personnes intéressées.

The author retains ownership of the copyright in his/her thesis. Neither the thesis nor substantial extracts from it may be printed or otherwise reproduced without his/her permission.

L'auteur conserve la propriété du droit d'auteur qui protège sa thèse. Ni la thèse ni des extraits substantiels de celle-ci ne doivent être imprimés ou autrement reproduits sans son autorisation.

ISBN 0-612-10568-7

Canada

UNIVERSITY OF ALBERTA

RELEASE FORM

NAME OF AUTHOR: YORAM APELBLAT

TITLE OF THESIS: ABSOLUTE INFRARED ABSORPTION INTENSITIES OF LIQUID CHLOROBENZENE AND TOLUENE

DEGREE: Ph.D.

YEAR THIS DEGREE GRANTED: 1996

Permission is hereby granted to the University of Alberta Library to reproduce single copies of this thesis and to lend or sell such copies for private, scholarly or scientific research purposes only.

The author reserves all other publication and other rights in association with the copyright in the thesis, and except as herein before provided neither the thesis nor any substantial portion thereof may be printed or otherwise reproduced in any material form whatever without the author's prior permission.

Yoram Apelblat
11111 - 87th AVE. #1404
Edmonton, Alberta
T6G 0X9

DATE: April 9, 1996

UNIVERSITY OF ALBERTA

FACULTY OF GRADUATE STUDIES AND RESEARCH

The undersigned certify that they have read, and recommend to the Faculty of Graduate Studies and Research for acceptance, a thesis entitled ABSOLUTE INFRARED ABSORPTION INTENSITIES OF LIQUID CHLOROBENZENE AND TOLUENE submitted by YORAM APELBLAT in partial fulfillment of the requirements for the degree of DOCTOR OF PHILOSOPHY.

J. E. Bertie, Supervisor

R. E. D. McClung

M. Palcic

F. Cantwell

A. M. Robinson

H. Wieser, External Examiner

DATE: April 9, 1996

To my parents for their continuous encouragement and support

Abstract

The optical constants of liquid toluene and chlorobenzene were measured across the entire mid-infrared region at 25°C. The estimated accuracy is ±0.2% for the real refractive index and ±2-3% for the imaginary refractive index. The optical constants were used to calculate the molar absorption coefficient and the molar polarizablity spectra of these liquids.

The optical constants and the molar absorption coefficient spectra of toluene and chlorobenzene, together with those of liquid benzene and dichloromethane measured separately, were used to establish secondary infrared intensity standards for liquids. These standards have been published by the International Union of Pure and Applied Chemistry.

Molecular properties are more directly reflected in the imaginary molar polarizability spectrum than in the imaginary refractive index spectrum or the molar absorption coefficient spectrum. In order to calculate the integrated intensities, the imaginary molar polarizability spectrum must be separated into contributions from different transitions. The separation was achieved by curve fitting the imaginary molar polarizability spectra with bands of classical damped harmonic oscillator shape, then calculating the integrated intensities from the parameters of the fitted bands. The accuracy of the integrated intensities is estimated at 3-5% for strong bands and 5-10% for weak bands. The results of this work are corrected for liquid dielectric effects and agree usually within a factor of two with literature values for the gas obtained by

experimental or by *ab initio* calculation. In these cases the agreement must mean that the vibrations in question have very similar intrinsic intensities in the liquid and gas phases.

The procedure used to determine the optical constants of the liquid from transmission measurements is exact but computationally complex. A simpler, approximate method was developed and the conditions under which it yields results of sufficient accuracy were explored.

Finally, a method for data reduction and presentation is given. The data is reduced and incorporated into a format that allows a spectrum to be tabulated in about 1/10 of the space required for a traditional table. The format allows direct retrieval of specific values, and also the retrieval, through a recovery program, of the entire spectrum without loss of intensity and line shape information.

Acknowledgments

I would like to thank Dr. John E. Bertie for suggesting this project to me and for his guidance and help throughout the course of the project and the preparation of the thesis. His knowledge, encouragement and patience over the last 4 years were invaluable in shaping my attitudes and views in science.

I express my appreciation to the following collaborators who supplied spectra that were used to estimate the accuracy of the intensities of chlorobenzene and toluene: V. Behnam, R. Cain, M. Smith, A. Oskam, R.D. Brown, K. Krishnan and A.N. Davies. I would like to thank G.R. Loppnow and M.S. Ngari for providing the Raman data used in the thesis.

I like to express my appreciation to the following persons for their discussion in my research; S.L. Zhang, Z. Lan, Dr. R. N. Jones and in particular to C.D. Keefe.

Permission is hereby granted to Yoram Apelblat to use in this thesis the work contained in

"Infrared Intensities of Liquids XIII: Accurate Optical Constants and Molar Absorption Coefficients Between 6500 and 435 cm^{-1} of Toluene at 25°C, from Spectra Recorded in Several Laboratories.", John E. Bertie, R. Norman Jones, Yoram Apelblat, and C. Dale Keefe, Applied Spectroscopy, **48**, 127 (1994).

C. Dale Keefe

Permission is hereby granted to Yoram Apelblat to use in his Ph.D. thesis the works contained in

"Compact Table for the Publication of Infrared Spectra That Are Quantitative on Both Intensity and Wavenumber Axes", J.E. Bertie, R. Norman Jones, Yoram Apelblat and C. Dale Keefe, Applied Spectroscopy, **47**, 1989 (1993).

"Infrared Intensities of Liquids XIII: Accurate Optical Constants and Molar Absorption Coefficients Between 6500 and 435 cm^{-1} of Toluene at 25°C, from Spectra Recorded in Several Laboratories", J.E. Bertie, R. Norman Jones, Yoram Apelblat and C. Dale Keefe, Applied Spectroscopy, **48**, 127 (1994).

"Infrared Intensities of Liquids XIV: Accurate Optical Constants and Molar Absorption Coefficients Between 4800 and 450 cm^{-1} of Chlorobenzene at 25°C from Spectra Recorded in Several Laboratories", J.E. Bertie, R. Norman Jones and Yoram Apelblat, Applied Spectroscopy, **48**, 144 (1994).

"Infrared Intensities of Liquids XIX: A Simple and Effective Approximate Method for the Calculation of Infrared Optical Constant Spectra of Liquids from Transmission Measurements", Applied Spectroscopy, Accepted for publication 1996.

John E Bertie

J.E. Bertie

Permission is hereby granted to Yoram Apelblat to use in his Ph.D. thesis the works contained in

"Compact Table for the Publication of Infrared Spectra That Are Quantitative on Both Intensity and Wavenumber Axes", J.E. Bertie, R. Norman Jones, Yoram Apelblat and C. Dale Keefe, Applied Spectroscopy, **47**, 1989 (1993).

"Infrared Intensities of Liquids XIII: Accurate Optical Constants and Molar Absorption Coefficients Between 6500 and 435 cm^{-1} of Toluene at 25°C, from Spectra Recorded in Several Laboratories", J.E. Bertie, R. Norman Jones, Yoram Apelblat and C. Dale Keefe, Applied Spectroscopy, **48**, 127 (1994).

"Infrared Intensities of Liquids XIV: Accurate Optical Constants and Molar Absorption Coefficients Between 4800 and 450 cm^{-1} of Chlorobenzene at 25°C from Spectra Recorded in Several Laboratories", J.E. Bertie, R. Norman Jones and Yoram Apelblat, Applied Spectroscopy, **48**, 144 (1994).

R. Norman Jones

R. Norman Jones

Table of Contents

Chapter 1 - Introduction 1

1.1 - Infrared absorption intensities 1

1.2 - Overview of thesis 3

1.3 - Electromagnetic theory and optical properties 7

1.4 - The relationship of integrated intensities to molecular properties 14

Chapter 2 - Accurate Optical Constants and Molar Absorption Coefficients Between 6500 and 435 cm^{-1} of Toluene at 25°C, from Spectra Recorded in Several Laboratories 17

2.1 - Introduction 17

2.2 - Method and experimental 19

2.3 - Results 21

2.3.1 Imaginary refractive index spectra 21

2.3.2 - Real refractive index spectrum 39

2.3.3 - Molar absorption coefficient spectrum 43

2.4 - The accuracy of the results 47

2.4.1 - Accuracy of absorption index values 49

2.4.2 - Accuracy of areas 52

2.4.3. - Accuracy of real refractive index values 53

2.5 - Summary 54

2.6 - References 55

Chapter 3 - Accurate Optical Constants and Molar Absorption Coefficients Between 4800 and 450 cm^{-1} of Chlorobenzene at 25°C from Spectra Recorded in Several Laboratories 56

3.1 - Introduction 56

3.2 - Methods and results 57

3.2.1 Absorption index spectrum 60

3.2.2 - Real refractive index spectrum. 71

3.2.3 - Molar absorption coefficient spectrum. 75

3.2.4 - Areas under $k(\widetilde{\nu})$ and $E_m(\widetilde{\nu})$ bands. 79

3.3 - Accuracy of results 83

3.3.1 - Accuracy of absorption indices and molar absorption coefficients 83

3.3.2. - Accuracy of areas. 87

3.3.3 - Accuracy of real refractive indices. 89

3.4 - Summary 89

3.5 - References 90

Chapter 4 - Assignments of Vibrations for Chlorobenzene and Toluene 92

4.1 - Symmetry and vibrational notations for benzene and monosubstituted benzenes 92

4.2 - Previous assignments of the chlorobenzene vibrations 98

4.2.1 - The 11 A_1 vibrations of chlorobenzene 103

4.2.2 - The 3 A_2 vibrations of chlorobenzene 105

4.2.3 - The 6 B_1 vibrations of chlorobenzene 107

4.2.4 - The 10 B_2 vibrations of chlorobenzene 107

4.3 - Assignments of the chlorobenzene vibrations 108

4.3.1 - Assignments of the 11 A_1 vibrations of chlorobenzene 122

4.3.2 - Assignment of the 3 A_2 vibrations of chlorobenzene 124

4.3.3 - Assignment of the 6 B_1 vibrations of chlorobenzene 124

4.3.4 - Assignment of the 10 B_2 vibrations of chlorobenzene 125

4.3.5 - Summary of the assignments of chlorobenzene 127

4.4 - Previous assignments of the toluene vibrations 130

4.4.1 - Previous assignments of the 11 A_1 phenyl group vibrations of toluene . 134

4.4.2 - Previous assignments of the 3 A_2 phenyl group vibrations of toluene ... 137

4.4.3 - Previous assignments of the 6 B_1 phenyl group vibrations of toluene ... 139

4.4.4 - Previous assignments of the 10 B_2 phenyl group vibrations of toluene . 139

4.4.5 - Previous assignment of the 9 CH_3 group vibrations of toluene 141

4.5 - Assignment of the vibrations of toluene 143

4.5.1 - Assignments of the 11 A_1 phenyl group vibrations of toluene 155

4.5.2 - Assignments of the 3 A_2 phenyl group vibrations of toluene 157

4.5.3 - Assignments of the 6 B_1 phenyl group vibrations of toluene 158

4.5.4 - Assignments of the 10 B_2 phenyl group vibrations of toluene 159

4.5.5 - Assignments of the 9 CH_3 vibrations of toluene 160

4.5.6 - Summary of the assignments of toluene 162

Chapter 5 - Infrared Integrated Intensities for Liquid Chlorobenzene and Toluene . 166
5.1 - Integrated intensities and dipole moment derivatives of liquid chlorobenzene 170
5.1.1 - Integrated intensities and dipole moment derivatives of the fundamental vibrations of liquid chlorobenzene 180
5.1.1a - Intensities of the CH stretching vibrations 183
5.1.1b - Intensities of the ν_4, ν_5, ν_{23} and ν_{24} vibrations 186
5.1.1c - Intensities of the ν_6, ν_{25}, ν_{26} and ν_{27} vibrations 189
5.1.1d - Intensities of the ν_7, ν_8, ν_9 and ν_{28} vibrations 191
5.1.1e - Intensities of the ν_{12}, ν_{13}, ν_{15} and ν_{16} vibrations 193
5.1.1f - Intensities of the ν_{10}, ν_{17} and ν_{18} vibrations 195
5.1.1g - Intensities of the ν_{11}, ν_{14}, ν_{19}, ν_{20}, ν_{29} and ν_{30} vibrations 197
5.1.2 - Summary of intensity assignment of chlorobenzene 199
5.2 - Integrated intensities and dipole moment derivatives of liquid toluene 201
5.2.1 - Integrated intensities and dipole moment derivatives of the fundamental vibrations of liquid toluene 209
5.2.1a - Integrated intensities of the CH stretching vibrations 213
5.2.1c - Integrated intensities of the ν_6, ν_7, ν_8, ν_9, ν_{25}, ν_{26}, ν_{27}, ν_{28}, ν_{36} and ν_{39} vibrations 219
5.2.1d - Integrated intensities of the ν_{10}, ν_{12}, ν_{13}, ν_{15} and ν_{16} vibrations 222
5.2.1e - Integrated intensities of the ν_{17} and ν_{18} vibrations 224

7.3 - Recovery of a spectrum from a Compact Table 277

7.4 - The accuracy in the recovered spectrum 281

7.5 - Summary 290

7.6 - Appendix A 291

  7.6.1 - Input file - Comptab.asc 291

  7.6.2 - Summary of variables used in program: 291

  7.6.3. - Program listings 292

7.7 - Appendix B 297

  7.7.1 - Input file - Trecover.asc 297

  7.7.2 - Summary of variables used in program 297

  7.7.3 - Program listings 298

7.8 - References 303

Chapter 8 - Summary 305

References 309

5.2.1f - Integrated intensities of the ν_{11}, ν_{14}, ν_{19}, ν_{20}, ν_{29}, ν_{30} and ν_{33} vibrations 226

5.2.2 - Summary of intensity assignments of toluene 226

5.3 - Comparison of integrated intensities of liquid chlorobenzene and liquid toluene 231

Chapter 6 - A simple and effective approximate method for the calculation of infrared optical constant spectra of liquids from transmission measurements 238

6.1 - Introduction 238

6.2 - Method 241

6.3 - Results 247

6.4 - Conclusions 257

6.5 - Appendix I 258

6.5.1. - Program ANCHORPT 258

6.5.2 - Program RNJ46A 259

6.5.3 - Program WIND8 262

6.6 - Appendix II 264

6.7 - References 264

Chapter 7 - A Compact Table for the Publication of Infrared Spectra That Are Quantitative on Both Intensity and Wavenumber Axes 266

7.1 - Introduction 266

7.2 - Construction of a Compact Table 269

List of Tables

Table 2.1 - linear absorption coefficients at anchor points for liquid toluene at 25°C. ... 22

Table 2.2 - path lengths, high-wavenumber refractive index, and number of spectra from each spectroscopist, for the regions processed. ... 23

Table 2.3 - spectroscopist average areas under the absorption index, $k(\tilde{\nu})$, bands. ... 24

Table 2.4 - spectroscopist average absorption index peak heights, k_{max} ... 25

Table 2.5 - overall average area under the absorption index bands. ... 30

Table 2.6 - overall average peak heights in the absorption index spectra. ... 33

Table 2.7 - absorption indices between 6500 and 435 cm^{-1} of liquid toluene at 25°C. ... 37

Table 2.8 - real refractive indices between 6500 and 435 cm^{-1} of liquid toluene at 25°C ... 41

Table 2.9 - molar absorption coefficients between 6500 and 435 cm^{-1} of liquid toluene at 25°C ... 45

Table 2.10 - overall average areas under molar absorption coefficient bands of liquid toluene at 25°C. ... 48

Table 2. 11 - overall average peak heights in the molar absorption coefficient spectrum of liquid toluene at 25°C. ... 50

Table 3 1 - linear absorption coefficients at the anchor points of liquid chlorobenzene at 25°C. ... 58

Table 3.2 - pathlengths, high-wavenumber refractive index, and number of spectra from each spectroscopist, for the regions processed. ... 59

Table 3.3 - spectroscopist average absorption index peak heights. 61

Table 3.4 - overall average absorption index peak heights. 64

Table 3.5 - absorption indices between 4800 and 435 cm^{-1} of liquid chlorobenzene at 25°C. 69

Table 3.6 - real refractive indices between 4800 and 435 cm^{-1} of liquid chlorobenzene at 25°C. 73

Table 3.7 - molar absorption coefficients between 4800 and 435 cm^{-1} of liquid chlorobenzene at 25°C. 77

Table 3.8 - peak heights in the molar absorption coefficient spectrum of liquid chlorobenzene at 25°C. 80

Table 3.9 - spectroscopist average areas under the absorption index bands. 81

Table 3.10 - overall average areas under the absorption index bands. 82

Table 3.11 - overall average areas under molar absorption coefficient bands of liquid chlorobenzene at 25°C. 84

Table 4.1 - assignments of benzene using Herzberg and Wilson notation schemes. 93

Table 4.2 - correlation table between D_{6H} and C_{2V} symmetry species for monosubstituted benzenes 94

Table 4.3 - conversion table for the pseudo notations for the assignments of vibrations of monosubstituted benzenes. 98

Table 4.4 - previous assignments of the A_1 vibrations of chlorobenzene 104

Table 4.5 - previous assignments of the A_2 vibrations of chlorobenzene 106

Table 4.6 - previous assignments of the B_1 vibrations of chlorobenzene 106

Table 4.8 - features in the experimental infrared spectra of gas and liquid chlorobenzene and raman spectra of liquid chlorobenzene 119

Table 4.9 - computed wavenumbers, eigenvectors and potential energy distributions for chlorobenzene. 121

Table 4.10 - assignments of the fundamental vibrations of chlorobenzene 128

Table 4.11 - previous assignments of the 11 A_1 phenyl vibrations of toluene 136

Table 4.12 - previous assignments of the 3 A_2 phenyl vibrations of toluene 137

Table 4.13 - previous assignments of the 6 B_1 phenyl vibrations of toluene 138

Table 4.14 - previous assignments of the 10 B_2 phenyl vibrations of toluene 140

Table 4.15 - previous assignments of the 9 CH_3 group vibrations of toluene 142

Table 4.16 - spectral features in infrared spectrum of gaseous toluene and infrared and spectra of the liquid 151

Table 4.17 - computed wavenumbers, eigenvectors and potential energy distributions for toluene. 154

Table 4.18 - assignments of the fundamental vibrations of liquid toluene 163

Table 5.1 - integrated intensities and dipole moment transitions of liquid chlorobenzene. 173

Table 5.2 - dipole moment derivatives of liquid chlorobenzene 181

Table 5.3 - integrated intensities of toluene 203

Table 5.4 - dipole moment derivatives and integrated intensities of toluene 211

Table 5.5 - experimental integrated intensities of toluene 230

Table 5.6 - integrated intensities of liquid chlorobenzene, toluene and benzene 232

Table 6.1 - linear absorption coefficients, $k(\tilde{\nu})$, of liquid chlorobenzene at anchor points in the baseline. 252

Table 6.2 - peak heights in the molar absorption coefficient spectrum, $E_m(\tilde{\nu})$, of liquid chlorobenzene. 253

Table 6.3 - areas under the molar absorption coefficient spectrum, $E_m(\tilde{\nu})$, of chlorobenzene. 254

Table 7.1 - reduced data of imaginary refractive index of chlorobenzene in xy format. 271

Table 7.2 - the compact table of the imaginary refractive index of chlorobenzene. 272

Table 7.3 - the compact table of the molar absorption coefficient of chlorobenzene. 274

Table 7.4 - the compact table of the real refractive indices of chlorobenzene. 276

List of Figures

Figure 2.1 - average areas and 95% confidence limits under the absorption index spectra in the regions 3150 to 2770 cm^{-1}, 1837 to 1735 cm^{-1}, and 1650 to 1555 cm^{-1} for the six spectroscopists 29

Figure 2.2 - absorption index (imaginary refractive index), $k(\tilde{\nu})$, spectrum between 6500 and 435 cm^{-1} of toluene at 25°C 36

Figure 2.3 - real refractive index, $n(\tilde{\nu})$, spectrum between 6500 and 435 cm^{-1} of toluene at 25°C 40

Figure 2.4 - molar absorption index, $E_m(\tilde{\nu})$, spectrum between 6500 and 435 cm^{-1} of toluene at 25°C. 44

Figure 3.1 - absorption index, $k(\tilde{\nu})$, spectrum between 4800 and 435 cm^{-1} of chlorobenzene at 25°C 68

Figure 3.2 - real refractive index, $n(\tilde{\nu})$, spectrum between 4800 and 435 cm^{-1} of chlorobenzene at 25°C 72

Figure 3.3 - molar absorption coefficient, $E_m(\tilde{\nu})$ spectrum between 4800 and 435 cm^{-1} of chlorobenzene at 25°C. 76

Figure 4.1 - qualitative band contour shapes for chlorobenzene 99

Figure 4.2 - imaginary molar polarizability, α''_m, spectrum of liquid chlorobenzene 112

Figure 4.3 - infrared spectra of gas and liquid chlorobenzene and raman parallel and perpendicular spectra of the liquid between 3125 and 2975 cm^{-1}. 113

Figure 4.4 - infrared spectra of gas and liquid chlorobenzene and raman parallel and perpendicular spectra of the liquid between 1625 and 1400 cm^{-1}. 114

Figure 4.5 - infrared spectra of gas and liquid chlorobenzene and raman parallel and perpendicular spectra of the liquid between 1400 and 1105 cm^{-1}. 115

Figure 4.6 - infrared spectra of gas and liquid chlorobenzene and raman parallel and perpendicular spectra of the liquid between 1105 and 900 cm^{-1}. 116

Figure 4.7 - infrared spectra of gas and liquid chlorobenzene and raman parallel and perpendicular spectra of the liquid between 900 and 650 cm^{-1}. 117

Figure 4.8 - infrared spectra of gas and liquid chlorobenzene and raman parallel and perpendicular spectra of the liquid between 650 and 175 cm^{-1}. 118

Figure 4.9 - imaginary molar polarizability, α''_m, spectrum of liquid toluene. 145

Figure 4.10 - infrared spectra of gas and liquid toluene and raman parallel and perpendicular spectra of the liquid between 3150 and 2800 cm^{-1}. 146

Figure 4.11 - infrared spectra of gas and liquid toluene and raman parallel and perpendicular spectra of the liquid between 1650 and 1350 cm^{-1}. 147

Figure 4.12 - infrared spectra of gas and liquid toluene and raman parallel and perpendicular spectra of the liquid between 1350 and 950 cm^{-1}. 148

Figure 4.13 - infrared spectra of gas and liquid toluene and raman parallel and perpendicular spectra of the liquid between 950 and 650 cm^{-1}. 149

Figure 4.14 - infrared spectra of gas and liquid toluene and raman parallel and perpendicular spectra of the liquid between 650 and 200 cm^{-1}. 150

Figure 5.1 - superimposed experimental imaginary molar polarizability, α''_m and curve fitted α''_m spectra of liquid chlorobenzene 171

Figure 5.2 - superimposed experimental imaginary molar polarizability, α''_m and curve fitted α''_m spectra of liquid chlorobenzene between 3125 and 2975 cm^{-1} 184

Figure 5.3 - superimposed experimental imaginary molar polarizability, α''_m and curve fitted α''_m spectra of liquid chlorobenzene between 1650 and 1400 cm^{-1} 187

Figure 5.4 - experimental imaginary molar polarizability, α''_m and curve fitted α''_m spectra of liquid chlorobenzene between 1400 and 1140 cm^{-1} 190

Figure 5.5 - superimposed experimental imaginary molar polarizability, α''_m and curve fitted α''_m spectra of liquid chlorobenzene between 1140 and 990 cm^{-1} 192

Figure 5.6 - superimposed experimental imaginary molar polarizability, α''_m and curve fitted α''_m spectra of liquid chlorobenzene between 990 and 800 cm^{-1} 194

Figure 5.7 - top - superimposed experimental imaginary molar polarizability, α''_m and curve fitted α''_m spectra of liquid chlorobenzene between 800 and 650 cm^{-1} 196

Figure 5.8 - top - superimposed experimental imaginary molar polarizability, α''_m and curve fitted α''_m spectra of liquid chlorobenzene between 650 and 350 cm^{-1} 198

Figure 5.9 - the experimental imaginary molar polarizability, α''_m, spectrum and curve fitted α''_m spectrum of liquid toluene 202

Figure 5.10 - superimposed experimental imaginary molar polarizability, α''_m and curve fitted α''_m spectra of liquid toluene between 3150 and 2800 cm^{-1} 214

Figure 5.11 - superimposed experimental imaginary molar polarizability, α_m'' and curve fitted α_m'' spectra of liquid toluene between 1650 and 1350 cm^{-1}. 218

Figure 5.12 - superimposed experimental imaginary molar polarizability, α_m'' and curve fitted α_m'' spectra of liquid toluene between 1350 and 990 cm^{-1}. 220

Figure 5.13 - superimposed experimental imaginary molar polarizability, α_m'' and curve fitted α_m'' spectra of liquid toluene between 990 and 750 cm^{-1}. 223

Figure 5.14 - superimposed experimental imaginary molar polarizability, α_m'' and curve fitted α_m'' spectra of liquid toluene between 750 and 650 cm^{-1}. 225

Figure 5.15 - superimposed experimental imaginary molar polarizability, α_m'' and curve fitted α_m'' spectra of liquid toluene between 650 and 442 cm^{-1}. 227

Figure 6.1 - the real and imaginary refractive index spectra of the strongest absorption band in liquid chlorobenzene. 245

Figure 6.2 - top and middle boxes: the apparent absorbance due to reflection calculated by the exact method and the approximate method for 100 μm of chlorobenzene(ℓ) between KBr windows and NaCl windows. Bottom box: the real refractive index spectrum of liquid chlorobenzene at 25°C. 246

Figure 6.3 - the $E_m(\tilde{\nu})$ spectrum of chlorobenzene(ℓ) in four regions. 249

Figure 6.4 - the percent difference between the $E_m(\tilde{\nu})$ spectra, $\frac{\text{approximate } E_m \text{ - exact } E_m}{\text{exact } E_m} \times 100\%$, of chlorobenzene($\ell$) in the four regions of Fig. 6.3. 250

Figure 6.5 - top box: the apparent absorbance due to reflection calculated by the exact method and the approximate method for 23.26 μm of $CH_3CN(\ell)$ between kbr windows. Middle box: the E_m spectra of $CH_3CN(\ell)$ calculated by the exact and approximate methods. Lower box: the % difference between the E_m spectra, defined as for fig. 6.4, of CH_3CN between KBr windows. 256

Figure 7.1 - illustration of the step-wise procedure for interpolating to the original wavenumber spacing at the boundary between regions of different spacings, as described in the text. 279

Figure 7.2 - the absorption index, $k(\tilde{\nu})$, spectrum of chlorobenzene at 25°C. 282

Figure 7.3 - two of the bands in Fig. 7.2, with the original spectrum superimposed on that recovered from a compact table and the percent difference between the recovered and original spectra. 283

Figure 7.4 - the percent difference between the recovered and original $k(\tilde{\nu})$ spectra when 4 digits or 6 digits were retained in the compact table. 284

Figure 7.5 - the original real refractive index, $n(\tilde{\nu})$, spectrum of chlorobenzene at 25°C superimposed on that recovered from a compact table of $n(\tilde{\nu})$ values and the percent differences between the recovered and original spectra and between the original $n(\tilde{\nu})$ spectrum and that calculated by Kramers-Kronig transform of the $k(\tilde{\nu}$ spectrum recovered from a compact table of $k(\tilde{\nu})$ values. 286

Figure 7.6 - two of the bands in the decadic molar absorption coefficient, $E_m(\tilde{\nu})$ spectrum of chlorobenzene at 25°C and the percent difference between the recovered and original spectra. 287

Figure 7.7 - the percent differences between the real and imaginary dielectric constants calculated from the original real and imaginary refractive index spectra and from real and imaginary refractive index spectra recovered from compact tables.......... 288

List of Symbols

General

λ	Vacuum wavelength.
$\tilde{\nu}$	Vacuum wavenumber; usual unit cm^{-1}. $\tilde{\nu} = 1/\lambda$.
c	Speed of light in vacuum.
C	Molar concentration; usual unit mole L^{-1}.
V_m	Molar volume: usual unit cm^3 $mole^{-1}$.
$\boldsymbol{E}$	Electric field strength vector.
$\boldsymbol{D}$	Electric displacement vector.
$\boldsymbol{P}$	Electric polarization vector.
$\boldsymbol{H}$	Magnetic field strength vector.
$\boldsymbol{I}$	Energy flux. $\boldsymbol{I} = \boldsymbol{E} \times \boldsymbol{H}$.
σ	Conductivity
ε_o	Permittivity of vacuum
μ_o	Permeability of vacuum
i	$\sqrt{-1}$
^	used to indicate a complex quantity.

Wavenumber dependent quantities

$\hat{n}(\tilde{\nu})$	Complex refractive index. $\hat{n}(\tilde{\nu}) = n(\tilde{\nu}) + \mathrm{i}\,k(\tilde{\nu})$.
$n(\tilde{\nu})$	Real refractive index.
$k(\tilde{\nu})$	Imaginary refractive index, also called the absorption index.
$\hat{\varepsilon}(\tilde{\nu})$	Complex dielectric constant. $\hat{\varepsilon}(\tilde{\nu}) = \varepsilon'(\tilde{\nu}) + \mathrm{i}\,\varepsilon''(\tilde{\nu})$.
$\varepsilon'(\tilde{\nu})$	Real dielectric constant, usually called the dielectric constant.
$\varepsilon''(\tilde{\nu})$	Imaginary dielectric constant, also called the dielectric loss.
$\hat{\alpha}_{\mathrm{m}}(\tilde{\nu})$	Complex molar polarizability. $\hat{\alpha}_{\mathrm{m}}(\tilde{\nu}) = \alpha'_{\mathrm{m}}(\tilde{\nu}) + \mathrm{i}\,\alpha''_{\mathrm{m}}(\tilde{\nu})$.
$\alpha'_{\mathrm{m}}(\tilde{\nu})$	Real molar polarizability.
$\alpha''_{\mathrm{m}}(\tilde{\nu})$	Imaginary molar polarizability.
$E_{\mathrm{m}}(\tilde{\nu})$	(Decadic) molar absorption coefficient.
$K\tilde{\nu})$	(Decadic) linear absorption coefficient.

Integrated intensities

A_j	Area under band j in 2.303 E_{m} spectrum. Usual units km mole^{-1}.
C_j	Area under band j in $\tilde{\nu}\alpha''_{\mathrm{m}}$ spectrum. Usual units km mole^{-1}.

Molecular properties

μ_j	Magnitude of the dipole moment derivative with respect to normal coordinate j.
$\vec{R_j}$	Dipole transition moment, $<f|\vec{\mu}|i>$, of the transition that causes band j.

Types of spectra

$n(\tilde{\nu})$ vs. $\tilde{\nu}$	Real refractive index spectrum.
$k(\tilde{\nu})$ vs. $\tilde{\nu}$	Absorption index spectrum.
$E_{\mathrm{m}}(\tilde{\nu})$ vs. $\tilde{\nu}$	Molar absorption coefficient spectrum.
$\alpha''_{\mathrm{m}}(\tilde{\nu})$ vs. $\tilde{\nu}$	Imaginary molar polarizability spectrum.

Chapter 1 - Introduction

1.1 - Infrared absorption intensities

The absorbance spectrum of a liquid in the mid infrared region (8000 - 400 cm^{-1}) is due mainly to transitions between vibrational energy levels of a molecule. A similar spectrum of the gas phase may show some rotational structure in addition to the vibrational structure. In either case, the vibrational bands in the spectrum are characterised by their positions, their intensities and their band shapes[1].

The band position, measured in wavenumber units, usually cm^{-1}, is the easiest of the three to determine accurately and over the years its measurement accuracy has been improved and has reached such a high degree of accuracy that it was possible already in the early 1960s to publish tables of standard wavenumbers to calibrate spectrometers[2] in the 4300-600 cm^{-1} region. The estimated accuracy of the standard wavenumbers was about 0.01-0.1 cm^{-1}. The tables were later revised[3] and the range extended to 1 cm^{-1} with an estimated accuracy of 0.001-0.005 cm^{-1} throughout the range and < 0.0002 cm^{-1} for the fundamental and first overtone of carbon monoxide.

The intensity and band shape are more difficult to measure accurately. Intensity measurements were done as early as the late 1920s, but their accuracy[4,5] wasn't as good as that of the wavenumber.

From the theoretical viewpoint, it was recognized that the intensity is proportional to the dipole transition moment. For fundamental vibrations, under the double harmonic approximation, this is proportional to the square of the dipole moment derivative with respect to the normal coordinate, $|\partial\mu/\partial Q_j|^2$. The intensities reflect the change in electron distribution in the molecule during the atomic displacements[4]. However, the use of the intensity was hampered by the ambiguity of the sign of $\partial\mu/\partial Q_j$ and by unreliable transformation of the observed $\partial\mu/\partial Q_j$ to related motions defined by internal coordinates, $\partial\mu/\partial R_j$.

During the 1970s the study of intensities improved considerably[4]. Advances in normal coordinate calculations combined with *ab initio* quantum mechanical calculations helped solve the sign ambiguity of the dipole moment derivatives. At the same time, the introduction of Fourier Transform Infra Red (FTIR) spectrometers based on Michelson's interferometer and the use of computer controlled instruments gave far more reproducible spectra than dispersive instruments. Later it was shown by V. Behnam and J.E. Bertie that FTIR spectrometers were also accurate in addition to being reproducible. Their studies[5,6] of intensities of several organic liquids made with a non-calibrated FTIR spectrometer showed that their intensity values were more precise and within the error limits of R.N. Jones and co-workers' earlier work, which was made on a dispersive instrument and calibrated against primary standards[7].

As laboratory computers, powerful software and stable FTIR spectrometers became increasingly available and inexpensive in the 1980s and 1990s, the measurement over a wide wavenumber range and interpretation of accurate absolute infrared intensities of molecules is possible today to an extent unthinkable 20 years ago. The studies reported in this thesis form part of a research program that is aimed at measuring and using both the intensity and the wavenumber information to improve our chemical and physical knowledge of molecular vibrations in the liquid phase.

An important feature of the program is that the real and imaginary refractive indices are measured over a wide wavenumber range in the infrared. The results of any infrared experiment can be calculated from these quantities. Thus, they are fundamental physical properties, obtained as a part of the program.

1.2 - Overview of thesis

The first goal of the work for this thesis was to assist in the development of infrared secondary intensity standards. The work started in 1985 when J.E. Bertie and V. Behnam[5,6], showed that FTIR intensity measurements were precise to ~1%[5,6] and probably accurate to ~3%[5-7]. Further investigation was needed to identify and eliminate the systematic errors influencing the measurements. This was done by comparing the intensities of four organic liquids[8-11] determined from transmission measurements made by different workers using different instruments in different laboratories. The equations relating the transmission measurement to various intensity quantities are given in Section 1.3.

The resulting good agreement led to the acceptance of the intensities of 43 selected bands as secondary standards by the International Union of Pure and Applied Chemistry (IUPAC). Later these secondary standards were published as a monograph[12].

The intensity measurements of liquid toluene and liquid chlorobenzene, which were part of this project, are given in Chapters 2 and 3, respectively.

The intensities reported as standards were the real and imaginary refractive index spectra, also known as the optical constant spectra. The molar absorption coefficient spectra of the liquids were also reported. The real and imaginary refractive indices are fundamental physical quantities, from which other measures of infrared absorption intensities such as the complex dielectric constant and the complex molar polarizability can be calculated. The relationship between these quantities is given in Section 1.3

The second goal of the work for this thesis was to determine the physical and chemical information contained in the intensities. For that purpose, the complex molar polarizability spectra of liquid toluene and chlorobenzene were calculated under the assumption of the Lorentz local field, to relate the local electric field that acts on the molecule in the liquid to the macroscopic electric field of the radiation. The imaginary molar polarizability can then be related to the transition dipole moment and under the assumption of electrically and mechanically harmonic vibration, to the square of the dipole moment derivative with respect to the normal coordinate[13].

To relate these experimental intensities to particular vibrational modes of the molecules, fundamental frequencies must first be assigned to particular vibrations of the molecule, e.g. the CC stretch, CH bend, etc. Despite a considerable number of experimental and theoretical studies reported in the literature on toluene[14-34] and chlorobenzene[18,22,23,35-47], there are still some disagreements about the assignments of the fundamentals. In Chapter 4, the assignment of the spectra of toluene and chlorobenzene is discussed, based on our experimental spectra, previous studies, and normal coordinate calculations which relate the vibrations of benzene to those of substituted benzene derivatives of C_{2v} symmetry, chlorobenzene and toluene. For the latter molecule the CH_3 group was approximated by a point of mass 15 in the calculations in order to correlate the assignment of the vibrations of the phenyl group with those in the other molecules.

Once the fundamentals are assigned, it is possible to relate the intensities to the vibrational transitions in the different molecules. This is done in Chapter 5 where experimental and curve-fitted spectra are used to relate the intensities of toluene and chlorobenzene to the dipole moment derivatives. The curve fitting is necessary in order to separate contributions from different transitions and to make sure that the intensities in the wings of a band are included in the band area. It is noteworthy that the bands are nearly Lorentzian, so that it is necessary to integrate over more than ±16 times the full width at half height in order to include >98% of the area[48].

The procedure used to determine the optical constants of the liquid from transmission measurements was first developed by R.N. Jones and co-workers at the National Research Council of Canada[49-53] and later improved by J.E. Bertie and C.D. Keefe[54] at the University of Alberta. During this iterative procedure, the reflection losses are calculated at all interfaces of the cell, namely air-window-liquid-window-air. The method is exact but computationally complex. In Chapter 6, an approximate method is developed to calculate the optical constants from transmission measurements. The conditions under which the approximation method yields results of sufficient accuracy are explored.

The presentation of quantitative spectral data for publication in the literature is not an easy task. A graph is necessary to convey the spectrum qualitatively. However, to convey the spectrum quantitatively, values of both wavenumber and intensity must be tabulated. Since the space required to publish all data points in a traditional table is very large, only selected pairs of wavenumber and intensity values have usually been given, mostly at peaks of bands[7,55,56]. This practice was satisfactory when the intensity accuracy and precision were sufficiently low that only strong bands were reported and the shapes of bands were not considered important. Today, however, both intensity and line shapes can be precisely and accurately measured, and have gained in potential importance. The practice of reporting just band peak data is no longer valid and a method is required to allow quantitative ordinate values to be reported over the whole spectrum range in an acceptably small space. The solution to this problem is appropriate data reduction and appropriate compression of the presentation format.

In Chapter 7, a method for data reduction and presentation is given. The data is reduced and incorporated into what we call a Compact Table. The Compact Table format allows a spectrum to be tabulated in about 1/10 of the space required for a traditional table. It allows specific values to be read from the table directly and also allows, through a recovery program, the entire spectrum to be retrieved without loss of intensity and line shape information, within the experimental error. The programs for the creation of the Compact Table and recovery of the data are given in Chapter 7 and their use is demonstrated with the spectra of chlorobenzene.

Finally, Chapter 8 contains a summary of the results of this thesis and presents some possible future extensions of the work.

1.3 - Electromagnetic theory and optical properties

When light is transmitted through a sample, part of it is absorbed by the molecules in the sample. The extent of the macroscopic response of the sample to the perturbation caused by the electric field is determined by the complex refractive index of the sample, $\hat{n} = n + ik$. The real part of the refractive index, n, is what is usually called simply the refractive index. The imaginary refractive index, k, is a measure of absorption intensity, and is sometimes called the absorption index. Together the refractive indices are frequently called the optical constants.

The fraction of light transmitted by a medium is related to the optical constants through Maxwell's equations[57]. For isotropic conducting media, the curl equations relate the time and space derivatives of the magnetic, $\boldsymbol{H}$, and electric fields, $\boldsymbol{E}$, by

$$\nabla \times \boldsymbol{E} = -\,\mu\,\mu_o \frac{\partial \boldsymbol{H}}{\partial t} \tag{1.3.1}$$

$$\nabla \times \boldsymbol{H} = \sigma \boldsymbol{E} + \varepsilon\,\varepsilon_o \frac{\partial \boldsymbol{E}}{\partial t} \tag{1.3.2}$$

and the divergence conditions denote the absence of charge[57]

$$\nabla \bullet \boldsymbol{E} = 0 \qquad (1.3.3)$$

$$\nabla \bullet \boldsymbol{H} = 0 \qquad (1.3.4)$$

Here μ is the relative permeability, μ_o is the permeability of vacuum, ε is the relative dielectric constant of the medium, ε_o is the permittivity of vacuum and σ is the conductivity of the medium.

Equations 1.3.3 and 1.3.4 and the fact that A x (B x C) = (A • C) B - (A • B) C give equations 1.3.5 and 1.3.6

$$\nabla \times (\nabla \times \boldsymbol{E}) = (\nabla \bullet \boldsymbol{E})\, \nabla - (\nabla \bullet \nabla)\, \boldsymbol{E} = 0 - \nabla^2 \boldsymbol{E} = -\nabla^2 \boldsymbol{E} \qquad (1.3.5)$$

$$\nabla \times (\nabla \times \boldsymbol{H}) = (\nabla \bullet \boldsymbol{H})\, \nabla - (\nabla \bullet \nabla)\, \boldsymbol{H} = 0 - \nabla^2 \boldsymbol{H} = -\nabla^2 \boldsymbol{H} \qquad (1.3.6)$$

Equations 1.3.5, 1.3.6, 1.3.1 and 1.3.2 give equations 1.3.7 and 1.3.8

$$-\nabla^2 \boldsymbol{E} = -\,\mu\, \mu_o\, \sigma \frac{\partial \boldsymbol{E}}{\partial t} - \mu\, \mu_o\, \varepsilon\, \varepsilon_o \frac{\partial^2 \boldsymbol{E}}{\partial t^2} \qquad (1.3.7)$$

$$-\nabla^2 \boldsymbol{H} = -\,\mu\, \mu_o\, \sigma \frac{\partial \boldsymbol{H}}{\partial t} - \mu\, \mu_o\, \varepsilon\, \varepsilon_o \frac{\partial^2 \boldsymbol{H}}{\partial t^2} \qquad (1.3.8)$$

One solution to these equations is[58]

$$\boldsymbol{E} = \boldsymbol{E}_o\, \mathrm{e}^{-i\omega\left(t - \frac{x}{\hat{v}}\right)} \qquad (1.3.9)$$

$$\boldsymbol{H} = \boldsymbol{H}_o\, \mathrm{e}^{-i\omega\left(t - \frac{x}{\hat{v}}\right)} \qquad (1.3.10)$$

which is a representation of a wave propagating in the x direction with angular frequency $\omega = 2\pi f$, f = frequency, and with complex velocity $\hat{v}$, that holds true provided that

$$\frac{1}{\hat{v}^2} = \mu\,\mu_o\,\varepsilon\,\varepsilon_o + \mathrm{i}\,\mu\,\mu_o\frac{\sigma}{\omega} \qquad (1.3.11)$$

$\hat{v}$ can be written as $\frac{c}{\hat{n}}$, where $\hat{n}$ is the complex refractive index and c is the speed of light in vacuum. Equation 1.3.11 shows that in vacuum, where $\sigma = 0$ and $\mu = \varepsilon = 1$, the velocity of light is real and denoted by c, where $c = (\mu_o\,\varepsilon_o)^{-1/2}$. The use of these expressions in equation 1.3.11 yields

$$\hat{n}^2 = \mu\,\varepsilon + \mathrm{i}\frac{\sigma\mu}{\varepsilon_o\omega} \qquad (1.3.12)$$

$\hat{n}$ can be defined as

$$\hat{n} = n + \mathrm{i}k \qquad (1.3.13)$$

where n is the real refractive index and k is the imaginary refractive index.

Substitution of equation 1.3.13 into equation 1.3.9 and the use of $\hat{v} = \frac{c}{\hat{n}}$, gives

$$\boldsymbol{E} = \boldsymbol{E}_0\,\mathrm{e}^{-i\omega\left(t-\frac{x}{\hat{v}}\right)} = \boldsymbol{E}_0\,\mathrm{e}^{-i\omega\left(t-\frac{x\hat{n}}{c}\right)} = \boldsymbol{E}_0\,\mathrm{e}^{-i\omega\left(t-\frac{xn}{c}\right)}\,\mathrm{e}^{-\left(\frac{\omega k}{c}x\right)} \qquad (1.3.14)$$

Similarly, use of equations 1.3.13 in 1.3.10 gives

$$\boldsymbol{H} = \boldsymbol{H}_0\,\mathrm{e}^{-i\omega\left(t-\frac{x}{\hat{v}}\right)} = \boldsymbol{H}_0\,\mathrm{e}^{-i\omega\left(t-\frac{x\hat{n}}{c}\right)} = \boldsymbol{H}_0\,\mathrm{e}^{-i\omega\left(t-\frac{xn}{c}\right)}\,\mathrm{e}^{-\left(\frac{\omega k}{c}x\right)} \qquad (1.3.15)$$

Equations 1.3.14 and 1.3.15 show that the real refractive index controls the phase of the field while the imaginary part controls the attenuation of the field with propagation distance.

The energy flux, $\boldsymbol{I}$, is given by

$$\boldsymbol{I} = \boldsymbol{E} \times \boldsymbol{H} = \boldsymbol{I}_0 \, \mathrm{e}^{-2i\omega\left(t - \frac{xn}{c}\right)} \, \mathrm{e}^{-2\left(\frac{\omega k}{c} x\right)} \tag{1.3.16}$$

where $\boldsymbol{I}_o = \boldsymbol{E}_o \times \boldsymbol{H}_o$.

In a transmission measurement, the reduction of the energy of a light beam passing through a unit thickness of the sample is given by

$$\frac{\mathrm{d}\boldsymbol{I}}{\mathrm{d}x} = -K' \boldsymbol{I} \tag{1.3.17}$$

where K' is the (Napierian) linear absorption coefficient. If the path length through the sample is d, equation 1.3.17 can be integrated to give

$$\boldsymbol{I} = \boldsymbol{I}_o \, \mathrm{e}^{-K'd} \tag{1.3.18}$$

$$\text{so that } K' = -\frac{1}{d} \ln \left(\frac{\boldsymbol{I}}{\boldsymbol{I}_o}\right) \tag{1.3.19}$$

Equation 1.3.18 is also known as Lambert's law[59]. Chemists, however prefer to use the Beer-Lambert law[59]

$$\boldsymbol{I} = \boldsymbol{I}_o \, 10^{-Kd} = \boldsymbol{I}_o \, 10^{-E_m Cd} \tag{1.3.20}$$

where K is the linear (decadic) absorption coefficient, E_m is the molar (decadic) absorption coefficient and C is the molar concentration. By rearrangement of equation 1.3.20, K can be written as

$$K = -\frac{1}{d}\log_{10}\left(\frac{I}{I_o}\right) \tag{1.3.21}$$

From equations 1.3.16 and 1.3.18, the energy attenuation per unit thickness or distance travelled by the wave is

$$e^{-K'd} = e^{-2\left(\frac{\omega dk}{c}\right)} \tag{1.3.22}$$

because $\omega = 2\pi f$, where f is the frequency, and $\tilde{\nu} = f/c$, the wavenumber in vacuum, the (Napierian) linear absorption coefficient, K', is related to the imaginary refractive index, k, by $K' = 4\pi\tilde{\nu}k$, whereas the decadic linear absorption coefficient is given by

$$K = \frac{K'}{\ln 10} = \frac{4\pi\tilde{\nu}k}{2.303} \tag{1.3.23}$$

The absorbance, A, is defined as $-\log_{10}\left(\frac{I}{I_o}\right)$. From equations 1.3.21 and 1.3.23 it is given by

$$A = \frac{4\pi\tilde{\nu}kd}{2.303} \tag{1.3.24}$$

It is important to note that the absorbance used here is the absorbance defined by IUPAC, namely that due only to loss of light by absorption by the sample[60]. In a typical experiment, the experimentally observed absorbance includes the absorbance by the sample and absorbance by other elements such as the windows of the cell. It is called in this laboratory the experimental absorbance, EA. The experimental absorbance must therefore be corrected for energy loss other than through absorption by the sample before it can be used in these equations. The procedure for this correction is implemented through program RNJ46A[53,54]. The program and an alternative approximate procedure are discussed in Chapter 6. Throughout the thesis, the term absorbance is used according to the IUPAC definition, namely as due solely to absorption by the sample.

From equations 1.3.20, 1.3.23 and 1.3.24, the molar absorption coefficient is given by

$$E_m = \frac{A}{Cd} = \frac{4\pi \tilde{\nu} k}{2.303C} \qquad (1.3.25)$$

Other infrared intensity quantities can be obtained from the refractive indices. Eq. 1.3.12 relates the square of the complex refractive index to the complex dielectric constant, $\hat{\varepsilon}$.

$$\hat{n}^2 = n^2 + 2ink - k^2 = \mu\,\varepsilon + \mathrm{i}\frac{\sigma\mu}{\varepsilon_0\omega} = \mu\,(\varepsilon + \mathrm{i}\frac{\sigma}{\varepsilon_0\omega}) = \mu\,\hat{\varepsilon} \qquad (1.3.26)$$

$\hat{\varepsilon}$ is defined in a similar manner to $\hat{n}$, as

$$\hat{\varepsilon} = \varepsilon' + \mathrm{i}\,\varepsilon'' \qquad (1.3.27)$$

where the real part, ε', is the (real) dielectric constant and the imaginary dielectric constant, ε'', is also known as the dielectric loss.

For diamagnetics, $\mu \approx 1$, so $\hat{n}^2 \approx \hat{\varepsilon}$. From Equations 1.3.13, 1.3.26 and 1.3.27, the real and imaginary parts of the dielectric constants can be related to the refractive indices as:

$$\varepsilon' = n^2 - k^2 \tag{1.3.28a}$$

$$\varepsilon'' = 2nk \tag{1.3.28b}$$

The electric displacement, $\boldsymbol{D}$, is given by[61]

$$\boldsymbol{D} = \hat{\varepsilon}\,\boldsymbol{E} \tag{1.3.29}$$

It is also the sum of the electric field vector and the polarization vector, $\boldsymbol{P}$, where all of these vectors can be complex.

$$\boldsymbol{D} = \boldsymbol{E} + 4\pi\boldsymbol{P} \tag{1.3.30}$$

The polarization, i.e. the electric dipole moment per unit volume, is also given in terms of the complex polarizability[61,62], $\hat{\alpha}$, as

$$\boldsymbol{P} = N\,\hat{\alpha}\,(\boldsymbol{E} + \frac{4\pi}{3}\boldsymbol{P}) \tag{1.3.31}$$

where N is the number of molecules per unit volume. $\boldsymbol{E} + \frac{4\pi}{3}\boldsymbol{P}$ is the Lorentz local field derived by calculating the field within a microscopic cavity in an isotropic dielectric medium[62,63].

Combination of equations 1.3.29, 1.3.30 and 1.3.31 yields the Lorentz-Lorenz equation[62],

$$\frac{\hat{n}^2-1}{\hat{n}^2+2} = \frac{\hat{\varepsilon}-1}{\hat{\varepsilon}+2} = \frac{4\pi}{3} N \hat{\alpha} \tag{1.3.32}$$

Since $\hat{\alpha}$ is a molecular property and, thus, has a small value, the complex molar polarizability is introduced as $\hat{\alpha}_m = N_A \hat{\alpha} = \alpha'_m + i\alpha''_m$ where N_A is Avogadro's number. Multiplication of equation 1.3.32 by N_A and the use of the molar volume, $V_m = \frac{N_A}{N}$, gives the real and imaginary parts of the molar polarizability in terms of ε' and ε''.

$$\alpha'_m = \frac{3V_m}{4\pi} \frac{(\varepsilon'-1)(\varepsilon'+2) + \varepsilon''^2}{(\varepsilon'+2)^2 + \varepsilon''^2} \tag{1.3.33a}$$

$$\alpha''_m = \frac{9V_m}{4\pi} \frac{\varepsilon''}{(\varepsilon'+2)^2 + \varepsilon''^2} \tag{1.3.33b}$$

It is important to note that all quantities are frequency or wavenumber dependent, and thus should really be denoted as $n(\tilde{\nu})$, $k(\tilde{\nu})$, $E_m(\tilde{\nu})$, $\varepsilon'(\tilde{\nu})$, $\varepsilon''(\tilde{\nu})$, $\alpha'_m(\tilde{\nu})$ and $\alpha''_m(\tilde{\nu})$.

1.4 - The relationship of integrated intensities to molecular properties

There are several methods to define the integrated intensity of band j. One is as the integrated intensity, A_j[48,64,65] which is the area under the $E_m(\tilde{\nu})$ spectrum

$$A_j = 2.303 \int E_m(\tilde{\nu})d\tilde{\nu} \tag{1.4.1}$$

Another definition of the integrated intensity is as C_j, the area under the $\tilde{\nu}\alpha''_{\mathrm{m}}(\tilde{\nu})$ spectrum[48]

$$C_j = \int \tilde{\nu}\alpha''_m(\tilde{\nu})\mathrm{d}\,\tilde{\nu} \tag{1.4.2}$$

In both equations, the integration is over the entire band j. These experimental integrated intensities must be related to molecular properties. Calculation of the complex molar polarizability of randomly oriented molecules from quantum mechanics yields[48,58,63,66]

$$C_j = \int \tilde{\nu}\alpha''_m(\tilde{\nu})\mathrm{d}\,\tilde{\nu} = \frac{\mathrm{N_A}\pi}{3\mathrm{h}c}\, g_j\, \tilde{\nu}_j\, |\,\overrightarrow{R_j}\,|^2 \tag{1.4.3}$$

where h is Planck's constant, c is the velocity of light in vacuum, g_j is the degeneracy and $\overrightarrow{R_j}$ is the dipole transition moment. Under the assumption of mechanical and electrical harmonicity and the assumption that all of the hot bands of the fundamental contribute to the fundamental band, and the expression for the transition moment[13] $<1|\,\overrightarrow{\mu}\,|0>$, equation 1.4.3 yields[48]

$$C_j = \int \tilde{\nu}\alpha''_m(\tilde{\nu})\mathrm{d}\,\tilde{\nu} = \frac{\mathrm{N_A}\, g_j}{24\pi c^2}\,\mu_j^2 \tag{1.4.4}$$

where μ_j^2 is the square of the dipole moment derivative with respect to the j^{th} normal coordinate, e.g. $\mu_j^2 = |\partial\mu/\partial Q_j|^2$. The same result is obtained using the classical damped harmonic oscillator (CDHO) model[48,58,63,66,67].

Equations 1.4.3 and 1.4.4 relate the experimental integrated intensity to molecular properties through the assumption of the Lorentz local field. If an additional assumption is made, namely that the absorption bands are far apart so that the contribution across band j from all oscillators other than j is real and constant, $n(\tilde{\nu})$ becomes $\underline{n}$, the constant refractive index the sample would have in the region of the band if the band were not present which is often (incorrectly) taken as the average across the band. Then Equations 1.4.1, 1.3.25 and $\hat{n}^2 = \hat{\varepsilon}$ are used to yield[68-70]

$$A_j = 2.303 \int E_{\mathrm{m}}(\tilde{\nu})\mathrm{d}\tilde{\nu} = \frac{\mathrm{N_A}\pi}{3c^2}\, g_j \frac{1}{\underline{n}} \left(\frac{\underline{n}+2}{3}\right)^2 \mu_j^2 \qquad (1.4.5)$$

Values of μ_j^2 can be obtained from the rearrangement of either Equation 1.4.4 or Equation 1.4.5. However, both equations involve integration, i.e. obtaining the area under either the $\tilde{\nu}\alpha''_{\mathrm{m}}$ or E_{m} spectra. The integration is not always easy, as the integration limits are not always clear because of overlapping bands. Equation 1.4.5 presents the further difficulties that values of either $\underline{n}$ or $\sqrt{\underline{\varepsilon}}$ are needed. Thus, Equation 1.4.4 is preferred to 1.4.5[48]. Since, for small oscillations the CDHO model yields the same results as the quantum mechanical treatment[65], it may be possible to fit the experimental α''_{m} spectrum with CDHO-shaped bands and use the total area under each fitted band instead of under the experimental spectrum. The integration limits of the fitted bands are no longer uncertain and C_j values are easily obtained. This approach is used in Chapter 5 to determine the integrated intensities and dipole moment derivatives of liquid chlorobenzene and toluene.

Chapter 2 - Accurate Optical Constants and Molar Absorption Coefficients Between 6500 and 435 cm^{-1} of Toluene at 25°C, from Spectra Recorded in Several Laboratories*

2.1 - Introduction

This paper continues the report of a program to measure quantitative infrared absorption intensities. It presents the agreement between absolute absorption intensities of liquid toluene at 25°C measured by different spectroscopists in this and other laboratories, using instruments made by several different manufacturers. A similar study of the absolute absorption intensities of liquid benzene was recently published[1] and a report of the absolute absorption intensities of liquid chlorobenzene accompanies this paper[2]. In part, this work contributes to the International Union of Pure and Applied Chemistry project[3] to develop secondary standards for intensity measurements in infrared spectroscopy.

In the present study, experimental absorbance spectra of liquid toluene at 25°C have been measured by three different spectroscopists in this laboratory (two for the current work and one about 8 years ago) and also by three spectroscopists in other laboratories. Spectroscopists in different laboratories used instruments from different manufacturers. From these experimental absorbance spectra, the real and imaginary refractive index spectra have been calculated in this laboratory by the methods described previously[1,4].

---

* A version of this chapter has been published. Bertie, Jones, Apelblat and Keefe, Appl. Spectrosc., **48**, 127 (1994)

Attention was focussed on the absorption index (imaginary refractive index) spectra, $k(\tilde{\nu})$ vs. $\tilde{\nu}$. For each spectroscopist the average $k(\tilde{\nu})$ spectrum was evaluated together with its precision. In order to determine the agreement between different spectroscopists, the peak heights and the areas beneath the bands in these average spectra were compared. The agreement was excellent. These average spectra, one from each spectroscopist, were themselves averaged, unweighted, to yield a final absorption index spectrum that is presented here as the best currently available.

This absorption index spectrum, $k(\tilde{\nu})$ vs. $\tilde{\nu}$, was used to calculate[1,4] the molar absorption coefficient spectrum, $E_m(\tilde{\nu})$ vs. $\tilde{\nu}$, and, via Kramers-Kronig transformation, the real refractive index spectrum, $n(\tilde{\nu})$ vs. $\tilde{\nu}$.

The real and imaginary refractive index spectra and the molar absorption coefficient spectrum are presented as graphs and as tables. We also report the average area under individual bands or groups of bands, and the average peak heights, in the $k(\tilde{\nu})$ spectrum obtained by each spectroscopist, as well as the weighted and unweighted averages of these averages. Further, the peak heights and the areas under the bands in the average molar absorption coefficient spectrum are reported. For certain spectral regions, the real and imaginary refractive indices and the molar absorption coefficients, as well as the areas under the molar absorption coefficient bands, will be submitted to Commission I.5 of the International Union of Pure and Applied Chemistry for consideration as secondary absorption intensity standards.

2.2 - Method and experimental

The toluene used in this laboratory was of spectroscopic or reagent grade. Samples were purified by fractional freezing one to three times and were checked by gas chromatography and infrared spectroscopy. No impurities were detected. Samples were kept over molecular sieve to ensure dryness.

The experimental and instrumental details of this work have been described[1,4,5] and are summarised briefly here. All of the spectra from this laboratory were measured with a Bruker IFS 113V spectrometer. Triangular apodization was used in the early work from this laboratory[5]. The recent work in this laboratory used trapezoidal apodization[1]. A Globar source, a 10 mm aperture, and a deuterated triglycine sulfate, DTGS, detector were used for all spectra measured in this laboratory. The optical retardation velocity was 0.665 cm s^{-1}. The spectra were recorded at nominal resolution of 1 cm^{-1} and one level of zero-filling was used in the Fourier transform.

Experimental absorbance spectra of toluene were measured[1,4] in fixed path length cells with KBr windows and path lengths between 11 and 500 μm . To determine the linear absorption coefficients at the anchor points[1,4], spectra were also measured in KBr cells with path lengths of 500 and 1500 μm, and in variable path length NaCl and CaF_2 cells with path lengths up to 5 mm. The path lengths of the cells were determined from the fringe patterns in the experimental absorbance spectra of the empty cells by program

RNJ22A[1]. For the variable path cells, which gave weaker fringe patterns than the cells with fixed path lengths, path lengths greater than 700 μm could not be determined in this way. They were found by calibrating the cell micrometer readings from the fringe patterns for path lengths up to 700 μm, and assuming the calibration held for thicknesses above 700 μm.

In addition to the experimental absorbance spectra recorded in this study, spectra reported previously[5,6] by V. Behnam were also used. Further, three spectroscopists in other laboratories kindly supplied spectra which were recorded under 1 or 2 cm^{-1} nominal resolution with normal conditions and "good analytical laboratory technique". Toluene used in other laboratories was generally of reagent, spectro- or HPLC grade, and spectra from other laboratories were taken to be acceptable if they showed no unexpected peaks. The spectra from other laboratories were recorded on Digilab and Nicolet spectrometers. One spectroscopist used a mercury cadmium telluride detector at 77 K, and the other two used room-temperature DTGS detectors. Happ-Genzel apodization was used in two cases, and triangular apodization in one case. In this way, we obtained from this and three other laboratories spectra recorded by six different spectroscopists on four different models of FT spectrometer by three different manufacturers.

The linear (decadic) absorption coefficient , $K(\tilde{\nu})$, is the absorbance per unit length, and is related to the molar absorption coefficient by $K(\tilde{\nu}) = C\,E_m(\tilde{\nu})$, where C is the molar concentration[1]. Values of $K(\tilde{\nu})$ are needed at anchor points in the baseline in order to correct the baselines[1,4]. They were determined from experimental absorbance spectra in cells with path lengths two to ten times greater than those used for studying the nearby peaks. The experimental absorbance spectra from all sources were then converted to absorption index spectra by program RNJ46A[4], using this anchor point information. With two exceptions, each spectrum was only used in those regions in which the bands had peak absorbances between 0.2 and 2.0. The exceptions were the two spectra of the very intense band at 729 cm^{-1} (see later) which were used with peak absorbances between 2.0 and 2.5.

2.3 - Results

2.3.1 Imaginary refractive index spectra.

The baseline correction procedure[1,4] requires the linear absorption coefficient of the liquid at two or more anchor points in the baseline of the spectral region under study. Table 2.1 summarizes the wavenumbers of the anchor points, the measured linear absorption coefficients, $K(\tilde{\nu})$, and their 95% confidence limits, and the cell path lengths used to determine them. Table 2.1 includes the uncertainties in the absorption index, $k(\tilde{\nu})$, values at the anchor points that result from the precision of the linear absorption coefficients.

Table 2.2 shows the spectral regions that were used in the calculation[4] of the absorption index spectra from the experimental absorbance spectra, together with the cell thicknesses used, the value of the real refractive index at high wavenumber, n_∞, and

Table 2.1 - Linear absorption coefficients at anchor points for liquid toluene at 25°C.

Wavenumber (cm^{-1})	Cell Pathlengths (mm)	$K(\tilde{\nu})$ (cm^{-1})	95 % confidence limit (cm^{-1})	Uncertainty in $k(\tilde{\nu})$[a]
6358.6	2 - 4.5	0[b]		$< 6.0 \times 10^{-7}$
5450.8	1.5 - 4.5	0.251	0.031	1.0×10^{-6}
4806.7	1.5 - 4.5	0.361	0.019	7.2×10^{-7}
4480.3	1.5 - 4.5	1.86	0.01	4.1×10^{-7}
4146.2	1.5 - 4.5	3.39	0.01	4.4×10^{-7}
3970.2	1.5 - 4.5	3.94	0.09	4.2×10^{-6}
3748.0	1.5 - 4.5	1.83	0.01	4.9×10^{-7}
3483.8	1.5 - 4.5	1.13	0.02	1.1×10^{-6}
3355.5	1.5 - 4.5	1.56	0.01	5.5×10^{-7}
3159.3	0.5 - 2.5	7.77	0.03	1.7×10^{-6}
2759.6	0.5 - 3.5	5.46	0.02	1.3×10^{-6}
2562.9	1.5 - 4.5	2.547	0.007	5.0×10^{-7}
2219.2	1.5 - 4.5	1.612	0.006	5.0×10^{-7}
1977.6	~1.5	5.97	0.01	9.3×10^{-7}
1909.7	0.5 - 1.5	4.97	0.03	2.9×10^{-6}
1754.9	~1.5	6.04	0.01	1.0×10^{-6}
1648.4	0.5 - 1.5	7.79	0.03	3.3×10^{-6}
1556.3	0.1 - 0.5	26.7	0.2	2.3×10^{-5}
1398.6	~0.5	33.0	0.3	3.9×10^{-5}
1231.3	0.5 - 1.5	7.49	0.03	4.5×10^{-6}
919.9	0.5 - 1.5	11.11	0.03	6.0×10^{-6}
776.7	~0.5	18.1	0.1	2.4×10^{-5}
708.7	~0.05	70.2	0.7	1.8×10^{-4}
636.9	0.5 - 1.5	5.07	0.03	8.6×10^{-6}
508.2	~1.5	3.99	0.02	7.2×10^{-6}
436.3	~1.5	6.21	0.03	1.3×10^{-5}

a - The uncertainty in $k(\tilde{\nu})$, $\Delta k(\tilde{\nu})$, was calculated from the 95% confidence limit of $K(\tilde{\nu})$, $\Delta K(\tilde{\nu})$, by $\Delta k(\tilde{\nu}) = 2.303\, \Delta K(\tilde{\nu})/(4\pi\tilde{\nu})$.

b - The value of $K(\tilde{\nu})$ was set to 0 for this anchor point because the absorbance is less than 0.01 in a 4.5 mm cell, so K is less than 0.02 cm^{-1}.

Table 2.2 - Path lengths, high-wavenumber refractive index, and number of spectra from each spectroscopist, for the regions processed.

Region (cm^{-1})	Pathlengths used (μm)	n_∞ [a]	CDK	A	B	C	VB	YA	Total
6500 - 4500	~ 500	1.476	3	0	0	0	1	2	6
4500 - 3150	~ 500	1.476	6	2	0	0	4	4	16
3170 - 2750	10 - 35	1.471	8	6	0	2	11	3	30
2775 - 1970	~ 500	1.475	6	2	0	0	4	4	16
2000 - 1640	50 - 210	1.474	2	2	1	2	3	1	11
1655 - 1540	10 - 60	1.456	11	6	0	2	16	4	39
1565 - 1390	8 - 20	1.456	4	2	0	4	10	2	22
1420 - 770	35 - 100	1.470	8	10	0	4	6	2	30
780 - 700	~ 8	1.419	0	0	0	2	0	0	2
715 - 630	8 - 14	1.520	4	0	0	2	7	2	15
670 - 475	~ 500	1.513	3	2	0	0	2	2	9
510 - 435	8 - 20	1.483	8	2	0	4	9	3	26

a - n_∞ is the real refractive index at the highest wavenumber in the region.

the number of spectra from each spectroscopist, for each region. The value of n_∞ for each region is required by the Kramers-Kronig transform in program RNJ46A, which yields the real refractive index spectrum for the region. The spectra recorded in this laboratory are labeled with the initials CDK, VB and YA, identifying C.D. Keefe, V. Behnam and Y. Apelblat, respectively. The other collaborators are identified simply by a single letter, A to C. The real refractive index at the highest wavenumber in each region, n_∞, was read either from the graphs in reference 7 or, in most cases, from tables of $n(\tilde{\nu})$ in this laboratory which were calculated from the $k(\tilde{\nu})$ spectra in reference 5.

The peak heights and the areas under the bands were measured for each

Table 2.3 - Spectroscopist average areas under the absorption index, $k(\tilde{\nu})$, bands.[a]

Region (cm^{-1})	CDK	A	B	C	VB	YA
6307.1 - 5445.0	0.0393 (43)				0.0391	0.0362(414)
4763.8 - 4518.9	0.0332 (10)				0.0332 (15)	0.0333 (23)
4478.4 - 4145.2	0.0786 (6)	0.0781 (1)			0.0786 (5)	0.0785 (11)
4145.2 - 3988.1	0.0685 (10)	0.0679 (4)			0.0683 (5)	0.0684 (15)
3988.1 - 3748.9	0.0441 (2)	0.0442 (1)			0.0442 (1)	0.0441 (3)
3748.9 - 3694.9	0.00632 (5)	0.00632 (6)			0.00632 (3)	0.00633 (8)
3694.9 - 3608.2	0.0138 (2)	0.0138 (1)			0.0138 (1)	0.0139 (2)
3608.2 - 3569.1	0.00378 (11)	0.0385 (0)			0.00385 (13)	0.00382 (14)
3569.1 - 3531.5	0.00330 (2)	0.00336 (0)			0.00334 (3)	0.00330 (2)
3531.5 - 3503.1	0.00204 (1)	0.00203 (0)			0.00207 (2)	0.00205 (2)
3484.3 - 3418.7	0.00572 (2)	0.00569 (6)			0.00570 (2)	0.00572 (4)
3418.7 - 3357.0	0.00592 (1)	0.00590 (0)			0.00591 (2)	0.00592 (3)
3150.1 - 2770.2	2.74 (2)	2.77 (2)		2.83 (31)	2.77 (1)	2.73 (1)
2759.6 - 2679.1	0.0412 (3)	0.0415 (4)			0.0412 (1)	0.0411 (6)
2679.1 - 2563.4	0.0351 (1)	0.0350 (0)			0.0352 (1)	0.0351 (1)
2563.4 - 2131.0	0.1258 (3)	0.1240 (3)			0.1257 (2)	0.1257 (6)
2131.4 - 2095.8	0.00429 (1)	0.00400 (6)			0.00418 (3)	0.00428 (3)
2095.8 - 2049.5	0.00570 (1)	0.00525 (13)			0.00551 (3)	0.00568 (5)
1977.6 - 1910.1	0.1271 (6)	0.1262 (10)	0.1268	0.1273 (15)	0.1269 (5)	0.1270
1910.1 - 1836.9	0.1321 (7)	0.1307 (9)	0.1318	0.1316 (15)	0.1322 (9)	0.1320
1836.9 - 1754.9	0.1336 (0)	0.1321 (2)	0.1334	0.1337 (8)	0.1332 (6)	0.1336
1754.9 - 1712.5	0.0526 (1)	0.0526 (5)	0.0521	0.0522 (7)	0.0525 (4)	0.0527
1713.0 - 1686.4	0.0177 (1)	0.0172 (1)	0.0178	0.0178 (4)	0.0177 (5)	0.0177
1686.4 - 1668.1	0.0137 (1)	0.0134 (1)	0.0138	0.0137 (3)	0.0138 (1)	0.0138
1650.3 - 1555.3	0.533 (2)	0.533 (7)		0.531 (11)	0.535 (4)	0.535 (4)
1531.7 - 1516.3	0.0982 (9)	0.1004 (6)		0.1033 (52)	0.1010 (3)	0.0979 (13)
1513.3 - 1400.1	2.02 (1)	2.03 (1)		2.03 (5)	2.04 (1)	2.02 (2)
1400.5 - 1338.4	0.293 (3)	0.294 (1)		0.292 (1)	0.290 (2)	0.291 (4)
1265.6 - 821.0	2.08 (6)	2.08 (9)		2.11 (12)	2.07 (38)	2.09 (37)
790.7 - 775.7	0.0826 (4)	0.0815 (4)		0.0820 (3)	0.0826 (4)	0.0828 (22)
769.9 - 710.2				7.33 (58)		
710.2 - 660.0	2.70 (2)			2.99 (17)	2.72 (8)	2.72 (3)
640.2 - 606.5	0.0580 (4)	0.0569 (20)			0.0578 (5)	0.0578 (18)
552.0 - 498.5	0.0947 (16)	0.0942 (26)			0.0941 (11)	0.0949 (120)
490.3 - 440.2	1.65 (3)	1.84 (10)		1.88 (18)	1.73 (5)	1.65 (9)

a - The unit of area is cm^{-1}. The numbers in parentheses are the 95% confidence limits in the last digit. In some cases only one spectrum was available, so no 95% confidence limit could be calculated, and in others no spectrum was available from that spectroscopist for that region.

Table 2.4 - Spectroscopist average absorption index peak heights, k_{max}. [a]

$\tilde{\nu}$ (cm^{-1})	CDK	A	B	C	VB	YA
5949.9	0.000179 (9)				0.000181	0.000178 (1)
4667.0	0.000258 (7)				0.000262	0.000255 (15)
4637.1	0.000226 (6)				0.000230 (10)	0.000224 (14)
4612.1	0.000342 (9)				0.000347 (13)	0.000339 (19)
4573.6	0.000206 (4)				0.000208 (7)	0.000204 (9)
4388.7	0.000304 (3)	0.000301 (1)			0.000304 (3)	0.000305 (6)
4311.0	0.000348 (5)	0.000345 (2)			0.000349 (3)	0.000347 (8)
4244.3	0.000341 (2)	0.000340 (4)			0.000340 (1)	0.000340 (7)
4186.3	0.000175 (1)	0.000173 (1)			0.000174 (1)	0.000175 (1)
4161.3	0.000162 (0)	0.000161 (2)			0.000163 (1)	0.000162 (1)
4132.3	0.000174 (0)	0.000175 (1)			0.000174 (1)	0.000174 (1)
4056.6	0.000829 (21)	0.000805 (13)			0.000814 (9)	0.000830 (28)
4036.3	0.000978 (27)	0.000974 (11)			0.000977 (20)	0.000975 (42)
3980.3	0.000216 (1)	0.000215 (1)			0.000218 (1)	0.000217 (1)
3951.2	0.000212 (1)	0.000210 (1)			0.000213 (1)	0.000212 (2)
3923.8	0.000215 (1)	0.000216 (0)			0.000217 (1)	0.000215 (0)
3909.9	0.000215 (0)	0.000214 (2)			0.000215 (2)	0.000215 (0)
3869.7	0.000224 (3)	0.000223 (4)			0.000224 (2)	0.000224 (4)
3847.2	0.000251 (3)	0.000253 (3)			0.000255 (2)	0.000251 (5)
3812.2	0.000176 (1)	0.000174 (5)			0.000176 (1)	0.000175 (3)
3786.3	0.000179 (1)	0.000177 (5)			0.000179 (1)	0.000179 (2)
3763.9	0.000108 (0)	0.000107 (78)			0.000109 (1)	0.000108 (1)
3724.1	0.000140 (0)	0.000139 (0)			0.000141 (1)	0.000141 (0)
3707.0	0.000139 (2)	0.000138 (2)			0.000138 (1)	0.000139 (3)
3675.0	0.000148 (6)	0.000144 (3)			0.000144 (5)	0.000150 (8)
3649.0	0.000269 (2)	0.000270 (4)			0.000270 (2)	0.000269 (3)
3624.0	0.000161 (1)	0.000162 (1)			0.000163 (1)	0.000161 (1)
3584.6	0.000126 (4)	0.000126 (1)			0.000126 (20)	0.000127 (5)
3549.8	0.000108 (1)	0.000108 (1)			0.000109 (1)	0.000108 (1)
3519.3	0.0000840 (1)	0.0000845 (30)			0.0000851 (10)	0.0000842 (10)
3439.7	0.000127 (1)	0.000127 (1)			0.000126 (0)	0.000127 (2)
3385.3	0.000109 (1)	0.000109 (1)			0.000109 (0)	0.000109 (1)
3167.5	0.000481 (2)	0.000481 (8)			0.000487 (1)	0.000480 (2)
3104.1	0.00364 (2)	0.00365 (4)		0.00371 (4)	0.00369 (6)	0.00364 (4)
3086.4	0.0115 (1)	0.0117 (3)		0.0117 (1)	0.0118 (1)	0.0115 (1)
3062.0	0.0133 (1)	0.0137 (2)		0.0139 (2)	0.0137 (1)	0.0132 (0)
3026.9	0.0305 (6)	0.0309 (8)		0.0312 (3)	0.0308 (5)	0.0301 (0)
2979.1	0.00821 (4)	0.00826 (5)		0.00843 (13)	0.00830 (2)	0.00820 (3)
2947.5	0.0101 (1)	0.0101 (1)		0.0103 (2)	0.0102 (0)	0.0101 (0)

Table 2.4 - Continued

$\tilde{\nu}$ (cm^{-1})	CDK	A	B	C	VB	YA
2919.8	0.0162 (1)	0.0165 (2)		0.0166 (2)	0.0164 (1)	0.0161 (1)
2872.2	0.00788 (4)	0.00802 (4)		0.00813 (10)	0.00797 (2)	0.00790 (6)
2734.1	0.00173 (5)	0.00175 (8)			0.00172 (1)	0.00171 (8)
2671.7	0.000230 (1)	0.000227 (2)			0.000230 (0)	0.000229 (1)
2631.9	0.000328 (1)	0.000325 (2)			0.000329 (0)	0.000328 (1)
2604.7	0.000422 (2)	0.000409 (1)			0.000415 (1)	0.000421 (3)
2585.9	0.000772 (5)	0.000762 (9)			0.000770 (1)	0.000770 (10)
2540.4	0.000280 (1)	0.000271 (1)			0.000276 (1)	0.000280 (2)
2509.2	0.000257 (0)	0.000252 (2)			0.000256 (1)	0.000256 (1)
2496.7	0.000254 (0)	0.000249 (1)			0.000254 (1)	0.000254 (1)
2465.4	0.000257 (0)	0.000254 (0)			0.000259 (1)	0.000257 (1)
2412.4	0.000530 (2)	0.000519 (6)			0.000529 (1)	0.000529 (4)
2389.0	0.000442 (1)	0.000433 (7)			0.000440 (2)	0.000441 (2)
2360.6	0.000708 (4)	0.000691 (12)			0.000708 (1)	0.000707 (8)
2335.3	0.000805 (5)	0.000779 (16)			0.000789 (5)	0.000803 (10)
2312.6	0.000623 (2)	0.000619 (8)			0.000620 (3)	0.000623 (4)
2280.7	0.000387 (2)	0.000380 (1)			0.000380 (0)	0.000386 (4)
2260.5	0.000440 (2)	0.000426 (2)			0.000439 (1)	0.000439 (3)
2237.3	0.000199 (0)	0.000194 (2)			0.000198 (2)	0.000199 (1)
2207.5	0.000278 (2)	0.000264 (4)			0.000273 (1)	0.000277 (3)
2185.3	0.000281 (2)	0.000272 (1)			0.000277 (1)	0.000281 (3)
2163.7	0.000498 (2)	0.000483 (4)			0.000493 (2)	0.000497 (4)
2116.6	0.000152 (0)	0.000142 (1)			0.000148 (0)	0.000151 (1)
2068.5	0.000170 (0)	0.000157 (1)			0.000164 (1)	0.000169 (1)
2032.0	0.000173 (0)	0.000162 (3)			0.000169 (1)	0.000173 (1)
2008.5	0.000363 (1)	0.000351 (0)			0.000358 (1)	0.000363 (1)
1991.1	0.000704 (1)	0.000692 (4)			0.000708 (1)	0.000702 (3)
1942.1	0.00437 (2)	0.00430 (4)	0.00435	0.00435 (6)	0.00436 (2)	0.00436
1872.0	0.00268 (1)	0.00266 (1)	0.00268	0.00268 (3)	0.00269 (3)	0.00267
1857.6	0.00434 (1)	0.00423 (3)	0.00430	0.00429 (5)	0.00433 (1)	0.00434
1802.6	0.00390 (0)	0.00381 (0)	0.00387	0.00386 (3)	0.00388 (3)	0.00389
1778.5	0.00123 (1)	0.00122 (1)	0.00124	0.00123 (1)	0.00123 (1)	0.00123
1735.6	0.00222 (1)	0.00221 (1)	0.00220	0.00221 (4)	0.00222 (1)	0.00222
1696.8	0.000832 (11)	0.000805 (3)	0.000820	0.000832 (106)	0.000823 (24)	0.000833
1676.7	0.000944 (15)	0.000917 (4)	0.000936	0.000925 (3)	0.000939 (4)	0.000946
1623.1	0.00434 (4)	0.00425 (2)		0.00428 (8)	0.00429 (5)	0.00434 (7)
1604.5	0.0317 (5)	0.0301 (41)		0.0302 (10)	0.0318 (3)	0.0321 (9)
1586.7	0.00496 (1)	0.00494 (10)		0.00496 (3)	0.00491 (4)	0.00496 (2)
1572.1	0.00521 (2)	0.00521 (1)		0.00518 (3)	0.00519 (5)	0.00521 (2)

Table 2.4 - Continued

$\tilde{\nu}$ (cm^{-1})	CDK	A	B	C	VB	YA
1550.3	0.00341 (4)	0.00345 (3)		0.00347 (82)	0.00359 (4)	0.00339 (20)
1523.6	0.00865 (5)	0.00864 (8)		0.00898 (58)	0.00879 (3)	0.00864 (13)
1495.6	0.118 (1)	0.112 (4)		0.112 (15)	0.114 (2)	0.119 (1)
1460.2	0.0276 (2)	0.0277 (1)		0.0297 (27)	0.0278 (1)	0.0275 (0)
1378.9	0.0134 (0)	0.0127 (1)		0.0127 (0)	0.0128 (3)	0.0132 (1)
1332.0	0.00206 (2)	0.00203 (2)		0.00205 (0)	0.00209 (4)	0.00208 (17)
1312.7	0.00219 (2)	0.00217 (1)		0.00219 (0)	0.00223 (3)	0.00221 (4)
1277.6	0.00116 (4)	0.00112 (1)		0.00114 (1)	0.00118 (3)	0.00121 (60)
1248.7	0.00181 (2)	0.00181 (0)		0.00182 (1)	0.00182 (2)	0.00185 (16)
1210.1	0.00452 (3)	0.00427 (3)		0.00434 (2)	0.00435 (12)	0.00451 (11)
1178.6	0.01002 (6)	0.00930 (8)		0.00949 (2)	0.00959 (29)	0.01006 (25)
1155.9	0.00410 (4)	0.00407 (3)		0.00417 (2)	0.00405 (10)	0.00413 (4)
1106.5	0.00672 (2)	0.00673 (4)		0.00681 (2)	0.00665 (15)	0.00674 (6)
1081.4	0.0306 (2)	0.0295 (3)		0.0298 (1)	0.0302 (8)	0.0308 (11)
1041.4	0.0151 (1)	0.0150 (1)		0.0153 (0)	0.0149 (5)	0.0151 (3)
1002.3	0.00446 (3)	0.00459 (7)		0.00460 (2)	0.00437 (9)	0.00448 (13)
980.7	0.00420 (3)	0.00439 (6)		0.00438 (3)	0.00417 (6)	0.00423 (18)
966.4	0.00393 (2)	0.00414 (6)		0.00408 (5)	0.00391 (5)	0.00395 (31)
929.6	0.00292 (1)	0.00303 (3)		0.00297 (2)	0.00292 (3)	0.00291 (8)
895.4	0.00939 (3)	0.00880 (8)		0.00916 (2)	0.00918 (23)	0.00943 (1)
872.9	0.00235 (2)	0.00196 (14)		0.00233 (4)	0.00240 (4)	0.00235 (7)
842.7	0.00378 (3)	0.00336 (11)		0.00367 (4)	0.00380 (4)	0.00377 (22)
785.6	0.00867 (5)	0.00809 (10)		0.00811 (2)	0.00838 (12)	0.00873 (17)
728.9				0.719 (60)		
694.5	0.354 (10)			0.384 (15)	0.360 (12)	0.361 (13)
622.0	0.00336 (5)	0.00314 (13)			0.00328 (4)	0.00334 (30)
537.8	0.00132 (2)	0.00130 (7)			0.00130 (3)	0.00132 (13)
521.0	0.00748 (34)	0.00695 (34)			0.00681 (3)	0.00748 (221)
464.2	0.288 (32)	0.356 (370)		0.289 (41)	0.284 (17)	0.288 (112)

a - The numbers in parentheses are the 95% confidence limits in the last digit. In some cases only one spectrum was available, so no 95% confidence limit could be calculated, and in others no spectrum was available from that group for that region.

absorption index, $k(\tilde{\nu})$, spectrum. For each spectroscopist the average $k(\tilde{\nu})$ spectrum was calculated along with the average area and peak height for each band. The average areas and peak heights obtained by the different spectroscopists are tabulated in Tables 2.3 and 2.4, respectively. Table 2.4 includes the $k(\tilde{\nu})$ peak wavenumbers which were determined, with the peak heights, by fitting the top three points of the band to a parabola and determining the maximum of the parabola.

The areas and peak heights from the different spectroscopists in Tables 2.3 and 2.4 are in excellent agreement. The agreement is not always within the precision of the data of each spectroscopist, which suggests that systematic errors or inadequate statistics may still affect the results by about 2% in some regions. The quality of the agreement is shown pictorially in Figure 2.1 for the regions 3150 to 2770 cm^{-1}, 1837 to 1755 cm^{-1}, and 1650 to 1555 cm^{-1}. In Fig. 2.1, the filled symbols show the average area for each spectroscopist, and the error bars show the 95% confidence limits.

For each region, the average spectra from the different spectroscopists were themselves averaged to yield a weighted average $k(\tilde{\nu})$ spectrum, with the weighting factor for each spectroscopist being the number of spectra which contributed to the average (Table 2.2). To check the influence of the fact that the three spectroscopists in this laboratory, CDK, VB and YA, used the same instrument and ran more spectra than the other collaborators, an unweighted average $k(\tilde{\nu})$ spectrum was also calculated. For each region, the overall average area and the overall average peak heights were measured from both the weighted and the unweighted average $k(\tilde{\nu})$ spectra.

The overall average areas are presented in Table 2.5. Because the integration ranges have different widths for different bands, Table 2.5 includes the height of the strongest peak in the region to indicate the prominence of the absorption. For each

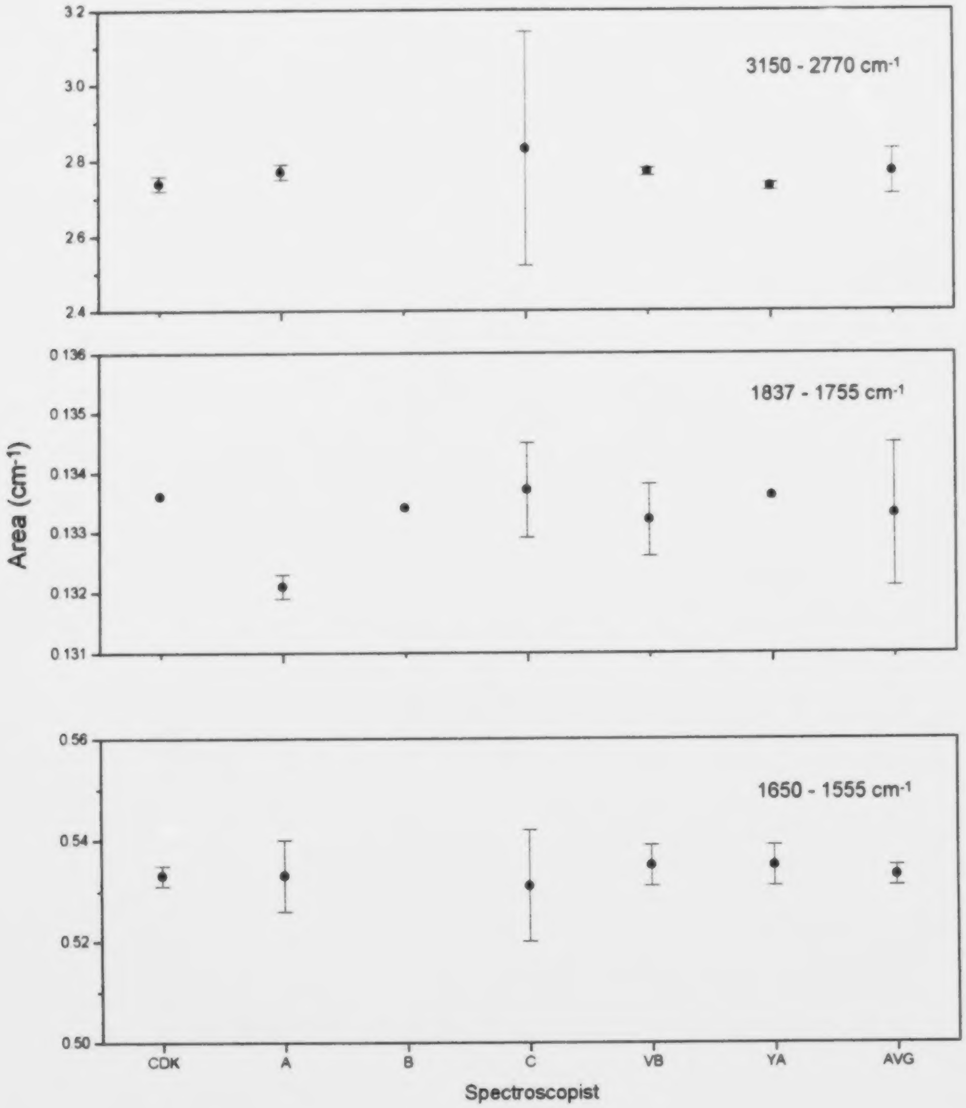

Figure 2.1 - Average areas and 95% confidence limits (vertical error bars) under the absorption index spectra in the regions 3150 to 2770 cm^{-1} (upper), 1837 to 1735 cm^{-1} (middle), and 1650 to 1555 cm^{-1} (bottom) for the six spectroscopists. The values are taken from Table 2.3. Also shown for each region above the label "AVG" is the unweighted average area from Table 2.5 with the maximum deviation from it indicated by a vertical error bar.

Table 2.5 - Overall average area under the absorption index bands.

Region (cm^{-1})	k_{max}[a]	Weighted Average Area[b]	Unweighted Average Area[b]	Maximum Deviation[b,c]	Anchor point Uncertainty[b,d]	% Estimated accuracy[e]
6307.1 - 5445.0	0.000179	0.0382	0.0382	± 0.0020	± 0.0007	7.1
4763.8 - 4518.9	0.000344	0.0332	0.0332	± 0.0001	± 0.0001	0.6
4478.4 - 4145.2	0.000347	0.0785	0.0784	± 0.0003	± 0.0001	0.5
4145.2 - 3988.1	0.000976	0.0683	0.0683	± 0.0004	± 0.0004	1.2
3988.1 - 3748.9	0.000251	0.0441	0.0441	± 0.0001	± 0.0006	1.6
3748.9 - 3694.9	0.000140	0.0632	0.00632	± 0.00001	± 0.00004	0.8
3694.9 - 3608.2	0.000269	0.0138	0.0138	± 0.0001	± 0.00007	1.2
3608.2 - 3569.1	0.000127	0.00382	0.00383	± 0.00005	± 0.00003	2.1
3569.1 - 3531.5	0.000108	0.00332	0.00333	± 0.00003	± 0.00003	1.8
3531.5 - 3503.1	0.000084	0.00205	0.00205	± 0.00002	± 0.00002	2.0
3484.3 - 3418.7	0.000126	0.00571	0.00571	± 0.00002	± 0.00005	1.2
3418.7 - 3357.0	0.000109	0.00592	0.00591	± 0.00001	± 0.00005	1.0
3150.1 - 2770.2	0.0308	2.76	2.77	± 0.06	± 0.0006	2.2
2759.6 - 2679.1	0.00172	0.0413	0.0413	± 0.0002	± 0.0001	0.7
2679.1 - 2563.4	0.000768	0.0351	0.0351	± 0.0001	± 0.0001	0.6
2563.4 - 2131.0	0.000793	0.1255	0.1253	± 0.0013	± 0.0002	1.2
2131.0 - 2095.8	0.000148	0.00423	0.00419	± 0.00019	± 0.00003	5.3
2095.8 - 2049.5	0.000165	0.00559	0.00554	± 0.00029	± 0.00003	5.8
1977.6 - 1910.1	0.00434	0.1269	0.1269	± 0.0007	± 0.0001	0.6
1910.1 - 1836.9	0.00429	0.1317	0.1317	± 0.0010	± 0.0001	0.8
1836.9 - 1754.9	0.00386	0.1332	0.1333	± 0.0012	± 0.0001	1.0
1754.9 - 1712.5	0.00221	0.0525	0.0524	± 0.0003	± 0.0001	0.8
1713.0 - 1686.4	0.000820	0.0176	0.0176	± 0.0004	± 0.00006	2.6
1686.4 - 1668.1	0.000931	0.0137	0.0137	± 0.0003	± 0.00004	2.5
1650.3 - 1555.3	0.0309	0.534	0.533	± 0.002	± 0.001	0.6
1531.2 - 1516.3	0.00867	0.01006	0.1002	± 0.0031	± 0.0005	3.6
1513.3 - 1400.1	0.112	2.03	2.03	± 0.01	± 0.004	0.7
1400.5 - 1338.4	0.0129	0.292	0.292	± 0.002	± 0.0001	0.7
1265.6 - 821.0	0.0302	2.08	2.09	± 0.02	± 0.005	1.2

Table 2.5 - Continued

Region (cm^{-1})	k_{max} [a]	Weighted Average Area[b]	Unweighted Average Area[b]	Maximum Deviation[b,c]	Anchor point Uncertainty[b,d]	% Estimated accuracy[e]
790.7 - 775.2	0.00837	0.0822	0.0823	± 0.0008	± 0.0002	1.2
769.9 - 710.2	0.719	7.33	7.33	± 0.58	± 0.006	8.0
710.2 - 660.0	0.365	2.75	2.78	± 0.21	± 0.005	7.7
640.2 - 606.5	0.00328	0.0577	0.0576	± 0.0007	± 0.0032	6.8
552.0 - 498.5	0.00716	0.0945	0.0945	± 0.0004	± 0.0005	1.0
490.3 - 440.2	0.295	1.73	1.75	± 0.13	± 0.0005	7.3

a - Height of the strongest peak in the region.

b - The unit of area is cm^{-1}.

c - The maximum deviation of the average of any one spectroscopist from the unweighted average, except for the region 769.9 - 710.2 cm^{-1}. In this case the maximum deviation is the 95% confidence limit of the area under the average spectrum for group C, the only spectroscopist who had spectra in this region.

d - The anchor point uncertainty is the integration range multiplied by the average of the uncertainties in $k(\tilde{\nu})$ (Table 2.1) at the two anchor points used for that range.

e - The % estimated accuracy is the sum of the maximum deviation and the anchor point uncertainty as a percentage of the unweighted average area.

band group, Table 2.5 also gives the maximum deviation of the average of any one spectroscopist from the unweighted average, which shows the agreement between the different spectroscopists. Table 2.5 includes the estimated accuracy of the overall unweighted average area of each band, which is discussed later. Again, a good sense of the quality of these results can be obtained from Fig. 2.1. Each box of Fig. 2.1 includes, above the label 'AVG', the unweighted average area and the maximum deviation.

The average agreement over the 35 band regions in Table 2.5 is ±1.8%. For the

11 regions between 3150 and 775 cm^{-1} with $k_{\max}$ between 0.002 and 0.112 the agreement between the areas is always better than ±3.1%, and averages ±1.1%. Such agreement between spectra measured in different laboratories on instruments by different manufacturers is very encouraging.

The agreement between the areas (Table 2.5) is only 5 to 8% for the very weak absorption between 6307 and 5445 cm^{-1} and for the very strong absorption below 770 cm^{-1}. The absorption between 770 and 710 cm^{-1} is so strong that cells with path lengths of 8 μm or less are needed to measure it accurately. There was only one spectroscopist who had such a cell and there were only two experimental absorbance spectra of suitable intensity to be measured accurately in this region. Additional measurements are needed to improve the intensities below 770 cm^{-1}.

The weighted and unweighted average areas in Table 2.5 agree to within 0.3% on average and they never disagree by more than 2.3%. This shows that the larger number of spectra from this laboratory did not unduly influence the average areas.

For each peak in the $k(\tilde{\nu})$ spectrum, the overall weighted and unweighted average peak heights are given in Table 2.6 along with the maximum deviation from the unweighted average of the averages of the different spectroscopists. Also given for each peak are the % estimated accuracy, which is discussed later, the previous value published from this laboratory[5] and the calibrated result of Jones and co-workers[7]. The weighted and unweighted averages agree to within 0.4% on average. Few of them disagree by more than 1% and the largest disagreement is 2.2% at 872.9 cm^{-1}. Thus, the

Table 2.6 - Overall average peak heights in the absorption index spectra.

$\tilde{\nu}$ (cm^{-1})	Unweighted Average[a]	% Estimated Accuracy[b]	Weighted Average	Ref 5[c]	Ref 7[d]
5949.9	0.000179 (2)	1.6	0.000179		
4667.0	0.000259 (4)	1.8	0.000258		
4637.1	0.000228 (4)	2.0	0.000226		
4612.1	0.000344 (5)	1.6	0.000342		
4573.6	0.000206 (2)	1.2	0.000206		
4388.7	0.000303 (2)	0.8	0.000304		
4311.0	0.000347 (2)	0.7	0.000348		
4244.3	0.000340 (1)	0.4	0.000340		
4186.3	0.000175 (2)	1.4	0.000175	0.000174 (5)	0.000171 (12)
4161.3	0.000162 (1)	0.9	0.000162	0.000162 (5)	0.000156 (11)
4132.3	0.000174 (1)	1.7	0.000174	0.000174 (5)	0.000174 (12)
4056.6	0.000812 (18)	2.5	0.000823	0.000815 (8)	0.000817 (31)
4036.3	0.000976 (2)	0.4	0.000977	0.000975 (5)	0.000980 (37)
3980.3	0.000217 (2)	1.8	0.000217	0.000221 (5)	0.000216 (15)
3951.2	0.000212 (2)	1.9	0.000212	0.000216 (4)	0.000214 (15)
3923.8	0.000216 (1)	1.4	0.000216	0.000219 (4)	0.000222 (16)
3909.9	0.000215 (2)	1.9	0.000215		
3869.7	0.000224 (1)	1.3	0.000224	0.000226 (5)	0.000227 (16)
3847.2	0.000251 (4)	2.4	0.000252	0.000255 (5)	0.000257 (18)
3812.2	0.000175 (1)	1.7	0.000176		
3786.3	0.000178 (1)	1.7	0.000179	0.000177 (4)	0.000178 (13)
3763.9	0.000109 (2)	3.7	0.000108		0.000111 (8)
3724.1	0.000140 (1)	1.3	0.000140	0.000138 (4)	0.000142 (10)
3707.0	0.000139 (1)	1.3	0.000139	0.000136 (4)	0.000144 (10)
3675.0	0.000146 (4)	3.2	0.000147		0.000160 (12)
3649.0	0.000269 (1)	0.7	0.000269	0.000268 (4)	0.000269 (19)
3624.0	0.000162 (1)	1.1	0.000162	0.000161(4)	0.000165 (12)
3584.6	0.000127 (1)	1.4	0.000126	0.000120 (9)	0.000127 (9)
3549.8	0.000108 (1)	1.7	0.000108	0.000108 (4)	0.000122 (9)
3519.3	0.0000843 (8)	1.9	0.0000844	0.000084 (4)	0.000093 (8)
3439.7	0.000126 (1)	1.4	0.000127		0.000128 (10)
3385.3	0.000109 (0)	0.7	0.000109		0.000122 (9)
3167.5	0.000484 (3)	0.8	0.000483		0.000509 (22)
3104.1	0.00366 (5)	1.4	0.00367		0.00357 (9)
3086.4	0.0116 (2)	1.7	0.0117	0.0119 (1)	0.0112 (4)
3062.0	0.0136 (4)	2.9	0.0136	0.0137 (1)	0.0134 (4)
3026.9	0.0308 (7)	2.3	0.0307	0.0313 (7)	0.0324 (6)
2979.1	0.00830 (13)	1.6	0.00827		0.00799 (22)

Table 2.6 - Continued

$\tilde{\nu}$ (cm^{-1})	Unweighted Average[a]	% Estimated Accuracy[b]	Weighted Average	Ref 5[c]	Ref 7[d]
2947.5	0.0102 (1)	1.0	0.0102	0.0103 (1)	0.00962 (30)
2919.8	0.0164 (3)	1.9	0.0164	0.0164 (1)	0.0161 (5)
2872.2	0.00800 (13)	1.7	0.00796	0.00803 (11)	0.00770 (21)
2734.1	0.00172 (3)	1.7	0.00172	0.00171 (1)	0.00171 (6)
2671.7	0.000229 (2)	1.3	0.000229	0.000226 (3)	0.000229 (16)
2631.9	0.000327 (2)	0.9	0.000328	0.000325 (3)	0.000319 (23)
2604.7	0.000417 (8)	2.1	0.000418	0.000410(3)	0.000406 (30)
2585.9	0.000768 (6)	0.9	0.000770	0.000766 (2)	0.000787 (59)
2540.4	0.000277 (6)	2.3	0.000278	0.000272 (4)	0.000277 (20)
2509.2	0.000255 (3)	1.4	0.000256	0.000252 (3)	0.000251 (18)
2496.7	0.000253 (4)	1.8	0.000253		0.000255 (18)
2465.4	0.000257 (3)	1.4	0.000257		0.000260 (18)
2412.4	0.000526 (5)	1.0	0.000528	0.000525 (3)	0.000512 (39)
2389.0	0.000439 (6)	1.5	0.000440	0.000436 (3)	0.000438 (32)
2360.6	0.000703 (12)	1.8	0.000706	0.000705 (3)	0.000769 (56)
2335.3	0.000793 (14)	1.8	0.000797	0.000784 (4)	0.000818 (60)
2312.6	0.000621 (2)	0.4	0.000622	0.000616 (2)	0.000614 (49)
2280.7	0.000382 (5)	1.4	0.000384		0.000374 (26)
2260.5	0.000436 (10)	2.4	0.000438	0.000436 (3)	0.000428 (31)
2237.3	0.000198 (4)	2.3	0.000198		0.000203 (15)
2207.5	0.000273 (9)	3.5	0.000275	0.000270 (3)	0.000274 (20)
2185.3	0.000277 (5)	2.0	0.000279	0.000274 (3)	0.000280 (20)
2163.7	0.000492 (9)	2.0	0.000495	0.000491 (3)	0.000434 (35)
2116.6	0.000148 (6)	4.5	0.000150		0.000158 (13)
2068.5	0.000165 (7)	4.7	0.000167	0.000163 (4)	0.000172 (14)
2032.0	0.000169 (7)	4.6	0.000171		0.000187 (15)
2008.5	0.000358 (7)	2.2	0.000360		
1991.1	0.000701 (9)	1.4	0.000703	0.000710 (3)	0.000678 (25)
1942.1	0.00434 (4)	1.0	0.00435	0.00441 (5)	0.00462 (11)
1872.0	0.00267 (1)	0.4	0.00268	0.00268 (1)	0.00270 (10)
1857.6	0.00429 (6)	1.4	0.00430	0.00458 (15)	0.00460 (11)
1802.6	0.00386 (5)	1.3	0.00387	0.00390 (4)	0.00390 (15)
1778.5	0.00123 (1)	0.9	0.00123		0.00123 (5)
1735.6	0.00221 (1)	0.6	0.00221	0.00220 (2)	0.00222 (8)
1696.8	0.000820 (15)	2.1	0.000824	0.000832 (4)	0.000809 (30)
1676.7	0.000931 (15)	1.8	0.000934	0.000947 (4)	0.000934 (34)
1623.1	0.00429 (5)	1.5	0.00430		0.00426 (10)
1604.5	0.0309 (12)	3.9	0.0315	0.0320 (1)	0.0304 (10)

Table 2.6 - Continued

$\tilde{\nu}$ (cm^{-1})	Unweighted Average[a]	% Estimated Accuracy[b]	Weighted Average	Ref 5[c]	Ref 7[d]
1586.7	0.00494 (5)	1.3	0.00494		
1572.1	0.00519 (2)	0.6	0.00520		0.00560 (14)
1550.3	0.00347 (12)	4.4	0.00350		0.00353 (13)
1523.6	0.00867 (31)	3.9	0.00877		0.00928 (22)
1495.6	0.115 (4)	3.4	0.115	0.115 (3)	0.116 (2)
1460.2	0.0278 (19)	6.9	0.0281	0.0280 (2)	0.0265 (9)
1378.9	0.0129 (5)	4.0	0.0129	0.0133 (2)	0.0137 (3)
1332.0	0.00206 (3)	2.4	0.00206		0.00217 (8)
1312.7	0.00220 (3)	2.3	0.00219		0.00230 (9)
1277.6	0.00116 (5)	6.0	0.00115		0.00118 (4)
1248.7	0.00182 (3)	2.7	0.00182		0.00181 (7)
1210.1	0.00439 (13)	3.1	0.00448		0.00446 (16)
1178.6	0.00967 (39)	4.1	0.00963	0.0100 (3)	0.0103 (3)
1155.9	0.00410 (7)	1.8	0.00409		0.00410 (15)
1106.5	0.00673 (8)	1.3	0.00672		0.00732 (18)
1081.4	0.0302 (7)	2.3	0.0301	0.0311 (2)	0.0305 (10)
1041.4	0.0151 (2)	1.3	0.0151		0.0158 (4)
1002.3	0.00450 (13)	3.0	0.00451		0.00442 (16)
980.7	0.00427 (12)	2.9	0.00428		0.00423 (16)
966.4	0.00400 (14)	3.6	0.00402		
929.6	0.00295 (8)	2.9	0.00296		0.00301 (11)
895.4	0.00919 (39)	4.4	0.00912	0.00968 (33)	0.0100 (5)
872.9	0.00228 (32)	14.7	0.00223		0.00235 (9)
842.7	0.00368 (32)	9.1	0.00363		0.00385 (14)
785.6	0.00837 (36)	4.5	0.00845		0.00839 (31)
728.9	0.719 (60)	8.3	0.719		0.658 (16)
694.5	0.365 (19)	5.2	0.362	0.342 (4)	0.380 (6)
622.0	0.00328 (10)	3.3	0.00329	0.00329 (1)	0.00320 (12)
537.8	0.00131 (1)	1.4	0.00131	0.00130 (0)	0.00126 (1)
521.0	0.00716 (35)	5.0	0.00721	0.00683 (5)	0.00667 (45)
464.2	0.295 (39)	13.2	0.292		0.120 (13)

a - In this column the number in parentheses is the maximum deviation from the unweighted average, except for the peak at 728.9 cm^{-1}. In this case the number is the 95% confidence limit in the average spectrum for C, the only spectroscopist who had spectra in this region.

b - The % estimated accuracy is the sum of the maximum deviation and the uncertainty due to the anchor points as a percentage of the unweighted average. The uncertainty due to the anchor points is the average of the uncertainties in k($\tilde{\nu}$) (Table 2.1) for the two anchor points either side of the peak.

c - In this column the number in parentheses is the 90% confidence limit in the last digit[5].

d - In this column the number in parentheses is the evaluated uncertainty in the value[7].

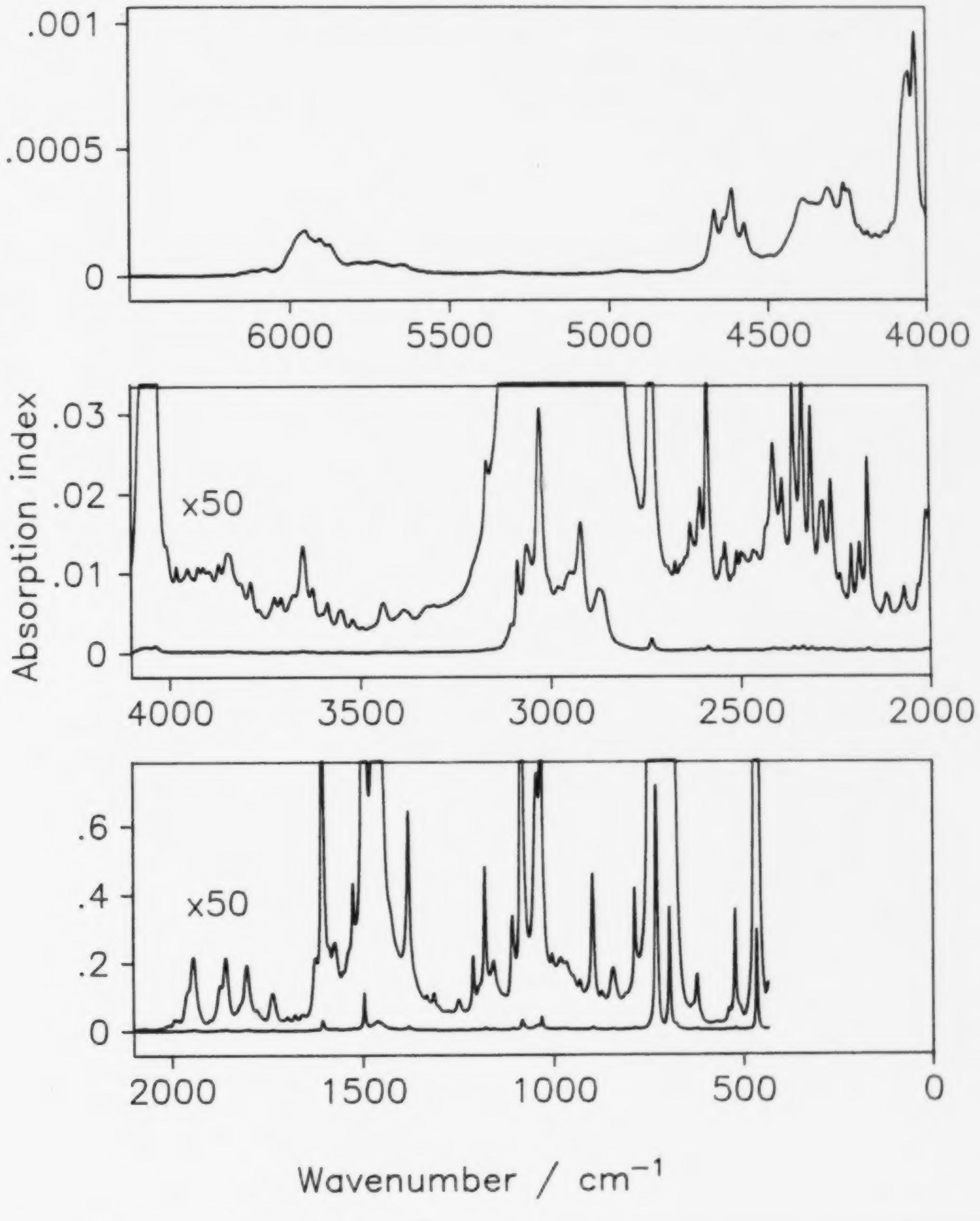

Figure 2.2 - Absorption index (imaginary refractive index), $k(\tilde{\nu})$, spectrum between 6500 and 435 cm^{-1} of toluene at 25°C. The scale labels in the middle and bottom boxes are for the lower spectrum in the box; they must be divided by 50 for the upper spectrum in the box.

Table 2.7 - Absorption indices between 6500 and 435 cm^{-1} of liquid toluene at 25°C.[a,b]

cm^{-1}	*XE*	*YE*	0	1	2	3	4	5	6	7	8	9	10	11	12	13	14	15	16
6499.90	3	-7	22	16	16	13	9	14	13	7	13	8	9	8	3	3	8	5	1
6368.76	3	-7	5	1	1	1	2	4	3	1	2	1	1	1	1	6	15	13	21
6237.63	3	-7	38	28	28	30	34	40	51	44	42	63	89	141	141	150	171	209	227
6106.49	3	-7	194	206	238	281	305	252	205	189	208	267	334	439	617	819	979	1128	1366
5975.35	3	-7	1513	1636	1723	1782	1721	1515	1439	1372	1357	1435	1404	1247	1181	1225	1143	966	776
5844.22	3	-7	633	528	471	439	446	483	508	525	534	514	495	501	512	523	546	562	532
5713.08	3	-7	502	485	443	416	393	379	394	424	439	436	418	350	280	246	227	193	165
5581.95	3	-7	172	147	117	138	121	108	126	117	108	99	113	104	87	91	83	82	81
5450.81	3	-7	84	81	81	81	83	85	92	90	96	107	112	111	121	128	138	144	140
5319.68	3	-7	118	120	121	98	100	96	84	81	77	74	79	89	85	75	74	73	69
5188.54	3	-7	65	59	46	56	72	69	63	64	65	63	64	62	65	68	69	67	68
5057.40	3	-7	71	71	80	85	87	92	100	111	127	147	159	175	178	177	174	170	162
4926.27	3	-7	163	152	147	134	125	119	125	133	140	141	141	144	142	142	140	137	138
4795.13	3	-7	148	164	186	204	213	226	233	259	296	346	403	455	532	683	1027		
4686.17	0	-7	1089	1148	1210	1278	1343	1409	1478	1546	1622	1696	1774	1863	1957	2056	2163	2268	2373
4666.89	2	-7	2592	2350	1957	1714	1655	1740	1980	2224	2269	2230	2332	2572	2851	3187	3424	3275	2730
4601.32	2	-7	2170	1818	1622	1524	1530	1677	1877	2054	1947	1650	1437	1274	1106	978	899	846	830
4531.90	3	-7	790	721	715	751	774	789	776	769	837	938	1055	1218	1411	1622	1822	2067	2453
4400.76	3	-7	2800	2996	3022	2920	2849	2847	2847	2817	2809	2878	3115	3397	3449	3261	2999	2713	2714
4269.63	3	-7	2983	3668	3376	3373	3230	2626	2105	1920									
4211.77	2	-7	1931	1869	1765	1672	1610	1613	1708	1730	1623	1530	1488	1500	1575	1617	1599	1561	1512
4146.20	2	-7	1497	1530	1618	1719	1741	1699	1683	1747	1879	2022	2062	2078	2180	2434	2885	3610	4674
4080.64	2	-7	5813	6573	7023	7474	7897	7991	8093	7828	7181	7278	8272	9467	9415	7922	6015	4443	3489
4015.07	2	-7	2992	2723	2699	2558	2293	2028	1860	1802	1916	2171	1955	1825	1825	1860	1900	1970	2090
3949.50	2	-7	2099	1989	1909	1872	1847	1896	2094	2150	2049	2044	2143	2098	2026	2033	2049	2024	1952
3883.93	2	-7	1859	1832	1930	2158	2214	2080	2016	2111	2332	2494	2509	2492	2419	2198	1994	1878	1795
3818.36	2	-7	1728	1739	1742	1642	1487	1387	1406	1560	1766	1693	1420	1198	1077	1046	1086	1039	963
3752.80	2	-7	911	894	903	944	1024	1110	1232	1381	1365	1233	1198	1306	1387	1255	1098	1064	1102
3687.23	2	-7	1203	1305	1398	1459	1446	1441	1525	1741	2118	2531	2688	2443	1982	1603	1436	1462	1597
3621.66	2	-7	1570	1291	1044	947	941	959	979	995	1094	1227							
3586.47	-1	-7	1238	1247	1255	1263	1267	1263	1250	1225	1192	1158	1124	1093	1064	1036	1011	988	965
3574.89	2	-7	817	745	730	783	900	1020	1073	1073	987	824	701	659	675	738	829	819	728
3509.33	2	-7	662	622	614	628	640	621	599	598	619	639	654	672	692	722	775	874	1039
3443.76	2	-7	1191	1261	1217	1108	983	887	839	827	839	865	897	925	957	1008	1058		
3382.05	3	-7	1079	1026	931	866	875	961	1063	1152	1167	1176	1201	1160	1171	1195	1224	1254	1307
3250.91	3	-7	1345	1405	1453	1547	1692	1892	2194	2392	2654	2931							
3179.56	1	-7	3032	3170	3359	3645	4074	4575	4829	4791	4667	4560	4510	4507	4586	4669	4767	4882	5025
3146.77	1	-6	514	531	550	574	597	625	656	696	745	808	891	999	1131	1294	1497	1718	1911
3113.99	1	-5	208	229	260	302	346	366	358	344	345	373	438	558	750	992	1152	1125	992
3079.28	2	-5	774	736	863	1134	1339	1342	1268	1172	1106	1134	1290	1700	2370	2952	3010	2358	1650
3013.71	2	-5	1234	1026	945	899	807	746	737	764	808	830	822	803	788	827	906	958	995
2948.14	2	-5	1017	1007	990	1002	1073	1224	1440	1621	1569	1270	949	724	593	528	514	539	593
2882.57	2	-6	6635	7363	7906	7984	7856	7641	7130	6029	4674	3524	2710	2165	1778	1490	1283	1184	1070
2817.01	2	-7	9537	9221	8845	7917	7032	6368	5771	5229	4868	4655	4476	4265	4051	3798	3646	3630	3684
2753.37	1	-6	377	392	416	454	514	607	752	972	1273	1583	1723	1574	1267	977	761	612	510
2720.58	1	-7	4394	3898	3536	3252	3021	2833	2675	2539	2429	2348	2273	2207	2163	2148	2153	2157	2134
2687.80	1	-7	2084	2037	2005	1976	1945	1937	1976	2099	2270	2234	2072	1990	1989	2039	2109	2170	2205
2655.02	1	-7	2206	2197	2215	2273	2341	2389	2397	2386	2408	2507	2734	3095	3272	3161	3002	2872	2779
2622.23	1	-7	2716	2678	2677	2734	2889	3180	3476	3619	3867	4164	3925	3479	3185	3110	3251	3675	4497
2589.45	1	-7	5770	7155	7658	6665	5213	4119	3408	2927	2564	2286	2088	1960	1876	1828	1821	1850	1905
2556.66	1	-7	1951	2012	2126	2273	2358	2354	2373	2522	2735	2710	2478	2255	2070	1921	1822	1788	1825
2523.88	1	-7	1901	1934	1933	1936	1978	2091	2286	2497	2533	2372	2236	2210	2281	2419	2526	2478	2442
2491.10	1	-7	2445	2437	2399	2350	2305	2280	2271	2270	2279	2301	2347	2421	2513	2564	2559	2538	2526
2458.31	1	-7	2514	2493	2453	2407	2364	2338	2329	2345	2394	2477	2588	2734	2941	3132	3187	3180	3213
2425.53	1	-7	3303	3460	3705	4044	4433	4804	5139	5258	5024	4634	4256	3942	3697	3533	3470	3517	3667
2392.74	1	-7	3894	4198	4387	4135	3702	3354	3084	2879	2759	2709	2705	2767	2911	3208	3802	4920	6521
2359.96	1	-7	6918	5941	5188	4755	4399	4068	3845	3814	4036	4541	5228	6106	7355	7887	6632	5063	4001
2327.18	1	-7	3393	3092	3009	3112	3436	4058	5016	6005	6061	5045	3977	3259	2827	2582	2474	2476	2577
2294.39	1	-7	2779	3064	3365	3625	3782	3757	3714	3815	3618	3226	2948	2803	2750	2790	2961	3289	3787
2261.61	1	-7	4263	4305	3879	3352	2910	2562	2291	2084	1939	1849	1823	1867	1949	1965	1842	1680	1563
2228.82	1	-7	1500	1469	1437	1392	1349	1330	1357	1463	1660	1916	2352	2730	2372	1856	1578	1485	1507
2196.04	1	-7	1600	1761	1981	2211	2450	2711	2728	2414	2103	1915	1834	1833	1920	2155	2638	3477	4526
2163.26	1	-7	4894	4180	3232	2504	1998	1665	1459	1335	1260	1203	1154	1116	1090	1072	1049	1013	976
2130.47	1	-7	963	988	1070	1162	1185	1219	1348	1479	1437	1395	1400	1353	1249	1146	1067	1016	991
2097.69	1	-7	987	987	984	989	1003	1027	1056	1083	1106	1134	1179	1243	1318	1402	1534	1644	1574

Table 2.7 - Continued.

cm^{-1}	*XE*	*YE*	0	1	2	3	4	5	6	7	8	9	10	11	12	13	14	15	16
2064.90	1	-7	1418	1296	1221	1169	1121	1087	1065	1053	1044	1045	1056	1077	1104	1150	1222	1340	1536
2032.12	1	-7	1689	1648	1644	1703	1812	1952	2126	2343	2614	2888	3152	3434	3580	3547	3451	3392	3445
1999.34	1	-7	3685	4243	5278	6463	6987	6862	6397	6192									
1981.98	2	-6	615	551	607	842	1295	1902	2291	2364	2640	3469	4274	4076	2882	1871	1316	1002	739
1916.41	2	-6	574	493	477	519	614	645	684	825	1042	1426	2042	2598	2628	2635	3322	4238	3842
1850.84	2	-6	2643	1688	1202	1001	995	1096	1196	1398	1578	1711	2054	2824	3693	3710	2803	1950	1512
1785.28	2	-6	1245	1180	1222	1077	939	831	741	669	631	711	967	1440	1985	2204	1894	1400	1002
1719.71	2	-7	7348	6267	6084	6145	6300	6974	8189										
1694.64	1	-7	7531	6936	6468	6124	5932	6025	6373	7203	8359	9241	9010	7989	7150	6714	6623	6904	7500
1661.85	1	-6	837	922	957	944	926	904	880	861	862	909	975	1061	1181	1340	1557	1894	2325
1629.07	1	-6	2879	3519	4077	4285	4205	4055	3985	4112	4566	5575	7823						
1608.82	0	-5	995	1335	1858	2532	3030	2999	2589	2102	1676	1344	1105	941	828	743	673	612	564
1591.47	1	-6	5081	4907	4919	4891	4562	4331	4367	4560	4813	5081	5193	5081	4783	4381	3976	3641	3373
1558.68	1	-6	3206	3152	3167	3296	3458	3452	3439	3545	3754	4031	4329	4549	4700	4795	4899	5143	5729
1525.90	1	-5	707	862	789	674	631	627	644	679	729	809	938	1143	1513	2215			
1499.86	0	-4	282	378	542	805	1081	1043	783	557	417	330	271	234	209	185	165	152	144
1480.58	2	-5	1388	1537	1811	2180	2555	2768	2712	2430	2055	1706	1341	1011	838	764	718	653	584
1415.01	2	-6	5286	4925	4671	4416	4324	4415	4777	5629	7438								
1382.23	1	-5	913	1178	1267	981	712	557	470	416	377	348	327	311	295	276	259	244	233
1349.44	1	-6	2242	2158	2070	1990	1930	1886	1871	1886	1961	2060	1955	1817	1729	1671	1642	1641	1690
1316.66	1	-6	1810	2027	2196	2016	1707	1524	1453	1439	1419	1371	1297	1222	1164	1126	1105	1097	1098
1283.87	1	-6	1109	1124	1146	1158	1156	1146	1129	1111	1095	1090	1094	1108	1131	1167	1221	1313	1468
1251.09	1	-6	1676	1815	1776	1645	1497	1371	1271	1197	1150	1122	1114	1119	1138	1171	1217	1286	1383
1218.31	1	-6	1518	1726	2124	3044	4324	3846	2877	2320	2122	2148	2309	2504	2628	2674	2709	2791	2963
1186.49	0	-6	3101	3295	3570	3959	4531	5402	6713	8436	9632	9066	7524	6117	5109	4441	4000	3709	3514
1169.13	1	-6	3292	3225	3269	3386	3567	3790	3992	4095	3815	3432	3113	2856	2658	2524	2423	2327	2230
1136.35	1	-6	2159	2114	2099	2097	2065	2019	1992	2006	2055	2153	2321	2613	3123	3987	5280	6545	6510
1103.56	1	-5	559	485	441	423	427	457	519	631	835	1219	1936	2847	2857	2158	1582	1211	962
1070.78	1	-5	785	669	599	561	547	552	573	612	669	749	854	986	1141	1304	1440	1506	1483
1038.96	0	-5	1447	1407	1373	1362	1388	1486	1720	2218	3133	3985	3577	2623	1890	1426	1142	967	859
1022.57	0	-6	7942	7342	6627	6007	5533	5170	4888	4669	4488	4341	4217	4121	4050	3997	3967	3959	3967
1006.17	0	-6	4000	4056	4171	4370	4494	4407	4249	4100	3984	3891	3829	3781	3750	3734	3733	3742	3770
986.89	2	-6	3946	4185	4222	3985	3915	3986	3940	3651	3388	3239	3173	3023	2781	2572			
934.82	1	-6	2563	2666	2870	2938	2726	2465	2299	2224	2212	2245	2309	2381	2468	2560	2678	2869	3213
902.04	1	-6	3823	4914	6757	8842	8711	6482	4560	3415	2763	2381	2148	2018	1985	2042	2177	2274	2227
867.33	2	-6	2012	1877	1885	2046	2410	3049	3613	3531	2945	2401	2041	1871	1839	1908	2048	2139	2180
804.65	0	-6	2199	2226	2254	2287	2331	2380	2426	2483	2540	2607	2700	2779	2904	3065	3259	3563	4027
788.26	0	-6	4790	6098	7784	8339	7439	6354	5546	5036	4719	4516	4382	4298	4279	4240	4233	4283	4321
771.87	0	-6	4317	4373	4471	4594	4749	4896	5065	5275	5481	5654	5878	6196	6551	6924	7373	7946	8642
755.47	0	-5	949	1048	1165	1310	1476	1651	1821	1991	2177	2393	2647	2953	3319	3766	4331	5055	5991
739.08	0	-4	722	887	1108	1408	1818	2371	3101	4023	5105	6214	7017	7116	6488	5421	4235	3182	2356
722.69	0	-4	1747	1313	1007	790	633	519	435	371	321	282	249	222	202	189	182	183	191
706.30	0	-4	207	233	273	326	393	471	565	694	899	1259	1896	2861	3616	3330	2498	1765	1251
689.91	0	-5	8951	6555	4974	3925	3215	2724	2384	2154	2005	1919	1880	1877	1872	1830	1733	1575	1386
673.52	0	-5	1202	1036	893	777	681	607	537	484	439	397	365	337	310	290	266	249	233
657.12	0	-6	2213	2048	1980	1863	1814	1705	1666	1574	1588	1495	1508	1433	1420	1370	1385	1311	1318
640.73	0	-6	1301	1330	1335	1424	1459	1468	1492	1532	1559	1558	1556	1569	1617	1708	1850	2055	2335
624.34	0	-6	2681	3035	3256	3221	2943	2567	2202	1902	1657	1464	1304	1171	1066	990	937	886	825
607.95	0	-7	7550	6906	6375	5953	5613	5359	5134	4934	4760	4600	4456	4341	4234	4146	4066	3962	3915
591.56	0	-7	3841	3796	3773	3760	3739	3720	3702	3744	3745	3786	3814	3867	3933	4020	4094	4211	4312
575.16	0	-7	4400	4460	4550	4619	4667	4701	4741	4766	4793	4803	4835	4805	4715	4627	4553	4489	4454
558.77	0	-7	4457	4485	4523	4576	4570	4656	4733	4842	4954	5093	5258	5454	5684	5946	6275	6675	7183
542.38	0	-6	787	881	1007	1155	1275	1303	1247	1177	1132	1118	1133	1171	1233	1321	1440	1597	1803
525.99	0	-6	2099	2527	3186	4245	5830	7135	6291	4480	3216	2508	2132	1904	1760	1653	1568	1508	1474
510.08	-1	-6	1462	1452	1445	1441	1394	1363	1307	1266	1274	1281	1225	1144	1134	1202	1153	1069	990
501.88	-1	-7	9312	9256	9572	9814	8861	8529	8491	8334	9016	9536	9728	9666	9111	8836	9190	9429	9337
493.69	-1	-6	982	1022	987	1012	1124	1268	1321	1301	1334	1391	1425	1491	1606	1683	1855	1983	2025
485.49	-1	-6	2095	2210	2303	2389	2688	2797	2787	2976	3165	3322	3443	3574	3681	3849	4106	4427	4839
477.29	-1	-5	524	574	638	704	774	862	963	1081	1218	1375	1568	1782	2027	2329	2693	3145	3708
469.10	-1	-4	439	526	640	787	979	1227	1544	1930	2362	2748	2953	2798	2443	2032	1649	1322	1061
460.90	-1	-5	8527	6935	5717	4764	4039	3473	2999	2593	2235	1928	1682	1459	1266	1120	1007	902	802
452.71	-1	-6	7250	6618	5960	5411	5043	4716	4349	4158	3898	3646	3523	3314	3193	3083	2978	2868	2577
444.51	-1	-6	2453	2525	2510	2400	2229	2075	2127	2296	2317	2333	2420	2345	2222	2287	2370	2354	2383
436.31	-1	-6	2463	2626	2694	2773	2989	3039											

a - The column headed cm^{-1} contains the wavenumber of the first $k(\tilde{\nu})$ value in the row. The columns headed *XE* and *YE* contain the X-exponent and the Y-exponent, respectively, for the row. The columns headed 0,1,2,$\cdots$16, contain the ordinate values, and the headings give the indices of the ordinate values in the row. In a row which starts with $\tilde{\nu}(0)$, the wavenumber corresponding to the ordinate indexed J is $\tilde{\nu}(J) = \tilde{\nu}(0) - \frac{15798.002}{16384} \cdot J \cdot 2^{XE}$. The $k(\tilde{\nu})$ values in that row are the ordinate value shown times 10^{YE}. Thus the entry indexed 16 in the first row of the table shows that $k = 1 \times 10^{-7}$ at $\tilde{\nu} = 6499.90 - \frac{15798.002}{16384} \cdot 16 \cdot 2^3 = 6376.48$ cm^{-1}.

b - The $k(\tilde{\nu})$ values in the table can be interpolated to the original wavenumber spacing, 0.482117 cm^{-1}, and yield the original $k(\tilde{\nu})$ values accurate to 1% below 4500 cm^{-1}, 2% between 4500 and 5000 cm^{-1} and 5% above 5000 cm^{-1}, via the 4-point spline interpolation program TRECOVER[8].

larger number of spectra from this laboratory did not unduly influence the average peak heights. Peak heights agreed between spectroscopists to ±2.1% on average. There was no evidence that resolution affected this agreement.

The unweighted average absorption index, $k(\tilde{\nu})$, spectrum, areas and peak heights were taken as the primary absorption intensity results of this work. This $k(\tilde{\nu})$ spectrum is shown in Fig. 2.2 and is tabulated in Table 2.7 in Compact Table format[8].

2.3.2 - Real refractive index spectrum.

The real refractive index spectrum, $n(\tilde{\nu})$, was determined by Kramers-Kronig transformation of the $k(\tilde{\nu})$ spectrum, with n = 1.4773±0.0004 at 8000 cm^{-1}. This value was obtained by fitting literature[9,10] values of the refractive index at eight wavelengths in the visible region to $n^2(\tilde{\nu}) = a\tilde{\nu}^4 + b\tilde{\nu}^2 + c$ and extrapolating to 8000 cm^{-1}. Further, we assumed that the $k(\tilde{\nu})$ values are all zero between 6500 and 8000 cm^{-1}. The final real refractive index spectrum is shown in Figure 2.3 and the values are in Table 2.8.

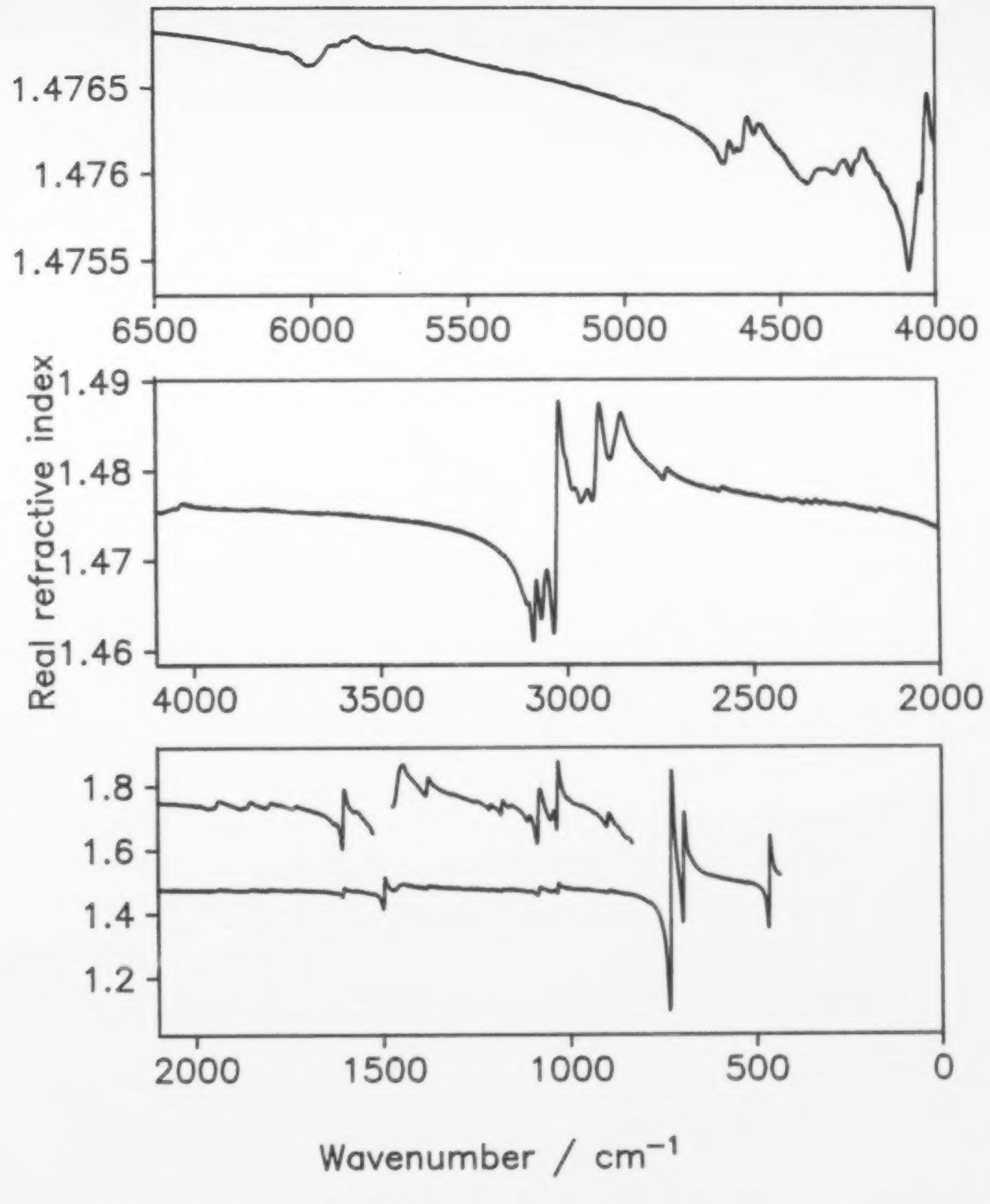

Figure 2.3 - Real refractive index, $n(\tilde{\nu})$, spectrum between 6500 and 435 cm^{-1} of toluene at 25°C. In the bottom box, the partial spectra shown by the upper curve are $(n(\tilde{\nu}) - 1.21) \times 6.6$, to magnify and offset the curves for clarity.

Table 2.8 - Real refractive indices between 6500 and 435 cm^{-1} of liquid toluene at 25°C.^{a,b}

cm^{-1}	*XE*	0	1	2	3	4	5	6	7	8	9	10	11	12	13	14	15	16
6499.90	3	14768	14768	14768	14768	14768	14768	14768	14768	14768	14768	14768	14768	14768	14768	14768	14768	14768
6368.76	3	14768	14767	14767	14767	14767	14767	14767	14767	14767	14767	14767	14767	14767	14767	14767	14767	14767
6237.63	3	14767	14767	14767	14767	14767	14767	14767	14767	14767	14767	14767	14767	14767	14767	14767	14767	14767
6106.49	3	14767	14767	14767	14767	14767	14767	14766	14766	14766	14766	14766	14766	14766	14766	14766	14766	14766
5975.35	3	14766	14766	14766	14767	14767	14767	14767	14767	14767	14767	14767	14767	14767	14767	14767	14768	14768
5844.22	3	14767	14767	14767	14767	14767	14767	14767	14767	14767	14767	14767	14767	14767	14767	14767	14767	14767
5713.08	3	14767	14767	14767	14767	14767	14767	14767	14767	14767	14767	14767	14767	14767	14767	14767	14767	14766
5581.95	3	14766	14766	14766	14766	14766	14766	14766	14766	14766	14766	14766	14766	14766	14766	14766	14766	14766
5450.81	3	14766	14766	14766	14766	14766	14766	14766	14766	14766	14766	14765	14765	14765	14765	14765	14765	14765
5319.68	3	14765	14765	14765	14765	14765	14765	14765	14765	14765	14765	14765	14765	14765	14765	14765	14765	14765
5188.54	3	14765	14765	14765	14765	14765	14765	14765	14764	14764	14764	14764	14764	14764	14764	14764	14764	14764
5057.40	3	14764	14764	14764	14764	14764	14764	14764	14764	14764	14764	14764	14764	14764	14763	14763	14763	14763
4926.27	3	14763	14763	14763	14763	14763	14763	14763	14763	14763	14763	14763	14763	14763	14763	14762	14762	14762
4795.13	3	14762	14762	14762	14762	14762	14762	14762	14762	14761	14761	14761	14761	14761	14760	14760		
4686.17	0	14760	14760	14760	14760	14760	14760	14760	14760	14760	14760	14760	14760	14760	14760	14760	14760	14760
4666.89	2	14761	14761	14761	14761	14761	14761	14761	14761	14761	14761	14761	14761	14761	14761	14762	14762	14763
4601.32	2	14763	14763	14762	14762	14762	14762	14762	14762	14762	14762	14762	14762	14762	14762	14762	14762	14762
4531.90	3	14762	14761	14761	14761	14761	14761	14760	14760	14760	14760	14760	14759	14759	14759	14759	14759	14759
4400.76	3	14759	14759	14760	14760	14760	14760	14760	14760	14760	14760	14759	14760	14760	14760	14760	14760	14760
4269.63	3	14759	14760	14760	14760	14761	14761	14761	14760									
4211.77	2	14760	14760	14760	14760	14760	14760	14759	14759	14759	14759	14759	14759	14759	14759	14759	14759	14758
4146.20	2	14758	14758	14758	14758	14758	14757	14757	14757	14757	14757	14756	14756	14756	14755	14755	14754	14754
4080.64	2	14754	14755	14755	14756	14757	14757	14758	14759	14759	14758	14758	14760	14762	14764	14764	14764	14763
4015.07	2	14762	14762	14761	14761	14761	14761	14761	14760	14760	14760	14760	14760	14759	14759	14759	14759	14759
3949.50	2	14759	14759	14759	14759	14758	14758	14758	14758	14758	14758	14758	14758	14758	14758	14758	14758	14758
3883.93	2	14758	14757	14757	14757	14757	14757	14757	14757	14757	14757	14757	14757	14757	14757	14757	14757	14757
3818.36	2	14757	14757	14757	14757	14757	14757	14756	14756	14756	14756	14756	14756	14756	14756	14756	14756	14755
3752.80	2	14755	14755	14755	14755	14755	14754	14754	14754	14754	14754	14754	14754	14754	14754	14754	14754	14753
3687.23	2	14753	14753	14753	14753	14753	14753	14752	14752	14752	14752	14753	14753	14753	14753	14753	14753	14752
3621.66	2	14753	14753	14752	14752	14752	14752	14752	14751	14751	14751							
3586.47	-1	14751	14751	14751	14751	14751	14751	14751	14751	14751	14751	14751	14751	14751	14751	14751	14751	14751
3574.89	2	14751	14751	14750	14750	14750	14750	14750	14750	14750	14750	14749	14749	14749	14749	14749	14748	14748
3509.33	2	14748	14748	14748	14748	14747	14747	14747	14747	14746	14746	14746	14746	14746	14745	14745	14745	14745
3443.76	2	14745	14744	14744	14744	14744	14744	14744	14743	14743	14743	14742	14742	14742	14742	14741		
3382.05	3	14741	14741	14740	14739	14739	14738	14737	14736	14736	14735	14734	14733	14732	14731	14730	14729	14728
3250.91	3	14727	14725	14724	14722	14721	14719	14717	14715	14712	14709							
3179.56	1	14709	14708	14707	14706	14705	14705	14704	14704	14703	14702	14702	14700	14699	14698	14697	14696	14695
3146.77	1	14694	14692	14691	14689	14688	14686	14684	14682	14680	14678	14675	14673	14670	14668	14665	14663	14661
3113.99	1	14659	14656	14653	14651	14651	14653	14653	14649	14643	14635	14625	14616	14611	14617	14639	14664	14676
3079.28	2	14673	14656	14640	14637	14656	14677	14687	14689	14679	14662	14641	14621	14632	14696	14795	14868	14875
3013.71	2	14858	14837	14822	14816	14810	14799	14789	14782	14779	14779	14779	14778	14773	14766	14765	14767	14771
2948.14	2	14775	14778	14778	14774	14769	14767	14776	14804	14844	14871	14874	14865	14853	14840	14829	14820	14814
2882.57	2	14812	14814	14821	14829	14836	14844	14854	14862	14864	14860	14855	14850	14845	14840	14836	14832	14829
2817.01	2	14826	14823	14821	14820	14818	14816	14814	14812	14810	14808	14807	14805	14804	14803	14801	14800	14798
2753.37	1	14797	14796	14795	14794	14793	14792	14791	14790	14790	14792	14796	14800	14802	14802	14802	14801	14800
2720.58	1	14799	14798	14797	14797	14796	14795	14795	14794	14794	14793	14793	14792	14792	14791	14791	14790	14790
2687.80	1	14790	14789	14789	14789	14788	14788	14787	14787	14787	14787	14786	14786	14786	14785	14785	14785	14785
2655.02	1	14784	14784	14784	14783	14783	14783	14783	14782	14782	14782	14781	14781	14781	14781	14781	14781	14781
2622.23	1	14781	14780	14780	14780	14779	14779	14779	14779	14779	14779	14779	14779	14779	14778	14778	14777	14776
2589.45	1	14776	14777	14779	14781	14781	14781	14780	14780	14780	14779	14779	14778	14778	14778	14777	14777	14777
2556.66	1	14776	14776	14776	14776	14776	14775	14775	14775	14775	14775	14775	14775	14775	14775	14774	14774	14774
2523.88	1	14774	14773	14773	14773	14773	14773	14772	14772	14772	14772	14772	14772	14772	14772	14772	14772	14771
2491.10	1	14771	14771	14771	14771	14771	14771	14770	14770	14770	14770	14770	14770	14770	14769	14769	14769	14769
2458.31	1	14769	14769	14769	14769	14768	14768	14768	14768	14768	14767	14767	14767	14767	14767	14767	14767	14766
2425.53	1	14766	14766	14766	14766	14766	14766	14766	14767	14767	14767	14767	14767	14767	14767	14766	14766	14766
2392.74	1	14766	14766	14766	14766	14766	14766	14766	14766	14765	14765	14764	14764	14763	14763	14762	14762	14762
2359.96	1	14764	14765	14765	14765	14765	14765	14764	14764	14763	14763	14762	14762	14763	14765	14766	14766	14766
2327.18	1	14765	14765	14764	14763	14763	14762	14762	14763	14764	14765	14765	14765	14764	14764	14763	14763	14762
2294.39	1	14762	14762	14762	14762	14762	14762	14762	14762	14762	14762	14762	14762	14761	14761	14761	14760	14760
2261.61	1	14761	14761	14762	14762	14762	14762	14761	14761	14761	14760	14760	14760	14760	14760	14760	14760	14759
2228.82	1	14759	14759	14759	14758	14758	14758	14758	14757	14757	14757	14757	14757	14757	14757	14757	14757	14756
2196.04	1	14756	14756	14755	14755	14755	14755	14756	14756	14756	14755	14755	14755	14754	14754	14753	14753	14754
2163.26	1	14755	14756	14756	14756	14756	14755	14755	14754	14754	14754	14754	14753	14753	14753	14753	14752	14752
2130.47	1	14752	14752	14751	14751	14751	14751	14751	14751	14751	14750	14750	14750	14750	14750	14750	14749	14749
2097.69	1	14749	14749	14748	14748	14748	14748	14747	14747	14747	14747	14747	14746	14746	14746	14746	14746	14746

Table 2.8 - Continued

cm^{-1}	XE	0	1	2	3	4	5	6	7	8	9	10	11	12	13	14	15	16
2064.90	1	14745	14745	14745	14745	14744	14744	14744	14743	14743	14743	14742	14742	14742	14741	14741	14741	14740
2032.12	1	14740	14740	14739	14739	14739	14738	14738	14737	14737	14737	14736	14736	14736	14736	14735	14735	14734
1999.34	1	14733	14732	14732	14732	14732	14733	14733	14732									
1981.98	2	14731	14729	14726	14723	14720	14720	14723	14725	14724	14725	14735	14750	14758	14757	14753	14750	14747
1916.41	2	14744	14741	14738	14735	14733	14731	14729	14726	14723	14720	14719	14722	14726	14725	14724	14733	14748
1850.84	2	14753	14751	14746	14741	14736	14733	14731	14728	14727	14725	14722	14721	14728	14741	14748	14748	14744
1785.28	2	14741	14738	14737	14737	14735	14733	14731	14729	14726	14722	14719	14717	14719	14724	14729	14730	14729
1719.71	2	14726	14722	14720	14717	14715	14713	14712										
1694.64	1	14712	14711	14710	14709	14707	14706	14704	14703	14702	14702	14702	14701	14700	14698	14696	14694	14693
1661.85	1	14691	14690	14689	14688	14687	14685	14683	14681	14678	14675	14672	14668	14665	14661	14656	14652	14648
1629.07	1	14645	14643	14645	14647	14647	14643	14637	14626	14612	14593	14565						
1608.82	0	14549	14533	14528	14554	14626	14713	14773	14802	14810	14807	14798	14788	14779	14772	14765	14759	14753
1591.47	1	14741	14732	14726	14723	14720	14715	14709	14705	14703	14702	14704	14706	14707	14706	14704	14700	14696
1558.68	1	14691	14686	14681	14676	14673	14670	14665	14660	14654	14650	14646	14643	14639	14635	14629	14621	14611
1525.90	1	14604	14612	14624	14618	14605	14591	14575	14558	14537	14511	14478	14436	14378	14299			
1499.86	0	14248	14190	14143	14178	14453	14894	15112	15140	15105	15063	15021	14983	14956	14933	14908	14884	14861
1480.58	2	14797	14758	14736	14733	14755	14799	14851	14892	14915	14924	14927	14913	14893	14878	14869	14863	14856
1415.01	2	14848	14840	14832	14825	14817	14808	14798	14789	14780								
1382.23	1	14779	14792	14835	14863	14864	14857	14850	14844	14839	14835	14831	14828	14826	14824	14821	14819	14816
1349.44	1	14814	14812	14810	14807	14805	14803	14801	14799	14797	14797	14797	14796	14794	14792	14790	14788	14786
1316.66	1	14784	14784	14786	14788	14788	14786	14784	14782	14781	14780	14779	14778	14776	14775	14773	14772	14770
1283.87	1	14769	14767	14766	14765	14764	14763	14762	14761	14760	14759	14757	14756	14754	14753	14751	14750	14748
1251.09	1	14748	14749	14751	14751	14751	14749	14748	14746	14744	14743	14741	14739	14737	14735	14732	14730	14727
1218.31	1	14724	14721	14717	14713	14722	14736	14738	14734	14730	14726	14723	14721	14720	14719	14716	14713	14709
1186.49	0	14707	14704	14701	14697	14694	14690	14690	14697	14718	14743	14755	14757	14756	14752	14749	14745	14743
1169.13	1	14738	14733	14730	14728	14726	14726	14727	14730	14733	14733	14732	14730	14728	14725	14723	14721	14718
1136.35	1	14715	14713	14710	14707	14705	14701	14698	14694	14689	14684	14678	14672	14665	14659	14657	14665	14679
1103.56	1	14683	14680	14673	14663	14653	14640	14625	14607	14585	14561	14554	14617	14741	14801	14810	14802	14791
1070.78	1	14777	14763	14750	14738	14726	14715	14705	14695	14686	14678	14670	14665	14664	14668	14679	14693	14705
1038.96	0	14708	14707	14703	14695	14682	14664	14641	14620	14630	14740	14883	14936	14935	14917	14898	14880	14865
1022.57	0	14854	14847	14841	14833	14826	14819	14813	14807	14802	14798	14793	14789	14785	14782	14778	14775	14772
1006.17	0	14769	14766	14764	14762	14763	14763	14763	14762	14760	14758	14756	14754	14752	14751	14749	14747	14745
986.89	2	14740	14737	14737	14735	14731	14728	14728	14726	14723	14718	14715	14712	14708	14702			
934.82	1	14699	14696	14694	14694	14694	14692	14688	14684	14680	14676	14673	14669	14665	14661	14657	14652	14645
902.04	1	14639	14632	14631	14648	14679	14694	14692	14685	14677	14670	14663	14657	14650	14645	14641	14638	14635
867.33	2	14628	14619	14608	14598	14587	14579	14576	14575	14570	14559	14546	14531	14515	14498	14482	14464	14445
804.65	0	14439	14434	14428	14423	14417	14410	14404	14398	14391	14384	14376	14369	14360	14352	14342	14332	14322
788.26	0	14310	14301	14303	14316	14323	14320	14311	14300	14289	14277	14265	14253	14240	14228	14214	14201	14187
771.87	0	14172	14156	14140	14123	14105	14087	14068	14047	14026	14004	13979	13954	13927	13898	13867	13833	13798
755.47	0	13760	13721	13678	13633	13587	13539	13489	13433	13370	13301	13222	13135	13037	12926	12799	12656	12492
739.08	0	12305	12094	11860	11605	11345	11113	10966	10997	11346	12173	13582	15325	16850	17901	18396	18462	18288
722.69	0	18004	17692	17392	17121	16881	16669	16484	16320	16174	16042	15920	15804	15693	15585	15479	15373	15268
706.30	0	15161	15053	14941	14829	14717	14601	14467	14301	14093	13858	13698	13947	15046	16394	17039	17160	17074
689.91	0	16919	16745	16581	16438	16315	16210	16120	16043	15977	15920	15873	15835	15808	15788	15773	15758	15740
673.52	0	15718	15695	15670	15646	15622	15600	15579	15558	15539	15521	15504	15487	15472	15457	15443	15430	15417
657.12	0	15405	15393	15381	15370	15360	15350	15340	15331	15322	15313	15305	15297	15289	15282	15274	15267	15260
640.73	0	15253	15246	15239	15233	15228	15222	15217	15211	15206	15201	15196	15191	15185	15180	15175	15170	15165
624.34	0	15162	15161	15162	15164	15165	15164	15161	15158	15154	15150	15146	15142	15137	15133	15130	15126	15123
607.95	0	15119	15116	15112	15109	15106	15102	15099	15096	15093	15090	15087	15084	15081	15078	15075	15072	15070
591.56	0	15067	15064	15062	15059	15057	15054	15052	15049	15047	15044	15042	15040	15037	15035	15033	15030	15028
575.16	0	15026	15024	15022	15020	15018	15016	15013	15011	15009	15007	15005	15003	15001	14999	14997	14995	14993
558.77	0	14991	14989	14987	14984	14982	14980	14978	14976	14973	14971	14969	14967	14964	14962	14959	14957	14954
542.38	0	14952	14949	14947	14945	14944	14943	14942	14940	14937	14935	14931	14928	14925	14921	14918	14914	14910
525.99	0	14905	14900	14895	14892	14895	14913	14936	14942	14938	14931	14925	14920	14915	14911	14907	14903	14899
510.08	-1	14897	14895	14893	14891	14890	14888	14886	14884	14881	14880	14878	14876	14873	14871	14869	14867	14864
501.88	-1	14862	14858	14856	14853	14851	14847	14845	14841	14838	14835	14832	14829	14826	14822	14818	14815	14811
493.69	-1	14807	14803	14799	14794	14789	14785	14782	14778	14772	14768	14762	14757	14751	14745	14739	14734	14728
485.49	-1	14722	14715	14708	14700	14692	14686	14678	14668	14659	14650	14640	14629	14617	14603	14590	14574	14558
477.29	-1	14541	14523	14503	14484	14461	14437	14411	14383	14352	14320	14284	14247	14203	14156	14102	14044	13979
469.10	-1	13910	13830	13748	13660	13584	13522	13513	13585	13820	14251	14903	15572	16030	16299	16409	16427	16383
460.90	-1	16317	16232	16153	16072	16001	15936	15883	15831	15787	15742	15703	15665	15631	15596	15568	15540	15517
452.71	-1	15492	15472	15451	15433	15414	15399	15383	15369	15356	15344	15332	15322	15311	15303	15293	15286	15278
444.51	-1	15269	15260	15255	15248	15243	15234	15227	15221	15218	15211	15209	15205	15201	15195	15193	15188	15187
436.31	-1	15182	15182	15178	15181	15178	15178											

a - The column headed cm^{-1} contains the wavenumber of the first $n(\tilde{\nu})$ value in the row. The column headed XE contains the X-exponent for the row. The columns headed 0,1,2,····16, contain the $n(\tilde{\nu})$ values with the decimal point implicitly after the first digit in each value, and the headings give the indices of the $n(\tilde{\nu})$ values in the row. In a row which starts with $\tilde{\nu}(0)$, the wavenumber corresponding to the ordinate indexed J is $\tilde{\nu}(J) = \tilde{\nu}(0) - \frac{15798.002}{16384} \cdot J \cdot 2^{XE}$. Thus, the entry indexed 16 in the first row of the table shows that $n = 1.4768$ at $\tilde{\nu} = 6499.90 - \frac{15798.002}{16384} \cdot 16\ 2^3 =$ 6376.48 cm^{-1}.

b - The $n(\tilde{\nu})$ values in the table can be interpolated to the original wavenumber spacing, 0.482117 cm^{-1}, and yield the original $n(\tilde{\nu})$ values accurate to 0.1%, via the 4-point spline interpolation program TRECOVER[8].

2.3.3 - Molar absorption coefficient spectrum.

To present the data in a form preferred by analytical chemists, we have used the final $k(\tilde{\nu})$ spectrum to calculate the molar absorption coefficient spectrum[1], by $E_m(\tilde{\nu}) = 4\pi\ \tilde{\nu}\ k(\tilde{\nu})/(2.303\ C)$, where C is the molar concentration. The $E_m(\tilde{\nu})$ spectrum is shown in Figure 2.4 and the values of $E_m(\tilde{\nu})$ are tabulated in Table 2.9 in Compact Table format[8]. For liquid toluene at 25°C, the molar concentration is 9.36 mol/L, as calculated from its density of 0.8623 g/ml[9]. The molar absorption coefficient is in the unit L mole^{-1} cm^{-1}. The areas under the molar absorption coefficient bands are in Table 2.10, with their estimated accuracies. The areas are in the unit used by analytical chemists, L mole^{-1} cm^{-2}. The values should be divided by 100 to put them in the km mole^{-1} unit usually used by physical chemists. The values of the molar absorption coefficient at the peaks of the bands are listed in Table 2.11.

For selected spectral regions, the molar absorption coefficient spectrum, the

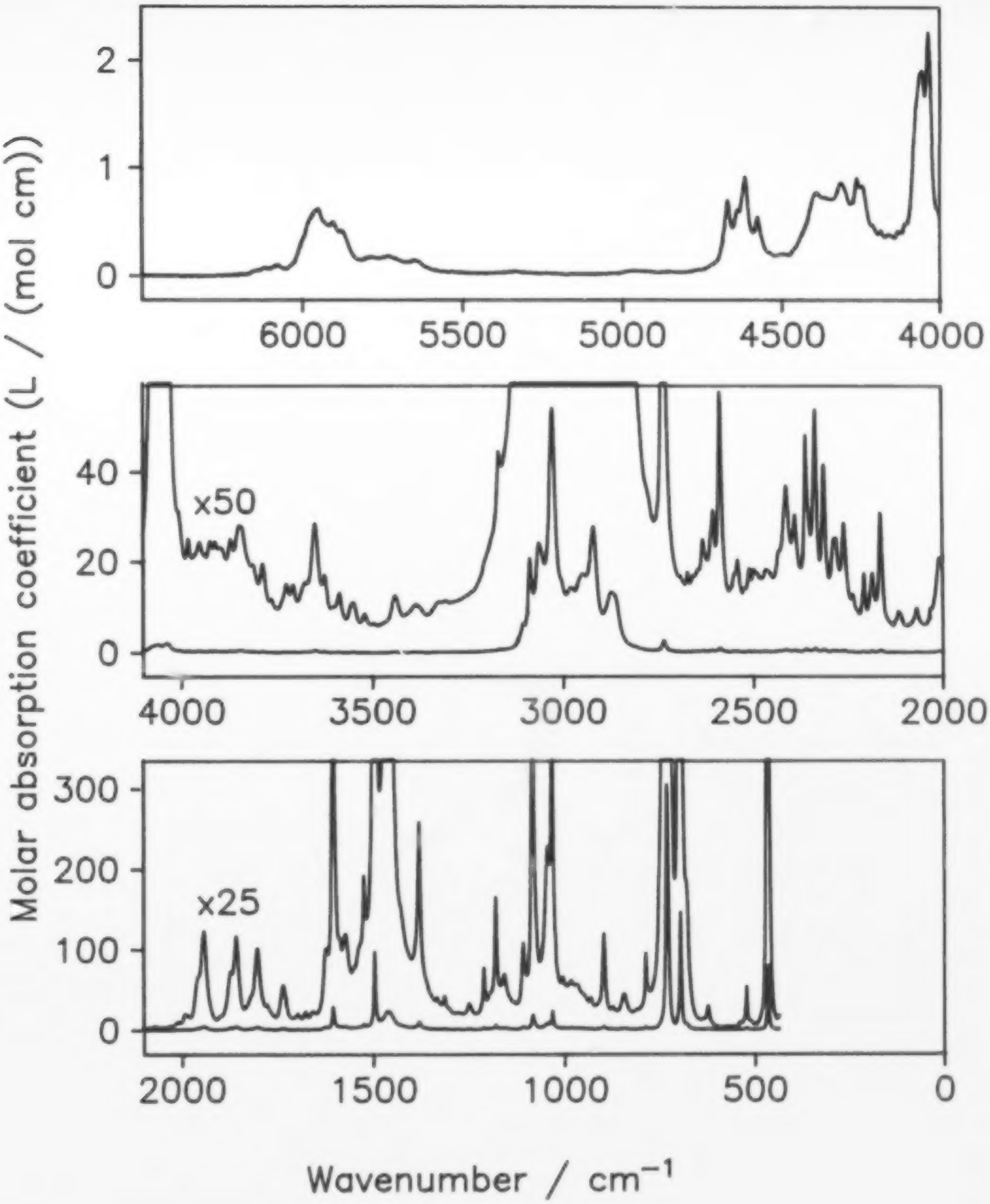

Figure 2.4 - Molar absorption index, $E_m(\tilde{\nu})$, spectrum between 6500 and 435 cm^{-1} of toluene at 25°C. The scale labels in the middle and bottom boxes are for the lower spectrum in the box; they must be divided by 50 or 25, as shown, for the upper spectrum in the box.

Table 2.9 - Molar absorption coefficients between 6500 and 435 cm^{-1} of liquid toluene at 25°C.[a,b,c]

cm^{-1}	*XE*	*YE*	0	1	2	3	4	5	6	7	8	9	10	11	12	13	14	15	16
6499.90	3	-6	8321	5917	6052	4844	3432	5247	5020	2708	4962	3057	3309	3052	988	1268	3069	1871	372
6368.76	3	-6	1862	371	371	370	822	1465	968	507	643	367	367	367	366	2355	5524	4745	7822
6237.63	3	-5	1389	1019	1017	1083	1233	1461	1840	1593	1527	2280	3195	5043	5035	5351	6096	7439	8100
6106.49	3	-4	691	732	844	995	1080	891	726	667	732	939	1172	1540	2161	2866	3423	3939	4763
5975.35	3	-4	5269	5690	5985	6180	5964	5244	4972	4735	4675	4938	4827	4282	4050	4193	3907	3298	2645
5844.22	3	-4	2158	1795	1600	1489	1511	1635	1717	1773	1800	1729	1663	1681	1715	1752	1824	1877	1772
5713.08	3	-4	1671	1614	1472	1381	1303	1255	1301	1399	1446	1436	1372	1149	917	803	740	628	536
5581.95	3	-5	5597	4790	3810	4477	3904	3485	4062	3756	3465	3184	3641	3331	2777	2906	2651	2626	2589
5450.81	3	-5	2681	2561	2571	2569	2607	2685	2894	2846	3016	3365	3505	3463	3764	4007	4289	4467	4362
5319.68	3	-5	3663	3706	3732	3030	3076	2951	2582	2498	2352	2265	2421	2712	2584	2270	2249	2204	2104
5188.54	3	-5	1973	1782	1400	1678	2169	2065	1874	1925	1940	1891	1903	1831	1931	2002	2030	1984	2000
5057.40	3	-5	2091	2094	2362	2492	2546	2699	2914	3227	3704	4270	4609	5069	5164	5106	5010	4895	4657
4926.27	3	-5	4692	4349	4196	3832	3574	3401	3554	3775	3963	4002	3993	4064	3992	3991	3943	3835	3863
4795.13	3	-4	412	457	519	568	591	625	645	716	816	952	1107	1249	1458	1869	2807		
4686.17	0	-4	2973	3135	3303	3489	3664	3844	4031	4215	4421	4623	4836	5077	5333	5601	5889	6174	6460
4666.89	2	-4	7050	6386	5313	4649	4487	4714	5357	6015	6130	6020	6290	6932	7679	8575	9206	8797	7328
4601.32	2	-4	5820	4872	4342	4077	4089	4478	5007	5476	5187	4392	3822	3384	2936	2594	2382	2241	2195
4531.90	3	-4	2088	1902	1883	1972	2031	2067	2030	2006	2181	2440	2739	3157	3650	4190	4697	5319	6303
4400.76	3	-4	7181	7672	7724	7450	7256	7238	7225	7136	7103	7266	7849	8546	8659	8173	7503	6775	6765
4269.63	3	-4	7422	9110	8371	8347	7980	6476	5181	4717									
4211.77	2	-4	4739	4584	4325	4093	3938	3940	4170	4219	3954	3725	3619	3645	3823	3921	3875	3780	3657
4146.20	2	-3	362	369	390	414	419	409	404	419	451	484	494	497	521	581	688	860	1113
4080.64	2	-3	1383	1562	1667	1772	1871	1892	1914	1849	1695	1716	1949	2228	2214	1861	1412	1042	817
4015.07	2	-4	7002	6366	6304	5968	5345	4722	4328	4188	4450	5036	4531	4226	4221	4298	4387	4543	4815
3949.50	2	-4	4832	4574	4386	4297	4236	4343	4792	4914	4679	4664	4884	4778	4609	4620	4651	4590	4423
3883.93	2	-4	4207	4143	4360	4871	4993	4685	4536	4746	5237	5595	5622	5578	5411	4910	4450	4187	3999
3818.36	2	-4	3845	3866	3869	3644	3296	3070	3110	3448	3899	3733	3127	2637	2367	2298	2382	2278	2109
3752.80	2	-4	1993	1953	1972	2058	2229	2416	2677	2999	2961	2671	2592	2824	2997	2709	2367	2291	2371
3687.23	2	-4	2586	2802	2998	3124	3094	3079	3257	3714	4513	5387	5715	5190	4207	3399	3040	3093	3375
3621.66	2	-4	3314	2722	2198	1993	1977	2014	2054	2084	2290	2566							
3586.47	-1	-4	2589	2605	2622	2639	2646	2638	2611	2559	2489	2417	2345	2281	2220	2162	2108	2060	2012
3574.89	2	-4	1702	1550	1517	1627	1867	2113	2221	2219	2039	1700	1444	1356	1388	1515	1701	1678	1491
3509.33	2	-4	1354	1270	1253	1281	1303	1263	1217	1215	1254	1294	1324	1357	1397	1456	1560	1758	2087
3443.76	2	-4	2389	2527	2438	2216	1963	1769	1672	1648	1669	1718	1781	1834	1895	1994	2091		
3382.05	3	-4	2126	2017	1826	1695	1709	1872	2067	2234	2259	2271	2314	2229	2245	2285	2336	2386	2483
3250.91	3	-4	2548	2656	2739	2910	3176	3543	4097	4457	4932	5434							
3179.56	1	-4	5619	5870	6217	6741	7531	8453	8916	8841	8607	8404	8307	8295	8436	8584	8758	8965	9221
3146.77	1	-3	942	974	1007	1050	1092	1143	1199	1270	1359	1474	1624	1820	2060	2355	2721	3122	3470
3113.99	1	-2	378	416	471	548	627	663	647	622	624	673	790	1005	1351	1786	2073	2022	1782
3079.28	2	-2	1388	1319	1545	2028	2392	2393	2258	2085	1965	2013	2286	3008	4189	5212	5307	4153	2902
3013.71	2	-2	2167	1800	1656	1573	1410	1301	1285	1330	1405	1440	1425	1390	1362	1429	1562	1650	1713
2948.14	2	-2	1747	1728	1697	1714	1834	2089	2456	2760	2668	2156	1609	1226	1003	892	866	907	997
2882.57	2	-2	1115	1235	1325	1336	1313	1275	1188	1003	777	585	449	358	294	246	211	195	176
2817.01	2	-3	1566	1512	1448	1294	1148	1038	940	850	791	755	725	690	654	613	587	584	592
2753.37	1	-3	604	628	667	727	822	970	1202	1552	2031	2524	2746	2506	2016	1553	1209	972	809
2720.58	1	-4	6967	6176	5599	5146	4776	4476	4224	4007	3830	3698	3578	3472	3401	3374	3380	3384	3345
2687.80	1	-4	3264	3189	3136	3088	3038	3023	3082	3272	3536	3477	3223	3093	3089	3165	3271	3363	3415
2655.02	1	-4	3413	3397	3422	3509	3611	3684	3693	3673	3705	3853	4199	4752	5020	4844	4598	4396	4250
2622.23	1	-4	4150	4090	4085	4169	4402	4843	5288	5502	5875	6321	5954	5275	4824	4707	4917	5555	6792
2589.45	1	-3	871	1079	1154	1004	784	619	512	439	385	343	313	293	281	273	272	276	284
2556.66	1	-4	2906	2995	3163	3380	3503	3495	3521	3738	4051	4011	3664	3332	3056	2834	2687	2635	2686
2523.88	1	-4	2796	2843	2840	2841	2900	3064	3346	3654	3703	3465	3264	3223	3324	3522	3677	3603	3549
2491.10	1	-4	3549	3535	3477	3404	3336	3297	3282	3278	3288	3318	3382	3485	3614	3685	3675	3642	3621
2458.31	1	-4	3602	3569	3509	3440	3377	3336	3321	3341	3409	3524	3679	3883	4174	4442	4515	4503	4546
2425.53	1	-4	4669	4888	5229	5703	6247	6764	7229	7392	7058	6504	5969	5524	5176	4943	4851	4912	5117
2392.74	1	-4	5430	5850	6108	5752	5146	4658	4280	3992	3823	3750	3741	3824	4021	4427	5243	6778	8977
2359.96	1	-3	952	816	712	652	603	557	526	522	552	620	713	832	1002	1073	902	688	543
2327.18	1	-4	4601	4190	4074	4211	4645	5480	6770	8097	8166	6791	5350	4380	3796	3465	3316	3316	3449
2294.39	1	-4	3716	4094	4492	4835	5040	5002	4942	5072	4805	4281	3910	3714	3640	3690	3913	4343	4996
2261.61	1	-4	5619	5670	5104	4407	3823	3363	3004	2731	2538	2418	2382	2437	2543	2561	2399	2187	2032
2228.82	1	-4	1949	1907	1864	1804	1746	1720	1753	1889	2141	2469	3029	3513	3049	2383	2025	1904	1930
2196.04	1	-4	2048	2252	2531	2822	3125	3454	3473	3071	2673	2431	2326	2323	2432	2726	3335	4392	5712
2163.26	1	-4	6171	5265	4067	3149	2510	2090	1830	1672	1577	1504	1442	1393	1359	1336	1306	1260	1213
2130.47	1	-4	1196	1226	1326	1439	1466	1507	1665	1825	1771	1717	1723	1663	1534	1406	1308	1244	1213
2097.69	1	-4	1207	1205	1201	1206	1222	1250	1283	1316	1342	1375	1429	1505	1593	1694	1851	1982	1896

Table 2.9 - Continued.

cm^{-1}	*XE*	*YE*	0	1	2	3	4	5	6	7	8	9	10	11	12	13	14	15	16
2064.90	1	-4	1707	1558	1467	1402	1344	1302	1275	1259	1247	1247	1259	1283	1313	1367	1452	1591	1821
2032.12	1	-4	2001	1949	1944	2011	2138	2301	2504	2756	3073	3392	3698	4024	4191	4149	4033	3961	4018
1999.34	1	-4	4294	4939	6139	7509	8111	7957	7411	7167									
1981.98	2	-3	710	636	699	967	1484	2176	2616	2693	3002	3937	4841	4607	3251	2107	1478	1124	827
1916.41	2	-3	641	549	530	577	681	713	755	909	1145	1564	2234	2837	2865	2866	3606	4590	4153
1850.84	2	-3	2851	1817	1291	1073	1064	1170	1274	1486	1673	1811	2170	2977	3884	3894	2935	2037	1577
1785.28	2	-3	1295	1225	1266	1113	968	855	761	686	645	725	985	1463	2012	2229	1911	1409	1006
1719.71	2	-4	7364	6267	6070	6117	6258	6912	8097										
1694.64	1	-4	7438	6842	6374	6027	5832	5917	6252	7057	8180	9033	8797	7791	6966	6533	6437	6703	7272
1661.85	1	-3	811	892	925	911	893	870	847	827	827	871	933	1015	1128	1278	1483	1802	2210
1629.07	1	-3	2734	3337	3861	4054	3973	3827	3757	3872	4294	5237	7340						
1608.82	0	-2	933	1251	1741	2370	2835	2804	2419	1963	1564	1253	1030	877	771	691	625	569	523
1591.47	1	-3	4713	4546	4551	4520	4211	3992	4021	4193	4421	4662	4759	4650	4372	4000	3625	3316	3068
1558.68	1	-3	2913	2860	2870	2983	3126	3116	3101	3193	3376	3621	3884	4076	4207	4286	4373	4586	5101
1525.90	1	-2	628	766	700	597	558	554	568	598	642	711	824	1003	1325	1937			
1499.86	0	-2	2465	3305	4727	7019	9428	9089	6815	4851	3627	2864	2352	2033	1815	1603	1429	1314	1247
1480.58	2	-2	1197	1323	1554	1866	2182	2357	2304	2059	1736	1438	1127	848	701	637	597	541	483
1415.01	2	-3	4359	4050	3831	3612	3527	3591	3875	4554	6000								
1382.23	1	-2	736	948	1018	787	571	446	375	332	300	277	260	247	234	219	204	193	183
1349.44	1	-3	1763	1695	1623	1558	1509	1473	1459	1469	1525	1599	1516	1407	1336	1290	1266	1263	1299
1316.66	1	-3	1389	1553	1680	1540	1303	1161	1105	1093	1076	1038	981	923	877	847	831	823	823
1283.87	1	-3	830	840	855	863	860	851	837	822	809	804	806	816	831	856	894	960	1072
1251.09	1	-3	1222	1321	1291	1194	1085	992	918	864	828	807	800	802	814	837	868	916	983
1218.31	1	-3	1078	1224	1503	2151	3050	2710	2023	1629	1487	1503	1614	1747	1830	1859	1881	1934	2050
1186.49	0	-3	2145	2277	2464	2731	3123	3720	4620	5800	6617	6223	5160	4192	3498	3038	2734	2533	2398
1169.13	1	-3	2243	2194	2220	2296	2414	2561	2693	2758	2566	2304	2086	1911	1775	1683	1613	1546	1480
1136.35	1	-3	1430	1398	1385	1382	1359	1326	1306	1313	1342	1404	1511	1698	2026	2582	3413	4224	4195
1103.56	1	-2	360	311	283	270	273	292	330	401	529	772	1224	1796	1799	1356	993	759	601
1070.78	1	-3	4898	4169	3725	3483	3388	3411	3537	3771	4112	4598	5233	6031	6967	7945	8761	9145	8987
1038.96	0	-2	876	851	830	822	837	896	1036	1334	1883	2393	2146	1572	1132	853	683	577	512
1022.57	0	-3	4733	4371	3942	3570	3285	3067	2897	2764	2654	2565	2490	2430	2386	2353	2333	2326	2329
1006.17	0	-3	2346	2376	2441	2555	2626	2572	2477	2388	2319	2262	2224	2194	2174	2162	2159	2163	2177
986.89	2	-3	2270	2398	2410	2265	2217	2248	2213	2042	1888	1797	1754	1664	1524	1404			
934.82	1	-3	1397	1449	1557	1591	1473	1329	1237	1194	1185	1200	1232	1268	1311	1357	1417	1515	1693
902.04	1	-3	2010	2578	3537	4619	4540	3371	2367	1768	1428	1228	1105	1036	1017	1044	1110	1157	1131
867.33	2	-3	1017	944	944	1020	1197	1507	1777	1729	1436	1165	986	900	880	909	971	1009	1023
804.65	0	-3	1031	1043	1054	1068	1088	1109	1129	1154	1180	1210	1251	1286	1342	1415	1503	1641	1852
788.26	0	-3	2200	2798	3567	3817	3401	2901	2529	2294	2147	2052	1988	1948	1937	1917	1911	1931	1946
771.87	0	-3	1942	1965	2006	2059	2125	2189	2261	2352	2441	2515	2611	2749	2903	3064	3259	3508	3810
755.47	0	-2	418	461	512	574	647	722	796	869	949	1041	1151	1282	1439	1631	1873	2183	2584
739.08	0	-1	311	381	476	604	779	1015	1325	1717	2176	2645	2983	3021	2751	2296	1791	1344	994
722.69	0	-2	7358	5523	4231	3313	2652	2173	1817	1547	1339	1172	1033	922	838	782	753	755	786
706.30	0	-1	85	96	112	134	161	193	231	283	366	512	770	1160	1464	1346	1009	712	504
689.91	0	-2	3599	2632	1994	1572	1286	1088	950	858	797	762	746	743	740	723	683	620	545
673.52	0	-3	4718	4060	3497	3036	2659	2365	2091	1880	1704	1539	1411	1302	1196	1116	1022	957	894
657.12	0	-4	8477	7830	7560	7103	6905	6481	6326	5968	6011	5649	5691	5399	5344	5147	5194	4910	4930
640.73	0	-4	4857	4959	4971	5294	5414	5441	5523	5659	5752	5738	5722	5761	5927	6252	6762	7499	8510
624.34	0	-3	976	1103	1181	1167	1064	927	794	685	596	525	467	419	381	353	334	315	293
607.95	0	-4	2675	2443	2252	2099	1976	1884	1802	1729	1665	1607	1554	1511	1472	1439	1409	1370	1352
591.56	0	-4	1324	1307	1296	1290	1281	1272	1264	1276	1274	1286	1293	1309	1330	1357	1379	1416	1448
575.16	0	-4	1475	1493	1520	1541	1554	1562	1573	1579	1585	1586	1594	1581	1549	1517	1491	1467	1453
558.77	0	-4	1451	1458	1468	1483	1478	1503	1526	1558	1591	1633	1683	1742	1813	1893	1994	2118	2275
542.38	0	-4	2486	2781	3170	3630	4001	4083	3901	3676	3526	3477	3518	3628	3813	4079	4437	4914	5537
525.99	0	-3	643	773	973	1294	1774	2167	1907	1356	972	756	642	572	528	495	468	450	439
510.08	-1	-4	4345	4314	4287	4271	4130	4032	3863	3737	3759	3777	3608	3366	3334	3529	3381	3134	2899
501.88	-1	-4	2724	2705	2794	2862	2582	2483	2469	2421	2617	2765	2818	2798	2634	2552	2652	2718	2689
493.69	-1	-4	2827	2938	2834	2903	3222	3630	3779	3718	3809	3967	4059	4243	4567	4780	5263	5623	5736
485.49	-1	-3	593	625	650	674	757	787	784	836	888	932	964	1000	1029	1075	1146	1234	1347
477.29	-1	-2	146	160	177	195	214	239	266	299	336	379	432	490	557	639	738	862	1015
469.10	-1	-2	1200	1438	1745	2145	2667	3338	4196	5239	6405	7444	7991	7563	6597	5481	4443	3557	2852
460.90	-1	-2	2291	1861	1533	1276	1080	928	800	692	595	513	447	388	336	297	266	239	212
452.71	-1	-3	1913	1744	1569	1423	1325	1238	1140	1089	1020	953	920	864	832	802	774	745	668
444.51	-1	-4	6355	6535	6489	6198	5748	5347	5475	5903	5950	5984	6202	6002	5682	5842	6048	5999	6067
436.31	-1	-4	6263	6671	6834	7028	7567	7684											

a - The column headed cm^{-1} contains the wavenumber of the first $E_m(\tilde{\nu})$ value in the row. The columns headed *XE* and *YE* contain the X-exponent and the Y-exponent, respectively, for the row. The columns headed 0,1,2,⋯16, contain the ordinate values, and the headings give the indices of the ordinate values in the row. In a row which starts with $\tilde{\nu}(0)$, the wavenumber corresponding to the ordinate indexed J is $\tilde{\nu}(J) = \tilde{\nu}(0) - \frac{15798.002}{16384} \cdot J \cdot 2^{XE}$. The $E_m(\tilde{\nu})$ values in that row are the ordinate value shown times 10^{YE}. Thus the entry indexed 16 in the first row of the table shows that $E_m = 372 \times 10^{-6} = 3.72 \times 10^{-4}$ at $\tilde{\nu} = 6499.90 - \frac{15798.002}{16384} \cdot 16 \cdot 2^3 = 6376.48$ cm^{-1}.

b - The $E_m(\tilde{\nu})$ values in the table can be interpolated to the original wavenumber spacing, 0.482117 cm^{-1}, and yield the original $E_m(\tilde{\nu})$ values accurate to 1% below 4500 cm^{-1}, 2% between 4500 and 5000 cm^{-1} and 5% above 5000 cm^{-1}, via the 4-point spline interpolation program TRECOVER[8].

c - The unit of E_m is L mole^{-1} cm^{-1}. Multiply the values by 1000 to convert to the unit cm^2 mol^{-1}.

areas under its bands, and the real and imaginary refractive index spectra will be proposed to Commission I.5 of the International Union of Pure and Applied Chemistry for consideration as secondary infrared intensity standards[3].

2.4 - The accuracy of the results

As noted previously[1], the purpose of this experimental study was to determine the accuracy of the measurements, rather than to obtain the highest possible precision. One must reveal the errors in the measurements in order to reveal accuracy, and to this end as few parameters as possible were kept constant in this work, as detailed previously[1]. A consequence is that the 95% confidence limits for the studies by VB, CDK and YA include the effects of factors that are usually kept constant when high precision is the goal. Thus they include errors that are usually systematic, as well as the random errors on which the use of confidence limits to indicate precision is based. They are therefore expected to reflect the accuracy of the measurements better than is usually the case. The comparison with the measurements from other laboratories should reveal

Table 2.10 - Overall average areas under molar absorption coefficient bands of liquid toluene at 25°C.

Region (cm^{-1})	Area[a]	Estimated accuracy of area[a,b]	Area above baseline[a,c]	Estimated accuracy of area above baseline[a,d]
6307.1 - 5445.0	132	± 9	121	± 6
4763.8 - 4518.9	89.5	± 0.5	59.2	± 0.2
4478.4 - 4145.2	196.8	± 1.0	103.1	± 0.4
4145.2 - 3988.1	160.7	± 1.9	99.2	± 0.6
3988.1 - 3748.9	99.6	± 1.6	26.13	± 0.06
3748.9 - 3694.9	13.73	± 0.11	2.266	± 0.004
3694.9 - 3608.2	29.4	± 0.4	10.9	± 0.1
3608.2 - 3569.1	8.13	± 0.17	1.30	± 0.02
3569.1 - 3531.5	6.86	± 0.12	1.45	± 0.01
3531.5 - 3503.1	4.20	± 0.08	0.490	± 0.005
3484.3 - 3418.7	11.45	± 0.14	2.064	± 0.007
3418.7 - 3357.0	11.64	± 0.12	1.344	± 0.002
3150.1 - 2770.2	4830	± 106	4535	± 100
2759.6 - 2679.1	65.6	± 0.5	29.9	± 0.1
2679.1 - 2563.4	53.5	± 0.3	20.2	± 0.1
2563.4 - 2131.0	171.8	± 2.1	87.0	± 0.9
2131.4 - 2095.8	5.22	± 0.28	0.92	± 0.04
2095.8 - 2049.5	6.69	± 0.39	1.01	± 0.05
1977.6 - 1910.1	143.8	± 0.9	104.4	± 0.6
1910.1 - 1836.9	143.2	± 1.1	85.3	± 0.7
1836.9 - 1754.9	139.7	± 1.4	70.2	± 0.6
1754.9 - 1712.5	52.97	± 0.4	26.4	± 0.2
1713.0 - 1686.4	17.52	± 0.46	1.71	± 0.04
1686.4 - 1668.1	13.41	± 0.34	2.15	± 0.05
1650.3 - 1555.3	497	± 3	320	± 1
1531.7 - 1516.3	90.9	± 3.3	14.3	± 0.4
1513.3 - 1400.1	1730	± 12	1201	± 6
1400.5 - 1338.4	234.0	± 1.6	78.6	± 0.5
1265.6 - 821.0	1266	± 15	891	± 9
790.7 - 775.7	36.7	± 0.4	10.5	± 0.1
769.9 - 710.2	3119	± 250	2823	± 223
710.2 - 660.0	1135	± 87	911	± 69

Table 2.10 - Continued.

Region (cm^{-1})	Area[a]	Estimated accuracy of area[a,b]	Area above baseline[a,c]	Estimated accuracy of area above baseline[a,d]
640.2 - 606.5	20.8	± 1.4	8.58	± 0.10
552.0 - 498.5	27.5	± 0.3	16.48	± 0.07
490.3 - 440.2	480	± 36	456	± 34

a - Unit: L mol^{-1} cm^{-2}. Divide the values by 100 to convert to the unit km mol^{-1}.

b - Calculated from the percent estimated accuracy of the area, which is the same for the $E_m(\tilde{\nu})$ and $k(\tilde{\nu})$ (Table 2.5) bands.

c - The baseline is a straight line drawn through the molar absorption coefficient value at each end of the integration range.

d - Calculated by scaling the maximum deviation from the corresponding area in the $k(\tilde{\nu})$ spectrum (Table 2.5), by the ratio of the $E_m(\tilde{\nu})$ and $k(\tilde{\nu})$ areas.

systematic errors associated with different instrument design, different laboratory, different environment, different cells, different samples, and different person.

2.4.1 - Accuracy of absorption index values.

For the above reasons, we believe the agreement between the results of the different spectroscopists gives a good indication of the accuracy of our final $k(\tilde{\nu})$ values. We use the maximum deviation from the unweighted mean to express this agreement. However, this is not a complete description of the accuracy because we introduce a systematic error by requiring all spectra to have the same $k(\tilde{\nu})$ value at each anchor point[1,4]. Accordingly, we define the estimated accuracy of our final average $k(\tilde{\nu})$ values as the maximum deviation from the unweighted mean plus the uncertainty in the $k(\tilde{\nu})$ values at the anchor points. The uncertainty in $k(\tilde{\nu})$ at the anchor points (column 5 of

Table 2. 11 - Overall average peak heights in the molar absorption coefficient spectrum of liquid toluene at 25°C.

$\tilde{\nu}$ (cm^{-1})	$E_m(\tilde{\nu})$	$\tilde{\nu}$ (cm^{-1})	$E_m(\tilde{\nu})$	$\tilde{\nu}$ (cm^{-1})	$E_m(\tilde{\nu})$	$\tilde{\nu}$ (cm^{-1})	$E_m(\tilde{\nu})$
5949.9	0.622 (10)	3584.6	0.265 (4)	2312.6	0.837 (3)	1460.3	23.6 (16)
4667.0	0.705 (13)	3549.9	0.224 (4)	2280.7	0.507 (7)	1378.9	10.4 (4)
4637.2	0.615 (12)	3519.3	0.173 (3)	2260.5	0.574 (14)	1332.0	1.60 (4)
4612.1	0.924 (15)	3439.7	0.253 (4)	2237.3	0.258 (6)	1312.8	1.68 (4)
4573.6	0.550 (7)	3385.4	0.214 (1)	2207.5	0.351 (12)	1277.7	0.863 (51
4388.8	0.775 (6)	3167.5	0.893 (7)	2185.3	0.353 (7)	1248.7	1.32 (4)
4311.0	0.871 (6)	3104.2	6.63 (9)	2163.7	0.621 (12)	1210.2	3.10 (10)
4244.4	0.840 (3)	3086.4	20.9 (4)	2116.6	0.183 (8)	1178.6	6.64 (27)
4186.4	0.426 (6)	3062.1	24.3 (7)	2068.5	0.198 (9)	1156.0	2.76 (5)
4161.3	0.392 (4)	3026.9	54.3 (12)	2032.0	0.200 (9)	1106.5	4.34 (6)
4132.4	0.420 (7)	2979.2	14.4 (2)	2008.6	0.420 (9)	1081.4	19.0 (4)
4056.7	1.92 (5)	2947.7	17.5 (2)	1991.1	0.814 (11)	1041.5	9.16 (12)
4036.3	2.28 (1)	2919.8	27.9 (5)	1942.1	4.91 (5)	1002.3	2.63 (8)
3980.3	0.504 (9)	2872.6	13.4 (2)	1872.1	2.92 (1)	980.8	2.44 (8)
3951.2	0.489 (9)	2734.1	2.75 (5)	1857.6	4.65 (7)	966.6	2.25 (8)
3923.8	0.495 (7)	2671.7	0.357 (5)	1802.6	4.06 (5)	929.6	1.60 (5)
3909.9	0.492 (9)	2632.0	0.502 (5)	1778.5	1.27 (1)	895.4	4.79 (21)
3869.8	0.504 (7)	2604.7	0.633 (13)	1735.6	2.23 (1)	873.0	1.16 (17)
3847.2	0.564 (14)	2585.9	1.16 (1)	1696.8	0.811 (17)	842.8	1.81 (16)
3812.2	0.389 (7)	2540.4	0.410 (9)	1676.7	0.910 (16)	785.6	3.84 (17)
3786.3	0.394 (7)	2509.2	0.373 (5)	1623.1	4.06 (6)	728.9	305 (25)
3764.0	0.238 (9)	2496.8	0.368 (7)	1604.5	28.9 (11)	694.5	148 (8)
3724.2	0.305 (4)	2465.5	0.369 (5)	1586.7	4.57 (6)	622.1	1.19 (4)
3707.0	0.300 (4)	2412.4	0.740 (7)	1572.2	4.76 (3)	537.8	0.410 (6)
3675.1	0.313 (10)	2389.0	0.611 (9)	1550.4	3.14 (14)	521.0	2.17 (11)
3649.0	0.572 (4)	2360.6	0.968 (17)	1523.6	7.70 (3)	464.2	79.9 (105)
3624.0	0.343 (4)	2335.3	1.08 (2)	1495.6	97.4 (33)		

a - The unit of $E_m(\tilde{\nu})$ is L mole^{-1} cm^{-1}. Multiply the values by 1000 to convert to the unit cm^2 mol^{-1}. The numbers in parentheses are the estimated accuracies in the last digit. The percent estimated accuracy is the same as that of the corresponding $k(\tilde{\nu})$ peak height.

Table 2.1) is ~±1 x10^{-6} above 1600 cm^{-1} , and ~±1 x10^{-5} below 1600 cm^{-1}. The estimated accuracy of $k(\tilde{\nu})$ is expressed as a percentage of $k(\tilde{\nu})$. The percent estimated accuracy of the $E_m(\tilde{\nu})$ values is the same as that of the $k(\tilde{\nu})$ values.

The percent estimated accuracies of the peak $k(\tilde{\nu})$ values are included in Table 2.6. They are generally good, but are poor for the six peaks at 1460, 1278, 873, 843, 728, and 464 cm^{-1}. These peaks are discussed below, and are excluded from the following general comments. The average estimated accuracy is ±2.5% for the heights of the 39 strong, medium and weak peaks below 4100 cm^{-1} which have $k_{max} > 0.002$. The average estimated accuracy is ±1.9% for the heights of the 51 very weak peaks below 4100 cm^{-1} which have $k_{max} < 0.002$. The average estimated accuracy is ±1.3% for the heights of the 11 very weak peaks above 4100 cm^{-1}, but the peaks above 4500 cm^{-1} were measured only in this laboratory.

The heights of the peaks at 1460, 1278, 873, 843, 728, and 464 cm^{-1} have estimated accuracies of 6.9, 6.0, 14.7, 9.1, 8.3, and 13.2%, respectively. There is no obvious reason why the peaks at 1460 and 843 cm^{-1} should have such large uncertainties. The peaks at 1278 and 873 cm^{-1} are very weak and form part of the baseline of surrounding peaks that are more intense. The peak at 728 cm^{-1} was poorly determined. It is very strong, requires cells of ≤ 8 μm path, and only two spectra from one spectroscopist were available. The peak at 464 cm^{-1} is near the transmission limit of the KBr windows but no reason for the poor accuracy is evident. It should be noted that the height of this 464 cm^{-1} peak reported here is about 2.5 times that reported by Jones and co-workers[7].

The peak $k(\tilde{\nu})$ values must be compared with the only calibrated results available, those of Jones and coworkers in Ref. 7. Of the 94 k_{max} values in Table 2.6 for which there is a calibrated value, 29 lie outside the evaluated uncertainty limits of Ref. 7. They are at the wavenumbers 3675, 3550, 3519, 3385, 3168, 3027, 2979, 2948, 2872, 2361, 2164, 2032, 1942, 1858, 1572, 1524, 1460, 1378, 1332, 1313, 1107, 1041, 895, 843, 729, 695, 538, 521, 464 cm^{-1}. The three values at 1460, 843, and 464 cm^{-1} had unusually poor accuracy in this work. Only the 13 peaks underlined in the above list disagree by more than the combined error limits, and only the 464 cm^{-1} peak is in serious disagreement.

The $k(\tilde{\nu})$ values in the baseline are not known as accurately as those in regions of significant absorption, except at the anchor points. From the agreement between different workers and the uncertainties in the anchor point values, we estimate the accuracy of the baseline $k(\tilde{\nu})$ values to be ±~2 x10^{-6} above 1600 cm^{-1}, and ±~1.5 x 10^{-5} below 1600 cm^{-1}. This corresponds to between ±3 and ±10% of the $k(\tilde{\nu})$ values in the baseline.

2.4.2 - Accuracy of areas.

The percent estimated accuracies of the areas under the $k(\tilde{\nu})$ bands are given in Table 2.5. Each was calculated by multiplying the uncertainty in $k(\tilde{\nu})$ at the anchor points (Table 2.1) by the integration range, adding the maximum deviation of the spectroscopist averages from the unweighted average (Table 2.5), and expressing the result as a percentage of the area. As was the situation for benzene[1], the uncertainty at the anchor points contributes about 0.5% to the percent estimated accuracies. The percent estimated accuracy of the area under an $E_m(\tilde{\nu})$ band equals that of the corresponding $k(\tilde{\nu})$ band. The estimated accuracies, rather than the percent estimated accuracies, of the $E_m(\tilde{\nu})$ bands are given in Table 2.10.

The average accuracy of all of the band areas is ±2.4% and it is an excellent ±1.2% for the eleven regions between 3150 and 775 cm^{-1} which contain a band with $0.002<k_{max}<0.112$.

The area we prefer for use as a secondary standard is the area under the molar absorption coefficient spectrum above a linear baseline drawn through the E_m values at the integration limits. This area is given in Table 2.10 with its estimated accuracy. The percent estimated accuracy of this area is the same as the maximum deviation of a spectroscopist's average area under a $k(\tilde{\nu})$ band from the unweighted average (Table 2.5) expressed as a percentage of the average.

2.4.3 - Accuracy of real refractive index values.

Three factors contribute to the accuracy of our $n(\tilde{\nu})$ values. First, our Kramers-Kronig transform procedure has an intrinsic accuracy of about 0.05%[11]. Second, we used $n(8000\ cm^{-1}) = 1.4773 \pm 0.0004$, an accuracy of 0.03%. Third, the approximately 2.5% accuracy of the absorption indices yields an approximately 2.5% accuracy in the values of $\Delta n = n(\tilde{\nu})\text{-}n(8000\ cm^{-1})$ from the Kramers-Kronig transform, which corresponds to an error of ~ 0.08% in $n(\tilde{\nu})$. The sum of these contributions gives

~0.2% as the estimated accuracy of our $n(\tilde{\nu})$ values.

2.5 - Summary

Transmission measurements by 6 spectroscopists in 4 laboratories have been recorded on four different instruments made by three different manufacturers. They have been converted to absorption index spectra which were compared and averaged, and the real refractive index and molar absorption coefficient spectra have been calculated from the average. The percent estimated accuracy of the absorption index and molar absorption coefficient values is on average ±2.5% at the peaks of the strong, medium and weak bands with $0.002<k_{\max}<0.112$, and ±1.9% and ±1.3% at the peaks of the very weak bands below and above 4100 cm^{-1}, respectively. The baseline values are accurate to between 3 and 10%. The percent estimated accuracy of areas under bands or groups of bands in $k(\tilde{\nu})$ and $E_m(\tilde{\nu})$ spectra is ±2.4% on average, and averages ±1.2% for the bands between 3150 and 775 cm^{-1} with $0.002< k_{\max} <0.112$. The estimated accuracy of the real refractive index values is 0.2%. For long-term reference, the complete numerical data are presented in Compact Table format[8], which is readable and allows the original spectra to be recovered by interpolation without loss of accuracy. The complete final $k(\tilde{\nu})$, $n(\tilde{\nu})$, and $E_m(\tilde{\nu})$ spectra obtained in this work are available on diskette from the authors. To provide continuity over the longer term, it is anticipated that they will be made available in the future on an internationally accessible data base.

2.6 - References

1. J.E. Bertie, R.N. Jones, and C.D. Keefe, Appl. Spectrosc., **47**, 891 (1993).
2. J.E. Bertie, R.N. Jones, and Y. Apelblat, Appl. Spectrosc., **48**, 144 (1994).
3. J.E. Bertie, C.D. Keefe, R.N. Jones, H.H. Mantsch, and D.J. Moffatt, Appl. Spectrosc., **45**, 1233 (1991).
4. J.E. Bertie, C.D. Keefe, and R.N. Jones, Can. J. Chem., **69**, 1609 (1991).
5. J.E. Bertie, R.N. Jones, and V. Behnam, Appl. Spectrosc., **40**, 427 (1986).
6. J.E. Bertie, R.N. Jones, and V. Behnam, Appl. Spectrosc., **39**, 401 (1985).
7. T.G. Goplen, D.G. Cameron, and R.N. Jones, Appl. Spectrosc., **34**, 657 (1980).
8. J.E. Bertie, R.N. Jones and Y. Apelblat, Appl. Spectrosc., **47**, 1989 (1993).
9. J. Timmermans. *Physico-Chemical Constants of Pure Organic Compounds,* (Elsevier, Amsterdam, 1965), Vol. 2, p. 100.
10. J. Timmermans. *Physico-Chemical Constants of Pure Organic Compounds,* (Elsevier, New York, 1950), pp. 152 - 153.
11. J.E. Bertie and S.L. Zhang. Can. J. Chem., **70**, 520 (1992).

Chapter 3 - Accurate Optical Constants and Molar Absorption Coefficients Between 4800 and 450 cm^{-1} of Chlorobenzene at 25°C from Spectra Recorded in Several Laboratories*

3.1 - Introduction

In previous papers[1,2] we have reported absolute infrared absorption intensities of benzene and toluene. The quantities reported have been the spectra of the real and imaginary refractive indices and the molar absorption coefficient, and the areas under bands in the imaginary refractive index and molar absorption coefficient spectra. The imaginary refractive index is also called the absorption index[3]. In this paper we report these same quantities between 4800 and 450 cm^{-1} for chlorobenzene at 25°C. The methods used were the same as have been described in detail for the spectra of benzene[1,4] and toluene[2].

For selected bands, the refractive indices, molar absorption coefficients, and areas under molar absorption coefficient bands, will be submitted to Commission I.5 of the International Union of Pure and Applied Chemistry for consideration as secondary infrared intensity standards for liquids[5].

---

* A version of this chapter has been published. Bertie, Jones and Apelblat, Appl. Spectrosc., **48**, 144 (1994).

3.2 - Methods and results

The chlorobenzene in this laboratory was of spectroscopic or reagent grade. Samples were purified by fractional freezing one to three times and were checked by gas chromatography and infrared spectroscopy. No impurities were detected. The samples were kept over molecular sieve to ensure dryness.

Experimental absorbance spectra of chlorobenzene were obtained from fixed path length cells with KBr windows and path lengths between 11 and 1500 μm and from a variable path length cell with NaCl windows and path lengths between 100 and 500 μm. Spectra were used only in the regions where the absorbances of the strongest bands were between 0.3 and 2.0.

To determine the linear absorption coefficients at the anchor points[4], spectra with strong baseline absorbance were also obtained in cells with path lengths from 50 μm to 3.5 mm. Table 3.1 summarizes the wavenumbers of the anchor points, the path lengths of the cells, the measured linear absorption coefficients and their 95% confidence limits, and the uncertainty in the absorption index, $k(\tilde{\nu})$, that results from the precision of the linear absorption coefficients.

In addition to the experimental absorbance spectra recorded in our laboratory, spectra recorded in this laboratory in 1984-5 by V. Behnam, and reported previously[6,7], were also reprocessed by our current improved methods to yield the refractive indices . In addition, three spectroscopists in three other laboratories kindly recorded and supplied experimental absorbance spectra of chlorobenzene. One set was recorded with 2 cm^{-1}

Table 3.1 - Linear Absorption coefficients at the anchor points of liquid chlorobenzene at 25°C

Wavenumber (cm^{-1})	cell path lengths (mm)	$K(\tilde{\nu})$ (cm^{-1})	95% confidence limit	Uncertainty in $k(\tilde{\nu})$
4795.1	1.5 - 3.5	0.32	0.09	3.5×10^{-6}
4475.0	1.5 - 3.5	0.617	0.021	8.6×10^{-7}
3849.2	1.5 - 3.5	1.303	0.031	1.5×10^{-6}
3333.3	1.5 - 3.5	0.682	0.025	1.4×10^{-6}
2931.2	1.3 - 3.5	3.152	0.021	1.3×10^{-6}
1908.2	0.7 - 3.5	4.723	0.017	1.6×10^{-6}
1835.9	0.7 - 3.5	4.428	0.021	2.1×10^{-6}
1754.9	0.7 - 3.5	5.846	0.018	1.9×10^{-6}
1676.8	0.7 - 3.5	4.114	0.017	1.9×10^{-6}
1630.5	0.5 - 1.5	11.64	0.03	3.6×10^{-6}
1534.0	0.5 - 1.7	9.081	0.030	3.6×10^{-6}
1404.8	0.5 - 1.7	7.056	0.032	4.2×10^{-6}
1345.1	1.3 - 3.5	3.526	0.016	2.2×10^{-6}
1251.5	0.5 - 3.5	6.235	0.025	3.7×10^{-6}
1197.5	0.5 - 1.7	9.545	0.020	3.1×10^{-6}
1141.6	0.2 - 0.7	17.65	0.10	1.7×10^{-5}
1045.2	0.2 - 1.3	16.52	0.09	1.6×10^{-5}
949.8	0.5 - 1.5	14.05	0.03	6.0×10^{-6}
801.3	0.2 - 1.5	12.66	0.08	1.7×10^{-5}
717.4	~0.05	65.7	0.6	1.5×10^{-4}
630.6	0.5 - 1.5	5.46	0.06	1.6×10^{-5}
528.4	~ 1.5	2.08	0.05	1.6×10^{-5}
437.8	0.5 - 1.5	7.47	0.20	8.5×10^{-5}

nominal resolution on a Nicolet 170SX spectrometer with a mercury cadmium telluride detector at 77K and Happ-Genzel apodization. For that work, the chlorobenzene was HPLC grade. The second set was recorded with 2 cm^{-1} nominal resolution on a Nicolet 510P spectrometer with room-temperature deuterated triglycine sulfate detector and

Table 3.2 - Pathlengths, high-wavenumber refractive index, and number of spectra from each spectroscopist[a], for the regions processed.

Region (cm^{-1})	Pathlengths (μm)	n_∞ [b]	YA	VB	A	B	C	Total
4800 - 3990	200-700	1.501	18	5	0	1	2	26
4000 - 3325	500-700	1.503	18	5	0	0	0	23
3335 - 2925	30-100	1.495	24	6	15	0	0	45
2940 - 1620	100-200	1.496	5	5	5	1	0	16
1640 - 1390	11-13	1.481	9	6	0	0	0	15
1415 - 1130	200-700	1.487	13	5	0	1	2	21
1150 - 935	11-13	1.473	5	6	0	0	0	11
960 - 790	25-100	1.493	14	6	15	1	2	38
810 - 705	~8	1.450	0	0	5	0	0	5
725 - 610	8-13	1.596	5	4	5	0	0	14
635 - 520	100-500	1.558	7	3	0	1	0	11
535 - 420	11-13	1.520	5	3	0	0	0	8

a - The spectroscopists are identified as YA, VB, A, B and C (see text).

b.- n_∞ is the real refractive index at the highest wavenumber in the region.

Happ-Genzel apodization. The chlorobenzene was 99%+ grade. No experimental details are available for the third set, but they were clearly run under comparable conditions. None of the spectra showed unexpected peaks.

Table 3.2 shows the spectral regions that were used in the computations, together with the cell thicknesses used, the value of n_∞, and the number of spectra from each spectroscopist, for each region. The value of n_∞ for each region is required by the Kramers-Kronig transform in program RNJ46A[1,4]. The spectra recorded in this laboratory are labeled YA for Y. Apelblat, and VB for V. Behnam. The other collaborators are identified by A, B and C. The real refractive index at the highest wavenumber in each region, n_∞, was taken from tables of $n(\tilde{\nu})$ in this laboratory which were calculated from the $k(\tilde{\nu})$ spectra in reference 7.

3.2.1 Absorption index spectrum.

The experimental absorbance spectra of each spectroscopist were converted to absorption index, $k(\tilde{\nu})$, spectra by program RNJ46A[1,4]. The peak heights, wavenumbers and areas were measured for each $k(\tilde{\nu})$ spectrum. For each region (Table 3.2), the $k(\tilde{\nu})$ spectra were averaged to give a single spectrum from each spectroscopist. Table 3.3 gives the peak wavenumber of each band and, for each spectroscopist, the average peak heights with their 95% confidence limits. The peak heights from different spectroscopists are in good agreement although, as was found for benzene[1] and toluene[2], the existence of systematic errors at the few percent level is indicated by the disagreement between spectroscopists sometimes being outside the combined confidence limits.

For each region, the average spectra from the different spectroscopists were themselves averaged to yield an unweighted average $k(\tilde{\nu})$ spectrum. The unweighted average peak heights are given in Table 3.4 with the maximum deviation of any spectroscopist's average from the unweighted average in parentheses. A weighted average $k(\tilde{\nu})$ spectrum was also calculated, with the weighting factor being the number of spectra which contributed to the spectroscopist's average. The weighted average peak heights are listed in Table 3.4 with their 95% confidence limits in parentheses. For

Table 3.3 - Spectroscopist average absorption index peak heights.[a]

$\tilde{\nu}$ (cm^{-1})	YA	VB	A	B	C
4656.4	0.000495(38)	0.000504(26)		0.000497	
4622.0	0.000163(12)	0.000168(10)		0.000168	
4595.3	0.000108(8)	0.000110(7)		0.000107	
4574.7	0.000243(14)	0.000251(10)		0.000244	
4514.6	0.000075(3)	0.000076(2)		0.000075	
4252.7	0.000111(1)	0.000111(1)		0.000109	0.000105
4145.7	0.000271(3)	0.000271(1)		0.000268	0.000262
4077.4	0.00120(10)	0.00117(5)		0.00111	0.00105
4066.5	0.00108(5)	0.00115(4)		0.00110	0.00105
4058.7	0.00129(14)	0.00120(6)		0.00118	0.00112
4000.5	0.000253(4)	0.000253(2)		0.000249	0.000246
3917.8	0.000103(2)	0.000102(1)			
3899.6	0.000109(1)	0.000109(1)			
3785.1	0.000354(4)	0.000355(2)			
3772.3	0.000265(2)	0.000260(1)			
3699.4	0.000521(7)	0.000532(6)			
3653.3	0.000104(2)	0.000107(1)			
3636.9	0.000137(2)	0.000138(1)			
3613.6	0.000143(2)	0.000145(1)			
3488.8	0.000080(1)	0.000078(1)			
3464.4	0.000077(1)	0.000075(1)			
3368.0	0.000065(1)	0.000065(1)			
3165.5	0.000658(7)	0.000664(2)	0.000671(7)		
3083.1	0.00659(2)	0.00682(3)	0.00671(3)		
3069.5	0.00981(2)	0.01007(5)	0.00989(5)		
3058.5	0.00811(2)	0.00793(5)	0.00793(5)		
3025.8	0.00316(1)	0.00319(2)	0.00318(1)		
3016.4	0.00279(1)	0.00273(1)	0.00275(1)		
2949.5	0.000338(4)	0.000337(2)	0.000343(2)		
2919.0	0.000439(3)	0.000426(1)	0.000417(1)	0.000425	
2885.6	0.000270(6)	0.000277(1)	0.000274(1)	0.000268	
2877.0	0.000284(5)	0.000279(1)	0.000282(1)	0.000275	
2849.2	0.000260(3)	0.000250(1)	0.000251(1)	0.000250	
2795.1	0.000102(8)	0.000099(2)	0.000103(1)	0.000093	
2772.9	0.000302(9)	0.000303(1)	0.000299(1)	0.000293	
2756.0	0.000128(7)	0.000126(1)	0.000129(1)	0.000121	
2739.0	0.000111(8)	0.000111(1)	0.000112(1)	0.000104	
2714.2	0.000087(8)	0.000089(1)	0.000092(1)	0.000084	

Table 3.3 - Continued

$\tilde{\nu}$ (cm^{-1})	YA	VB	A	B	C
2703.0	0.000094(5)	0.000096(2)	0.000098(1)	0.000090	
2663.5	0.000460(6)	0.000464(2)	0.000470(1)	0.000456	
2648.1	0.000302(8)	0.000299(1)	0.000302(1)	0.000292	
2616.3	0.000426(5)	0.000420(2)	0.000418(1)	0.000410	
2599.8	0.000409(7)	0.000415(1)	0.000419(1)	0.000407	
2582.2	0.000336(5)	0.000328(1)	0.000324(1)	0.000319	
2557.4	0.000295(5)	0.000295(1)	0.000302(1)	0.000292	
2544.3	0.000335(6)	0.000336(1)	0.000335(1)	0.000326	
2510.9	0.000103(6)	0.000107(1)	0.000106(1)	0.000100	
2496.0	0.000146(6)	0.000148(1)	0.000152(1)	0.000142	
2471.4	0.000198(6)	0.000199(1)	0.000201(1)	0.000193	
2446.6	0.000152(8)	0.000154(1)	0.000155(1)	0.000148	
2427.3	0.000195(5)	0.000197(1)	0.000201(1)	0.000193	
2406.4	0.000337(4)	0.000338(1)	0.000339(1)	0.000331	
2390.3	0.000452(7)	0.000452(1)	0.000453(1)	0.000444	
2365.7	0.000193(5)	0.000196(1)	0.000210(12)	0.000208	
2331.0	0.000766(5)	0.000770(1)	0.000787(8)	0.000776	
2319.8	0.000781(7)	0.000768(1)	0.000781(3)	0.000770	
2271.8	0.000318(6)	0.000321(1)	0.000320(1)	0.000314	
2240.5	0.000571(7)	0.000569(1)	0.000566(2)	0.000557	
2194.0	0.000187(7)	0.000189(1)	0.000185(1)	0.000182	
2178.7	0.000360(6)	0.000363(1)	0.000355(1)	0.000351	
2150.5	0.000145(6)	0.000148(1)	0.000145(1)	0.000142	
2132.5	0.000086(5)	0.000090(1)	0.000085(1)	0.000084	
2089.1	0.000140(6)	0.000145(1)	0.000139(1)	0.000137	
2058.2	0.000131(5)	0.000138(1)	0.000131(1)	0.000130	
2045.6	0.000149(6)	0.000149(1)	0.000143(1)	0.000145	
2023.7	0.000249(5)	0.000248(1)	0.000236(1)	0.000236	
2002.5	0.000279(5)	0.000289(1)	0.000284(1)	0.000283	
1962.2	0.00207(1)	0.00207(1)	0.00209(1)	0.00206	
1942.9	0.00410(3)	0.00406(4)	0.00413(1)	0.00409	
1881.4	0.00240(1)	0.00240(1)	0.00240(1)	0.00238	
1861.9	0.00441(4)	0.00444(6)	0.00443(1)	0.00438	
1787.8	0.00354(3)	0.00357(2)	0.00358(1)	0.00354	
1730.5	0.00345(2)	0.00349(3)	0.00346(1)	0.00342	
1685.9	0.000663(8)	0.000649(1)	0.000646(1)	0.000649	
1645.5	0.00229(1)	0.00227(1)	0.00227(1)	0.00225	
1622.2	0.00270(3)	0.00263(2)			

Table 3.3 - Continued

$\tilde{\nu}$ (cm^{-1})	YA	VB	A	B	C
1583.8	0.0826(5)	0.0803(4)			
1566.1	0.0149(1)	0.0146(1)			
1477.4	0.245(3)	0.262(22)			
1445.4	0.110(1)	0.097(1)			
1387.1	0.00303(1)	0.00304(1)		0.00303	0.00304
1370.7	0.00303(1)	0.00303(1)		0.00302	0.00304
1325.2	0.00252(1)	0.00254(1)		0.00248	0.00254
1298.1	0.00377(2)	0.00373(1)		0.00369	0.00383
1272.5	0.00366(5)	0.00385(1)		0.00373	0.00377
1235.2	0.00278(1)	0.00277(1)		0.00276	0.00278
1210.9	0.00233(1)	0.00235(1)		0.00234	0.00236
1171.6	0.00522(1)	0.00521(1)		0.00512	0.00527
1156.4	0.00459(1)	0.00459(2)		0.00454	0.00466
1122.7	0.0265(1)	0.0270(1)			
1083.2	0.180(1)	0.176(1)			
1068.1	0.0529(2)	0.0513(2)			
1022.6	0.197(1)	0.175(3)			
1001.9	0.0461(2)	0.0426(2)			
963.7	0.00384(4)	0.00369(6)			
935.0	0.00785(1)	0.00784(2)	0.00780(1)	0.00837	0.00787
902.9	0.0315(1)	0.0317(1)	0.0312(1)	0.0330	0.0320
866.3	0.00304(1)	0.00302(5)	0.00294(1)	0.00291	0.00291
830.0	0.00585(2)	0.00587(6)	0.00576(1)	0.00594	0.00554
812.2	0.00354(2)	0.00352(4)	0.00349(1)	0.00353	0.00346
739.5			0.747(16)		
702.2	0.305(2)	0.292(4)	0.320(2)		
684.8	0.372(2)	0.353(12)	0.395(2)		
661.9	0.0170(1)	0.0171(4)	0.0185(1)		
614.0	0.00847(5)	0.00792(2)		0.00776	
547.7	0.00100(1)	0.00098(1)		0.00093	
533.7	0.00141(1)	0.00138(2)		0.00140	
467.8	0.289(3)	0.275(6)			

a The numbers in parentheses are the 95% confidence limits in the last digit.

reference, we include in Table 3.4 the peak heights of chlorobenzene published previously from this laboratory[7] and the results of the only measurements that have been made against a primary standard[8]. The latter have an evaluated uncertainty[8] of ~6%.

Table 3.4 - Overall average absorption index peak heights.

$\tilde{\nu}$ ($\mathrm{cm^{-1}}$)	Weighted average[a]	Unweighted average[b]	Uncertainty due to anchor points[c]	% estimated accuracy	Ref. 8	Ref. 7
4656.4	0.000497 (28)	0.000499 (42)	2.2×10^{-6}	1.4		
4622.0	0.000165 (9)	0.000166 (3)	2.2×10^{-6}	3.1		
4593.3	0.000108 (6)	0.000108 (2)	2.2×10^{-6}	3.9		
4574.7	0.000245 (10)	0.000246 (5)	2.2×10^{-6}	2.9		
4514.6	0.000075 (3)	0.000076 (2)	2.2×10^{-6}	5.5		
4252.7	0.000110 (1)	0.000109 (4)	1.2×10^{-6}	4.8		
4145.7	0.000270 (2)	0.000268 (6)	1.2×10^{-6}	2.7	0.000276 (21)	
4077.4	0.00118 (7)	0.00113 (8)	1.2×10^{-6}	7.2	0.00113 (5)	
4066.5	0.00110 (3)	0.00110 (5)	1.2×10^{-6}	4.7	0.00115 (5)	
4058.7	0.00125 (9)	0.00120 (9)	1.2×10^{-6}	7.6	0.00112 (5)	
4000.5	0.000252 (3)	0.000250 (4)	1.2×10^{-6}	2.1	0.000252 (19)	
3917.4	0.000103 (2)	0.000103 (1)	1.2×10^{-6}	2.1	0.000110 (9)	0.000103 (1)
3899.6	0.000109 (1)	0.000109 (1)	1.2×10^{-6}	2.0	0.000115 (9)	0.000109 (1)
3785.1	0.000354 (3)	0.000354 (1)	1.5×10^{-6}	0.7	0.000352 (28)	0.000356 (2)
3772.3	0.000264 (2)	0.000263 (3)	1.5×10^{-6}	1.7	0.000270 (20)	0.000261 (2)
3699.4	0.000524 (6)	0.000527 (6)	1.5×10^{-6}	1.4	0.000541 (37)	0.000532 (4)
3653.3	0.000105 (1)	0.000106 (2)	1.5×10^{-6}	3.3	0.000109 (9)	0.000107 (2)
3636.9	0.000137 (1)	0.000138 (1)	1.5×10^{-6}	1.8	0.000144 (11)	0.000138 (2)
3613.6	0.000143 (2)	0.000144 (1)	1.5×10^{-6}	1.7	0.000146 (11)	0.000145 (1)
3488.8	0.000079 (1)	0.000079 (1)	$1.5 \times 10^{-}$	3.2	0.000083 (7)	0.000077 (1)
3464.4	0.000077 (1)	0.000076 (1)	1.5×10^{-6}	3.3	0.000082 (7)	0.000075 (1)
3368.0	0.000065 (1)	0.000065 (1)	1.5×10^{-6}	3.8	0.000071 (7)	0.000064 (1)
3165.5	0.000663 (4)	0.000664 (7)	1.4×10^{-6}	1.3	0.000709 (32)	
3083.1	0.00666 (3)	0.00671 (12)	1.4×10^{-6}	1.8	0.00670 (30)	0.00689 (2)
3069.5	0.00987 (3)	0.00992 (15)	1.4×10^{-6}	1.5	0.00991 (20)	0.01015 (4)
3058.5	0.00802 (3)	0.00799 (12)	1.4×10^{-6}	1.5	0.00796 (17)	0.00800 (3)
3025.8	0.00317 (1)	0.00318 (2)	1.4×10^{-6}	0.7	0.00321 (14)	0.00325 (1)
3016.4	0.00277 (1)	0.00276 (3)	1.4×10^{-6}	1.1	0.00278 (13)	0.00279 (1)
2949.5	0.000339 (2)	0.000339 (3)	1.4×10^{-6}	1.3	0.000364 (27)	
2919.0	0.000427 (5)	0.000427 (12)	1.5×10^{-6}	3.2	0.000444 (35)	

Table 3.4 - Continued

$\tilde{\nu}$ (cm^{-1})	Weighted average[a]	Unweighted average[b]	Uncertainty due to anchor points[c]	% estimated accuracy	Ref. 8	Ref. 7
2885.6	0.000274 (2)	0.000273 (5)	1.5 x 10^{-6}	2.4	0.000300 (22)	
2877.0	0.000281 (2)	0.000280 (5)	1.5 x 10^{-6}	2.3	0.000300 (22)	
2849.2	0.000253 (3)	0.000253 (7)	1.5 x 10^{-6}	3.4	0.000268 (20)	
2795.1	0.000101 (2)	0.000099 (4)	1.5 x 10^{-6}	5.6	0.000117 (10)	
2772.9	0.000301 (2)	0.000299 (6)	1.5 x 10^{-6}	2.5	0.000301 (22)	
2756.0	0.000127 (2)	0.000126 (5)	1.5 x 10^{-6}	5.2	0.000148 (11)	
2739.0	0.000111 (2)	0.000109 (5)	1.5 x 10^{-6}	6.0	0.000128 (10)	
2714.2	0.000089 (2)	0.000088 (4)	1.5 x 10^{-6}	6.3	0.000108 (9)	
2703.0	0.000096 (2)	0.000094 (4)	1.5 x 10^{-6}	5.9	0.000115 (9)	
2663.5	0.000464 (3)	0.000462 (8)	1.5 x 10^{-6}	2.1	0.000480 (38)	0.000470 (2)
2648.1	0.000300 (2)	0.000299 (7)	1.5 x 10^{-6}	2.8	0.000310 (23)	
1616.3	0.000421 (3)	0.000418 (8)	1.5 x 10^{-6}	2.3	0.000437 (33)	0.000425 (1)
2599.8	0.000414 (3)	0.000413 (6)	1.5 x 10^{-6}	1.8	0.000434 (33)	0.000421 (1)
2582.2	0.00329 (3)	0.000327 (9)	1.5 x 10^{-6}	3.2	0.000344 (25)	0.000333 (1)
2557.4	0.000297 (2)	0.000296 (6)	1.5 x 10^{-6}	2.5	0.000316 (23)	
2544.3	0.000335 (2)	0.000333 (7)	1.5 x 10^{-6}	2.6	0.000356 (26)	0.000341 (1)
2510.9	0.000105 (2)	0.000104 (4)	1.5 x 10^{-6}	5.3	0.000124 (11)	
2496.0	0.000148 (2)	0.000147 (5)	1.5 x 10^{-6}	4.4	0.000161 (13)	0.000153 (1)
2471.4	0.000199 (2)	0.000198 (5)	1.5 x 10^{-6}	3.3	0.000219 (10)	0.000204 (1)
2446.6	0.000153 (2)	0.000152 (4)	1.5 x 10^{-6}	3.6	0.000171 (13)	
2427.3	0.000197 (2)	0.000197 (4)	1.5 x 10^{-6}	2.8	0.000216 (16)	
2406.4	0.000337 (1)	0.000336 (5)	1.5 x 10^{-6}	1.9	0.000344 (25)	0.000342 (1)
2390.3	0.000452 (2)	0.000450 (6)	1.5 x 10^{-6}	1.7	0.000466 (35)	0.000456 (2)
2365.7	0.000200 (5)	0.000202 (9)	1.5 x 10^{-6}	5.2	0.000220 (17)	
2331.0	0.000774 (5)	0.000775 (12)	1.5 x 10^{-6}	1.7	0.000801 (55)	0.000775 (1)
2319.8	0.000776 (4)	0.000775 (7)	1.5 x 10^{-6}	1.1	0.000842	0.000773 (1)
2271.8	0.000319 (2)	0.000318 (4)	1.5 x 10^{-6}	1.7	0.000331 (24)	0.000325 (1)
2240.5	0.000568 (2)	0.000566 (9)	1.5 x 10^{-6}	1.9	0.000598 (48)	0.000573 (1)
2194.0	0.000187 (2)	0.000186 (4)	1.5 x 10^{-6}	3.0	0.000206 (16)	0.000192 (2)
2178.7	0.000359 (3)	0.000357 (6)	1.5 x 10^{-6}	2.1	0.000376 (27)	0.000366(1)

Table 3.4 - Continued

$\tilde{\nu}$ (cm^{-1})	Weighted average[a]	Unweighted average[b]	Uncertainty due to anchor points[c]	% estimated accuracy	Ref. 8	Ref. 7
2150.5	0.000145 (2)	0.000145 (3)	1.5×10^{-6}	3.1	0.000170 (14)	
2132.5	0.000087 (2)	0.000086 (4)	1.5×10^{-6}	6.4	0.000108 (10)	
2089.1	0.000141 (2)	0.000140 (5)	1.5×10^{-6}	4.6	0.000154 (13)	0.000147 (1)
2058.2	0.000133 (2)	0.000132 (6)	1.5×10^{-6}	5.7	0.000149 (13)	
2045.6	0.000147 (2)	0.000147 (4)	1.5×10^{-6}	3.7	0.000164 (14)	0.000150 (1)
2023.7	0.000244 (3)	0.000242 (7)	1.5×10^{-6}	3.5	0.000266 (20)	0.000249 (1)
2002.5	0.000284 (2)	0.000284 (5)	1.5×10^{-6}	2.3	0.000306 (23)	
1962.2	0.00208 (1)	0.00207 (2)	1.5×10^{-6}	1.0	0.00213 (8)	
1942.9	0.00410 (2)	0.00409 (4)	1.5×10^{-6}	1.0	0.00441 (11)	
1881.4	0.00240 (1)	0.00239 (1)	1.9×10^{-6}	0.5	0.00243 (9)	0.00239 (1)
1861.9	0.00442 (2)	0.00442 (4)	1.9×10^{-6}	0.9	0.00465 (12)	0.00445 (3)
1787.8	0.00356 (1)	0.00355 (3)	2.0×10^{-6}	0.9	0.00357 (13)	0.00355 (2)
1730.5	0.00346 (1)	0.00345 (3)	1.9×10^{-6}	0.9	0.00347 (13)	0.00348 (1)
1685.9	0.000652 (4)	0.000652 (11)	1.9×10^{-6}	2.0	0.000673 (25)	0.00652 (1)
1645.5	0.00227 (1)	0.00227 (2)	2.8×10^{-6}	1.0	0.00233 (8)	0.00230 (1)
1622.2	0.00267 (3)	0.00267 (4)	3.6×10^{-6}	1.6	0.00267 (10)	0.00264 (1)
1583.8	0.0816 (7)	0.0814 (12)	3.6×10^{-6}	1.5	0.0811 (20)	0.0805 (5)
1566.1	0.0148 (1)	0.0147 (2)	3.6×10^{-6}	1.4	0.0141 (3)	
1477.4	0.252 (9)	0.254 (9)	3.9×10^{-6}	3.5	0.323 (8)	
1445.4	0.105 (4)	0.103 (7)	3.9×10^{-6}	6.8	0.109 (3)	0.098 (1)
1387.1	0.00303 (1)	0.00303 (1)	3.2×10^{-6}	0.4	0.00315 (111)	
1370.7	0.00303 (1)	0.00303 (1)	3.2×10^{-6}	0.4	0.00313 (12)	
1325.2	0.00253 (1)	0.00252 (4)	3.0×10^{-6}	1.7	0.00268 (10)	
1298.1	0.00376 (5)	0.00375 (8)	3.0×10^{-6}	2.2	0.00390 (15)	
1272.5	0.00372 (5)	0.00375 (10)	3.0×10^{-6}	2.7	0.00402 (15)	
1235.2	0.00278 (1)	0.00277 (1)	3.4×10^{-6}	0.5	0.00285 (11)	
1210.9	0.00234 (1)	0.00235 (2)	3.4×10^{-6}	1.0	0.00246 (9)	
1171.6	0.00522 (1)	0.00520 (8)	1.0×10^{-5}	1.7	0.00532 (20)	
1156.4	0.00459 (1)	0.00459 (7)	1.0×10^{-5}	1.7	0.00480 (18)	
1122.7	0.0267 (2)	0.0268 (3)	1.7×10^{-5}	1.2	0.0258 (5)	

Table 3.4 - Continued

$\tilde{\nu}$ (cm^{-1})	Weighted average[a]	Unweighted average[b]	Uncertainty due to anchor points[c]	% estimated accuracy	Ref. 8	Ref. 7
1083.2	0.178 (2)	0.178 (2)	1.7 x 10^{-5}	1.1	0.179 (5)	0.176 (1)
1068.1	0.0520 (6)	0.0521 (8)	1.7 x 10^{-5}	1.6	0.0515 (10)	0.0517 (3)
1022.6	0.185 (8)	0.186 (11)	1.1 x 10^{-5}	5.9	0.194 (5)	0.175 (2)
1001.9	0.0442 (12)	0.0444 (17)	1.1 x 10^{-5}	3.9	0.0434 (8)	0.0427 (4)
963.7	0.00376 (6)	0.00376 (8)	1.1 x 10^{-5}	2.4	0.00395 (15)	
935.0	0.00784 (3)	0.00795 (42)	1.2 x 10^{-5}	5.4	0.00812 (24)	
902.9	0.0315 (1)	0.0319 (11)	1.2 x 10^{-5}	3.5	0.0304 (6)	
866.3	0.00299 (2)	0.00296 (8)	1.2 x 10^{-5}	3.1	0.00314 (12)	
830.0	0.00582 (2)	0.00579 (25)	1.2 x 10^{-5}	4.5	0.00609 (23)	
812.2	0.00352 (1)	0.00351 (5)	1.2 x 10^{-5}	1.8	0.00366 (14)	
739.5	0.747 (16)	0.747 (16)	8.4 x 10^{-5}	2.2	0.785 (20)	
702.2	0.307 (7)	0.306 (14)	8.4 x 10^{-5}	4.6	0.311 (8)	0.293 (3)
684.8	0.375 (10)	0.373 (22)	8.3 x 10^{-5}	5.9	0.389 (11)	0.355 (6)
661.9	0.0176 (4)	0.0175 (10)	8.3 x 10^{-5}	6.2	0.0175 (4)	
614.0	0.00826 (20)	0.00805 (42)	1.6 x 10^{-5}	5.4	0.00902 (30)	
547.7	0.00099 (1)	0.00097 (4)	1.6 x 10^{-5}	5.8	0.00101 (4)	
533.7	0.00140 (1)	0.00140 (2)	1.6 x 10^{-5}	2.6	0.00144 (5)	
467.8	0.284 (6)	0.282 (7)	5.1 x 10^{-5}	2.5	0.263 (39)	

a - In this column the number in parentheses is the 95% confidence limit in the last digit.

b - In this column the number in parentheses is the maximum deviation from the unweighted average, except for the 739.5 cm^{-1} band where it is the 95% confidence limit in the last digit of the data of A, the only spectroscopist to measure that band.

c - The uncertainty is calculated as the average uncertainty in the anchor points (Table 3.1) at each side of the band.

d - The estimated accuracy is the sum of the maximum deviation from the unweighted average and the uncertainty due to the anchor points, as a percentage of the unweighted average.

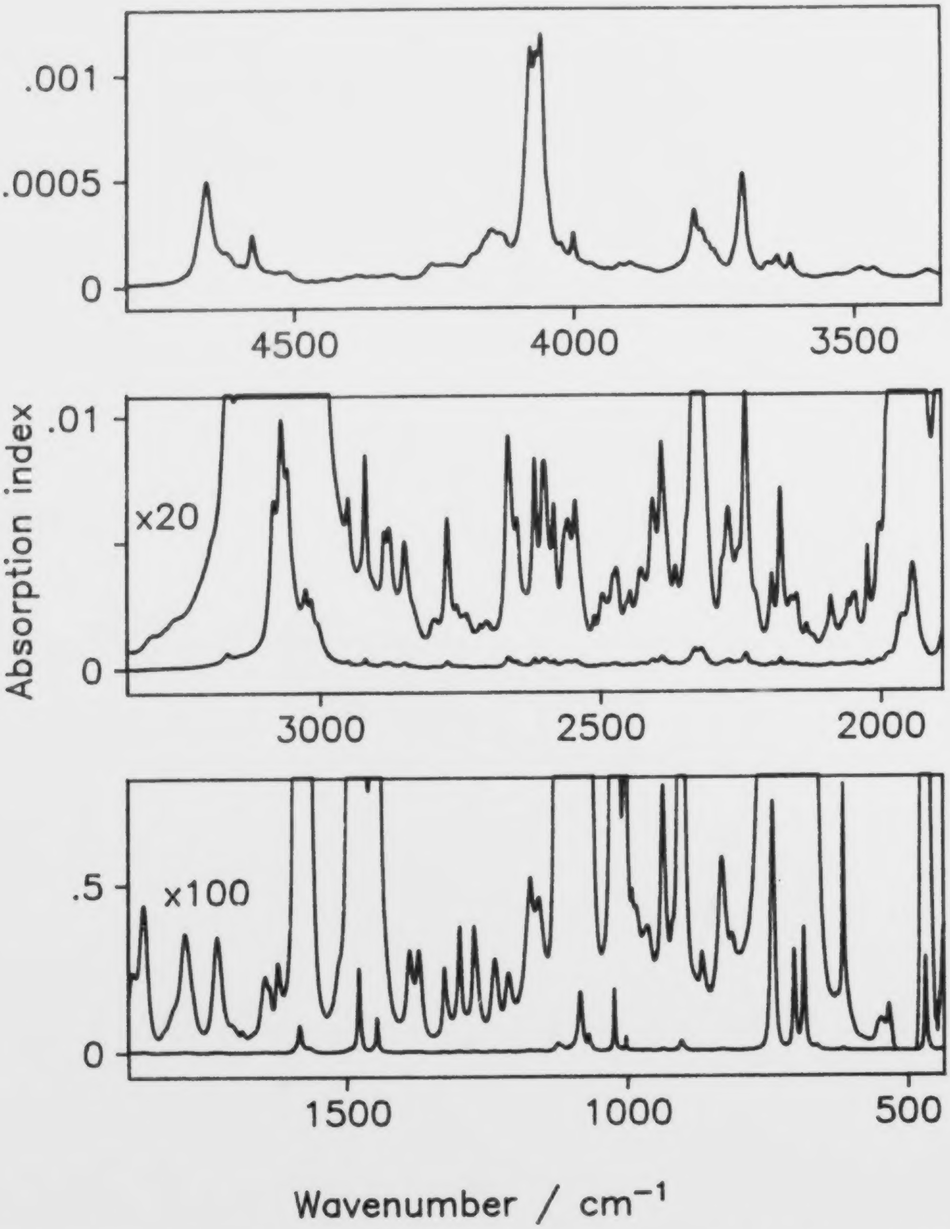

Figure 3.1 - Absorption index, $k(\tilde{\nu})$, spectrum between 4800 and 435 cm^{-1} of chlorobenzene at 25°C. The ordinate scale labels in the middle and bottom boxes are for the lower spectrum in the box; they must be divided by 20 and 100, as shown, for the upper spectrum in the box.

Table 3.5 - Absorption indices between 4800 and 435 cm^{-1} of liquid chlorobenzene at 25°C.[a,b]

cm^{-1}	*XE*	*YE*	0	1	2	3	4	5	6	7	8	9	10	11	12	13	14	15	16
4799.95	0	-7	124	127	126	127	123	118	122	125	123	125	129	132	131	132	133	137	141
4783.56	0	-7	139	143	143	147	142	150	154	155	157	154	153	155	156	154	153	156	153
4766.20	1	-7	152	156	161	161	162	173	180	191	191	198	203	204	210	207	205	208	214
4731.49	2	-7	230	248	257	273	298	330	373	430	498	556	615	703	867	1129	1562	2165	2723
4665.92	2	-7	3361	4145	4873	4821	4009	3178	2563	2132	1882	1770	1643	1649	1639	1563	1420	1250	1093
4600.35	2	-7	1040	1070	1035	965	1039	1420	2206	2386	1799	1304	1063	943	822	758	758	739	707
4534.79	2	-7	675	673	725	721	718	746	728	665	547	437	376	339	314	282	267	255	256
4469.22	2	-7	281	280	262	257	272	297	298	306	348	387	390	360	346	345	349	389	435
4403.65	2	-7	463	457	467	509	546	542	536	516	473	461	475	491	500	488	473	488	512
4338.08	2	-7	511	518	541	554	562	530	469	422	393	388	391	402	405	404	415	434	466
4272.51	2	-7	526	609	708	839	987	1088	1043	997	987	999	1008	1018	1037	1028	1023	1008	987
4206.95	2	-7	956	935	940	985	1096	1253	1419	1529	1534	1588	1711	1911	2147	2257	2384	2591	2674
4141.38	2	-6	259	249	247	248	242	234	209	189	185	193	216	256	328	436	613	828	1066
4077.74	1	-6	1131	1108	1056	1035	1054	1094	1109	1093	1102	1158	1195	1104	921	739	604	519	469
4044.95	1	-7	4230	3708	3220	2848	2592	2400	2229	2091	1990	1947	1972	2025	2021	1923	1788	1678	1597
4012.17	1	-7	1527	1487	1495	1589	1826	2217	2497	2293	1896	1588	1395	1284	1234	1187	1154	1130	1101
3977.46	2	-7	1048	1037	1063	1030	940	870	827	816	785	769	821	780	766	804	878	1000	1009
3911.89	2	-7	966	959	1007	1086	1056	980	912	881	839	824	788	762	758	730	672	637	621
3846.32	2	-7	621	639	670	709	740	771	810	861	931	1013	1092	1196	1412	1797	2309	3067	
3786.54	1	-7	3438	3534	3325	2990	2715	2579	2575	2617	2610	2525	2375	2196	2058	2002	1979	1894	1765
3753.76	1	-7	1663	1641	1665	1640	1536	1424	1312	1211	1128	1068	1017	974	944	929	926	950	1003
3720.97	1	-7	1103	1267	1475	1670	1844	2066	2410	2933	3621	4416	5021	5253	5138	4623	3836	3069	2486
3688.19	1	-7	2080	1794	1584	1411	1259	1130	1024	941	874	816	762	723	711	747	839	952	1012
3655.40	1	-7	1041	1055	1045	1013	990	997	1043	1127	1241	1351	1364	1246	1089	985	935	880	806
3622.62	1	-7	763	785	887	1098	1358	1424	1223	982	797	692	634	594	549	498	450	412	385
3589.84	1	-7	374	388	405	426	395	367	353	341	333	326	322	323	323	325	331	338	351
3557.05	1	-7	365	378	391	404	420	431	431	430	428	432	439	453	466	476	475	466	459
3522.34	2	-7	445	453	478	508	548	607	667	724	770	782	738	685	663	677	730	762	721
3456.77	2	-7	626	533	471	439	409	376	348	326	316	321	320	312	313	313	316	324	346
3391.20	2	-7	384	435	480	519	567	623	647	624	570	517	465	420	393	379	374	375	
3332.39	0	-7	376	370	372	375	383	394	396	405	408	415	423	433	438	448	458	470	479
3315.99	0	-7	489	516	524	537	549	556	578	593	601	616	639	646	656	668	671	682	
3299.60	1	-7	699	706	697	701	696	700	708	720	737	752	775	799	822	824	843	867	906
3261.03	3	-7	1007	1041	1078	1162	1303	1476	1693	1939	2248	2609	2989	4020					
3174.25	1	-7	4429	4871	5361	5969	6535	6604	6288	5914	5633	5444	5341	5320	5349	5424	5537	5670	5844
3141.47	1	-7	5986	6095	6180	6261	6359	6479	6616	6779	6971	7188	7441	7705	8019	8377	8772	9245	9767
3108.68	1	-6	1034	1101	1183	1292	1439	1641	1912	2280	2771	3325	4036	5061	6140	6689	6615	6381	6236
3075.90	1	-6	6569	7592	9004	9870	9732	8988	8160	7685	7740	7989	7561	6448	5351	4628	4218	3819	3425
3043.12	1	-6	3112	2860	2658	2504	2421	2435	2543	2738	3008	3174	2989	2687	2554	2659	2754	2582	2289
3010.33	1	-6	2033	1883	1842	1840	1761	1593	1393	1205	1050	927	829	747	676	616	563	517	479
2977.55	1	-7	4474	4204	3977	3790	3626	3487	3348	3223	3099	2991	2906	2869	2900	3079	3356	3305	2909
2944.76	1	-7	2550	2301	2149	2059	1985	1949	1945	1963	2007	2083	2218	2510	3178	4147			
2918.73	0	-7	4248	3947	3473	3021	2657	2380	2181	2043	1947	1887	1843	1813	1791	1770	1748	1721	1691
2902.34	0	-7	1664	1636	1611	1596	1585	1581	1580	1588	1597	1615	1643	1690	1759	1874	2045	2288	2558
2885.95	0	-7	2713	2695	2605	2534	2514	2551	2621	2698	2766	2798	2787	2727	2624	2494	2348	2194	2044
2868.59	1	-7	1799	1641	1553	1507	1496	1522	1599	1752	2003	2333	2524	2417	2186	1949	1722	1535	1396
2835.81	1	-7	1313	1259	1193	1116	1035	951	872	799	745	700	666	640	627	626	631	656	700
2803.02	1	-7	782	876	949	979	992	982	958	927	909	923	974	1086	1282	1636	2224	2855	2936
2770.24	1	-7	2508	2023	1626	1366	1222	1175	1200	1251	1239	1150	1064	1024	1033	1043	1053	1073	1089
2737.45	1	-7	1078	1028	950	874	810	768	741	730	727	740	758	823	880	844	817	833	879
2704.67	1	-7	928	943	929	902	870	835	805	786	780	780	796	822	869	949	1069	1245	1505
2671.89	1	-7	1887	2443	3226	4096	4585	4530	4139	3660	3231	2914	2760	2810	2966	2891	2488	2078	1806
2639.10	1	-7	1635	1551	1516	1503	1490	1477	1526	1680	1944	2318	2894	3745					
2616.92	0	-7	4094	4164	3899	3469	3056	2745	2548	2440	2407	2439	2535	2701	2957	3293	3652	3929	4069
2599.57	1	-7	4123	4024	3663	3148	2705	2447	2364	2444	2819	3265	2829	2205	1826	1634	1591	1695	1963
2566.78	1	-7	2306	2580	2716	2801	2907	2955	2850	2669	2557	2625	2900	3231	3305	3000	2619	2293	2009
2534.00	1	-7	1769	1554	1361	1181	1032	915	835	788	761	754	788	916	1040	941	866	887	986
2501.22	1	-7	1138	1316	1439	1463	1422	1363	1315	1288	1289	1328	1431	1636	1832	1823	1865	1958	1956
2468.43	1	-7	1811	1565	1298	1134	1073	1087	1158	1242	1298	1328	1390						
2448.18	0	-7	1449	1507	1515	1447	1355	1282	1237	1214	1212	1219	1237	1268	1312	1375	1455	1551	1655
2430.83	1	-7	1842	1941	1963	1924	1854	1774	1727	1743	1855	2086	2457	2917	3279	3344	3163	2920	2733
2398.04	1	-7	2671	2816	3296	4077	4499	4217	3740	3310	2941	2606	2273	1962	1737	1627	1644	1774	1949
2365.26	1	-7	2014	1864	1675	1596	1625	1728	1872	2072	2374	2739	2952	3092	3451	4078	4885	5818	6796
2332.48	1	-7	7550	7728	7373	6912	6765	7082	7621	7674	7025	6110	5211	4406	3695	3088	2573	2159	1837
2299.69	1	-7	1583	1384	1260	1197	1172	1220	1395	1718	2038	2157	2203	2350	2622	2935	3153	3149	2932

Table 3.5 - Continued

cm^{-1}	*XE*	*YE*	0	1	2	3	4	5	6	7	8	9	10	11	12	13	14	15	16
2266.91	1	-7	2630	2365	2179	2096	2115	2213	2311	2345	2362	2483	2834	3481	4412	5370	5604	4847	3820
2234.12	1	-7	2963	2316	1877	1628	1525	1499	1456	1360	1219	1064	919	808	736	699	696	727	798
2201.34	1	-7	921	1112	1383	1714	1845	1594	1316	1199	1276	1590	2264	3224	3537	2895	2131	1660	1416
2168.56	1	-7	1283	1214	1222	1294	1378	1386	1343	1326	1370	1438	1418	1256	1012	822	718	673	672
2135.77	1	-7	726	823	856	772	699	660	647	636	624	595	549	511	487	482	491	521	560
2102.99	1	-7	609	666	723	770	828	925	1147										
2090.45	0	-7	1294	1392	1381	1292	1200	1130	1073	1018	963	906	852	810	779	759	747	741	740
2074.06	0	-7	744	756	777	809	843	876	898	914	929	942	959	979	1007	1053	1127	1228	1313
2057.67	0	-7	1312	1252	1208	1199	1223	1273	1336	1395	1433	1447	1447	1448	1458	1461	1413	1307	1187
2041.28	0	-7	1081	997	943	907	885	873	869	870	877	893	923	972	1044	1136	1237	1411	1698
2024.89	0	-7	2102	2405	2310	1984	1704	1519	1407	1340	1306	1295	1308	1341	1392	1455	1542	1650	1783
2008.49	0	-7	1952	2144	2344	2530	2683	2791	2838	2822	2773	2727	2697	2690	2719	2789	2915	3113	3400
1992.10	0	-7	3783	4231	4645	4927	5079	5192	5329	5481	5594	5642	5639	5629	5661	5771	5994	6344	6842
1974.74	1	-6	832	1042	1297	1567	1809	1981	2062	2064	2028	2002	2028	2141	2365	2731	3220	3711	4045
1941.96	1	-6	4058	3797	3351	2827	2316	1872	1519	1262	1084	950	834	732	647	578	527	496	472
1907.25	2	-6	456	512	620	821	1198	1800	2291	2377	2251	2433	3199	4112	4374	3455	2104	1206	746
1841.68	2	-6	532	448	456	550	661	738	883	1068	1248	1389	1548	1869	2478	3226	3553	3280	2710
1776.11	2	-6	2066	1634	1154	860	697	618	623	716	953	1425	2205	3124	3435	2911	2105	1445	1051
1710.54	2	-7	8674	8392	8091	7158	6164	5304											
1689.33	1	-7	5373	6089	6452	5664	5313	4872	4494	4520	4698	5026	5348	5584	5784	6082	6509	7049	7916
1656.55	1	-6	929	1138	1427	1732	2028	2223	2263	2174	2023	1918	1953						
1636.30	0	-6	1938	1816	1631	1471	1362	1306	1308	1345	1431	1576	1778	2028	2293	2518	2638	2658	2586
1619.91	0	-6	2456	2301	2139	2002	1893	1800	1744	1724	1717	1739	1785	1842	1906	1996	2109	2247	2425
1603.51	0	-5	264	291	323	362	411	477	567	692	861	1077	1333	1604	1866	2118	2384	2710	3166
1587.12	0	-5	3882	5116	6860	8035	8017	7346	6287	5116	4054	3195	2555	2103	1802	1617	1518	1471	1435
1569.77	1	-5	1374	1415	1473	1341	1078	822	623	468	357	278	224	186	161	144	132	122	116
1536.98	1	-6	1087	1069	1103	1163	1226	1296	1398	1516	1705	1920	2188	2460	2678	2819	2949	3196	3633
1504.20	1	-5	441	569	749	931	1046	1119	1230	1417	1678	2067	2746						
1483.95	0	-4	331	414	543	756	1121	1713	2365	2467	2135	1490	1013	735	577	463	363	274	209
1467.56	0	-5	1662	1371	1173	1031	928	855	807	783	778	796	837	904	999	1127	1291	1489	1713
1451.17	0	-4	196	225	265	337	493	800	1033	783	504	340	245	192	163	137	109	86	70
1433.81	1	-6	5156	4193	3559	3047	2608	2224	1893	1624	1414	1271	1162	1056	983	941	916	919	940
1401.03	1	-6	976	1047	1180	1410	1766	2252	2755	3022	2941	2655	2335	2112	2058	2214	2559	2927	3016
1368.24	1	-6	2718	2224	1739	1339	1042	837	703	615	557	519	496	483	480	485	497	517	546
1335.46	1	-6	594	676	830	1139	1753	2464	2300	1808	1537	1327	1144	1032	992	1008	1074	1201	1430
1303.64	0	-6	1612	1869	2231	2701	3227	3645	3737	3455	2962	2436	2005	1688	1469	1329	1244	1194	1166
1287.25	0	-6	1149	1139	1135	1137	1150	1174	1213	1271	1352	1472	1647	1916	2330	2910	3470	3738	3699
1269.89	1	-6	3311	2893	2443	1982	1614	1345	1150	1019	942	911	922	980	1092	1275	1545	1897	2289
1237.11	1	-6	2629	2773	2634	2317	1969	1647	1407	1277	1249	1325	1512	1795	2104	2309	2331	2192	1968
1204.32	1	-6	1743	1575	1483	1454	1471	1524	1610	1729	1888	2093	2349	2674	3077	3531	3974	4439	4945
1171.54	1	-6	5201	4965	4573	4297	4193	4235	4373	4530	4591	4454	4142	3786	3458	3162	2955	2851	2825
1138.75	1	-5	293	322	376	479	655	960	1455	2129	2636	2558	2241	2051	1875	1587	1315	1145	1073
1105.97	1	-4	108	118	137	167	208	252	303	382	504	717	1095	1595	1764	1417	950	606	401
1074.15	0	-5	3391	2992	2804	2872	3277	4161	5137	4936	3874	3070	2577	2182	1807	1469	1199	990	829
1057.76	0	-6	7024	6034	5284	4744	4297	3932	3606	3377	3214	3097	3012	2974	2926	2896	2912	2966	3008
1041.37	0	-5	310	320	330	340	358	379	409	450	500	570	664	795	980	1235	1604	2219	3310
1024.97	0	-4	552	1031	1772	1726	1104	662	412	273	193	150	126	115	121	126	107	86	76
1008.58	0	-5	704	703	733	826	1088	1616	3063	4433	2907	1500	1005	734	613	537	484	466	451
992.19	0	-6	4491	4756	4851	4544	4441	4385	4301	4271	4302	4324	4316	4242	4148	4013	3884	3769	3656
974.83	1	-6	3437	3417	3510	3566	3631	3713	3744	3697	3518	3273	3014	2846	2693	2709	2772	2937	3256
942.05	1	-6	3809	4727	6125	7578	7845	6726	5316	4244	3593	3293	3318	3608	3875	3949	4227	4920	6298
909.27	1	-5	907	1451	2362	3134	2949	2215	1541	1050	719	515	399	327	283	256	240	230	223
876.48	1	-6	2161	2112	2091	2210	2565	2942	2862	2604	2342	2107	1933	1825	1772	1776	1839	1954	2110
843.70	1	-6	2343	2663	3057	3571	4199	4901	5501	5787	5628	5144	4575	4090	3703	3446	3328	3372	3494
810.91	1	-6	3456	3256	3075	2962	2909	2895	2889	2913	2955	3013	3094	3191	3332	3481	3609	3812	4105
778.13	1	-4	45	49	54	60	67	76	86	100	118	142	176	227	305	433	657	1077	1858
745.35	1	-4	3172	4938	6619	7450	6104	3723	2025	1120	676	450	326	253	209	183			
719.31	0	-4	175	170	168	169	173	180	192	209	233	269	321	398	518	709	1012	1492	2179
702.92	0	-4	2870	3019	2581	1976	1440	1056	802	638	545	510	524	576	652	753	908	1186	1691
686.53	0	-4	2511	3425	3690	3083	2232	1564	1099	784	577	441	349	286	242	210	186	168	155
670.14	0	-5	1457	1399	1376	1362	1371	1420	1513	1642	1745	1717	1546	1321	1123	961	826	713	620
653.74	0	-6	5387	4749	4276	3849	3500	3203	2971	2742	2533	2391	2275	2146	2026	1946	1835	1798	1757
637.35	0	-6	1745	1695	1654	1648	1645	1608	1623	1584	1599	1625	1658	1680					
626.26	-1	-6	1679	1679	1675	1670	1674	1678	1693	1708	1737	1766	1814	1862	1937	2013	2126	2239	2416
618.07	-1	-6	2594	2886	3178	3697	4217	5100	5982	6969	7957	7581	7205	6035	4864	4105	3346	2989	2633
609.87	-1	-6	2476	2318	2219	2120	2022	1924	1826	1728	1652	1577	1516	1456	1406	1356	1308	1260	1213

Table 3.5 - Continued

cm^{-1}	*XE*	*YE*	0	1	2	3	4	5	6	7	8	9	10	11	12	13	14	15	16
601.19	0	-6	1123	1040	965	897	835	776	721	671	627	588	554	523	496	477	457	440	431
584.80	0	-7	4262	4222	4151	4039	3907	3796	3719	3645	3588	3546	3479	3402	3323	3241	3174	3136	3137
568.41	0	-7	3142	3140	3160	3204	3279	3407	3581	3799	4070	4365	4718	5202	5833	6607	7435	8089	8459
552.02	0	-7	8660	8854	9125	9433	9641	9633	9507	9358	9129	8804	8466	8204	8088				
539.97	-1	-6	808	812	816	831	845	884	922	985	1047	1130	1212	1287	1362	1374	1387	1315	1243
531.77	-1	-6	1144	1045	968	892	839	787	756	722	633	549	454	374	328	278	199	118	76
516.34	3	0	0	0	0	0	0												
484.52	0	-4	0	2	6	10	17	25	35	51	71	99	141	202	299	462	758	1302	2119
468.13	0	-4	2767	2566	1798	1121	697	454	316	238	191	150	113	86	66	52	40	30	23
451.74	0	-6	1585	1048	978	1003	866	560	1029	1106	1257	1455	1727	1664	2024	2425	2925	3196	3487
435.35	0	-6	3616	4147															

Note: Footnotes follow Table 3.7

The average agreement between the weighted and unweighted average peak heights is 0.6% which shows that, as was found previously[1,2], the fact that more spectra were run in this laboratory than elsewhere did not have an important influence on the averages. The agreement between spectroscopists is shown by the maximum deviations from the unweighted average peak heights, which average 2.4% for the 108 peak heights in Table 3.4.

The unweighted average $k(\tilde{\nu})$ spectrum, is taken as the primary intensity result of this work. It is shown in Fig. 3.1 and tabulated in Compact Table format[9] in Table 3.5.

3.2.2 - Real refractive index spectrum.

The real refractive index spectrum $n(\tilde{\nu})$ was obtained by Kramers-Kronig transformation of the unweighted average $k(\tilde{\nu})$ spectrum[1,10] with the value of n at 8000 cm^{-1} equal to 1.5043±0.0005. This value was found by fitting the literature values[11-13] of

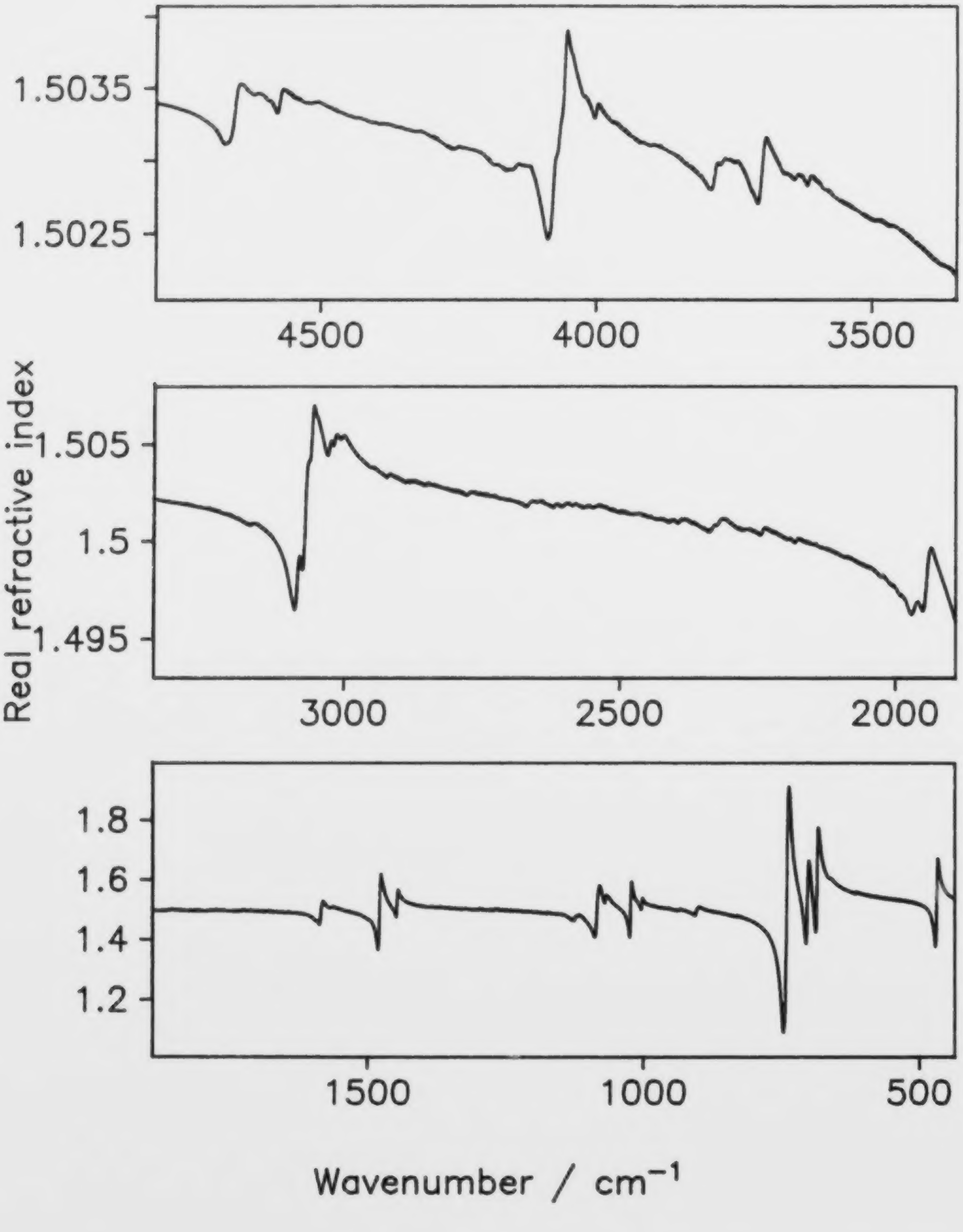

Figure 3.2 - Real refractive index, $n(\tilde{\nu})$, spectrum between 4800 and 435 cm^{-1} of chlorobenzene at 25°C.

Table 3.6 - Real refractive indices between 4800 and 435 cm^{-1} of liquid chlorobenzene at 25°C.^{a,b}

cm^{-1}	*XE*	0	1	2	3	4	5	6	7	8	9	10	11	12	13	14	15	16
4799.95	0	15033	15033	15033	15033	15033	15033	15033	15033	15033	15033	15033	15033	15033	15033	15033	15033	15033
4783.56	0	15033	15033	15033	15033	15033	15033	15033	15033	15033	15033	15033	15033	15033	15033	15033	15033	15033
4766.20	1	15033	15033	15033	15033	15033	15033	15033	15033	15033	15033	15033	15033	15033	15033	15033	15033	15033
4731.49	2	15033	15033	15033	15032	15032	15032	15032	15032	15032	15032	15032	15031	15031	15031	15031	15031	15031
4665.92	2	15031	15031	15032	15034	15035	15035	15035	15035	15034	15034	15034	15034	15034	15034	15034	15034	15034
4600.35	2	15034	15034	15034	15033	15033	15033	15033	15034	15034	15034	15034	15034	15034	15034	15034	15034	15034
4534.79	2	15034	15034	15033	15033	15033	15033	15034	15034	15034	15033	15033	15033	15033	15033	15033	15033	15033
4469.22	2	15033	15033	15033	15033	15033	15033	15033	15033	15032	15032	15032	15032	15032	15032	15032	15032	15032
4403.65	2	15032	15032	15032	15032	15032	15032	15032	15032	15032	15032	15032	15032	15032	15032	15032	15032	15032
4338.08	2	15032	15032	15032	15032	15032	15032	15031	15031	15031	15031	15031	15031	15031	15031	15031	15031	15031
4272.51	2	15031	15030	15030	15030	15030	15030	15031	15030	15030	15030	15030	15030	15030	15030	15030	15030	15030
4206.95	2	15030	15030	15030	15030	15029	15029	15029	15029	15029	15029	15029	15029	15029	15029	15029	15029	15029
4141.38	2	15029	15029	15029	15029	15029	15029	15029	15029	15028	15028	15027	15026	15025	15025	15024	15024	15026
4077.74	1	15028	15029	15030	15030	15030	15031	15032	15032	15033	15033	15035	15037	15038	15039	15038	15038	15037
4044.95	1	15037	15037	15036	15036	15036	15035	15035	15035	15035	15034	15034	15034	15034	15034	15034	15034	15034
4012.17	1	15033	15033	15033	15033	15033	15033	15033	15033	15034	15033	15033	15033	15033	15033	15033	15033	15033
3977.46	2	15032	15032	15032	15032	15032	15032	15032	15032	15032	15031	15031	15031	15031	15031	15031	15031	15031
3911.89	2	15031	15031	15031	15031	15031	15031	15031	15031	15030	15030	15030	15030	15030	15030	15030	15030	15030
3846.32	2	15030	15029	15029	15029	15029	15029	15029	15029	15029	15029	15028	15028	15028	15028	15028	15028	
3786.54	1	15028	15029	15029	15029	15029	15029	15029	15029	15030	15030	15030	15030	15030	15030	15030	15030	15030
3753.76	1	15030	15029	15029	15030	15030	15029	15029	15029	15029	15029	15029	15029	15029	15029	15028	15028	15028
3720.97	1	15028	15028	15027	15027	15027	15027	15027	15027	15027	15027	15028	15029	15030	15031	15031	15031	15031
3688.19	1	15031	15031	15031	15030	15030	15030	15030	15030	15030	15029	15029	15029	15029	15029	15029	15029	15029
3655.40	1	15029	15029	15029	15029	15029	15028	15028	15028	15028	15028	15029	15029	15029	15029	15029	15028	15028
3622.62	1	15028	15028	15028	15028	15028	15028	15029	15029	15029	15028	15028	15028	15028	15028	15028	15028	15028
3589.84	1	15028	15028	15028	15028	15028	15028	15027	15027	15027	15027	15027	15027	15027	15027	15027	15027	15027
3557.05	1	15027	15027	15027	15027	15027	15027	15027	15027	15027	15026	15026	15026	15026	15026	15026	15026	15026
3522.34	2	15026	15026	15026	15026	15026	15026	15026	15025	15025	15025	15025	15025	15025	15025	15025	15025	15025
3456.77	2	15025	15025	15025	15025	15025	15025	15024	15024	15024	15024	15024	15024	15024	15024	15023	15023	15023
3391.20	2	15023	15023	15023	15023	15023	15022	15022	15022	15022	15022	15022	15022	15022	15022	15021	15021	
3332.39	0	15021	15021	15021	15021	15021	15021	15021	15021	15021	15021	15021	15021	15021	15021	15020	15020	15020
3315.99	0	15020	15020	15020	15020	15020	15020	15020	15020	15020	15020	15020	15020	15020	15020	15020	15020	
3299.60	1	15020	15020	15020	15019	15019	15019	15019	15019	15019	15019	15019	15019	15018	15018	15018	15018	15018
3261.03	3	15018	15017	15017	15016	15015	15015	15014	15013	15012	15011	15010	15009					
3174.25	1	15009	15008	15008	15008	15008	15009	15009	15009	15009	15009	15008	15008	15007	15007	15007	15006	15006
3141.47	1	15005	15005	15004	15004	15003	15003	15002	15001	15001	15000	14999	14998	14997	14996	14995	14994	14992
3108.68	1	14991	14989	14987	14985	14982	14979	14976	14973	14970	14968	14965	14965	14971	14981	14989	14992	14991
3075.90	1	14987	14985	14992	15007	15024	15036	15041	15041	15043	15050	15062	15069	15070	15067	15065	15064	15062
3043.12	1	15060	15058	15055	15053	15050	15048	15046	15044	15045	15048	15051	15052	15050	15050	15052	15054	15055
3010.33	1	15055	15054	15053	15053	15054	15055	15055	15054	15053	15052	15051	15050	15049	15048	15048	15047	15046
2977.55	1	15045	15044	15044	15043	15043	15042	15042	15041	15041	15040	15040	15039	15039	15038	15038	15038	15038
2944.76	1	15038	15037	15037	15037	15036	15036	15035	15035	15035	15034	15034	15033	15033	15033			
2918.73	0	15034	15035	15035	15035	15035	15035	15034	15034	15034	15034	15033	15033	15033	15033	15033	15033	15033
2902.34	0	15033	15032	15032	15032	15032	15032	15032	15032	15031	15031	15031	15031	15031	15031	15030	15030	15030
2885.95	0	15031	15031	15031	15031	15031	15031	15031	15031	15031	15031	15031	15031	15031	15031	15031	15031	15031
2868.59	1	15031	15030	15030	15030	15030	15029	15029	15029	15029	15029	15029	15029	15029	15029	15029	15029	15029
2835.81	1	15029	15029	15029	15028	15028	15028	15028	15028	15028	15027	15027	15027	15027	15027	15027	15026	15026
2803.02	1	15026	15026	15026	15026	15026	15026	15025	15025	15025	15025	15025	15024	15024	15024	15024	15024	15025
2770.24	1	15025	15026	15025	15025	15025	15025	15025	15025	15024	15024	15024	15024	15024	15024	15024	15024	15024
2737.45	1	15024	15024	15023	15023	15023	15023	15023	15023	15023	15023	15022	15022	15022	15022	15022	15022	15022
2704.67	1	15022	15022	15021	15021	15021	15021	15021	15021	15021	15020	15020	15020	15020	15020	15019	15019	15019
2671.89	1	15018	15018	15018	15018	15019	15020	15021	15021	15021	15021	15021	15020	15020	15021	15021	15021	15021
2639.10	1	15020	15020	15020	15019	15019	15019	15019	15018	15018	15018	15017	15018					
2616.92	0	15018	15019	15019	15019	15019	15019	15019	15019	15019	15018	15018	15018	15018	15018	15018	15018	15018
2599.57	1	15019	15019	15020	15020	15020	15019	15019	15019	15018	15019	15019	15019	15019	15019	15018	15018	15017
2566.78	1	15017	15017	15017	15017	15018	15018	15018	15018	15018	15017	15017	15018	15018	15018	15019	15018	15018
2534.00	1	15018	15018	15018	15018	15018	15017	15017	15017	15017	15016	15016	15016	15016	15016	15016	15015	15015
2501.22	1	15015	15015	15015	15015	15015	15015	15015	15015	15014	15014	15014	15014	15014	15014	15014	15014	15014
2468.43	1	15014	15014	15014	15014	15014	15013	15013	15013	15013	15013	15013						
2448.18	0	15013	15013	15013	15013	15013	15013	15012	15012	15012	15012	15012	15012	15012	15012	15012	15011	15011
2430.83	1	15011	15011	15011	15011	15011	15011	15011	15011	15010	15010	15010	15010	15010	15010	15011	15011	15011
2398.04	1	15010	15010	15009	15010	15010	15011	15011	15011	15011	15011	15011	15011	15011	15010	15010	15009	15009
2365.26	1	15009	15009	15009	15009	15008	15008	15007	15007	15007	15006	15006	15006	15006	15005	15005	15005	15005
2332.48	1	15006	15007	15008	15009	15008	15008	15009	15010	15011	15012	15012	15012	15012	15011	15011	15011	15010
2299.69	1	15010	15009	15009	15008	15008	15007	15007	15007	15006	15006	15006	15006	15006	15006	15006	15006	15007

Table 3.6 - Continued

cm^{-1}	*XE*	0	1	2	3	4	5	6	7	8	9	10	11	12	13	14	15	16
2266.91	1	15007	15006	15006	15006	15005	15005	15005	15005	15005	15004	15004	15003	15003	15004	15005	15007	15007
2234.12	1	15007	15007	15006	15006	15005	15005	15005	15005	15004	15004	15004	15004	15003	15003	15003	15002	15002
2201.34	1	15002	15001	15001	15001	15001	15001	15001	15001	15000	15000	14999	15000	15001	15001	15001	15001	15001
2168.56	1	15000	15000	15000	15000	14999	14999	14999	14999	14999	14999	14999	14999	14999	14998	14998	14998	14997
2135.77	1	14997	14997	14997	14997	14996	14996	14996	14996	14996	14995	14995	14995	14995	14994	14994	14994	14993
2102.99	1	14993	14993	14993	14992	14992	14992	14992										
2090.45	0	14992	14992	14992	14992	14992	14992	14992	14991	14991	14991	14991	14991	14991	14991	14990	14990	14990
2074.06	0	14990	14990	14990	14990	14989	14989	14989	14989	14989	14989	14989	14988	14988	14988	14988	14988	14988
2057.67	0	14988	14988	14988	14987	14987	14987	14987	14987	14987	14987	14987	14986	14986	14986	14986	14986	14986
2041.28	0	14986	14986	14985	14985	14985	14985	14984	14984	14984	14984	14983	14983	14983	14983	14982	14982	14982
2024.89	0	14982	14982	14982	14982	14982	14982	14982	14981	14981	14981	14980	14980	14980	14979	14979	14979	14978
2008.49	0	14978	14978	14978	14977	14977	14977	14977	14977	14977	14976	14976	14976	14975	14975	14974	14974	14973
1992.10	0	14973	14973	14972	14972	14972	14972	14972	14972	14971	14971	14971	14970	14970	14969	14968	14967	14967
1974.74	1	14965	14964	14963	14963	14964	14966	14967	14969	14969	14969	14968	14967	14965	14965	14966	14969	14975
1941.96	1	14983	14989	14994	14996	14997	14996	14995	14993	14991	14989	14988	14986	14985	14983	14981	14980	14978
1907.25	2	14975	14972	14968	14965	14961	14960	14963	14966	14966	14963	14962	14968	14982	14995	14997	14992	14986
1841.68	2	14981	14977	14973	14969	14967	14964	14962	14960	14958	14957	14955	14952	14951	14954	14962	14970	14975
1776.11	2	14975	14974	14971	14967	14963	14959	14954	14950	14945	14940	14938	14942	14952	14960	14963	14960	14956
1710.54	2	14952	14948	14946	14943	14940	14936											
1689.33	1	14934	14933	14932	14931	14929	14927	14925	14923	14921	14919	14916	14914	14912	14910	14907	14905	14902
1656.55	1	14898	14895	14893	14891	14891	14892	14893	14893	14892	14889	14887						
1636.30	0	14887	14887	14885	14883	14880	14877	14874	14871	14867	14864	14861	14859	14858	14857	14857	14858	14858
1619.91	0	14857	14855	14853	14849	14846	14842	14837	14833	14828	14823	14817	14812	14806	14799	14792	14785	14776
1603.51	0	14768	14758	14747	14736	14723	14708	14691	14673	14655	14638	14625	14615	14608	14600	14588	14570	14544
1587.12	0	14512	14495	14562	14743	14942	15099	15208	15264	15278	15265	15238	15206	15174	15145	15121	15103	15091
1569.77	1	15071	15057	15064	15080	15086	15079	15067	15052	15037	15022	15008	14995	14983	14972	14962	14952	14943
1536.98	1	14934	14924	14915	14906	14897	14887	14878	14868	14857	14847	14836	14825	14814	14802	14787	14770	14749
1504.20	1	14726	14702	14680	14663	14646	14620	14581	14532	14469	14383	14258						
1483.95	0	14173	14069	13943	13794	13663	13713	14237	15138	15853	16190	16153	16023	15912	15835	15771	15700	15624
1467.56	0	15553	15490	15436	15389	15346	15308	15272	15239	15207	15177	15147	15118	15090	15063	15036	15011	14986
1451.17	0	14961	14929	14885	14821	14749	14808	15215	15592	15656	15609	15551	15497	15460	15438	15416	15390	15365
1433.81	1	15322	15290	15266	15246	15229	15214	15201	15188	15177	15167	15157	15148	15140	15132	15125	15118	15111
1401.03	1	15105	15098	15092	15086	15080	15077	15076	15078	15080	15080	15078	15075	15070	15066	15063	15064	15067
136[illegible].24	1	15071	15071	15069	15066	15062	15058	15054	15051	15047	15044	15040	15037	15034	15031	15028	15025	15022
1335.46	1	15019	15015	15011	15007	15004	15008	15015	15016	15014	15012	15010	15006	15003	14999	14996	14992	14988
1303.64	0	14986	14984	14982	14982	14984	14989	14996	15002	15005	15006	15005	15002	15000	14997	14995	14993	14991
1287.25	0	14989	14987	14986	14984	14982	14980	14978	14976	14974	14971	14969	14966	14964	14964	14967	14972	14977
1269.89	1	14983	14985	14986	14985	14982	14979	14975	14972	14968	14964	14960	14957	14953	14949	14946	14944	14943
1237.11	1	14945	14948	14950	14951	14950	14948	14944	14940	14936	14931	14927	14924	14923	14923	14924	14924	14923
1204.32	1	14920	14916	14912	14908	14903	14899	14895	14890	14886	14881	14876	14872	14868	14865	14864	14862	14863
1171.54	1	14867	14870	14869	14865	14860	14856	14852	14849	14847	14845	14842	14837	14829	14821	14810	14798	14785
1138.75	1	14769	14751	14731	14707	14680	14652	14632	14640	14697	14762	14786	14792	14800	14799	14779	14748	14712
1105.97	1	14671	14627	14580	14532	14486	14441	14382	14306	14213	14113	14088	14388	15078	15634	15803	15745	15610
1074.15	0	15535	15460	15386	15312	15247	15221	15296	15429	15489	15478	15458	15441	15422	15398	15372	15344	15318
1057.76	0	15293	15269	15247	15226	15207	15189	15172	15155	15139	15124	15109	15094	15080	15066	15052	15038	15024
1041.37	0	15009	14994	14978	14962	14944	14924	14903	14880	14853	14823	14789	14749	14702	14644	14571	14474	14344
1024.97	0	14175	14068	14544	15495	15927	15904	15786	15666	15564	15481	15415	15360	15320	15306	15297	15271	15241
1008.58	0	15211	15182	15151	15114	15072	15018	15009	15199	15377	15361	15310	15276	15248	15227	15209	15194	15181
992.19	0	15169	15160	15156	15150	15143	15137	15132	15126	15121	15117	15114	15110	15107	15104	15100	15096	15092
974.83	1	15084	15075	15068	15062	15056	15051	15047	15043	15039	15035	15028	15022	15014	15006	14998	14989	14980
942.05	1	14970	14962	14958	14966	14982	14992	14991	14983	14972	14960	14947	14936	14926	14915	14899	14879	14854
909.27	1	14825	14799	14809	14901	15021	15081	15092	15081	15061	15039	15019	15002	14987	14974	14963	14953	14944
876.48	1	14935	14927	14918	14908	14900	14897	14895	14890	14884	14877	14868	14860	14851	14842	14832	14823	14814
843.70	1	14804	14794	14785	14776	14769	14763	14761	14761	14761	14758	14751	14742	14731	14718	14705	14692	14680
810.91	1	14669	14656	14641	14625	14608	14591	14572	14552	14531	14509	14486	14460	14433	14404	14373	14338	14300
778.13	1	14260	14215	14165	14110	14049	13979	13899	13807	13699	13571	13415	13223	12983	12673	12270	11763	11217
745.35	1	10897	11291	12770	15432	18216	19110	18712	18021	17420	16958	16603	16320	16084	15880			
719.31	0	15785	15693	15602	15512	15422	15329	15232	15129	15018	14895	14757	14599	14417	14214	14009	13863	13954
702.92	0	14554	15526	16281	16616	16640	16504	16314	16107	15897	15692	15499	15322	15155	14976	14760	14507	14280
686.53	0	14308	14992	16271	17318	17725	17728	17583	17392	17202	17032	16886	16762	16655	16564	16485	16416	16354
670.14	0	16299	16249	16205	16166	16130	16097	16070	16052	16048	16053	16055	16046	16030	16011	15991	15971	15951
653.74	0	15932	15913	15894	15877	15861	15845	15830	15816	15803	15790	15777	15765	15754	15743	15732	15721	15711
637.35	0	15702	15693	15684	15675	15667	15659	15651	15643	15635	15628	15621	15614					
626.26	-1	15611	15607	15604	15601	15597	15594	15590	15586	15583	15579	15576	15572	15568	15564	15560	15556	15552
618.07	-1	15548	15544	15539	15535	15532	15529	15531	15533	15547	15561	15570	15579	15578	15576	15572	15567	15563
609.87	-1	15558	15555	15551	15548	15546	15543	15540	15538	15535	15533	15530	15528	15525	15523	15521	15518	15516

Table 3.6 - Continued

cm^{-1}	XE	0	1	2	3	4	5	6	7	8	9	10	11	12	13	14	15	16
601.19	0	15512	15508	15503	15499	15495	15491	15487	15483	15479	15476	15472	15468	15465	15461	15458	15454	15451
584.80	0	15447	15444	15441	15438	15435	15432	15429	15426	15423	15420	15417	15414	15412	15409	15406	15403	15400
568.41	0	15397	15395	15392	15389	15386	15384	15381	15378	15375	15373	15370	15367	15365	15362	15360	15358	15357
552.02	0	15355	15353	15351	15349	15347	15346	15344	15342	15340	15338	15336	15333	15331				
539.97	-1	15330	15328	15327	15326	15324	15323	15322	15320	15319	15318	15318	15317	15317	15317	15317	15318	15317
531.77	-1	15317	15316	15315	15314	15313	15312	15310	15310	15309	15308	15306	15305	15303	15302	15300	15298	15296
516.34	3	15268	15239	15201	15146	15045												
484.52	0	15025	15001	14976	14947	14914	14877	14833	14784	14723	14652	14563	14453	14312	14137	13933	13787	13994
468.13	0	14912	16097	16680	16726	16576	16399	16244	16121	16033	15970	15911	15856	15811	15770	15736	15705	15676
451.74	0	15651	15628	15603	15587	15571	15555	15538	15528	15516	15507	15499	15491	15482	15477	15472	15471	15470
435.35	0	15471	15474															

Note: Footnotes follow Table 3.7

the refractive index at five wavelengths in the visible region to $n^2(\tilde{\nu}) = a\tilde{\nu}^4 + b\tilde{\nu}^2 + c\tilde{\nu}$ and extrapolating to 8000 cm^{-1}. $k(\tilde{\nu})$ is less than 5 $\times 10^{-5}$ above 4800 cm^{-1}, apart from a doublet of height 2.5 $\times 10^{-4}$ near 6000 cm^{-1}. We did not make reliable measurements in this region, so we assumed that $k(\tilde{\nu}) = 0.0$ between 4800 and 8000 cm^{-1}. The real refractive index spectrum is shown in Figure 3.2 and tabulated in Compact Table format[9] in Table 3.6.

3.2.3 - Molar absorption coefficient spectrum.

The molar absorption coefficient spectrum was calculated from the unweighted average $k(\tilde{\nu})$ spectrum. The molar concentration of liquid chlorobenzene at 25°C is 9.783 mole L^{-1}, as calculated from the density[12] 1.10118 g cm^{-3}. The $E_m(\tilde{\nu})$ spectrum is shown in Figure 3.3 and the values are tabulated in Table 3.7. The molar absorption coefficient peak heights are listed in Table 3.8.

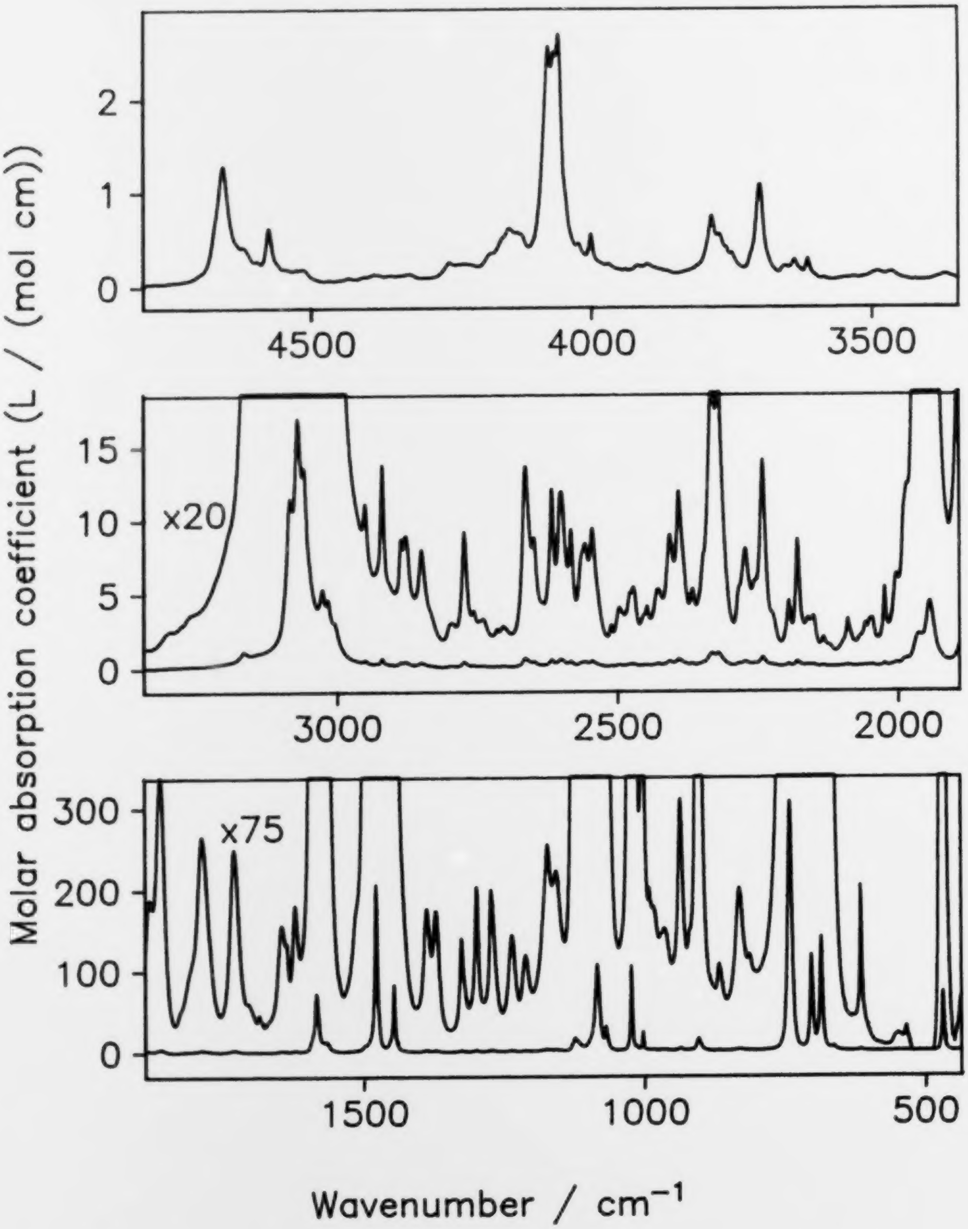

Figure 3.3 - Molar absorption coefficient, $E_m(\tilde{\nu})$ spectrum between 4800 and 435 cm^{-1} of chlorobenzene at 25°C. The ordinate scale labels in the middle and bottom boxes are for the lower spectrum in the box; they must be divided by 20 and 75, as shown, for the upper spectrum in the box.

Table 3.7 - Molar absorption coefficients between 4800 and 435 cm^{-1} of liquid chlorobenzene at 25°C^{a,b,c}

cm^{-1}	*XE*	*YE*	0	1	2	3	4	5	6	7	8	9	10	11	12	13	14	15	16
4799.95	0	-5	3309	3389	3374	3411	3304	3145	3254	3350	3282	3346	3460	3529	3501	3535	3551	3649	3752
4783.56	0	-5	3714	3806	3806	3912	3783	3993	4101	4132	4193	4091	4079	4121	4157	4103	4060	4149	4079
4766.20	1	-5	4043	4156	4271	4272	4302	4597	4776	5055	5069	5242	5377	5393	5553	5484	5419	5488	5647
4731.49	2	-4	607	654	678	720	784	867	981	1129	1307	1457	1610	1838	2266	2949	4075	5642	7093
4665.92	2	-3	875	1078	1266	1251	1040	824	664	552	487	457	424	425	422	402	365	321	281
4600.35	2	-4	2668	2744	2651	2471	2656	3629	5633	6086	4586	3320	2704	2398	2087	1923	1923	1872	1791
4534.79	2	-4	1706	1700	1830	1820	1810	1878	1832	1673	1374	1097	943	850	787	704	668	637	639
4469.22	2	-4	701	697	651	638	675	738	740	759	863	956	964	888	855	849	859	956	1070
4403.65	2	-4	1138	1120	1146	1246	1337	1325	1311	1261	1154	1124	1156	1195	1216	1185	1147	1182	1240
4338.08	2	-4	1235	1251	1308	1336	1355	1277	1128	1015	945	932	937	963	969	967	991	1036	1113
4272.51	2	-4	1254	1451	1684	1995	2343	2580	2471	2362	2335	2361	2380	2403	2445	2421	2408	2369	2318
4206.95	2	-4	2242	2193	2203	2304	2561	2928	3311	3565	3573	3696	3978	4439	4982	5232	5521	5996	6183
4141.38	2	-3	599	574	571	571	558	538	480	435	424	443	494	586	748	996	1398	1887	2425
4077.74	1	-3	2573	2518	2400	2351	2392	2483	2514	2477	2497	2623	2704	2497	2083	1670	1364	1171	1058
4044.95	1	-4	9543	8363	7259	6417	5837	5401	5015	4701	4473	4374	4427	4545	4534	4311	4007	3760	3577
4012.17	1	-4	3417	3327	3342	3552	4078	4949	5571	5114	4228	3538	3107	2858	2746	2641	2565	2510	2445
3977.46	2	-4	2324	2298	2353	2278	2077	1920	1824	1799	1727	1692	1803	1713	1680	1761	1922	2186	2204
3911.89	2	-4	2107	2090	2193	2362	2295	2128	1977	1909	1815	1781	1703	1645	1634	1573	1446	1368	1333
3846.32	2	-4	1332	1370	1435	1516	1582	1646	1727	1834	1981	2153	2319	2538	2994	3804	4885	6480	
3786.54	1	-4	7261	7461	7015	6306	5722	5434	5421	5508	5490	5308	4990	4611	4320	4201	4150	3970	3697
3753.76	1	-4	3482	3435	3483	3429	3210	2973	2738	2526	2352	2225	2119	2029	1964	1932	1925	1974	2083
3720.97	1	-3	229	263	306	346	382	428	499	606	748	912	1037	1084	1060	953	790	632	512
3688.19	1	-4	4278	3688	3254	2898	2585	2319	2100	1929	1790	1671	1560	1479	1454	1526	1714	1944	2064
3655.40	1	-4	2123	2149	2128	2062	2014	2028	2121	2290	2520	2742	2766	2525	2206	1994	1893	1780	1630
3622.62	1	-4	1541	1585	1791	2216	2739	2869	2464	1978	1604	1391	1273	1194	1103	1000	902	825	772
3589.84	1	-5	7498	7760	8108	8522	7892	7326	7047	6798	6637	6506	6410	6433	6417	6462	6577	6709	6961
3557.05	1	-5	7241	7489	7759	8010	8306	8537	8519	8491	8458	8521	8662	8941	9183	9369	9348	9170	9033
3522.34	2	-4	873	890	937	994	1072	1185	1302	1411	1500	1522	1435	1329	1285	1312	1413	1472	1393
3456.77	2	-4	1207	1026	906	843	786	722	666	623	605	614	611	594	596	595	600	615	654
3391.20	2	-4	726	822	906	978	1068	1171	1215	1170	1068	968	869	785	734	706	697	697	
3332.39	0	-5	6988	6871	6910	6958	7107	7318	7353	7512	7569	7686	7832	8024	8118	8303	8484	8705	8871
3315.99	0	-4	905	953	968	992	1014	1027	1066	1094	1108	1137	1178	1191	1210	1230	1235	1256	
3299.60	1	-4	1287	1299	1281	1288	1278	1285	1298	1319	1351	1376	1418	1461	1503	1505	1540	1581	1651
3261.03	3	-4	1832	1888	1951	2098	2348	2652	3036	3468	4011	4644	5309	7122					
3174.25	1	-3	784	862	948	1055	1154	1166	1109	1043	992	959	940	936	940	953	972	995	1025
3141.47	1	-3	1049	1067	1081	1095	1111	1132	1155	1183	1215	1252	1296	1341	1395	1456	1524	1605	1694
3108.68	1	-2	179	191	205	224	249	284	330	394	478	573	696	872	1057	1150	1137	1096	1071
3075.90	1	-2	1127	1302	1543	1690	1665	1537	1395	1313	1321	1363	1289	1099	911	788	717	649	582
3043.12	1	-3	5282	4851	4506	4242	4099	4119	4299	4626	5080	5357	5040	4529	4301	4476	4632	4341	3845
3010.33	1	-3	3414	3160	3088	3084	2949	2666	2329	2015	1754	1548	1382	1246	1126	1025	936	860	796
2977.55	1	-4	7430	6977	6596	6283	6006	5773	5539	5328	5121	4939	4795	4731	4779	5070	5523	5435	4781
2944.76	1	-4	4188	3776	3525	3375	3251	3191	3182	3209	3279	3401	3618	4093	5179	6753			
2918.73	0	-4	6916	6424	5650	4914	4319	3869	3543	3317	3162	3063	2991	2940	2905	2870	2833	2788	2739
2902.34	0	-4	2693	2647	2607	2581	2562	2555	2552	2564	2579	2607	2651	2725	2836	3020	3296	3686	4119
2885.95	0	-4	4367	4336	4190	4074	4042	4100	4211	4333	4440	4490	4472	4374	4207	3996	3762	3514	3272
2868.59	1	-4	2879	2624	2482	2407	2386	2427	2549	2791	3188	3710	4011	3839	3469	3091	2730	2431	2210
2835.81	1	-4	2076	1991	1885	1762	1633	1499	1373	1258	1172	1100	1046	1005	984	981	989	1027	1096
2803.02	1	-4	1222	1368	1482	1528	1546	1531	1492	1443	1414	1433	1513	1685	1988	2535	3444	4418	4540
2770.24	1	-4	3874	3124	2509	2106	1883	1809	1846	1924	1903	1766	1632	1569	1583	1596	1611	1640	1664
2737.45	1	-4	1646	1568	1449	1332	1234	1168	1127	1109	1104	1122	1149	1246	1333	1277	1235	1258	1327
2704.67	1	-4	1400	1421	1399	1357	1308	1255	1209	1180	1169	1170	1192	1230	1300	1418	1597	1858	2244
2671.89	1	-4	2812	3639	4800	6091	6812	6727	6142	5427	4788	4314	4084	4154	4382	4268	3671	3063	2661
2639.10	1	-4	2407	2281	2228	2208	2186	2166	2237	2460	2845	3389	4229	5468					
2616.92	0	-4	5976	6075	5687	5058	4455	4000	3710	3553	3502	3548	3686	3927	4297	4784	5303	5704	5904
2599.57	1	-4	5977	5830	5303	4555	3911	3535	3412	3525	4063	4703	4071	3171	2624	2347	2283	2430	2812
2566.78	1	-4	3302	3691	3883	4001	4150	4215	4062	3800	3639	3732	4120	4588	4689	4253	3710	3245	2842
2534.00	1	-4	2501	2194	1920	1665	1454	1288	1175	1108	1069	1058	1105	1284	1456	1317	1211	1239	1376
2501.22	1	-4	1588	1835	2004	2037	1978	1895	1826	1787	1787	1840	1981	2263	2533	2517	2574	2700	2695
2468.43	1	-4	2493	2153	1785	1557	1472	1490	1587	1701	1776	1816	1899						
2448.18	0	-4	1979	2056	2067	1974	1847	1747	1685	1653	1650	1659	1683	1724	1783	1868	1976	2105	2245
2430.83	1	-4	2497	2629	2657	2603	2505	2396	2331	2350	2499	2808	3305	3920	4404	4487	4241	3912	3659
2398.04	1	-4	3573	3764	4401	5440	5998	5618	4978	4402	3909	3461	3016	2601	2301	2153	2175	2344	2574
2365.26	1	-4	2657	2456	2207	2101	2136	2270	2458	2718	3112	3586	3862	4042	4508	5323	6371	7581	8849
2332.48	1	-3	982	1005	958	897	877	918	987	993	908	789	672	568	476	397	331	277	236
2299.69	1	-4	2031	1774	1614	1531	1499	1559	1781	2191	2596	2746	2802	2987	3329	3724	3996	3988	3711

Table 3.7 -Continued

cm^{-1}	*XE*	*YE*	0	1	2	3	4	5	6	7	8	9	10	11	12	13	14	15	16
2266.91	1	-4	3325	2988	2750	2643	2665	2786	2907	2947	2967	3115	3553	4360	5522	6714	7001	6050	4764
2234.12	1	-4	3692	2883	2335	2024	1894	1860	1805	1685	1508	1316	1135	997	908	861	857	894	981
2201.34	1	-4	1131	1364	1695	2099	2257	1948	1607	1463	1556	1937	2756	3921	4297	3513	2585	2011	1715
2168.56	1	-4	1552	1468	1475	1561	1661	1670	1616	1594	1645	1725	1700	1504	1211	983	858	803	801
2135.77	1	-4	865	979	1018	917	830	783	766	753	737	704	649	603	574	568	578	613	658
2102.99	1	-4	715	780	847	901	968	1080	1338										
2090.45	0	-4	1509	1622	1609	1505	1396	1314	1248	1183	1119	1051	989	940	903	880	865	858	856
2074.06	0	-4	861	874	898	934	974	1012	1036	1054	1070	1085	1104	1127	1159	1211	1296	1411	1507
2057.67	0	-4	1505	1436	1385	1374	1401	1457	1528	1595	1638	1654	1653	1653	1664	1667	1611	1490	1352
2041.28	0	-4	1231	1135	1073	1031	1006	992	986	987	995	1012	1046	1101	1182	1285	1399	1595	1918
2024.89	0	-4	2374	2715	2606	2238	1921	1711	1585	1508	1469	1457	1470	1507	1563	1633	1729	1850	1999
2008.49	0	-4	2187	2400	2623	2831	2999	3119	3170	3151	3095	3042	3007	2998	3028	3105	3244	3462	3779
1992.10	0	-4	4204	4699	5156	5466	5633	5755	5904	6069	6191	6241	6235	6221	6253	6372	6615	6998	7543
1974.74	1	-3	916	1146	1426	1721	1985	2171	2258	2258	2217	2186	2212	2332	2574	2969	3498	4028	4386
1941.96	1	-3	4396	4108	3622	3053	2499	2018	1636	1357	1165	1020	895	784	692	618	563	529	503
1907.25	2	-3	485	543	656	868	1264	1895	2407	2493	2356	2541	3334	4277	4540	3579	2175	1244	768
1841.68	2	-3	546	459	466	562	673	750	896	1081	1261	1400	1557	1876	2481	3223	3542	3264	2690
1776.11	2	-3	2047	1615	1138	846	685	605	609	699	928	1384	2137	3021	3314	2802	2022	1385	1005
1710.54	2	-4	8276	7988	7684	6783	5828	5004											
1689.33	1	-4	5063	5731	6065	5318	4983	4564	4205	4225	4386	4687	4982	5195	5376	5645	6035	6528	7322
1656.55	1	-3	858	1050	1315	1595	1865	2042	2077	1992	1851	1753	1783						
1636.30	0	-3	1769	1656	1487	1340	1241	1188	1189	1223	1300	1431	1613	1839	2078	2280	2388	2405	2338
1619.91	0	-3	2219	2078	1930	1805	1706	1621	1570	1551	1544	1563	1603	1653	1710	1790	1890	2012	2170
1603.51	0	-2	236	260	288	323	367	425	505	617	767	958	1185	1425	1657	1879	2114	2402	2804
1587.12	0	-2	3437	4526	6065	7099	7079	6483	5545	4510	3571	2813	2248	1849	1584	1420	1332	1290	1258
1569.77	1	-2	1203	1237	1286	1170	939	715	541	406	309	240	194	161	139	124	114	105	99
1536.98	1	-3	932	915	943	994	1046	1104	1189	1288	1447	1627	1853	2080	2261	2377	2484	2688	3052
1504.20	1	-2	370	477	627	778	873	933	1024	1178	1394	1714	2274						
1483.95	0	-1	274	343	449	624	926	1413	1950	2032	1758	1226	833	604	473	380	298	224	171
1467.56	0	-2	1360	1122	959	842	757	697	658	638	634	648	680	735	811	914	1047	1206	1387
1451.17	0	-2	1588	1818	2145	2723	3979	6457	8329	6310	4057	2734	1968	1539	1309	1103	874	687	560
1433.81	1	-3	4123	3348	2838	2427	2075	1766	1501	1286	1118	1004	917	832	773	739	719	720	736
1401.03	1	-3	763	817	920	1098	1372	1747	2135	2339	2273	2049	1799	1626	1582	1699	1961	2240	2305
1368.24	1	-3	2074	1694	1324	1017	791	634	532	464	420	391	373	363	360	363	371	386	408
1335.46	1	-3	443	503	616	845	1298	1822	1698	1333	1131	975	839	756	726	737	784	875	1041
1303.64	0	-3	1172	1358	1620	1959	2339	2641	2705	2499	2141	1760	1447	1217	1059	957	895	858	837
1287.25	0	-3	825	817	813	815	823	840	867	908	965	1049	1174	1365	1658	2069	2465	2654	2624
1269.89	1	-3	2345	2046	1725	1398	1136	945	807	714	659	636	643	682	760	885	1071	1313	1582
1237.11	1	-3	1814	1911	1812	1591	1350	1127	962	871	851	902	1027	1218	1424	1561	1573	1477	1324
1204.32	1	-3	1171	1056	993	972	982	1016	1071	1148	1252	1386	1552	1765	2027	2322	2609	2910	3237
1171.54	1	-3	3399	3239	2978	2794	2721	2745	2829	2926	2960	2868	2662	2429	2215	2022	1886	1817	1797
1138.75	1	-2	186	204	238	302	414	605	915	1336	1652	1600	1399	1278	1167	986	815	709	663
1105.97	1	-1	67	73	84	103	127	154	185	232	307	436	664	965	1065	854	571	364	241
1074.15	0	-2	2032	1791	1677	1716	1956	2482	3061	2939	2304	1825	1530	1294	1071	870	709	585	489
1057.76	0	-3	4144	3556	3112	2791	2526	2309	2116	1980	1882	1812	1761	1737	1707	1688	1696	1726	1748
1041.37	0	-2	180	186	191	197	207	219	236	260	288	328	382	457	563	709	919	1271	1894
1024.97	0	-1	316	589	1011	984	629	377	234	155	110	85	71	65	68	71	60	48	43
1008.58	0	-2	396	395	412	463	610	905	1713	2477	1623	836	560	408	341	298	269	258	250
992.19	0	-3	2485	2629	2679	2507	2448	2415	2366	2348	2362	2372	2365	2322	2269	2193	2120	2055	1992
974.83	1	-3	1869	1854	1901	1927	1959	1999	2012	1982	1882	1748	1607	1514	1429	1435	1465	1549	1714
942.05	1	-3	2001	2479	3205	3957	4088	3498	2759	2198	1857	1698	1708	1853	1986	2020	2157	2506	3201
909.27	1	-2	460	734	1193	1579	1483	1111	772	524	359	256	198	162	140	126	118	113	109
876.48	1	-3	1057	1030	1018	1073	1243	1422	1381	1254	1125	1010	924	870	843	843	871	924	995
843.70	1	-3	1103	1250	1432	1669	1958	2280	2553	2680	2600	2371	2103	1876	1695	1573	1516	1532	1584
810.91	1	-3	1563	1469	1384	1330	1303	1294	1288	1295	1311	1333	1366	1406	1464	1526	1578	1663	1786
778.13	1	-2	194	211	232	258	289	324	369	426	502	601	745	957	1284	1817	2753	4499	7745
745.35	1	-1	1319	2047	2737	3073	2511	1528	829	457	275	183	132	102	84	74			
719.31	0	-2	704	682	672	674	689	718	763	830	926	1066	1269	1574	2046	2794	3986	5866	8554
702.92	0	-1	1125	1182	1009	772	561	411	312	248	211	197	202	222	251	290	349	455	648
686.53	0	-1	961	1309	1409	1175	850	595	417	297	218	167	132	108	91	79	70	63	58
670.14	0	-3	5446	5223	5128	5070	5094	5269	5606	6075	6446	6333	5695	4861	4124	3524	3025	2609	2262
653.74	0	-3	1964	1729	1554	1397	1269	1159	1074	990	913	860	817	770	726	696	655	641	625
637.35	0	-4	6205	6016	5863	5830	5811	5672	5719	5570	5615	5698	5806	5872					
626.26	-1	-4	5866	5860	5840	5821	5830	5840	5886	5933	6029	6125	6287	6449	6705	6960	7346	7732	8337
618.07	-1	-3	894	994	1094	1272	1449	1751	2053	2389	2726	2595	2464	2063	1661	1401	1141	1018	896
609.87	-1	-4	8421	7879	7536	7194	6857	6520	6183	5846	5585	5325	5118	4911	4737	4564	4399	4234	4075

Table 3.7 -Continued

cm^{-1}	*XE*	*YE*	0	1	2	3	4	5	6	7	8	9	10	11	12	13	14	15	16
601.19	0	-4	3765	3481	3227	2994	2781	2581	2394	2226	2076	1944	1828	1722	1631	1565	1499	1440	1409
584.80	0	-4	1390	1375	1349	1311	1266	1228	1201	1175	1155	1139	1116	1089	1062	1035	1011	998	996
568.41	0	-4	996	994	998	1011	1032	1071	1124	1190	1273	1363	1470	1618	1812	2048	2301	2499	2609
552.02	0	-4	2666	2721	2800	2889	2948	2940	2896	2846	2771	2668	2561	2477	2438				
539.96	-1	-4	2433	2442	2452	2495	2537	2650	2762	2947	3131	3374	3617	3838	4058	4091	4124	3907	3691
531.77	-1	-4	3394	3097	2867	2638	2481	2324	2229	2129	1864	1614	1334	1099	962	814	583	345	223
516.34	3	0	0	0	0	0	0												
484.52	0	-2	0	7	15	27	45	67	94	135	189	263	372	533	788	1217	1992	3414	5544
468.13	0	-2	7224	6686	4676	2909	1806	1173	815	613	490	384	288	219	169	133	102	75	57
451.74	0	-4	3994	2635	2454	2512	2163	1395	2561	2745	3113	3596	4258	4095	4970	5940	7151	7795	8486
435.35	0	-3	878	1005															

Footnotes to Tables 3.5, 3.6 and 3.7

a - The column headed cm^{-1} contains the wavenumber of the first ordinate value in the row. The columns headed *XE* and *YE* contain the X-exponent and the Y-exponent, respectively, for the row. The columns headed $0,1,2,\cdots 16$, contain the ordinate values, and the headings give the indices of the ordinate values in the row. In a row which starts with $\tilde{\nu}(0)$, the wavenumber corresponding to the ordinate indexed J is $\tilde{\nu}(J) = \tilde{\nu}(0) - \frac{15798.002}{16384} \cdot J \cdot 2^{XE}$. For Tables 3.5 & 3.7, the $k(\tilde{\nu})$ and $E_m(\tilde{\nu})$ values in that row are the ordinate value shown times 10^{YE}. In Table 3.6, the $n(\tilde{\nu})$ values are given directly with the decimal point implicitly after the first digit. Thus the entry indexed 16 in the first row of Tables 3.5, 3.6 and 3.7 shows that at $\tilde{\nu} = 4799.95 - \frac{15798.002}{16384} \cdot 16 \cdot 2^{0} = 4784.52$ cm^{-1} the ordinate values are: $k = 141 \times 10^{-7} = 1.41 \times 10^{-5}$, $n = 1.5033$ and $E_m = 3752 \times 10^{-5} = 3.752 \times 10^{-2}$.

b - The 4-point spline interpolation program TRECOVER[9], interpolated the $k(\tilde{\nu})$ and $E_m(\tilde{\nu})$ values in the table to the original wavenumber spacing, 0.482117 cm^{-1}, and yielded the original values accurate to 1% below 4000 cm^{-1}, and to 1-2% between 4000 and 4800 cm^{-1}. The original $n(\tilde{\nu})$ values were similarly recovered accurate to 0.1%.

c - The unit of the E_m values is L $mole^{-1}$ cm^{-1}. Multiply the values by 1000 to change the unit to cm^2 $mole^{-1}$.

3.2.4 - Areas under $k(\tilde{\nu})$ and $E_m(\tilde{\nu})$ bands.

Table 3.9 contains the average area under the $k(\tilde{\nu})$ spectrum for each spectroscopist in the integration ranges given in Table 3.1. The areas were measured

Table 3.8 - Peak heights in the molar absorption coefficient spectrum of liquid chlorobenzene at 25°C.[a,b]

$\tilde{\nu}$ (cm^{-1})	$E_m(\tilde{\nu})$	$\tilde{\nu}$ (cm^{-1})	$E_m(\tilde{\nu})$	$\tilde{\nu}$ (cm^{-1})	$E_m(\tilde{\nu})$	$\tilde{\nu}$ (cm^{-1})	$E_m(\tilde{\nu})$
4656.4	1.29(2)	3016.3	4.64(5)	2331.0	1.01(2)	1370.7	2.32(1)
4622.4	0.429(13)	2949.8	0.559(8)	2319.8	1.00(1)	1325.2	1.86(3)
4595.3	0.276(11)	2919.0	0.694(22)	2271.8	0.403(7)	1298.1	2.72(6)
4574.7	0.627(18)	2885.6	0.438(11)	2240.5	0.706(13)	1272.5	2.66(7)
4514.6	0.189(10)	2877.0	0.449(10)	2194.0	0.227(7)	1235.2	1.91(1)
4252.9	0.258(12)	2849.2	0.401(14)	2178.7	0.434(9)	1210.9	1.58(2)
4145.8	0.619(17)	2795.2	0.155(9)	2150.5	0.173(5)	1171.6	3.40(6)
4077.4	2.58(19)	2773.0	0.463(12)	2132.5	0.103(7)	1156.5	2.96(5)
4066.5	2.52(12)	2755.9	0.194(10)	2089.1	0.163(7)	1122.7	16.8(2)
4058.7	2.71(21)	2738.9	0.167(10)	2058.2	0.152(9)	1083.3	107.(1)
4000.5	0.558(12)	2714.3	0.133(8)	2045.6	0.167(6)	1068.1	31.0(5)
3917.7	0.225(7)	2703.1	0.142(8)	2023.7	0.273(10)	1022.6	106.(6)
3899.5	0.237(7)	2663.5	0.687(14)	2002.5	0.317(7)	1001.9	24.8(10)
3785.1	0.748(10)	2648.1	0.441(12)	1962.3	2.27(2)	964.0	2.01(5)
3772.3	0.552(9)	2616.3	0.610(14)	1942.9	4.43(4)	935.0	4.14(22)
3699.4	1.09(2)	2599.8	0.598(11)	1881.5	2.51(1)	902.9	16.1(6)
3653.4	0.215(11)	2582.2	0.470(15)	1862.0	4.58(4)	866.3	1.43(4)
3636.9	0.279(7)	2557.4	0.428(11)	1787.9	3.54(3)	830.1	2.68(12)
3613.6	0.290(9)	2544.3	0.472(12)	1730.6	3.33(3)	812.3	1.59(3)
3488.8	0.153(7)	2510.9	0.146(8)	1685.9	0.611(12)	739.7	308.(7)
3464.1	0.147(5)	2496.0	0.204(9)	1645.5	2.08(2)	702.2	119.(5)
3368.5	0.122(7)	2471.4	0.272(9)	1622.1	2.41(4)	684.8	142.(8)
3165.4	1.17(2)	2446.6	0.208(7)	1583.8	71.9(11)	662.1	6.47(40)
3083.1	11.5(2)	2427.3	0.266(7)	1566.1	12.9(2)	614.1	2.74(15)
3069.5	17.0(3)	2406.4	0.451(9)	1477.6	207.(7)	547.7	0.296(17)
3058.5	13.6(2)	2390.3	0.600(10)	1445.4	83.3(57)	533.4	0.414(11)
3025.8	5.36(4)	2365.7	0.266(14)	1387.1	2.35((1)	467.8	73.5(18)

a - The unit of $E_m(\tilde{\nu})$ is L mole^{-1} cm^{-1}. Multiply the values by 1000 to change the unit to cm^2 mole^{-1}.

b - The number in parentheses is the estimated accuracy in the last digit. The % estimated accuracy is the same as for the corresponding $k(\tilde{\nu})$ value.

above zero ordinate. The 95% confidence limit is given in parentheses except when only one spectrum was available. These spectroscopist average areas were themselves averaged to give an overall unweighted average area and an overall weighted average

Table 3.9 - Spectroscopist average areas under the absorption index bands[a].

Region (cm^{-1})	YA	VB	A	B	C
4785.0-4475.0	0.0328(26)	0.0343(22)		0.0337	
4301.9-3850.2	0.0981(33)	0.0978(15)			
3850.2-3665.5	0.0320(3)	0.0326(2)			
3239.8-2930.3	0.5355(19)	0.5423(21)	0.5430(25)		
2930.3-2895.1	0.00809(8)	0.00796(2)	0.00804(1)	0.00798	
2895.1-2811.2	0.0144(5)	0.0142(1)	0.0145(1)	0.0140	
2811.2-2688.3	0.0133(9)	0.0134(2)	0.0137(1)	0.0127	
2688.3-2517.1	0.0407(11)	0.0412(2)	0.0419(1)	0.0402	
2517.1-2111.7	0.0880(21)	0.0893(2)	0.0902(5)	0.0879	
2000.3-1905.3	0.1377(6)	0.1363(29)	0.1390(2)	0.1372	
1905.3-1835.4	0.1335(8)	0.1324(5)	0.1342(2)	0.1327	
1835.4-1754.4	0.1262(6)	0.1258(3)	0.1269(2)	0.1256	
1754.4-1690.3	0.0933(5)	0.0931(3)	0.0936(1)	0.0928	
1605.4-1545.2	1.080(5)	1.073(5)			
1530.2-1410.2	2.772(14)	2.756(40)			
1405.9-1345.1	0.1013(2)	0.1014(1)		0.1017	0.1013
1345.1-1252.1	0.1491(4)	0.1500(1)		0.1487	0.1496
1252.1-1198.5	0.0948(1)	0.0951(1)		0.0946	0.0950
1198.5-1141.7	0.1959(3)	0.1967(3)		0.1952	0.1975
1140.2-1050.1	2.988(15)	3.002(13)			
1045.2- 970.0	1.308(5)	1.266(6)			
950.3- 851.9	0.6002(4)	0.6028(32)	0.5958(5)	0.6195	0.5942
799.6- 717.1			8.354(56)		
719.3- 649.9	5.065(29)	4.997(46)	5.442(31)		
630.6- 569.9	0.0941(2)	0.0931(3)		0.0898	

a - The unit of area is cm^{-1}. The numbers in parentheses are the 95% confidence limits in the last digit.

area for each band. The weighting was the number of spectra that contributed to the spectroscopist's average. These average areas are listed in Table 3.10. The weighted and unweighted average areas agree well, and the unweighted average areas are taken as the integrated intensities that result from this study.

The agreement between different spectroscopists is shown in Table 3.10 by the

Table 3.10 - Overall average areas under the absorption index bands.

Region (cm^{-1})	k_{max} [a]	Weighted Average Area[b]	Unweighted Average Area[b]	Maximum Deviation[b,c]	Anchor point Uncertainty[b,d]	% Estimated accuracy [e]
4785.0-4475.0	0.000474	0.0332	0.0336	±0.0008	±0.0014	6.55
4301.9-3850.2	0.00128	0.0981	0.0980	±0.0002	±0.0011	1.33
3850.2-3665.5	0.000521	0.0321	0.0323	±0.0003	±0.00027	1.76
3239.8-2930.3	0.00993	0.5389	0.5403	±0.0048	±0.00042	0.97
2930.3-2895.1	0.000424	0.00802	0.00802	±0.00007	±0.00005	1.50
2895.1-2811.2	0.000279	0.0143	0.0143	±0.0003	±0.00012	2.94
2811.2-2688.3	0.000298	0.0134	0.0133	±0.0006	±0.00018	5.86
2688.3-2517.1	0.000461	0.0412	0.0410	±0.0009	±0.00025	2.80
2517.1-2111.7	0.000774	0.0891	0.0889	±0.0013	±0.0006	2.14
2000.3-1905.3	0.00409	0.1376	0.1375	±0.0015	±0.00015	1.20
1905.3-1835.4	0.00442	0.1333	0.1332	±0.0010	±0.00013	0.85
1835.4-1754.4	0.00355	0.1263	0.1261	±0.0008	±0.00016	0.76
1754.4-1690.3	0.00345	0.0933	0.0932	±0.0004	±0.00012	0.56
1605.4-1545.2	0.0813	1.077	1.077	±0.004	±0.00022	0.39
1530.2-1410.2	0.254	2.765	2.764	±0.008	±0.00047	0.31
1405.9-1345.1	0.00303	0.1014	0.1014	±0.0003	±0.0002	0.49
1345.1-1252.1	0.00375	0.1493	0.1493	±0.0007	±0.00027	0.65
1252.1-1198.5	0.00277	0.0949	0.0949	±0.00025	±0.00018	0.45
1198.5-1141.7	0.00520	0.1962	0.1963	±0.0012	±0.0011	1.17
1140.2-1050.1	0.178	2.996	2.995	±0.007	±0.0015	0.28
1045.2- 970.0	0.186	1.285	1.287	±0.021	±0.00083	1.70
950.3- 851.9	0.0319	0.5990	0.6025	±0.0170	±0.00011	2.84
799.6- 717.1	0.747	8.354	8.354	±0.056[f]	±0.014	0.84
719.3- 649.9	0.373	5.181	5.168	±0.274	±0.0058	5.41
630.6- 569.9	0.00796	0.0934	0.0923	±0.0026	±0.0010	3.90

a - Height of the strongest peak in the region.

b - The unit of area is cm^{-1}.

c - Maximum deviation from the unweighted average.

d - The anchor point uncertainty is the integration range multiplied by the average of the uncertainties in $k(\tilde{\nu})$ (see Table 3.1) at the two anchor points used for that range.

e - The estimated accuracy is taken as the sum of the maximum deviation and the anchor point uncertainty.

f - This value is the 95% confidence limit of the measurements of A, the only spectroscopist who measured this band.

maximum deviation of any spectroscopist's average from the unweighted average. The average agreement over all bands is 1.9%. The average agreement for strong, medium and weak bands with $k_{max} > 0.002$ is 1.3%. The average agreement is 3.1% for very weak bands with $k_{max} < 0.002$.

The areas under the molar absorption coefficient, $E_m(\tilde{\nu})$, spectrum are more widely used in analytical chemistry. They are listed in Table 3.11. In addition to the area above zero ordinate, Table 3.11 contains the area above a linear baseline drawn through the E_m values at the integration limits. This latter area is the more accurate, and is the area we recommend as an intensity calibration standard (*vide infra)*.

3.3 - Accuracy of results

3.3.1 - Accuracy of absorption indices and molar absorption coefficients.

We have described previously[1,2] our reasons for regarding the agreement between different spectroscopists as a good measure of the accuracy of our results. We must also consider the systematic error in our absorption index values due to the uncertainties in the values at the anchor points[1,2,4]. Thus, the estimated accuracy of our $k(\tilde{\nu})$ values is taken as the sum of the maximum deviation from the unweighted average (in parentheses in column 3 of Table 3.4) plus the uncertainty due to the anchor points. For the peak heights, the latter is given in column 4 of Table 3.4 and was calculated as the average of the uncertainties in $k(\tilde{\nu})$ at the anchor points on either side of the band (Table 3.1).

Table 3.11 - Overall average areas under molar absorption coefficient bands of liquid chlorobenzene at 25°C

Region (cm^{-1})	Area[a]	Estimated accuracy of area[a,b]	Area above baseline[a]	Estimated accuracy of area above baseline[a,c]
4785.0-4475.0	86.66	5.68	71.14	1.69
4301.9-3850.2	218.9	2.9	167.8	0.3
3850.2-3665.5	67.41	1.19	41.62	0.39
3239.9-2930.3	923.8	9.0	841.8	7.5
2930.3-2895.1	13.03	0.20	2.80	0.02
2895.1-2811.2	22.74	0.67	7.84	0.16
2811.2-2688.3	20.41	1.20	7.20	0.32
2688.3-2517.1	59.53	1.67	40.44	0.89
2517.1-2111.7	115.0	2.5	81.98	1.20
2000.3-1905.3	149.5	1.8	110.8	1.2
1905.3-1835.4	139.1	1.2	105.2	0.8
1835.4-1754.4	126.0	1.0	83.36	0.53
1754.4-1690.3	89.72	0.50	54.49	0.23
1605.4-1545.2	948.8	3.7	849.5	3.2
1530.2-1410.2	2266	7	2159	6
1405.9-1345.1	77.98	0.38	45.19	0.13
1345.1-1252.1	107.7	0.7	61.30	0.29
1252.1-1198.5	64.79	0.29	21.68	0.06
1198.5-1141.7	127.8	1.5	48.72	0.30
1140.2-1050.1	1817	5	1650	4
1045.2- 970.0	729.7	12.4	593.8	9.7
950.3- 851.9	304.3	8.6	192.4	5.4
799.6- 717.1[d]	3451	29	3120	21
719.3- 649.9	1994	108	1705	90
630.6- 569.9	31.45	1.23	11.34	0.32

a - The unit of area is L mole^{-1} cm^{-2}. Divide the values by 100 to obtain areas in the unit km mole^{-1}.

b - Calculated from the percent estimated accuracy of the area, which is the same for $E_m(\tilde{\nu})$ and $k(\tilde{\nu})$ (Table 3.10) bands.

c - The percent estimated accuracy of the area under $E_m(\tilde{\nu})$ above baseline equals the maximum deviation from the unweighted average $k(\tilde{\nu})$ area (Table 3.10) as a percentage of the unweighted average $k(\tilde{\nu})$ area (Table 3.10). This percentage, multiplied by the area under $E_m(\tilde{\nu})$ above baseline gives the numbers in this column.

d - These results are from 5 spectra from spectroscopist A.

The percent estimated accuracies of the $k(\tilde{\nu})$ values at the peak heights are included in Table 3.4. For the 108 peaks, the average accuracy is ±2.9%. This is somewhat larger than the 2.4% agreement between spectroscopists, because of the large number of very weak bands for which the uncertainty due to anchor points is comparable to the maximum deviation from the unweighted average. Thus, for the 65 peaks which have $k_{max} <0.002$, all except 3 of which are above 2000 cm^{-1}, the average accuracy is ±3.3% while the average agreement is ±2.4%. The heights of the remaining 43 peaks with $k_{max} >0.002$ are accurate to ±2.4% on average and the agreement between spectroscopists is 2.3%.

There are only 19 peaks for which the estimated accuracy is no better than 5%, and the poorest accuracy is 7.6% . 13 of these 19 peaks are very weak peaks with $k_{max} <0.002$, and 9 of them have $k_{max} <0.0002$. Three of the 19 peaks are among the 10 strong peaks which have $k_{max} >0.05$, and which have an average accuracy of 3.6%. If these 3 poorly known peaks are excluded, the accuracy of the remaining 7 strong peaks is 2.4%.

The $k(\tilde{\nu})$ values at the peaks can be compared with those of Jones and co-workers[8] which are the only calibrated measurements available. The calibrated results were obtained from samples held at either 20°C or 28°C[8], not at the 25°C of this work. The density change for a 5°C temperature change affects the $k(\tilde{\nu})$ values by about 0.5%, and it is unlikely that a 5°C temperature difference would affect the $k(\tilde{\nu})$ values by more than 2% overall. Köser's results[14] indicate that the heights of the peaks at 1477 and 1023 cm^{-1} decrease by about 2% when the temperature increases from 20 to 25°C, while the peak at 740 cm^{-1} is almost independent of temperature.

There are 102 peak heights reported in both this paper and ref. 8. Forty two of our values lie outside of the evaluated uncertainty limits of Ref. 8, but only twenty values lie outside of the combined error limits of the two studies. Ten of these are very weak peaks between 2100 and 2800 cm^{-1}. In fact only two peaks disagree substantially, those at 1477 and 614 cm^{-1}. The estimated accuracy of the 1477 cm^{-1} peak is 3.5%, but the band was really too intense to yield good measurements in the cells available. This may contribute to the disagreement. As noted above, Köser's results[14] argue that sample temperature is not the cause of our 1477 cm^{-1} peak being 27% lower than the calibrated value[8].

The $k(\tilde{\nu})$ values in the baseline are not known as accurately as those in regions of significant absorption, except at the anchor points. From the agreement between different workers and the uncertainties in the anchor point values, we estimate the accuracy of the baseline $k(\tilde{\nu})$ values to be approximately $\pm 2\times10^{-6}$ above 3000 cm^{-1}, $\pm 6\times10^{-6}$ between 3000 and 1650 cm^{-1}, and $\pm 6\times10^{-5}$ below 1650 cm^{-1}. These values corresponds to about ±5% and ±2.5% of the weakest $k(\tilde{\nu})$ values above and below 3000 cm^{-1}, respectively.

The percent estimated accuracy of the molar absorption coefficient, $E_m(\tilde{\nu})$, values is that of the corresponding $k(\tilde{\nu})$ value. The accuracies are given in Table 3.8 in parentheses as absolute values, not as percentages.

3.3.2. - Accuracy of areas.

To calculate the estimated accuracy of the areas under the $k(\tilde{\nu})$ bands given in Table 3.10, the average uncertainty in $k(\tilde{\nu})$ at the anchor points (Table 3.1) on each side of the integration range was multiplied by the integration range and added to the maximum deviation from the unweighted average area (Table 3.10). The estimated accuracy is given in Table 3.10 for each band, as a percentage of the unweighted area. The average accuracy over all 25 spectral regions is an excellent 1.9%. Of the 17 bands, for which $k_{\max} > 0.002$ the average accuracy is 1.3%. The only regions for which the accuracy of the area is poor are the regions of very weak absorption from 4785 to 4475 cm^{-1}, 2811 to 2688 cm^{-1}, and 719 to 650 cm^{-1}. The latter may have been influenced by the very strong neighbouring band at 739.5 cm^{-1}, for which spectra were only available from one spectroscopist.

A comparison was made with the areas under three $k(\tilde{\nu})$ bands reported by Köser from dispersive transmission measurements[15]. For the integration ranges 1550.0 - 1350.0, 1100.0 - 825.0, and 825.0 - 615.0 cm^{-1}, the areas are 2.89, 4.53 and 13.65 cm^{-1} from our spectrum and 2.97, 1.86 and 13.71 cm^{-1} from Köser's spectrum. Two regions show excellent agreement. The agreement in the 1100-825 cm^{-1} region is extremely poor. However, the integration range 1100 - 825 cm^{-1} includes a large region of weak absorption, and it is probable that baseline accuracy plays a large part in the disagreement.

The percent estimated accuracy of the area under a molar absorption coefficient band equals that of the corresponding absorption index band (Table 3.10). The accuracy is given in Table 3.11 as an absolute value, not as a percentage.

Table 3.11 includes the areas under the molar absorption coefficient spectrum above *a linear baseline drawn through the molar absorption coefficients at the integration limits*. These areas are free from error due to the anchor points, so their estimated accuracy simply reflects the agreement between spectroscopists that is shown by the maximum deviation from the unweighted average area under the corresponding $k(\tilde{\nu})$ band (Table 3.10). The percent accuracy of the area above the baseline thus equals the maximum deviation as a percentage of the unweighted mean area (Table 3.10). In Table 3.11 we report the actual estimated accuracy of the area above the baseline, not the percent accuracy.

For selected regions, these $E_m(\tilde{\nu})$ areas above baseline and the real and imaginary refractive index and molar absorption coefficient values, will be submitted to Commission I.5 of the International Union of Pure and Applied Chemistry for consideration as secondary intensity standards for infrared spectroscopy of liquids.

3.3.3 - Accuracy of real refractive indices.

The real refractive indices, $n(\tilde{\nu})$, were calculated by adding the value n = 1.5043±0.0005 at 8000 cm^{-1} to the value of $\Delta n(\tilde{\nu})$ that is calculated by the Kramers-Kronig transform[10] of the $k(\tilde{\nu})$ spectrum. The accuracy of $n(\tilde{\nu})$ is, then, the sum of the 0.05% accuracy intrinsic to our Kramers-Kronig transform[10], the 0.03% accuracy of the value 1.5043 at 8000 cm^{-1} plus the ~0.08% accuracy of $\Delta n(\tilde{\nu})$ which results from the accuracy of the $k(\tilde{\nu})$ values. The accuracy of the $n(\tilde{\nu})$ values is, thus, ~0.2%.

3.4 - Summary

Transmission spectra of liquid chlorobenzene at 25°C that were measured by 5 spectroscopists in 4 different laboratories have been transformed to absorption index spectra. These $k(\tilde{\nu})$ spectra were compared and averaged to yield spectra between 4800 and 450 cm^{-1} of the absorption index, the real refractive index and the molar absorption coefficient that are believed to be the most accurate currently available. Absorption index, $k(\tilde{\nu})$, and molar absorption coefficient, $E_m(\tilde{\nu})$, values are believed accurate to ±2.4% on average at the peaks of stronger bands , and ±3.3% at weaker bands (k<0.002). The baseline $k(\tilde{\nu})$ values are known to ~5% above 3000 cm^{-1} and ±2.5% below 3000 cm^{-1}. The areas under 17 bands or band groups in $k(\tilde{\nu})$ and $E_m(\tilde{\nu})$ spectra for which k_{max} >0.002 are known to ±1.3% on average. The real refractive index, $n(\tilde{\nu})$, values are believed accurate to 0.2%.

For future reference, the complete numerical data is presented in Compact Table format[9] to allow the original spectra to be recovered by interpolation without loss of accuracy. The complete final $k(\tilde{\nu})$, $n(\tilde{\nu})$, and $E_m(\tilde{\nu})$ spectra obtained in this work are available on diskette from the authors. To make them available over the longer term, it is planned to place them on an internationally accessible data base.

3.5 - References

1. J.E. Bertie, R.N. Jones, and C.D. Keefe, Appl. Spectrosc., **47**, 891 (1993).
2. J.E. Bertie, R.N. Jones, Y. Apelblat, and C.D. Keefe, Appl. Spectrosc., **48**, 127 (1994).
3. I. Mills, T. Cvitas, K. Homann, N. Kallay, and K. Kuchitsu, *Quantities, Units and Symbols in Physical Chemistry. International Union of Pure and Applied Chemistry* (Blackwell Scientific Publications, Oxford 1988)
4. J.E. Bertie, C.D. Keefe and R.N. Jones, Can. J. Chem., **69**, 1609 (1991).
5. J.E. Bertie, C.D. Keefe, R.N. Jones, H.H. Mantsch, and D.J. Moffatt, Appl. Spectrosc., **45**, 1233 (1991)
6. J.E. Bertie, R.N. Jones, and V. Behnam, Appl. Spectrosc., **39**, 401 (1985).
7. J.E. Bertie, R.N. Jones and V. Behnam, Appl. Spectrosc., **40**, 427 (1986).

8. T.G. Goplen, D.G. Cameron and R.N. Jones, Appl. Spectrosc., **34**, 657 (1980).

9. J.E. Bertie, R. N. Jones and Y. Apelblat, Appl. Spectrosc., **47**, 1989 (1993).

10. J.E. Bertie and S.L. Zhang, Can. J. Chem., **70**, 520 (1992).

11. J. Timmermans. *Physico-chemical constants of pure organic compounds*, (Elsevier, New York, 1950) p. 285.

12. J. Timmermans. *Physico-chemical constants of pure organic compounds*, Vol. 2 (Elsevier, Amsterdam, 1965) p.241-2.

13. *International critical tables of numerical data, physics, chemistry and technology*, (1st Ed. McGraw-Hill, 1930) p. 38, vol VII.

14. H.J.K. Köser, Ber. Bunsenges. Phys. Chem., **88**, 24 (1984).

15. H.J.K. Köser, Spectrochim. Acta A, **40**, 117 (1984).

Chapter 4 - Assignments of Vibrations for Chlorobenzene and Toluene

Despite numerous experimental and theoretical studies reported in the literature on toluene[14-36] and chlorobenzene[18,22,23,35-47] there are still some disagreements about the assignments of the fundamental vibrations, especially for toluene. While some of the disagreements are simply due to the use of different notation systems, others are due to different choice of wavenumbers or the assignment of similar wavenumbers to different symmetry modes.

4.1 - Symmetry and vibrational notations for benzene and monosubstituted benzenes

The differences in notation arise from two main numbering schemes for the vibrations of the benzene molecule: Wilson's[13,71] and Herzberg's[72]. A third notation system of using letters for the assignments was used by Whiffen[37] for halogen substituted benzenes but was not used afterwards.

Wilson's notation was introduced first and has only been used for benzene and substituted derivatives of benzenes. Herzberg's notation was introduced later and is in general use. In both numbering schemes, vibrations are numbered according to their symmetry species. Within each symmetry species, Herzberg numbers the vibrations in order of decreasing wavenumber. Wilson, on the other hand, numbers them in order of increasing wavenumber with one or two exceptions. An additional difference between the two systems is the order in which the symmetry species for D_{6h} molecules such as

Table 4.1 - Assignments of benzene using Herzberg and Wilson notation schemes.

Symmetry Species	Assignment[a,b]	Herzberg's Notation	Wilson's Notation
A_{1g}	CH stretch	ν_1	ν_2
A_{1g}	CC stretch	ν_2	ν_1
A_{2g}	HCC bend	ν_3	ν_3
A_{2u}	oop HCC bend (75), CCC deformation (25)	ν_4	ν_{11}
B_{1u}	CH stretch	ν_5	ν_{13}
B_{1u}	CCC deformation	ν_6	ν_{12}
B_{2g}	oop HCC bend (65), CCC deformation (35)	ν_7	ν_5
B_{2g}	oop CCC deformation (85), HCC bend (15)	ν_8	ν_4
B_{2u}	CC stretch (75), HCC bend (25)	ν_9	ν_{14}
B_{2u}	HCC bend (65), CC stretch (35)	ν_{10}	ν_{15}
E_{1g}	oop HCC bend	ν_{11}	ν_{10}
E_{1u}	CH stretch	ν_{12}	ν_{20}
E_{1u}	HCC bend (70), CC stretch (30)	ν_{13}	ν_{19}
E_{1u}	CC stretch (65), HCC bend (35)	ν_{14}	ν_{18}
E_{2g}	CH stretch	ν_{15}	ν_7
E_{2g}	CC stretch (65), HCC bend (25), CCC deformation (20)	ν_{16}	ν_8
E_{2g}	HCC bend (80), CC stretch (20)	ν_{17}	ν_9
E_{2g}	CCC deformation	ν_{18}	ν_6
E_{2u}	oop HCC bend (80), CCC deformation (20)	ν_{19}	ν_{17}
E_{2u}	oop CCC deformation (85), HCC bend (15)	ν_{20}	ν_{16}

a - Potential energy distribution in percent is given in brackets. Contributions over 90% are omitted.

b - oop indicate out-of-plane displacements. The remaining vibrations are in-plane.

benzene are listed. Wilson's character table[13] lists the species in the following order: A_{1g}, A_{2g}, B_{1g}, B_{2g}, E_{1g}, E_{2g}, A_{1u}, A_{2u}, B_{1u}, B_{2u}, E_{1u} and E_{2u}. Herzberg[69] lists them in the following order: A_{1g}, A_{1u}, A_{2g}, A_{2u}, B_{1g}, B_{1u}, B_{2g}, B_{2u}, E_{1g}, E_{1u}, E_{2g} and E_{2u}. Table 4.1 lists the vibrational assignments of benzene under both, Wilson's and Herzberg's

Table 4.2 - Correlation table between D_{6h} and C_{2v} symmetry species for monosubstituted benzenes

D_{6h}	C_{2v}[a]	D_{6h}	C_{2v}[a]
A_{1g}	A_1	B_{2u}	B_2
A_{2g}	B_2	E_{1g}	$A_2 + B_1$
A_{2u}	B_1	E_{1u}	$A_1 + B_2$
B_{1u}	A_1	E_{2g}	$A_1 + B_2$
B_{2g}	B_1	E_{2u}	$A_2 + B_1$

a - The A_1 and B_2 displacements are in the plane of the ring.

notations. The potential energy distributions were obtained from earlier normal coordinate calculations of benzene made by C.D. Keefe[73].

Monosubstituted benzenes have C_{2v} symmetry which indicates a lower symmetry than benzene. The lower symmetry has the effect of splitting some of the degenerate vibrations in benzene into non degenerate vibrations in the substituted benzenes. The symmetry species for C_{2v} symmetry are: A_1, A_2, B_1 and B_2. The A_1 and A_2 vibrations are the in-plane and out-of-plane modes, respectively, that are symmetric with respect to the 2-fold rotation axis. The B_1 and B_2 modes are antisymmetric with respect to the 2-fold rotation and they depend on the coordinate system used. In a coordinate system in which the plane of molecule is the YZ plane, the B_1 modes are the out-of-plane modes and the B_2 are the in-plane modes. This notation is used throughout the thesis, as recommended by the Joint Commission for Spectroscopy of IUPAP and IUPAC[74]. These C_{2v} species can be related to the D_{6h} species through the correlation table[13] given in Table 4.2.

The difference in symmetry species for D_{6h} and C_{2v} should result in different numbering of related vibrations for the substituted benzenes. Chlorobenzene, a representative of the monosubstituted benzenes, has 12 atoms which leads to 12x3-6 = 30 vibrational modes. These 30 vibrational modes are distributed among the C_{2v} symmetry species as $11A_1+3A_2+6B_1+10B_2$. If either Wilson's or Herzberg's notation is used, the 11 A_1 vibrations would be numbered 1 through 11, the 3 A_2 vibrations would be numbered 12 through 14, the 6 B_1 vibrations would be numbered 15 through 20 and the 10 B_2 vibrations would be numbered 21 through 30. The vibration numbers would be different from those of the parent vibration of benzene. Thus, under Herzberg's notation, ν_{15} (E_{2g}) of benzene, is split under C_{2v} symmetry into an A_1 and a B_2 vibration. The vibration numbers would be between 1 and 11 for the A_1 mode and between 21 and 30 for the B_2 mode.

Clearly, such a rigorous application of Herzberg's or Wilson's notation makes comparison of similar vibrations in different molecules very difficult. Differences of this nature always occur between benzene and monosubstituted benzenes, and even occur among the monosubstituted benzenes themselves as the number given to a vibration within a symmetry species depends on its wavenumber. The wavenumber of a particular vibration, such as the A_1, CX stretching vibration, may change significantly with the change of mass of the substituent X, and this may result in the CX stretching mode being in a different position in the sequence of the A_1 vibrations ordered according to wavenumber. For example, the A_1 CD stretching vibration of monodeuterobenzene is ν_4 while the CCl stretching vibration of chlorobenzene is regarded as ν_{11}.

It is clear from the above example that there is an incentive to use a similar numbering scheme for substituted benzenes to that used for benzene. By doing so, the comparison of similar vibrations in different molecules is simplified. The practice of most authors is to use either Wilson's or Herzberg's notation for benzene. Whenever a degenerate vibration in benzene is split, the benzene vibration number is kept and the letter "a" or "b" is added. All "a" vibrations in monosubstituted benzenes are symmetric with respect to 2-fold rotation, and so are either A_1 or A_2 species under C_{2v}, while all "b" vibrations in monosubstituted benzenes are antisymmetric with respect to 2-fold rotation and so are either B_1 or B_2 species. Thus, under Herzberg's notation and the above practice, ν_{15} (E_{2g}), the CH stretch in benzene, is split under C_{2v} symmetry into ν_{15a} (A_1) and ν_{15b} (B_2). Under Wilson's notation, the same vibration in benzene is labeled ν_7 (E_{2g}) and is split into ν_{7a} (A_1) and ν_{7b} (B_2) under C_{2v} symmetry. These notations do not follow either Wilson's or Herzberg's notations for C_{2v} molecules, but are commonly used. Throughout the thesis they are termed either pseudo-Wilson or pseudo-Herzberg notation.

It must be realized that the pseudo-Wilson and pseudo-Herzberg notations only approximately indicate the relation between a vibration of the C_{2v} molecule and the parent vibration of benzene. To understand this, consider the A_1 vibrations under C_{2v}. The reduction of symmetry from D_{6h} to C_{2v} causes a mixing of all the benzene vibrations that correlate with A_1 vibrations under C_{2v}. In most cases the vibration under C_{2v} can not be described by just one vibration under D_{6h}, which is what the pseudo-Wilson or pseudo-Herzberg notations attempt. Nevertheless, these notations have been widely used and the pseudo-Herzberg notation will be used, together with the true Herzberg notation in the thesis.

The disagreements that result from the use of different notations can be easily resolved by a) adopting a single notation scheme[75], or b) quoting previous authors and pointing out the correlation between the previous authors assignments and the current assignments. Throughout the thesis, the recommendation by Miller[75], to use the Herzberg notation, is followed. In addition, the pseudo-Herzberg notation is preferred to the pseudo- Wilson and consequently assignments using the pseudo-Wilson notation made by various authors are converted to the pseudo-Herzberg notation in this thesis using Table 4.3.

In order to relate the true Herzberg notation to the pseudo-Herzberg notation, the relation between the form of the C_{2v} vibration and that of the D_{6h} vibration must be known. The origin of the relation used must be stated with each table in which the two notations appear.

The disagreements due to notation are not important to the understanding of the vibrations and therefore will be considered to have been resolved. Other differences in assignments are discussed in Section 4.2 for chlorobenzene and in Section 4.4 for toluene.

Table 4.3 - Conversion table for the pseudo notations for the assignments of vibrations of monosubstituted benzenes.

pseudo-Herzberg	pseudo-Wilson	pseudo-Herzberg	pseudo-Wilson
ν_{1}	ν_{2}	ν_{13b}	ν_{19b}
ν_{2}	ν_{1}	ν_{14a}	ν_{18a}
ν_{3}	ν_{3}	ν_{14b}	ν_{18b}
ν_{4}	ν_{11}	ν_{15a}	ν_{7a}
ν_{5}	ν_{13}	ν_{15b}	ν_{7b}
ν_{6}	ν_{12}	ν_{16a}	ν_{8a}
ν_{7}	ν_{5}	ν_{16b}	ν_{8b}
ν_{8}	ν_{4}	ν_{17a}	ν_{9a}
ν_{9}	ν_{14}	ν_{17b}	ν_{9b}
ν_{10}	ν_{15}	ν_{18a}	ν_{6a}
ν_{11a}	ν_{10a}	ν_{18b}	ν_{6b}
ν_{11b}	ν_{10b}	ν_{19a}	ν_{17a}
ν_{12a}	ν_{20a}	ν_{19b}	ν_{17b}
ν_{12b}	ν_{20b}	ν_{20a}	ν_{16a}
ν_{13a}	ν_{19a}	ν_{20b}	ν_{16b}

4.2 - Previous assignments of the chlorobenzene vibrations

All of the 30 fundamental vibrations of chlorobenzene are Raman active, and all except the 3 A_2 vibrations are infrared active. In principle, theoretical calculations[72,76-79] of band contours of asymmetric top molecules allow the determination of the symmetry species of the vibrations which cause bands in the observed gas phase infrared spectrum. These calculations yield three different types of band for each C_{2v} molecule, A, B and C, due to the rotational transitions associated with the vibrational transitions. The band

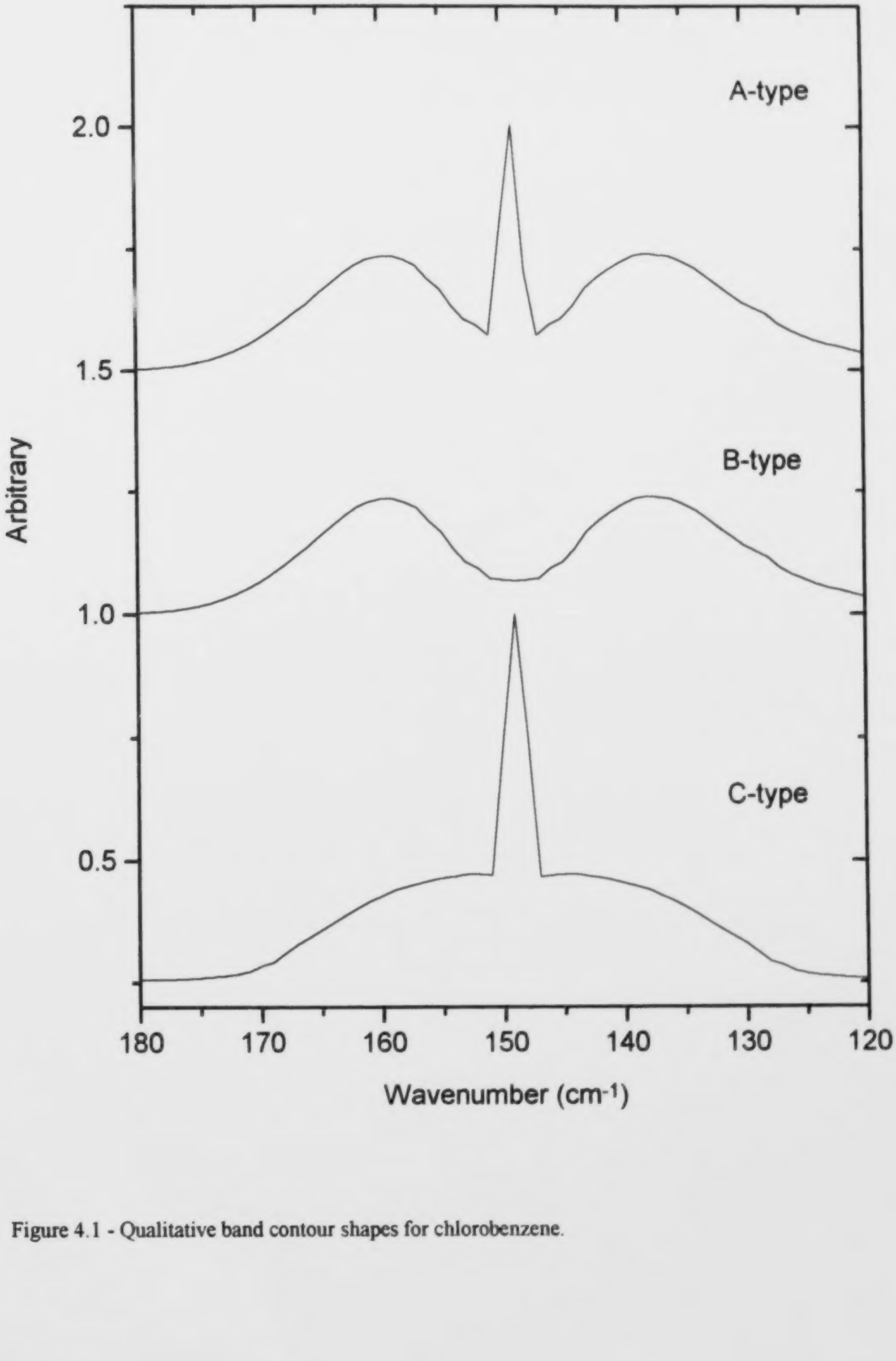

Figure 4.1 - Qualitative band contour shapes for chlorobenzene.

shapes depend on the moments of inertia. For chlorobenzene[80-82] these are I_a = 89.1±0.1 a.m.u Å^2, I_b = 320.5±0.1 a.m.u Å^2 and I_c = 409.7±0.1 a.m.u Å^2 and for toluene[83] are I_a = 89.2 a.m.u Å^2, I_b = 200.8 a.m.u Å^2 and I_c = 289.1 a.m.u Å^2. According to Ueda and Shimanouchi[79] the moments of inertia yield the three band shapes shown in Fig. 4.1, which are qualitatively the same for chlorobenzene and toluene. In type A, a strong sharp central peak due to Q branch transitions is observed as well as medium side-bands due to P and R branches. In type B, the Q branch is absent and only the unresolved P and R branches are observed. In the C type, a strong Q branch is observed with weak P and R branches. For chlorobenzene and toluene, an A-type band indicates an A_1 vibration, a B-type band indicates a B_2 vibration and a C-type band indicates a B_1 vibration.

In practice, a complete assignment based just on the gas phase infrared spectrum is not possible. First, some wavenumbers of fundamental and/or combination transitions are very similar which results in overlapping and distortion of band shapes. Second, the A_2 vibrations are infrared inactive and are unobserved in the gas phase spectrum. However, in the liquid phase, where adjacent molecules can induce a dipole moment change, the A_2 vibrations can be observed with weak intensity. Further information about the symmetry of vibrations can be obtained from the Raman spectrum. According to Herzberg[72], the A_1 modes are polarized in the Raman spectrum, with depolarization ratio for linearly polarized incident light $\rho_\ell \leq 0.75$, while the other modes are depolarized, with depolarization ratio $\rho_\ell = 0.75$. Cross correlation of observed wavenumbers from infrared and Raman measurements permitted several authors to present a complete assignment for the fundamental vibrations of chlorobenzene. The assignment of the fundamental vibrations made by several authors are summarized in Tables 4.4 to 4.7. The differences between them are not due to notation but rather to the use of different wavenumbers or different symmetry species. It is important though, to clarify the notation used by each author and his data source.

The first major study of chlorobenzene since 1950 was by Whiffen[37]. For the 30 vibrations he used the letters a through y for the assignment of 25 vibrations and z_1 through z_5 for the remaining 5 vibrations, the CH stretches. Whiffen's letters define a C_{2v} symmetry coordinate through Fig. 1 in his paper. His notation was quoted in later studies but was not adopted. He used wavenumbers from experimental infrared and Raman spectra collected from various studies cited in his paper. He took the plane of the molecule as XZ and, thus, his B_1 species are interchanged with our B_2 species.

In 1960, Schmid, Brandmuller and Nonnenmacher[18] performed normal coordinate calculations with a constant force field and obtained the wavenumbers of benzene and monosubstituted benzenes including chlorobenzene and toluene. In addition to the calculated wavenumbers, experimental wavenumbers obtained from gas and liquid phase infrared and liquid phase Raman measurements were also given, some measured by the authors and some taken from earlier studies. The authors use a true Herzberg notation but their B_1 and B_2 species are interchanged with ours. The authors also gave the pseudo-Wilson notation.

In the early 1970s, Bist and co-workers[40,42] reported vibrational data for gaseous chlorobenzene from measurements of the infrared spectrum and the UV electronic spectrum. The authors used the pseudo-Wilson notation.

In the early 1970's, two books were published which, *inter alia*, summarized the vibrations of monosubstituted benzenes. Sverdlov, Kovner and Krainov[22] selected without explanation fundamental wavenumbers from a variety of authors, several of whom published in unobtainable USSR journals. The true Herzberg notation was used with the B_1 and B_2 vibrations interchanged with ours. The second book, written by Varsanyi[23], is specific to benzene and its derivatives. Varsanyi again selected without explanation fundamental frequencies from a variety of authors including Sverdlov, Kovner and Krainov[22]. The pseudo-Wilson notation was used.

In 1992-3, Pulay and co-workers[47] reported the fundamental vibrational wavenumbers obtained from scaled *ab initio* calculations. The experimental wavenumbers which guided the scaling were taken from Bist *et al.*[40,42] and Whiffen[37]. The notation used is a true Herzberg notation.

Several other authors have reported vibrational studies on chlorobenzene. However, the studies either gave only partial wavenumbers and assignments[38,41,44-46] or, as is the case for some theoretical studies[39,43], used wavenumbers and assignments from previous studies without change. These studies will be cited when deemed necessary.

In the following sub-sections, the assignment of the fundamentals by these authors is reviewed. The differences will be pointed out, however, a critical evaluation of the authors' choices is left to Section 4.3 where an assignment is proposed, based on all available data, including data measured for this thesis.

4.2.1 - The 11 A_1 vibrations of chlorobenzene

Previously reported wavenumbers and assignments for the 11 A_1 vibrations of chlorobenzene are given in Table 4.4. The first column gives the true Herzberg notation, and, for convenience, the pseudo-Herzberg notation is given in the second column. In Table 4.4 and in the later Tables 4.5 to 4.7, the pseudo notation was taken from Schmid *et al.*[18], who determined the relation between the C_{2v} vibrations and those of benzene in the early 1960's. Schmid's pseudo-Wilson notation was converted to the pseudo-Herzberg notation in column 2.

The remaining columns in Table 4.4 contain each author's wavenumbers and assignments. Bist's[40,42] and Varsanyi's[23] pseudo-Wilson notations have been converted to pseudo-Herzberg notation in Table 4.4. No assignment is given for Pulay[47], Schmid[18] and Sverdlov[22]. Pulay and Sverdlov used only the true Herzberg notation which is shown in column 1 of Table 4.4. The experimental wavenumbers listed in the table are those from infrared measurement in the liquid phase except for those of Bist. When the Raman wavenumber is used, it is denoted by the letter R next to the wavenumber.

The agreement on the fundamental wavenumbers is generally very good among the experimental studies. In several cases, Bist's wavenumber is high by up to 8 cm^{-1}, but this is likely due to differences in the wavenumber calibration. There are however

Table 4.4 - Previous assignments of the A_1 vibrations of chlorobenzene

		Experimental							Theoretical	
		Whiffen[a] [Ref 37]		Bist[b,c] [Ref 40]		Sverdlov[d] [Ref 22]	Varsanyi[b] [Ref 23]		Schmid[d,e] [Ref 18]	Pulay[d,e] [Ref 47]
Herzberg notation true	pseudo	cm^{-1}		cm^{-1}		cm^{-1}	cm^{-1}		cm^{-1}	cm^{-1}
ν_1	ν_{12a}	3071	Z_1	3082	ν_{12a}	3086	3086	ν_{12a}	3075	3087
ν_2	ν_1	3050	Z_2	3054	ν_1	3050R	3071	ν_1	3069	3071
ν_3	ν_5	3029	Z_3	3031	ν_5	3029	3029	ν_5	3053	3047
ν_4	ν_{16a}	1580	k	1586	ν_{16a}	1580	1580	ν_{16a}	1632	1590
ν_5	ν_{13a}	1477	m	1482	ν_{13a}	1475	1477	ν_{13a}	1513	1475
ν_6	ν_{15a}	1174	a	1153	ν_{17a}	1175	1174	ν_{17a}	1225	1179
ν_7	ν_{17a}	1085	q	1093	ν_{15a}	1085	1085	ν_2	1140	1097
ν_8	ν_{14a}	1026	b	1026	ν_{14a}	1027	1026	ν_{14a}	1023	1017
ν_9	ν_6	1003	p	1004	ν_2	1002	1003	ν_6	1000	989
ν_{10}	ν_{18a}	701	r	706	ν_6	702	701	ν_{18a}	708	698
ν_{11}	ν_2	415	t	417	ν_{18a}	418	420	ν_{15a}	389	413

a - Author used his own notation scheme.

b - Assignments in pseudo-Wilson notation were converted to pseudo-Herzberg notation using Table 4.3.

c - Wavenumbers of the infrared spectrum of the gas.

d - Authors used the true Herzberg notation in column 1.

e - Calculated wavenumbers.

three significant wavenumber differences. Bist *et al.*[40] reported ν_6 at 1153 cm^{-1} while Whiffen[37], Sverdlov *et al.*[22] and Varsanyi[23], all put it at 1174±1 cm^{-1}. Other wavenumber differences occur for two CH stretching vibrations, ν_1 and ν_2. ν_2 is given as

3052±2 cm^{-1} by Whiffen[37], Bist[40] and Sverdlov[22], while Varsanyi[23] places it about 20 cm^{-1} higher at 3071 cm^{-1}. ν_1 is given as 3071 cm^{-1} by Whiffen[37], while Bist[40], Sverdlov[22] and Varsanyi[23] placed it at 3084±2 cm^{-1}.

There are also deviations from the pseudo-Herzberg notation. Varsanyi[23] and Bist[40] disagree with each other and with Schmid[18] about the pseudo-Herzberg description of ν_6, ν_7, ν_9, ν_{10} and ν_{11}. ν_6 is assigned as ν_{17a}, HCC deformation and CC stretch (Table 4.1), by both Varsanyi and Bist, while Schmid[18] assigns it as ν_{15a}, the E_{2g} CH stretch which, near 1160 cm^{-1}, means it is related to the CX stretching mode. Miller[75] has noted that ν_9 derives from ν_6 of benzene not ν_2. However, in the other cases, the authors give little evidence to help evaluate the other assignments which, in any case, probably arise from the limitations of the pseudo-Herzberg description.

The computed frequencies by Schmid *et al.*[18] and Pulay *et al.*[47] agree reasonably well with the experimental wavenumbers. However both are to some extent fitted to their chosen experimental data, so can not really settle disagreements.

4.2.2 - The 3 A_2 vibrations of chlorobenzene

The wavenumbers and assignments of the A_2 vibrations are given in Table 4.5. The table is arranged in a similar manner to Table 4.4. All wavenumbers and assignments from the different experimental studies are in excellent agreement, and the computed wavenumbers are in satisfactory agreement with experiment.

Table 4.5 - Previous assignments of the A_2 vibrations of chlorobenzene

		Experimental							Theoretical	
		Whiffen[a]		Bist[b,c]		Sverdlov[d]	Varsanyi[b]		Schmid[d,e]	Pulay[d,e]
Herzberg notation		[Ref 37]		[Ref 42]		[Ref 22]	[Ref 23]		[Ref 18]	[Ref 47]
true	pseudo	cm^{-1}		cm^{-1}		cm^{-1}	cm^{-1}		cm^{-1}	cm^{-1}
ν_{12}	ν_{14a}	965	h	961	ν_{14a}	965	965	ν_{14a}	979	956
ν_{13}	ν_{11a}	830	g	832	ν_{11a}	830	830	ν_{11a}	848	821
ν_{14}	ν_{20a}	400	w	400R	ν_{20a}	400R	400	ν_{20a}	405	404

a - Author used his own notation scheme.

b - Assignments in pseudo-Wilson notation were converted to pseudo-Herzberg notation using Table 4.3.

c - Wavenumbers of the infrared spectrum of the gas.

d - Authors used the true Herzberg notation in column 1.

e - Calculated wavenumbers.

Table 4.6 - Previous assignments of the B_1 vibrations of chlorobenzene[*]

		Experimental							Theoretical	
		Whiffen[a]		Bist[b,c]		Sverdlov[d]	Varsanyi[b]		Schmid[d,e]	Pulay[d,e]
Herzberg notation		[Ref 37]		[Ref 42]		[Ref 22]	[Ref 23]		[Ref 18]	[Ref 47]
true	pseudo	cm^{-1}		cm^{-1}		cm^{-1}	cm^{-1}		cm^{-1}	cm^{-1}
ν_{15}	ν_{7}	985	j	981	ν_{7}	984	985	ν_{7}	984	981
ν_{16}	ν_{19b}	902	i	902	ν_{19b}	903	902	ν_{19b}	919	899
ν_{17}	ν_{11b}	740	f	740	ν_{11b}	740	740	ν_{4}	752	740
ν_{18}	ν_{8}	682	v	685	ν_{8}	682	682	ν_{8}	700	679
ν_{19}	ν_{4}	467	y	467	ν_{20b}	469	467	ν_{20b}	490	466
ν_{20}	ν_{20b}	196R	x	198R	ν_{4}	196R	196	ν_{11b}	224	187

[*] - See footnotes to Table 4.5

4.2.3 - The 6 B_1 vibrations of chlorobenzene

The wavenumbers and assignments of the B_1 vibrations are given in Table 4.6 which is arranged in a similar manner to Table 4.4. All wavenumbers are in excellent agreement from the different experimental studies and the computed wavenumbers are in satisfactory agreement with the experimental values.

Differences in assignment or description of the vibration by the pseudo-Herzberg notation exist for ν_{17}, ν_{19} and ν_{20} with different authors assigning different vibrations to ν_4, ν_{11b} and ν_{20b}. However, these pseudo-Herzberg description all indicate a mixture of out-of-plane HCC and CCC deformations, so the differences are of detail, not principle.

4.2.4 - The 10 B_2 vibrations of chlorobenzene

The wavenumber and assignments of the B_2 vibrations are given in Table 4.7 which is arranged in a similar manner to Table 4.4.

The only significant wavenumber disagreement is for ν_{21}, ν_{22} and ν_{23}. For the CH stretching modes, there is no agreement within 25 cm^{-1} about the wavenumber of ν_{21}, and Bist[40] preferred 3067 cm^{-1} to 3052 cm^{-1} for ν_{22}. For ν_{23}, Bist's wavenumber is 18 cm^{-1} higher than that of Whiffen[37], Sverdlov[22] and Varsanyi[23]. This difference is at the high end of what can be expected from calibration errors.

The only disagreement in notation is Varsanyi's assignment of ν_{28} and ν_{30} to ν_{14b} and ν_{10} instead of the reverse. ν_{14b} and ν_{10} are, however, both mixtures of HCC in-plane

Table 4.7 - Previous assignments of the B_2 vibrations of chlorobenzene

		Experimental							Theoretical	
		Whiffen[a]		Bist[b,c]		Sverdlov[d]	Varsanyi[b]		Schmid[d,e]	Pulay[d,e]
Herzberg notation		[Ref 37]		[Ref 40]		[Ref 22]	[Ref 23]		[Ref 18]	[Ref 47]
true	pseudo	cm^{-1}		cm^{-1}		cm^{-1}	cm^{-1}		cm^{-1}	cm^{-1}
ν_{21}	ν_{12b}	3071	Z_4	3096	ν_{12b}	3086	3050	ν_{12b}	3079	3082
ν_{22}	ν_{15b}	3052R	Z_5	3067	ν_{15b}	3052R	3052	ν_{15b}	3044	3058
ν_{23}	ν_{16b}	1580	ℓ	1598	ν_{16b}	1580	1570	ν_{16b}	1592	1596
ν_{24}	ν_{13b}	1445	n	1448	ν_{13b}	1445	1445	ν_{13b}	1445	1438
ν_{25}	ν_9	1326	o	1326	ν_9	1326	1326	ν_9	1324	1320
ν_{26}	ν_3	1271	e	1271	ν_3	1271	1271	ν_3	1298	1272
ν_{27}	ν_{17b}	1157	c	---	ν_{17b}	1157R	1157	ν_{17b}	1141	1162
ν_{28}	ν_{10}	1068	d	1068	ν_{10}	1068	1068	ν_{14b}	1064	1069
ν_{29}	ν_{18b}	616	s	615	ν_{18b}	617	616	ν_{18b}	629	618
ν_{30}	ν_{14b}	297	u	295	ν_{14b}	296	297	ν_{10}	321	291

a - Author used his own notation scheme.

b - Assignments in pseudo-Wilson notation were converted to pseudo-Herzberg notation using Table 4.3.

c - Wavenumbers of the infrared spectrum of the gas.

d - Authors use the true Herzberg notation in column 1.

e - Calculated wavenumbers.

bend and CC stretching, so the difference is again one of detail not principle.

4.3 - Assignments of the chlorobenzene vibrations

There is good but not complete agreement between the assignments of the fundamentals of chlorobenzene in the literature. Unfortunately very little experimental evidence has been cited in support of any of these assignments, so it is impossible to evaluate the disagreements. For this reason, it was decided to collect some evidence in this work to help to evaluate the assignments. Three types of evidence were collected in addition to the quantitative infrared spectrum of the liquid reported in Chapter 3.

First, the infrared spectrum of the gas was recorded in order to observe the contours of the different bands, and, hence, deduce the symmetry of the vibration that causes the band. As discussed previously, for chlorobenzene an A-type indicates an A_1 vibration, B-type indicates a B_2 vibration and a C-type indicates a B_1 vibration. A_2 vibrations are unobserved in the gas phase spectrum.

Second, the Raman spectrum of the liquid was recorded under parallel ($I_\parallel$) and perpendicular ($I_\perp$) polarizations, with linearly polarized incident light. Frequently bands that are weak in the infrared are strong in the Raman so additional vibrations can sometimes be observed in the Raman. Further, values of the depolarization ratio, $\rho_\ell = \frac{I_\perp}{I_\parallel}$ that are less than 0.75 indicate that the band arises from an A_1 vibration under C_{2v}. For A_2, B_1 and B_2 vibrations under C_{2v}, $\rho_\ell = 0.75$.

Third, the selection of fundamental vibrations was guided by a very simple normal coordinate calculation that showed the changes in fundamental wavenumbers that must occur simply from the change in mass of the substituent atom. Thus the latest force field and geometry for liquid benzene[73] were used without change, and only the mass of the substituent atom was changed. This was done for C_6H_5D, $C_6H_5CH_3$ and C_6H_5Cl, where a single atom of mass 15 was used to substitute the CH_3 group in toluene. These calculations indicated the approximate wavenumber of the fundamentals in the monosubstituted benzenes, with C_6H_5Cl being of interest in this section. Further, when the symmetry coordinates under D_{6h} that were written for benzene, were used in the calculations for the molecules of C_{2v} symmetry, the relation between the C_{2v} vibration and the D_{6h} symmetry coordinates was directly given by the eigenvectors. Thus, the pseudo-Herzberg notation for the vibration was made by choosing the D_{6h} symmetry coordinate that contributed the most to the C_{2v} vibration.

The experimental data and the results of the calculations are presented below so as to form a basis for the evaluation of the assignments. The liquid phase real and imaginary refractive index spectra, obtained for the secondary intensity standards project and reported in Chapter 3, were converted into the real and imaginary molar polarizability spectra by use of Equations 1.3.33 and 1.3.28. The wavenumbers assigned in this section are the wavenumbers of peaks in the imaginary molar polarizability, α_m'', spectrum. The experimental spectra of chlorobenzene are shown in Figures 4.2 to 4.8. First, the entire infrared α_m'' spectrum of the liquid is given in Fig. 4.2. Figures 4.3 to 4.8 show the same infrared spectrum, the infrared bands of the gas, and the parallel and perpendicular Raman spectra for smaller wavenumber ranges, and thus provide a better view of the various features of the spectra. In addition, Table 4.8

gives information from all the three spectra for every feature observed in the regions where the fundamentals are expected, i.e. 3150 - 2950 cm^{-1} and 1700 - 175 cm^{-1}. The first three columns give the wavenumber, a brief description and the peak height of the band in the infrared α_m'' spectrum of the liquid. When the feature is a shoulder its position and height are estimated and are indicated by a ~. In columns 4 and 5 the infrared gas phase band's wavenumber and shape are given. The labels ? and ?? are used to indicate uncertainty and great uncertainty, respectively, in the determination of the band shape. The wavenumber of a B-type vibration was taken at the minimum of the R and P branches while the peak of the Q branch is given for the A-type and C-type bands. In columns 6 and 7 the Raman wavenumber and the depolarization ratio are given for the liquid. When the feature is too weak or noisy to obtain a reliable ratio, the labels p and dp are used to indicate a polarized or depolarized band.

The computed wavenumbers, eigenvectors and potential energy distribution (PED) for chlorobenzene are given in Table 4.9. Only the main contributions are given in the eigenvector and PED columns. It is clear from this table that the fundamental vibrations are a mixture of several symmetry coordinates. Hence, attempts in the past to describe them as being derived from a single vibration in benzene, which is what the pseudo notations do, were bound to fail and create disagreements in notations.

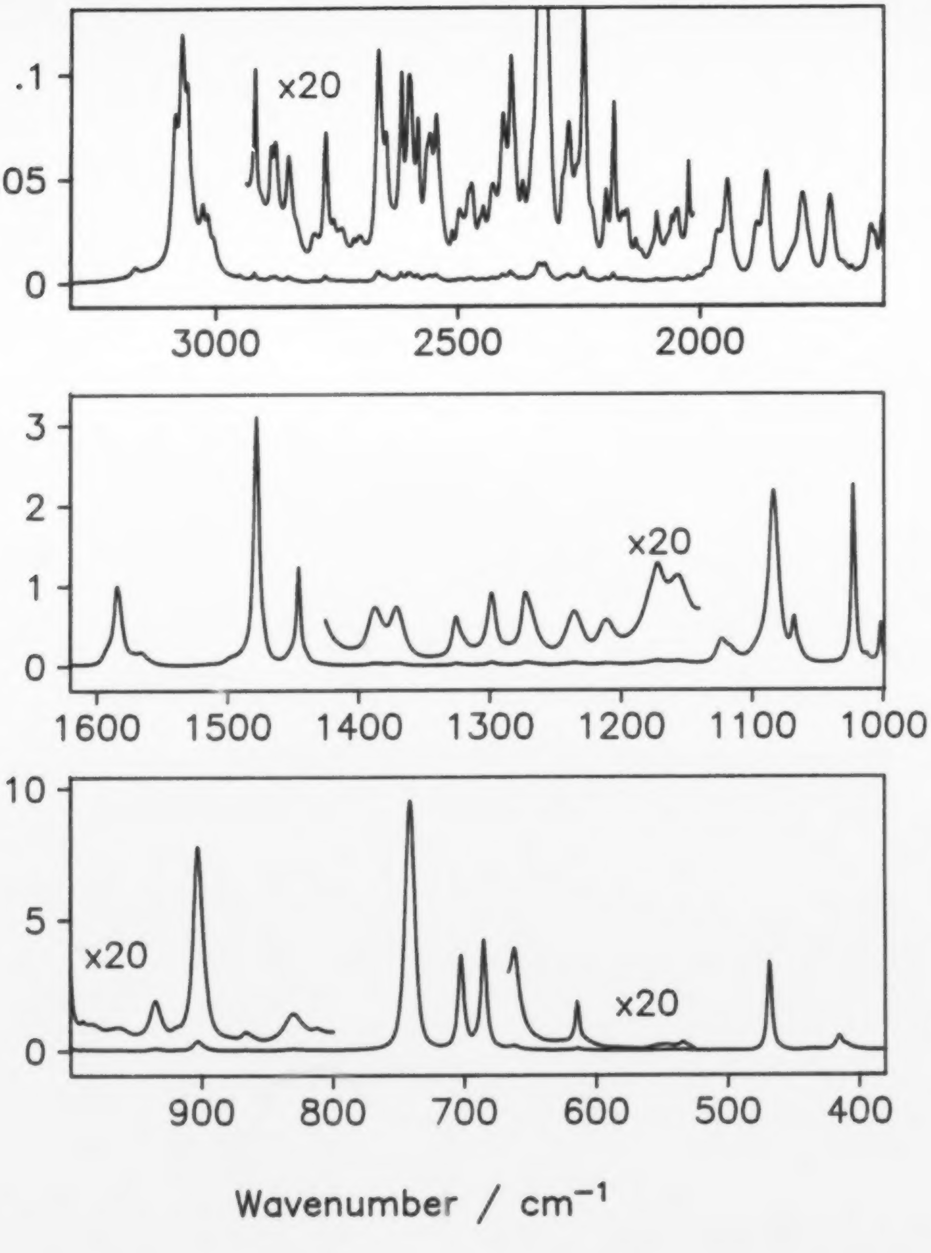

Figure 4.2 - Imaginary molar polarizability, α''_{m}, spectrum of liquid chlorobenzene. Units are $\mathrm{cm}^3\ \mathrm{mol}^{-1}$. In each box, the ordinate scale is for the lower curve. It needs to be divided by 20 for the upper curve.

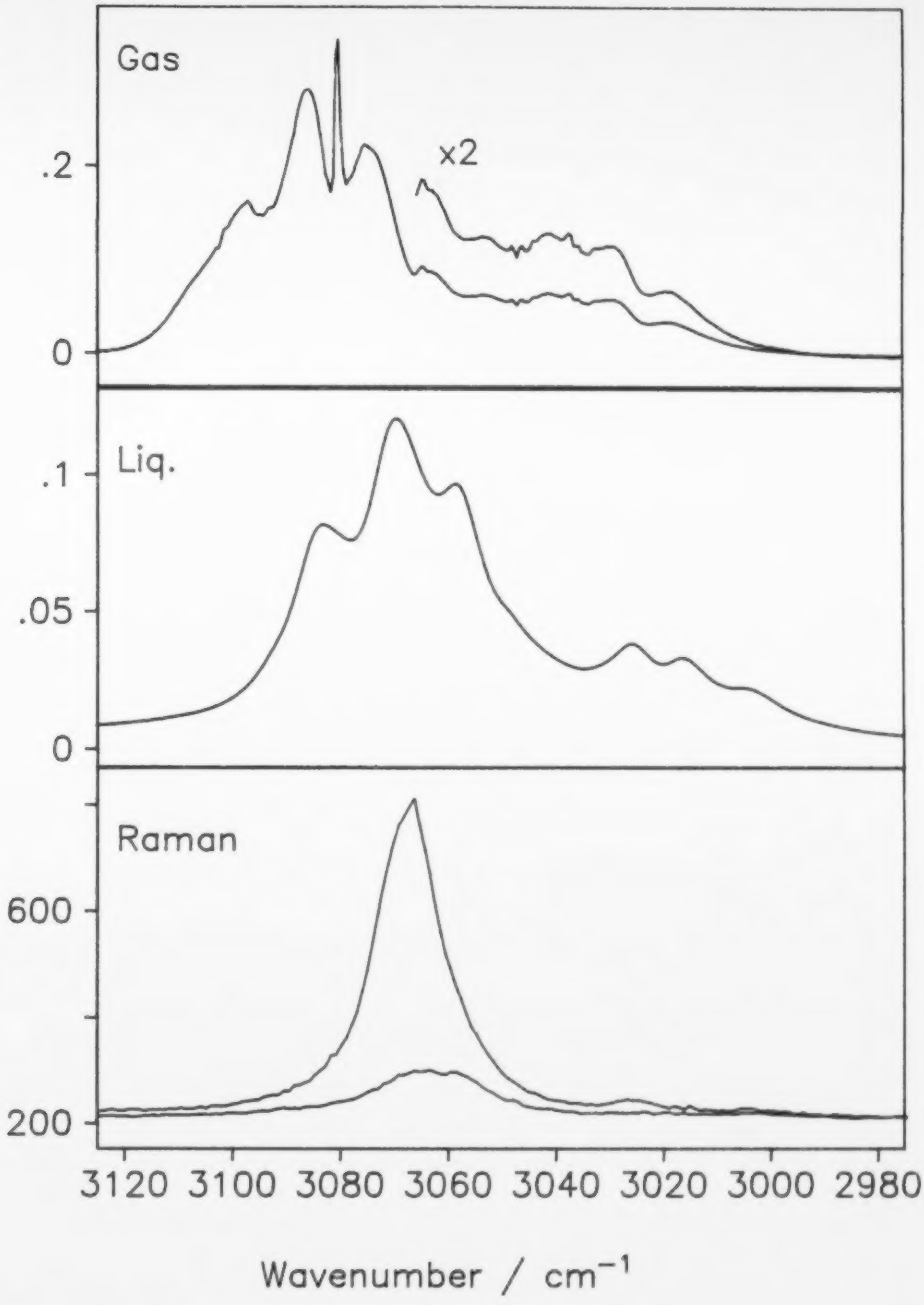

Figure 4.3 - Infrared spectra of gas and liquid chlorobenzene and Raman parallel (upper) and perpendicular (lower) spectra of the liquid between 3125 and 2975 cm^{-1}. In each box, the ordinate scale is for the lower curve. It needs to be divided by the multiplication factor for the upper curve.

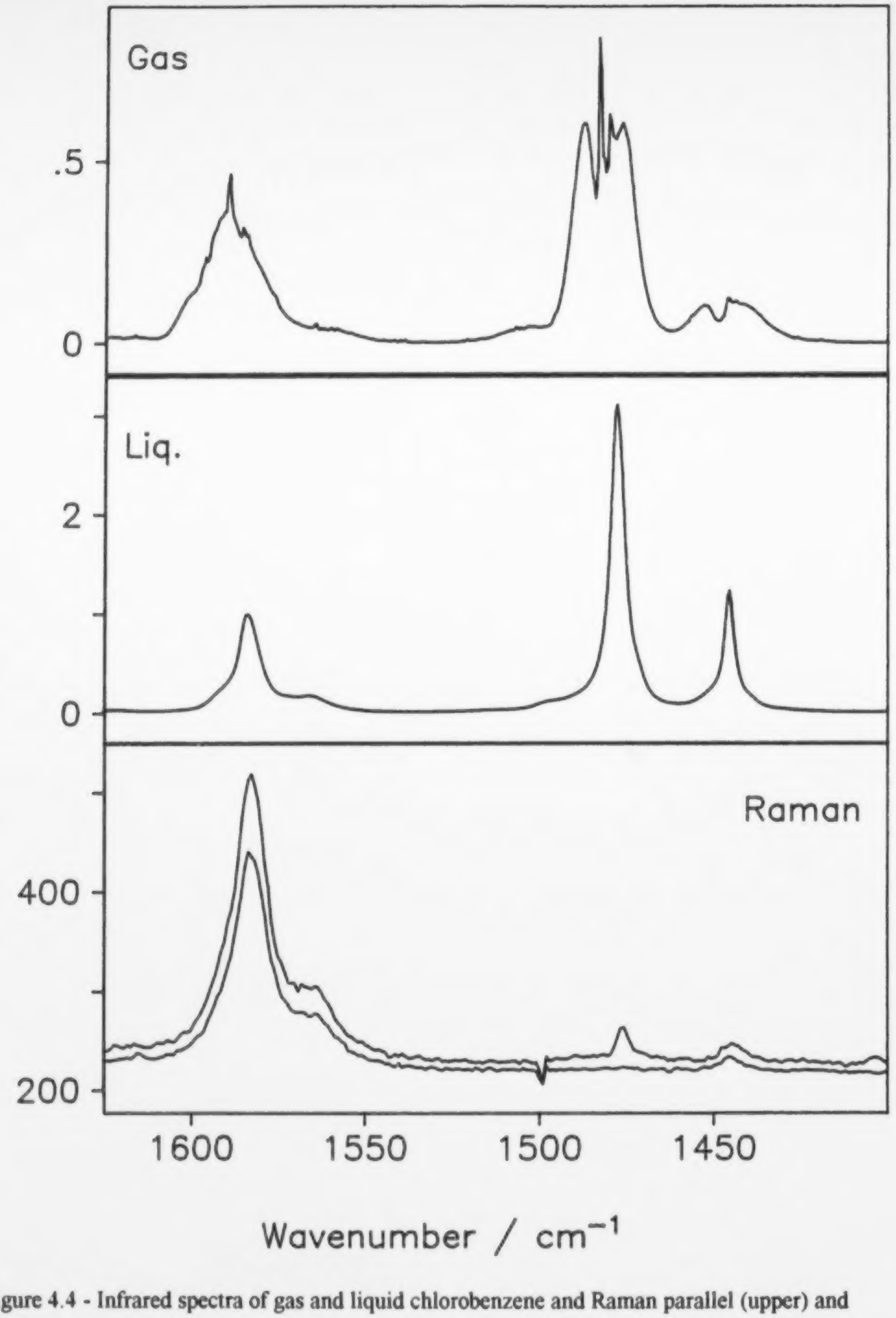

Figure 4.4 - Infrared spectra of gas and liquid chlorobenzene and Raman parallel (upper) and perpendicular (lower) spectra of the liquid between 1625 and 1400 cm^{-1}. In each box, the ordinate scale is for the lower curve. It needs to be divided by the multiplication factor for the upper curve.

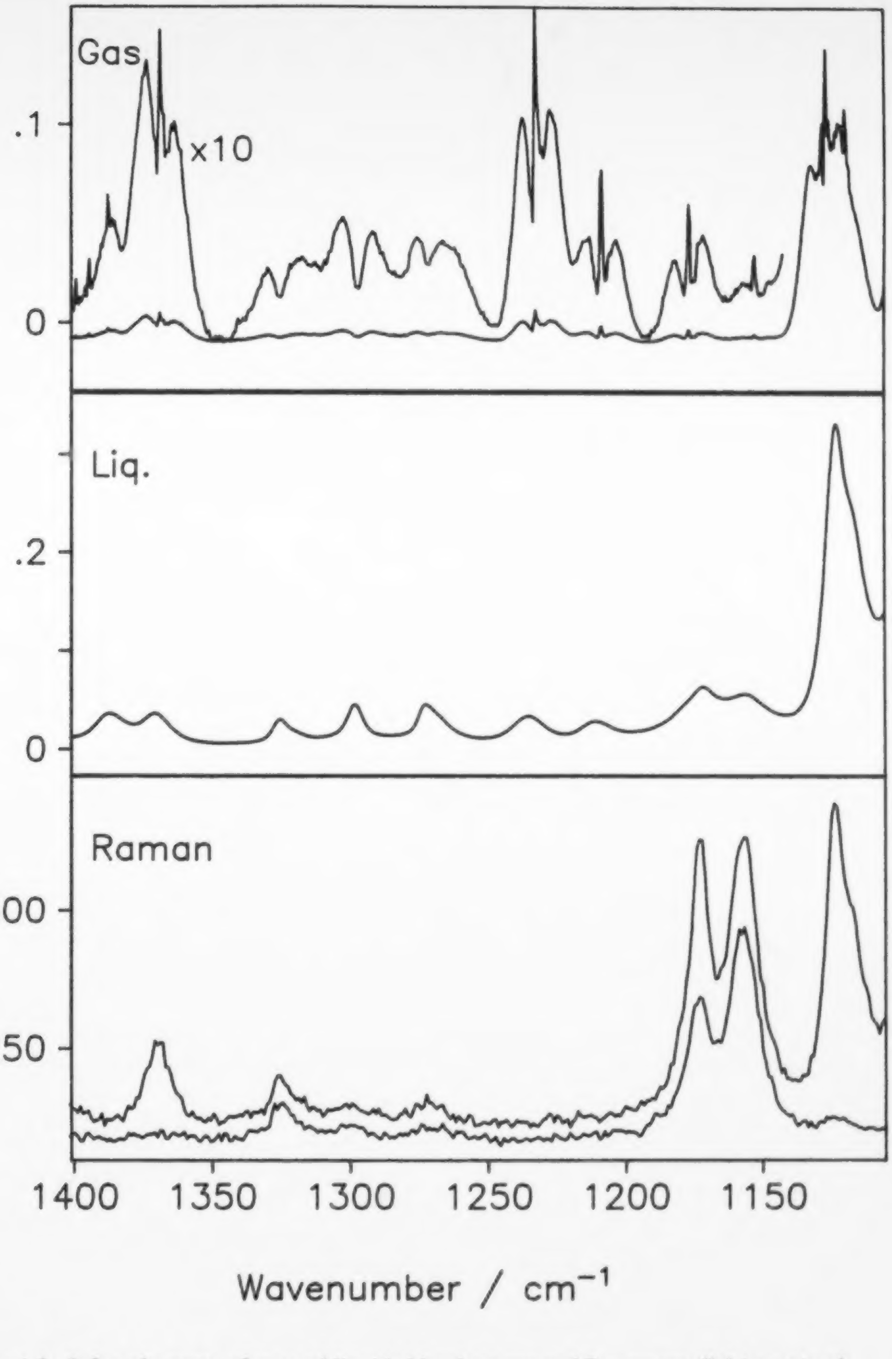

Figure 4.5 - Infrared spectra of gas and liquid chlorobenzene and Raman parallel (upper)and perpendicular (lower) spectra of the liquid between 1400 and 1105 cm^{-1}. In each box, the ordinate scale is for the lower curve. It needs to be divided by the multiplication factor for the upper curve.

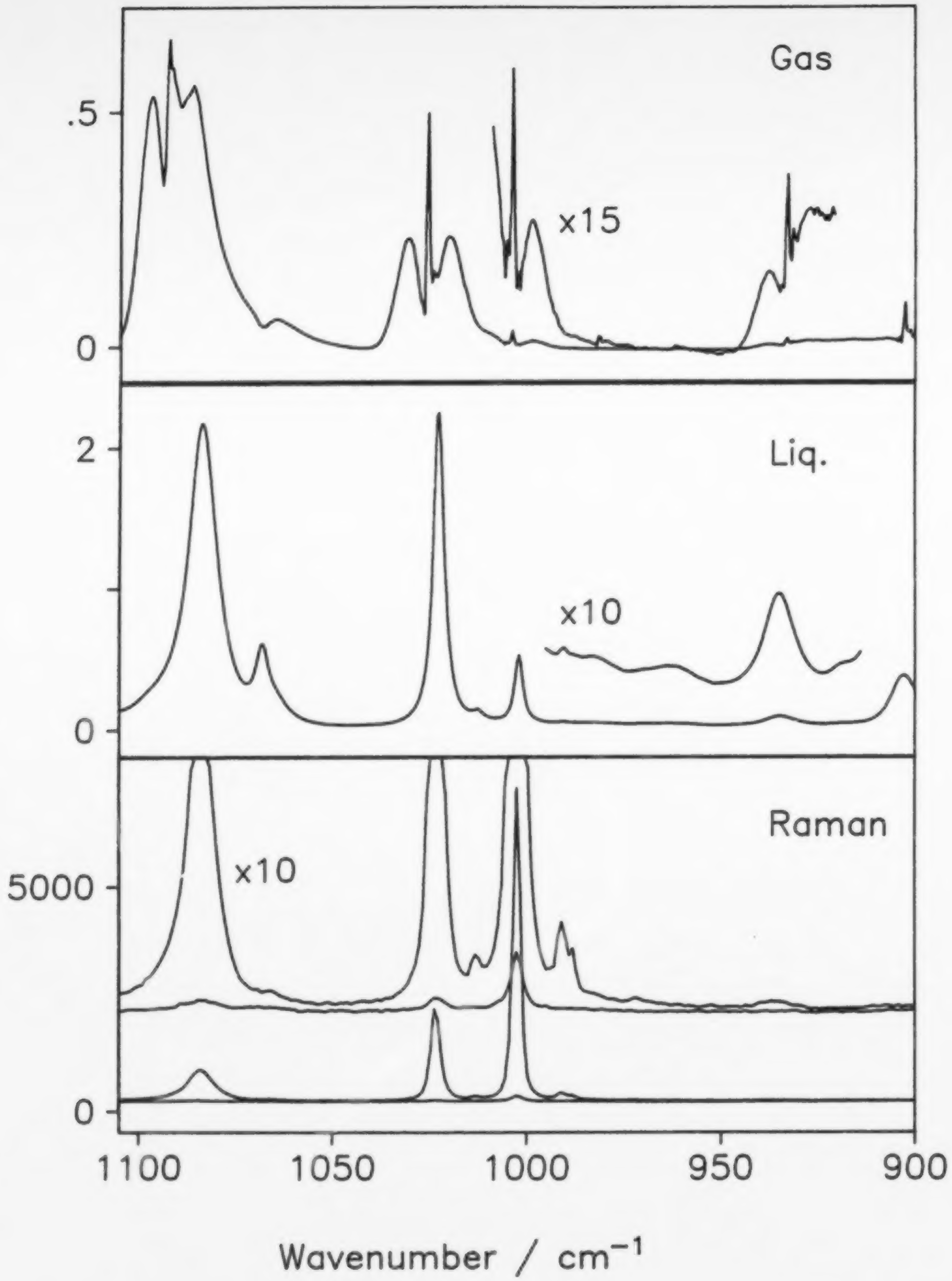

Figure 4.6 - Infrared spectra of gas and liquid chlorobenzene and Raman parallel (upper) and perpendicular (lower) spectra of the liquid between 1105 and 900 cm^{-1}. In each box, the ordinate scale is for the lower curve. It needs to be divided by the multiplication factor for the upper curve.

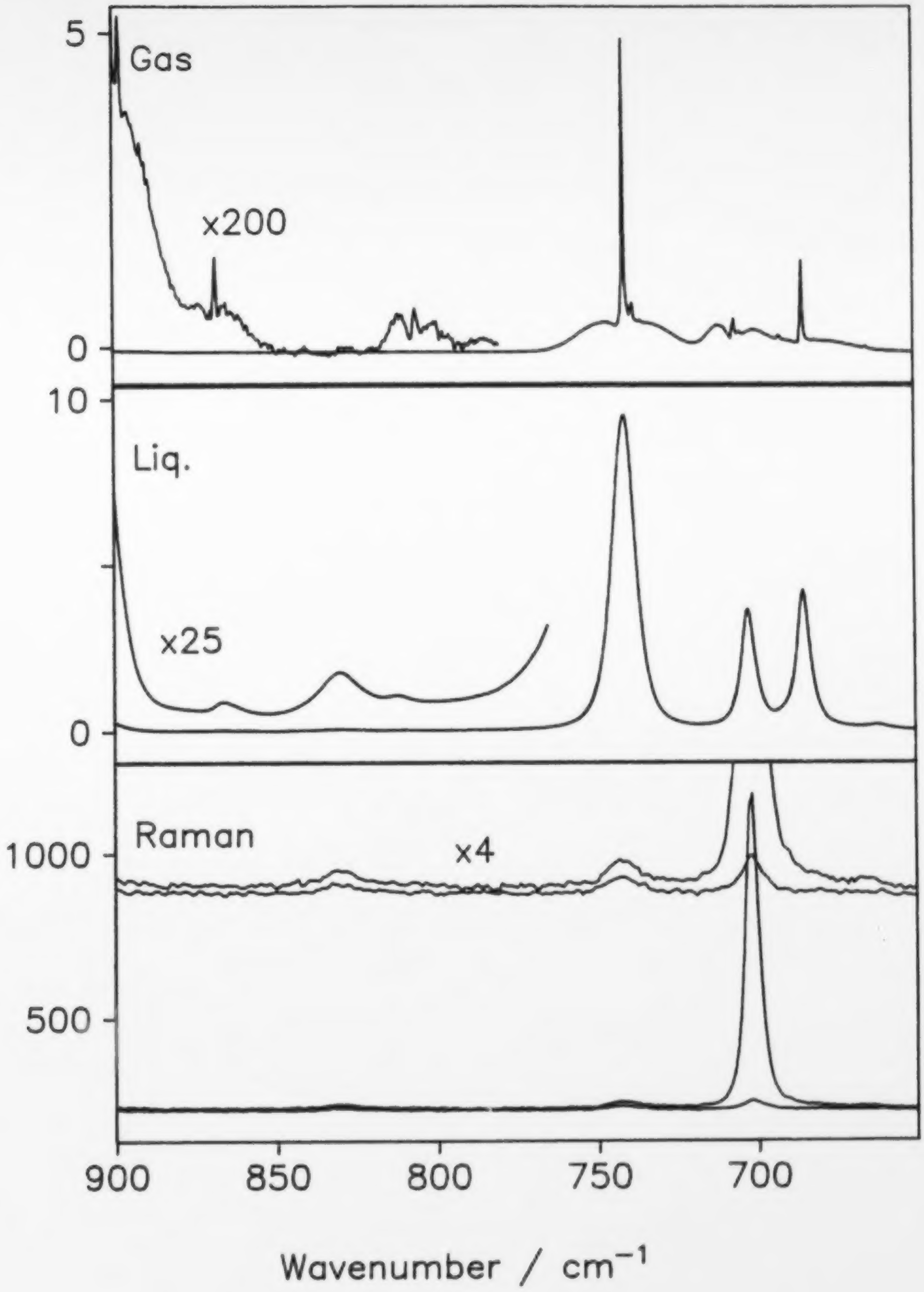

Figure 4.7 - Infrared spectra of gas and liquid chlorobenzene and Raman parallel (upper) and perpendicular (lower) spectra of the liquid between 900 and 650 cm^{-1}. In each box, the ordinate scale is for the lower curve. It needs to be divided by the multiplication factor for the upper curve.

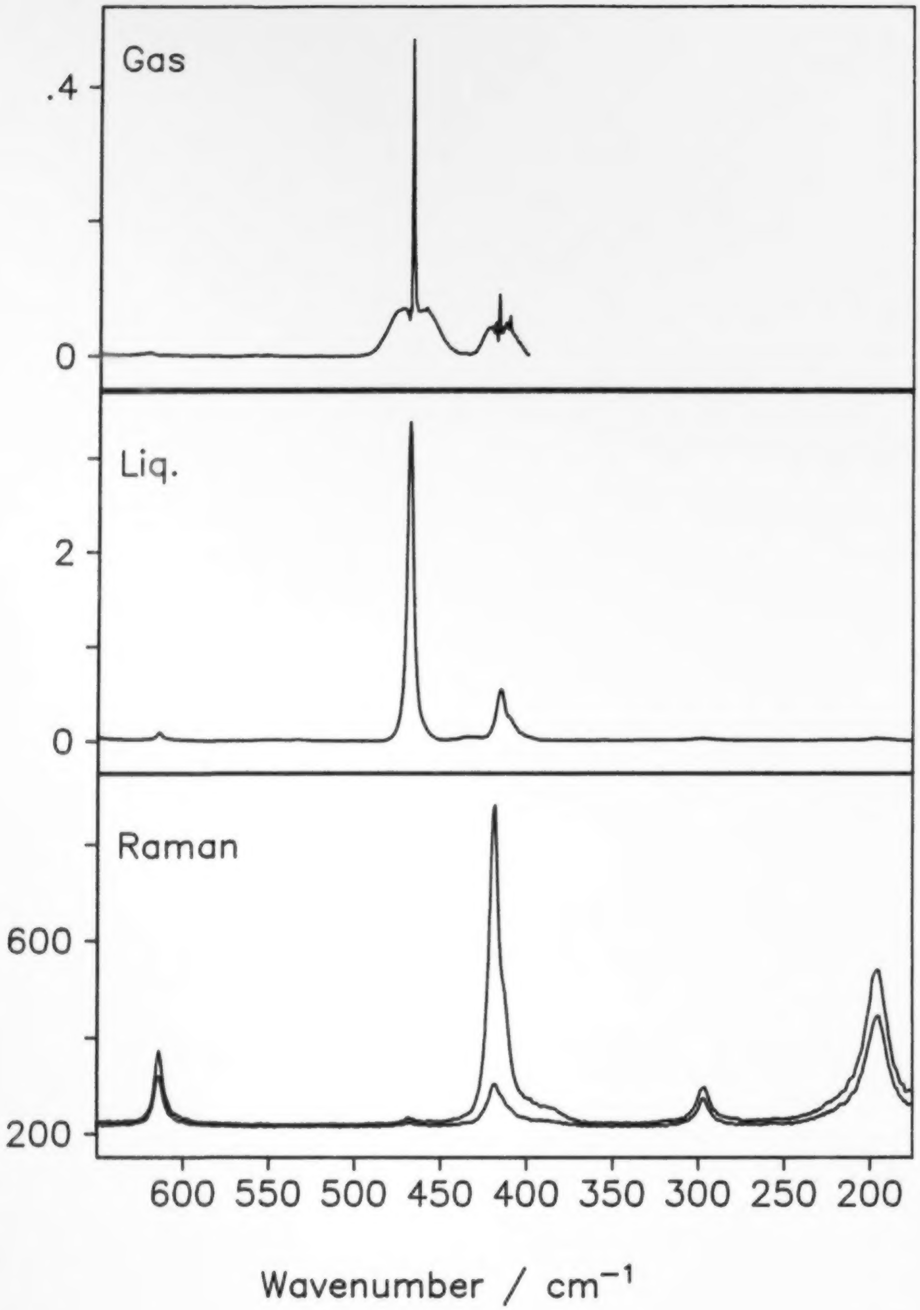

Figure 4.8 - Infrared spectra of gas and liquid chlorobenzene and Raman parallel (upper) and perpendicular (lower) spectra of the liquid between 650 and 175 cm^{-1}.

Table 4.8 - Features in the experimental infrared spectra of gas and liquid chlorobenzene and Raman spectra of liquid chlorobenzene

Infrared liquid [a]			Infrared gas [d]		Raman liquid [b]		
cm^{-1}	Desc.[b]	α''_m [c]	cm^{-1}	Contour	cm^{-1}	ρ_ℓ [e]	comments
3083.1	m	0.0817	~3095	B?			
3069.5	s	0.121	3080	A	3066 s	0.20	
3058.5	m br	0.0968	3065	A??			
~3050	m sh	0.0545	~3055	B??			
3025.8	w	0.0385	~3037	A??	3027 vw	0.07	
3016.3	w	0.0334	~3022	B?			
~3004	w sh	~0.02			3005 vw	0.41	
~1703	vw sh	~0.01					
1685.9	vw	0.008					
1645.5	w	0.0278					
1636.9	w p/sh	0.0240					
1622.1	w br	0.0327					
~1591	s sh	~0.25	1589	A?			
1583.9	vs	1.00	~1586	B??	1583 m	0.76	
1566.1	s br sh	0.178			~1565 w sh	dp	
~1496	s sh	0.13					
1477.8	vs	3.11	1483	A	1476 vw	0.05	
1445.5	vs	1.24	~1449	B	1445 vw	0.78	
1387.1	w	0.0367					
1370.7	w	0.0367	1369	A	1370 vw	0.05	
1325.2	w	0.0306	1325	B?	1326 vw	0.79	
1298.1	m	0.0456	1297	B	1300	dp	
1272.5	m	0..0457	~1271	B?	1272 vw	dp	
1235.2	w	0.0339	1232	A			
1210.9	w	0.0287	1208	A			
1171.6	m	0.0639	1176	A	1173 w	0.42	
1156.4	m	0.0565			1157 w	0.79	
1122.7	s	0.332	1126	A?	1124 w	0.03	
			1128	A?			
~1116	s sh	0.244	~1119	C??			
1083.6	vs	2.18	1092	A	1084 s	0.04	
1068.1	s	0.617	~1068	B?	~1069 vw	dp	
1022.8	vs	2.27	1025	A	~1023 vs	0.03	
1012.6	s	0.151			1013 w	0.003	
1001.9	s	0.532	1004	A?	1002 vs	0.04	
990.5	m	0.0585			991	p	

Table 4.8 - Continued

Infrared liquid [a]			Infrared gas [d]		Raman liquid [b]		
cm^{-1}	Desc. [b]	α''_m [c]	cm^{-1}	Contour	cm^{-1}	ρ_ℓ [e]	comments
983.2	m br sh/p	0.0521	982	??	972? vw	p	
963.7	m br	0.0454					
935.0	m	0.0967	933	A	937 vw	0.17	
~919	m sh/p	~0.0469					
903.0	s	0.389	903	C? A?	~904? vw	dp	
866.3	w	0.0363	868	A? C?			
830.0	m	0.0717			831 vw	0.71	
812.2	m	0.0437	806	A?			
			811	A??			
741.2	vs	9.52	741	C	743 vw	0.78	
702.5	vs	3.67	706	A? C?	702 vs	0.04	
685.2	vs	4.25	685	C			
			692				
662.1	s	0.197	665	C??			
			666	B??			
614.1	m	0.0933	615	B	614 w	0.73	
~552	w sh	~0.0102					
547.7	w	0.0115					
533.4	w	0.0165					
468.1	vs	3.39	467	C	468 vw	dp	
~434	m br sh/p	0.049					
415.0	s	0.548	417	A	418 s	0.15	
~400	m sh	~0.0549					literature
297.5	w	0.0292			296 vw	0.73	
195.9	w	0.0326			195 m	0.72	

a - Features are from the α''_m spectrum.

b - Abbreviations used: v- very, w- weak, m- medium, s- strong, sh- shoulder, br- broad, sh/p- shoulder or a peak.

c - Peak heights in the α''_m spectrum in cm^3 mol^{-1}.

d - Peak positions in the absorbance spectrum of the gas. Wavenumbers of B-type bands are measured at the minimum between the R and P branches. ? and ?? indicate degrees of uncertainty in the determination of the band shape.

e - Depolarization ratio are $\rho_\ell = \frac{I_\perp}{I_\parallel}$. When the feature is too weak or noisy to obtain a reliable ratio, p or dp are used to indicate polarized and depolarized, respectively.

Table 4.9 - Computed wavenumbers, eigenvectors and potential energy distributions for chlorobenzene

ν_i	cm^{-1}	Eigenvectors^a				PED^b
ν_1	3177	S_5 -0.84	S_1 -0.59			CH
ν_2	3171	S_1 -0.73	S_{15a} -0.55	S_5 0.42		CH
ν_3	3158	S_{12a} -0.80	S_{15a} 0.62			CH
ν_4	1595	S_{18a} 0.85	S_{16a} 0.43	S_{17a} 0.39		CC (75), HCC (25)
ν_5	1541	S_{14a} -1.17	S_{13a} 0.27			HCC (60), CC (40)
ν_6	1270	S_{18a} 0.69	S_{14a} -0.59			HCC (55), CC (25), CCl (20)
ν_7	1148	S_{18a} 0.79	S_{14a} 0.30			HCC (55), CCl (30), CC (15)
ν_8	1029	S_{14a} 0.49	S_6 -0.31	S_{13a} 0.20		CC (55), HCC (22), CCC (22)
ν_9	1001	S_6 -0.47	S_2 -0.20			CCC (50), CC (50)
ν_{10}	773	S_{17a} -0.31	S_6 0.18			CCC (50), CC (30), CCl (20)
ν_{11}	398	S_{17a} 0.20	S_{18a} -0.10			CCC (60), CCl (40)
ν_{12}	971	S_{19a} 1.25	S_{20a} 0.44			oop H
ν_{13}	852	S_{11a} 1.03				oop H
ν_{14}	403	S_{20a} 0.70	S_{19a} 0.26			oop C
ν_{15}	987	S_7 1.13	S_{19b} 0.64	S_8 -0.59		oop H (70), oop C (30)
ν_{16}	915	S_{19b} -0.84	S_{11b} -0.67	S_7 0.49		oop H
ν_{17}	748	S_8 0.72	S_4 0.61	S_{11b} -0.53	S_7 -0.45	oop H (67), oop C (33)
ν_{18}	698	S_8 1.04	S_4 -0.52	S_7 -0.41		oop C (67), oop H (33)
ν_{19}	481	S_{20b} 0.66	S_{19b} 0.39	S_4 -0.32		oop C (50), oop Cl (50)
ν_{20}	230	S_{20b} 0.24	S_4 0.13	S_{11b} 0.11		oop C (60), oop Cl (40)
ν_{21}	3157	S_{15b} 0.84	S_{12b} -0.59			CH
ν_{22}	3151	S_{12b} -0.85	S_{15b} -0.59			CH
ν_{23}	1584	S_{18b} -0.80	S_{16b} -0.43	S_{17b} -0.37		CC (75), HCC (25)
ν_{24}	1452	S_{14b} 1.09	S_3 -0.54			HCC (65), CC (35)
ν_{25}	1330	S_3 -1.08	S_{10} -0.66			HCC (70), CC (30)
ν_{26}	1293	S_3 0.59	S_{10} -0.49	S_9 0.40	S_{18b} -0.35	CC (75), HCC (25)
ν_{27}	1158	S_{10} -0.80	S_{18b} -0.61			HCC (65), CC (35)
ν_{28}	1073	S_{14b} 0.44	S_{10} 0.39	S_{18b} -0.38	S_{13b} 0.22	CC (55), HCC (45)
ν_{29}	615	S_{17b} 0.40				CCC
ν_{30}	329	S_{18b} 0.20	S_{14b} 0.18	S_{10} -0.15	S_3 0.11	HCC

a - The numbers are the $\partial S_i/\partial Q_j$ elements of the indicated symmetry coordinate in the particular vibration. Only the dominant terms are shown.

b - CH, CC or CCl are stretches, HCC is CH bend, CCC is ring deformation. Out-of-plane vibrations are denoted by oop. Percent contributions are given in brackets..

4.3.1 - Assignments of the 11 A_1 vibrations of chlorobenzene

There are five CH stretches in chlorobenzene: three A_1 vibrations and two B_2 vibrations. According to the calculations all are expected within ~30 cm^{-1} and allowing for anharmonicity should be at 3100 - 3050 cm^{-1}, about 100 cm^{-1} lower than the calculated values.

The strong A-type band at 3080 cm^{-1} in the infrared spectrum of the gas, has a counterpart in the strong infrared band in the liquid at 3070 cm^{-1} (Fig 4.3). The wavenumber shift between the gas and liquid is in agreement with observations of benzene[69]. There is a strong polarized Raman band at 3066 cm^{-1}. The Raman wavenumber calibration is such that this band may coincide with the infrared band at 3070 cm^{-1} or there may be two A_1 vibrations at 3070 cm^{-1} and 3066 cm^{-1}.

No other obvious A_1 vibrations are observed. The peak at 3058 cm^{-1} in the infrared spectrum of the liquid is often assigned to an A_1 fundamental and we do the same, clearly for lack of a better alternative.

Calculations predict that ν_4 is near 1595 cm^{-1} with ν_{23} (B_2) nearby at 1584 cm^{-1}. In the Raman spectra a depolarized band is observed at 1583 cm^{-1} and a depolarized, weak shoulder at 1565 cm^{-1} (Fig. 4.4). The gas's infrared band contour is not easy to interpret, but has a Q branch at 1589 cm^{-1}. In the infrared spectrum of the liquid there is a strong band at 1584 cm^{-1}, a peak at 1566 cm^{-1} and a shoulder at ~1590 cm^{-1}. The evidence is not clear, but the gas phase Q branch and complex band shape lead us to assign ν_4 (A_1) to the Q branch at 1589 cm^{-1} in the gas and at 1584 cm^{-1} in the liquid, in both cases very close to ν_{23} (B_2).

The calculated wavenumber for ν_5 (A_1) is 1541 cm^{-1} and that of ν_{24} (B_2) is 1452 cm^{-1}. Both are due to the splitting of the strong ring mode of benzene. ν_5 (A_1) is clearly at 1483 cm^{-1} in the infrared spectrum of the gas and 1478 cm^{-1} in the liquid where the liquid infrared and polarized Raman band essentially coincide (Fig. 4.4).

The next four A_1 vibrations are expected near 1270 cm^{-1} for ν_6, 1150 cm^{-1} for ν_7, 1030 cm^{-1} for ν_8 and 1000 cm^{-1} for ν_9. The A-type contours in the infrared spectrum of the gas are located at 1232 cm^{-1}, 1208 cm^{-1}, 1176 cm^{-1}, 1126 cm^{-1}, 1092 cm^{-1}, 1025 cm^{-1} and probably at 1004 cm^{-1} (Fig. 4.5 and 4.6). All these bands have a corresponding band within 5 cm^{-1} to low wavenumber in the infrared spectrum of the liquid. The polarized Raman bands in this region are located at 1173 cm^{-1}, 1124 cm^{-1}, 1084 cm^{-1}, 1023 cm^{-1} and 1002 cm^{-1}. The bands at 1023 cm^{-1} and 1002 cm^{-1}, for which the calculated wavenumbers agree with those from all three experimental spectra, are assigned to ν_8 and ν_9 respectively. The very strong band at 1084 cm^{-1} in the liquid and 1092 cm^{-1} in the gas is assigned to ν_7. We follow Whiffen[37] by assigning 1172 cm^{-1} in the liquid and 1176 cm^{-1} in the gas to ν_6 and assigning the stronger band at 1123 cm^{-1} in the infrared spectrum of the liquid to the combination $\nu_{10}+\nu_{11}$.

The last two A_1 vibrations are expected near 775 cm^{-1} and 400 cm^{-1}. There are two strong polarized Raman bands at 702 cm^{-1} and 418 cm^{-1} (Fig. 4.7 and 4.8). A weak A-type band is observed in the spectrum of the gas at 706 cm^{-1} and a very strong band in the liquid is at 703 cm^{-1}. It is assigned to ν_{10}. ν_{11} is assigned to the infrared and Raman bands of the liquid near 415 cm^{-1} correlated with the A-type band at 417 cm^{-1} in the spectrum of the gas.

4.3.2 - Assignment of the 3 A_2 vibrations of chlorobenzene

The three A_2 vibrations are expected near 970, 850 and 400 cm^{-1}. These vibrations are inactive in the infrared but may appear as very weak bands in the liquid. They are active in the Raman spectra and should be depolarized but are possibly weak.

The only weak, depolarized Raman band without a corresponding band in the infrared spectrum of the gas is found at 831 cm^{-1} (Fig. 4.7). The band is essentially coincident with the 830 cm^{-1} band in the infrared spectrum of the liquid and is assigned to ν_{13}.

The weak Raman bands at 991 cm^{-1} and 972 cm^{-1} are clearly polarized and can not be assigned to ν_{12}, while the strong, polarized Raman band at 418 cm^{-1} masks the 400 cm^{-1} region. Without evidence, we follow Whiffen[37] in assigning ν_{12} at 964 cm^{-1} and ν_{14} at 400 cm^{-1} at 400 cm^{-1}.

4.3.3 - Assignment of the 6 B_1 vibrations of chlorobenzene

The computed wavenumbers of the six B_1 fundamentals of chlorobenzene are: 987 cm^{-1} for ν_{15}, 915 cm^{-1} for ν_{16}, 748 cm^{-1} for ν_{17}, 698 cm^{-1} for ν_{18}, 481 cm^{-1} for ν_{19} and 230 cm^{-1} for ν_{20}. These bands should be depolarized in the Raman spectrum and should have a C-type contour in the infrared gas spectrum.

Three strong bands at 903, 741 and 468 cm^{-1} are observed in all experimental spectra (Fig. 4.6 to 4.8) with the appropriate contour and depolarization. They are assigned to ν_{16}, ν_{17} and ν_{19}, respectively. The band at 685 cm^{-1} is very strong in the liquid and has a C-type contour in the spectrum of the gas. Although no Raman band is observed nearby, it is assigned to ν_{18}.

As the gas spectrum was not recorded below 400 cm^{-1}, the choice for ν_{20} is based on the Raman bands and the computed wavenumbers. Of the two depolarized Raman bands at 296 and 195 cm^{-1}, ν_{20} is assigned at 195 cm^{-1} because its computed wavenumber is 100 cm^{-1} lower than that of ν_{30} (B_2).

ν_{15} was previously[22,23,37,42] assigned at ~985 cm^{-1}. A band at 983 cm^{-1} is observed in the infrared spectrum of the liquid. A band of undetermined shape is observed in the gas at 982 cm^{-1} but the Raman shoulder observed in that area is clearly polarized. For lack of better evidence, we follow the previous assignments and assign ν_{15} at 983 cm^{-1}.

4.3.4 - Assignment of the 10 B_2 vibrations of chlorobenzene

The computed wavenumbers for the two B_2 CH stretches are 3157 and 3151 cm^{-1}. Allowing for anharmonicity the observed wavenumbers should be about 100 cm^{-1} lower. A possible B-type contour is observed at ~3095 cm^{-1} in the infrared spectrum of the gas corresponding to a band at 3083 cm^{-1} in the infrared spectrum of the liquid (Fig 4.3). These features are assigned to ν_{21}. More questionable B-type contours are observed at 3067, 3055 and 3022 cm^{-1}. The observed infrared bands of the liquid are a shoulder at ~3050 cm^{-1} and peaks at 3059 (ν_3 A_1), 3026 and 3016 cm^{-1}. There is a depolarized Raman band at ~3060 cm^{-1} that is not coincident with the strong polarized band at 3066 cm^{-1}. As the computation suggest that all five CH stretches should be within 30 cm^{-1}, we assign ν_{22} at ~3060 cm^{-1}. Thus we assign ν_3 (A_1) and ν_{22} (B_2) nearly coincident at 3060 cm^{-1}.

ν_{23} is expected near 1585 cm^{-1}. As was discussed previously, the depolarized Raman band at 1583 cm^{-1} and the infrared band at 1584 cm^{-1} can be assigned to ν_{23}. ν_{23} (B_2) and ν_4 (A_1) combine to give the confused gas phase band in Fig. 4.4.

ν_{24} is expected at 1450 cm^{-1}. It is assigned to the very strong band at 1446 cm^{-1} in the infrared spectrum of the liquid, the corresponding depolarized Raman band at 1445 cm^{-1}, and the B-type contour at ~1449 cm^{-1} in the infrared spectrum of the gas.

ν_{25} is expected near 1330 cm^{-1}. It is assigned to the weak band at 1325 cm^{-1} in the infrared spectrum of the liquid that is essentially coincident with a depolarized Raman band and a B-type band in the infrared spectrum of the gas.

ν_{26} is expected at 1290 cm^{-1}. Two bands are observed in the infrared spectrum of the liquid, at 1298 cm^{-1} and 1272 cm^{-1}. Both bands correspond to depolarized Raman bands and B-type contours in the infrared spectrum of the gas. We follow Whiffen[37] in assigning ν_{26} at 1272 cm^{-1} and the combination ν_{14}+ν_{16} at 1299 cm^{-1}.

ν_{27} is expected near 1160 cm^{-1}. It is assigned to the band at 1156 cm^{-1} in the infrared spectrum of the liquid that is essentially coincident with a depolarized Raman band.

ν_{28} is expected near 1075 cm^{-1}. It is assigned to the band at 1068 cm^{-1} in the infrared spectrum of the liquid coincident with a B-type band in the infrared spectrum of the gas. A probable depolarized Raman band at 1069 cm^{-1} is observed on the side of the strong polarized Raman band at 1084 cm^{-1}.

ν_{29} is expected near 615 cm^{-1}. It is assigned to the medium-weak band at 614 cm^{-1} in the infrared spectrum of the liquid and the corresponding depolarized Raman band and B-type gas phase band.

Finally, ν_{30} is expected near 330 cm^{-1}. As discussed in Section 4.3.3, the depolarized Raman band at 296 cm^{-1} is assigned to ν_{30} while that at 196 cm^{-1} is assigned to ν_{20} (B_1).

4.3.5 - Summary of the assignments of chlorobenzene

The proposed assignments are given in Table 4.10. The true Herzberg description is given in the first column followed by the proposed wavenumber. When a wavenumber was chosen with imperfect or no supporting evidence from the experimental data gathered for this thesis, it is indicated by ? or ??, respectively.

In the pseudo-Herzberg or pseudo-Wilson notations for the vibrations of the

Table 4.10 - Assignments of the fundamental vibrations of chlorobenzene

true Herzberg	cm^{-1}[a]	pseudo-Herzberg[b]	Description[c]
ν_{1}	3069.5	ν_{5}, ν_{1}	CH
ν_{2}	3069 ??	ν_{1}, ν_{15a}, ν_{5}	CH
ν_{3}	3058.5 ??	ν_{12a}, ν_{15a}	CH
ν_{4}	1584 ??	ν_{18a}, ν_{16a}	HCC, CC
ν_{5}	1477.8	ν_{14a}	HCC
ν_{6}	1171.6 ?	ν_{18a}, ν_{14a}	HCC
ν_{7}	1083.6	ν_{18a}	HCC
ν_{8}	1022.8	ν_{14a}, ν_{6}	HCC, CCC
ν_{9}	1001.9	ν_{6}	CCC
ν_{10}	702.5	ν_{17a}, ν_{6}	CCC
ν_{11}	415.0	ν_{17a}, ν_{18a}	CCC, HCC
ν_{12}	963.7 ??	ν_{19a}	oop H
ν_{13}	830.0	ν_{11a}	oop H
ν_{14}	400 ??	ν_{20a}	oop C
ν_{15}	983.2 ??	ν_{7}, ν_{19b}, ν_{8}	oop H, oop C
ν_{16}	903.0	ν_{19b}, ν_{11b}, ν_{7}	oop H
ν_{17}	741.2	ν_{8}, ν_{4}, ν_{11b}, ν_{7}	oop C, oop H
ν_{18}	685.2	ν_{8}, ν_{4}	oop C, oop H
ν_{19}	468.1	ν_{19b}, ν_{4}	oop C, oop H
ν_{20}	195.9	ν_{20b}, ν_{4}	oop C, oop H
ν_{21}	3083.1 ?	ν_{15b}, ν_{12b}	CH
ν_{22}	3060 ??	ν_{12b}, ν_{15b}	CH
ν_{23}	1583.9	ν_{18b}, ν_{16}, ν_{17b}	HCC, CC, CCC
ν_{24}	1445.5	ν_{14b}	HCC
ν_{25}	1325.2	ν_{3}, ν_{10}	HCC
ν_{26}	1272.5 ?	ν_{3}, ν_{10}, ν_{9}, ν_{18b}	HCC, CC
ν_{27}	1156.4	ν_{10}, ν_{18b}	HCC
ν_{28}	1068.1	ν_{14b}, ν_{10}, ν_{18b}, ν_{13b}	HCC
ν_{29}	614.1	ν_{17b}	CCC
ν_{30}	297.5	ν_{18b}, ν_{14b}, ν_{10}, ν_{3}	HCC

a - Peak wavenumbers in the imaginary molar polarizability spectrum of liquid chlorobenzene.

b - Contributions greater than 50% of the largest contribution.

c - CH, CC are stretches, HCC is CH bend, CCC is ring deformation and oop is out-of-plane.

monosubstituted benzenes the symbol ν_j has been used to relate the vibration to one symmetry coordinate of benzene, not to one vibration of benzene[68]. We follow this practice, except that it is clear from Table 4.9 that most of the chlorobenzene vibrations are mixtures of more than one symmetry coordinate of benzene and therefore more than one ν_j is required in the pseudo-Herzberg notation. In column 3, ν_j is given for each symmetry coordinate that contributed ≥ 50 % of the largest contribution. Note that ν_2 and ν_{13a}, both CC stretching displacements, do not appear in this table. Although these displacements contribute to many vibrations they are always minor contributors. The last column gives a chemical description of the vibration.

A question arises from the table. Where are the C-Cl stretching vibration and the Cl-C-C in-plane and out-of-plane bending vibrations? From the unsymmetrized eigenvectors, $\frac{\partial R_{C\text{-}Cl}}{\partial Q_k}$, the C-Cl stretch contributes with HCC, CC and CCC to the following A_1 vibrations: ν_4 (1595), ν_5 (1541), ν_6 (1270), ν_7 (1148), ν_{10} (773) and ν_{11} (398). It does not make the major contribution to any of these vibrations. From the potential energy distribution (PED), the C-Cl stretch is among the three main contributors to ν_6 (1270), ν_7 (1148), ν_{10} (773) and ν_{11} (398) but is the major contributor to none of these. Therefore we conclude that no single vibration can be identified as the C-Cl stretch.

Both the unsymmetrized eigenvectors and the PED show that ν_{30} (B_2) is the Cl-C-C in-plane deformation vibration. They also show that ν_{19} and ν_{20} are both heavy mixtures of the Cl-C-C and C-C-C-C out-of-plane deformations, so the Cl-C-C oop deformation can not be assigned to any one vibration.

4.4 - Previous assignments of the toluene vibrations

Toluene, has 15 atoms and 15x3-6 = 39 fundamental vibrations. Technically the symmetry of the molecule is at most C_s but often the CH_3 group is considered to be freely rotating which means that the CH_3 group can be approximated by a point of mass 15, and thus the molecule has C_{2v} symmetry. Assuming C_{2v} symmetry, the 39 vibrational modes are distributed among the symmetry species as $13A_1+4A_2+9B_1+13B_2$. As is the case for chlorobenzene, all of the vibrations in toluene are Raman active, and all except the $4A_2$ vibrations are infrared active. Of the 39 vibrations, 30 vibrations are similar to the 30 vibrations of chlorobenzene and 9 vibrations are related to the CH_3 vibrations. The CH_3 related modes form the representation $2A_1+1A_2+3B_1+3B_2$ under C_{2v}.

Although the CH_3 group can be approximated in simple calculations as an atom of mass 15, the 9 vibrations of the CH_3 group cause problems in notation. If true Herzberg notation is used, the A_2, B_1 and B_2 vibrations would be assigned different number ranges compared with other monosubstituted benzenes. Therefore, the common practice is to treat the phenyl group vibrations separately and to number them using either the true Herzberg notation, ν_1 to ν_{30}, or the pseudo-Wilson or pseudo-Herzberg notations. The CH_3 vibrations are considered then extra and are usually labeled as ν_s, ν_a, δ_s, δ_a, and r, where ν, δ and r indicate CH bond stretching, HCH angle deformation and CH_3 rocking vibrations, and the "s" and "a" designate symmetric and antisymmetric vibrations, respectively. ν_a and δ_a are sometimes marked with ′ or ″ to differentiate between the B_1 and B_2 species.

As was the case for chlorobenzene, the use of different spectra is necessary in order to determine the symmetry species of toluene. However, the difference between shapes[74] of A-type and C-type bands in the gas phase infrared spectrum of toluene, is less obvious than for chlorobenzene, so the assignment of symmetry species is more ambiguous. The infrared and Raman spectra of the liquid provide similar information to that obtained for chlorobenzene. Comparison of observed wavenumbers in infrared and Raman spectra permitted several authors to present a complete assignment of the fundamental vibrations of toluene.

The first major study of toluene since 1950, was by Wilmshurst and Bernstein[15]. The authors reported spectra of toluene and toluene-α-d_3. They also used literature data for toluene-p-d. They included figures of their infrared spectra of the gas and liquid and their Raman spectra of the liquid, and tabulated all the wavenumbers they observed. They reported gas-phase band types and whether the Raman bands were polarized or depolarized. They assigned wavenumbers to fundamental vibrations and to overtone and combination transitions. On the basis of the CH_3 to CD_3 isotope shifts, they related some of the fundamentals to the vibrations of benzene using the pseudo-Wilson notation, which was converted in this thesis to the pseudo-Herzberg notation.

They took the plane of the molecule as XZ. Thus, their B_1 species are interchanged with our B_2 species.

In 1960, Fuson *et al.*[17] reported the spectra of $C_6H_5CH_3$, $C_6H_5CD_3$ and $C_6D_5CD_3$. The authors tabulated all the wavenumbers they observed in the infrared spectra of the gas and liquid phases and included Raman data from Wilmshurst and Bernstein[15] which was confirmed by measurements in their laboratory. For the phenyl group vibrations the authors used the pseudo-Wilson notation, which was converted to the pseudo-Herzberg notation throughout this thesis. Their B_1 species are interchanged with our B_2 species. For the CH_3 group vibrations, the authors used ′ and ″ to differentiate between the B_1 and B_2 species. The authors also compared their assignments and those of Wilmshurst and Bernstein[15] and those of Kovner[16].

In 1960, Schmid, Brandmuller and Nonnenmacher[18] performed normal coordinate calculations on toluene with the same force field as for benzene and obtained the wavenumbers of the 30 phenyl group vibrations in toluene. The CH_3 group was approximated in the calculations by an atom of mass 15. In addition to the calculated wavenumbers, experimental wavenumbers obtained from gas and liquid phase infrared and liquid phase Raman measurements were also given. Their B_1 species are interchanged with our B_2 species. and for the 30 ring vibrations the authors used the true Herzberg notation. Alongside, a pseudo-Wilson notation is also given.

In 1971, La Lau and Snyder[19] derived a valence force field for methyl substituted benzenes from 303 observed wavenumbers of benzene, toluene, p-xylene, m-xylene, mesitylene and some of their deuterated derivatives. For toluene, they gave figures of the infrared spectrum of the crystalline phase and tabulated the observed fundamental wavenumbers and their computed wavenumbers together with their potential energy distribution. In a separate table, they gave the wavenumbers of fundamentals below 1606 cm^{-1} of the Raman spectrum of the liquid with the polarization of the band.

As was the case for chlorobenzene, the books by Sverdlov *et al.*[22] and by Varsanyi[23] give the wavenumbers and assignments for toluene without explanation. In the book by Sverdlov *et al.*, the B_1 and B_2 species are interchanged with our B_2 and B_1 species. Sverdlov *et al.* used the true Herzberg notation system for all 39 vibrations. In the book by Varsanyi, the pseudo-Wilson notation is used.

In 1985, Draeger[25] reported experimental and theoretical wavenumbers for benzene, toluene and some of their deuterated derivatives. The experimental wavenumbers were obtained from Raman and infrared measurements of the gas. The wavenumbers were classified according to symmetry species and a potential energy distribution was given.

In 1986, Xie and Boggs[26] reported fundamental wavenumbers obtained from scaled *ab initio* calculations. The experimental wavenumbers used in the scaling were those of Wilmshurst and Bernstein[15], Kovner *et al.*[16], Fuson *et al.*[17] and Draeger[25]. Xie and Boggs numbered the wavenumbers of all 39 vibrations in order of increasing wavenumber regardless of symmetry species.

In 1995, Schrotter and co-workers[32,33] reported experimental Raman wavenumbers of the gas and liquid phases and wavenumbers obtained from normal coordinate calculation based on the experimental wavenumbers. The B_1 and B_2 species were interchanged with our notation and the authors used the true Herzberg notation for all vibrations. However, one A_2 vibration was omitted and, consequently, the numbering scheme is off by one for the subsequent vibrations.

In the following sub-sections, the wavenumbers and assignments of the 30 phenyl group vibrations by these authors are given for each symmetry species, followed by the assignments and wavenumbers of the 9 CH_3 vibrations. Differences in assignment will be pointed out. However a critical evaluation of the authors' assignment is left to Section 4.5 where the assignment is evaluated on the basis of all available data, including data measured for this thesis.

Other studies either gave only partial wavenumbers and assignments[27,29] or used wavenumbers and assignments from previous studies without change[28,30,31,34]. These studies will be quoted and used when deemed necessary.

4.4.1 - Previous assignments of the 11 A_1 phenyl group vibrations of toluene

The wavenumbers and assignments of the 11 A_1 phenyl group vibrations of liquid toluene are given in Table 4.11. The first column gives the true Herzberg notation for the 30 phenyl vibrations under the qualification that the CH_3 group vibrations are numbered 31 to 39 regardless of symmetry species. The pseudo-Herzberg notation is given in the second column. In Table 4.11 and later in Tables 4.12 to 4.14, the pseudo notation is taken from Schmid *et al.*[18] who determined the relation between the vibrations of substituted benzenes and those of benzene. Schmid's original pseudo-Wilson notation was converted to the pseudo-Herzberg notation through use of Table 4.3. The remaining columns contain the wavenumbers and assignments of the different authors. The experimental wavenumbers listed in the table are those from the infrared measurement of the liquid phase. When only the Raman band was observed, it is denoted by the letter R next to the wavenumber.

In general, the agreement between the different experimental studies, on the A_1 phenyl wavenumbers is very good, with differences that can be attributed to calibration errors, often within ±5 cm^{-1} of each other. There are, however, two major differences in wavenumbers and several differences in the pseudo-Herzberg notation. The latter involve interchange of ν_1, ν_5, ν_{12a} and ν_{15a}, all CH stretches, and interchange of ν_2 and ν_{18a}, a CC stretch and a HCC deformation, respectively.

Two assigned wavenumbers for the three aromatic A_1 CH stretching vibrations are in good agreement among the different experimental studies, 3063±4 cm^{-1} and 3055±1 cm^{-1}. The third A_1 CH stretching vibration was assigned by Wilmshurst and Bernstein[15], Varsanyi[23] and Schrotter *et al.*[32] at 3003 cm^{-1}. Sverdlov *et al.*[22] placed it at 3060 cm^{-1}. Fuson *et al.*[17] placed it at 3087 cm^{-1}, above their other two CH stretches, and Draeger[25] placed it at 3039 cm^{-1}, below the other CH stretches. Consequently the true Herzberg notation, for, e.g., 3063 cm^{-1} is different for different workers (Table 4.11).

The second major difference is the wavenumber of ν_4. Wilmshurst and

Table 4.11 - Previous assignments of the 11 A_1 phenyl vibrations of toluene

		Experimental									Theoretical		
Herzberg notation		Wilmshurst[a] [Ref 15]		Fuson[a] [Ref 17]		Sverdlov[b] [Ref 22]	Varsanyi[a] [Ref 23]		Draeger[c] [Ref 25]	Schrotter[d] [Ref 32]	Schmid[e] [Ref 18]	Snyder[c] [Ref 19]	Boggs[f] [Ref 26]
true	pseudo	cm^{-1}		cm^{-1}		cm^{-1}	cm^{-1}		cm^{-1}	cm^{-1}	cm^{-1}	cm^{-1}	cm^{-1}
ν_1	ν_{12a}	3067	ν_{12a}	3087	ν_{15a}	3060	3063	ν_{12a}	3067	3065R	3075	3057	3088
ν_2	ν_1	3056	ν_1	3063	ν_{12a}	3060	3055	ν_1	3056	3055R	3069	3056	3063
ν_3	ν_5	3003	ν_5	3055R	ν_1	3060	3003	ν_{15a}	3039	3003R	3053	3055	3049
ν_4	ν_{16a}	1585R	ν_{16a}	1605	ν_{16a}	1608	1605	ν_{16a}	1611	1606R	1656	1614	1620
ν_5	ν_{13a}	1491	ν_{13a}	1494	ν_{13a}	1500	1494	ν_{13a}	1500	1495R	1524	1503	1504
ν_6	ν_{15a}	1209	ν_{15a}	1208	ν_5	1218	1208	ν_5	1212	1210R	1299	1205	1214
ν_7	ν_{17a}	1178	ν_{17a}	1175	ν_{17a}	1184	1175	ν_{17a}	1178	1180R	1157	1182	1189
ν_8	ν_{14a}	1029	ν_{14a}	1030	ν_{14a}	1030	1030	ν_{14a}	1030	1030R	1023	1026	1034
ν_9	ν_6	1002	ν_6	1003	ν_6	1004R	1003	ν_6	1004	1005R	1000	1005	1001
ν_{10}	ν_{18a}	785	ν_2	784	ν_2	774	784	ν_2	786	787R	778	793	784
ν_{11}	ν_2	521	ν_{18a}	521	ν_{18a}	521	521	ν_{18a}	521	521R	506	526	519

a - Assignments in pseudo-Wilson notation were converted to pseudo-Herzberg notation using Table 4.3.

b - Authors used the true Herzberg notation for 39 vibrations.

c - No notation was used.

d - Authors used the true Herzberg notation for 38 vibrations. See Section 4.4.

e - Authors used the true Herzberg notation for 30 ring vibrations.

f - Authors numbered all 39 vibrations in order of increasing wavenumber.

Bernstein placed it at 1585 cm^{-1} with a B_2 vibration at 1604 cm^{-1}. Other experimental studies reverse these assignments.

The wavenumbers calculated by Schmid *et al.*[18] and Boggs *et al.*[26] are in

Table 4.12 - Previous assignments of the 3 A_2 phenyl vibrations of toluene

		Experimental									Theoretical		
Herzberg notation		Wilmshurst[a] [Ref 15]		Fuson[a] [Ref 17]		Sverdlov[b] [Ref 22]	Varsanyi[a] [Ref 23]		Draeger[c] [Ref 25]	Schrotter[d] [Ref 32]	Schmid[e] [Ref 18]	Snyder[c] [Ref 19]	Boggs[f] [Ref 26]
true	pseudo	cm^{-1}		cm^{-1}		cm^{-1}	cm^{-1}		cm^{-1}	cm^{-1}	cm^{-1}	cm^{-1}	cm^{-1}
ν_{12}	ν_{19a}	994R	ν_{19a}	964	ν_{19a}	970R	964	ν_{19a}	964R	990R	979	975	965
ν_{13}	ν_{11a}	842	ν_{11a}	844	ν_{11a}	836	843	ν_{11a}	843R	844R	848	847	836
ν_{14}	ν_{20a}	407	ν_{20a}	408R	ν_{20a}	414R	408	ν_{20a}	405R	408R	405	403	401

a - Assignments in pseudo-Wilson notation were converted to pseudo-Herzberg notation using Table 4.3.

b - Authors used the true Herzberg notation for 39 vibrations.

c - No notation was used.

d - Authors used the true Herzberg notation for 38 vibrations. See Section 4.4.

e - Authors used the true Herzberg notation for 30 ring vibrations.

f - Authors numbered all 39 vibrations in order of increasing wavenumber.

satisfactory agreement with the experimental values, while the wavenumbers computed by La Lau and Snyder[19], are in excellent agreement with the different experimental values with the exception of the wavenumbers of the CH stretches.

4.4.2 - Previous assignments of the 3 A_2 phenyl group vibrations of toluene

The wavenumbers and assignments of the A_2 vibrations are given in Table 4.12 which is arranged similarly to Table 4.11. One major disagreement is the assignment of ν_{12}. Wilmshurst and Bernstein[15] and Schrotter *et al.*[32] placed it at 992±2 cm^{-1}, while the other experimental studies[17,22,23,25] placed it at about 25 cm^{-1} lower at 967±3 cm^{-1}. The

Table 4.13 - Previous assignments of the 6 B_1 phenyl vibrations of toluene

		Experimental									Theoretical		
Herzberg notation		Wilmshurst[a] [Ref 15]		Fuson[a] [Ref 17]		Sverdlov[b] [Ref 22]	Varsanyi[a] [Ref 23]		Draeger[c] [Ref 25]	Schrotter[d] [Ref 32]	Schmid[e] [Ref 18]	Snyder[c] [Ref 19]	Boggs[f] [Ref 26]
true	pseudo	cm^{-1}		cm^{-1}		cm^{-1}	cm^{-1}		cm^{-1}	cm^{-1}	cm^{-1}	cm^{-1}	cm^{-1}
ν_{15}	ν_7	966	ν_7	978	ν_7	993R	978	ν_7	980	974R	984	989	976
ν_{16}	ν_{19b}	895	ν_{11b}	893	ν_{19b}	892	893	ν_{19b}	894	897R	920	909	892
ν_{17}	ν_{11b}	729	ν_4	728	ν_4	716	728	ν_4	730	731R	754	734	721
ν_{18}	ν_8	695	ν_8	695	ν_8	702	695	ν_8	695	—	700	698	688
ν_{19}	ν_4	464	ν_{20b}	464	ν_{20b}	465	464	ν_{20b}	462	466R	497	463	457
ν_{20}	ν_{20b}	216	ν_{19b}	217R	ν_{11b}	217R	217	ν_{11b}	205	217R	254	210	201

a - Assignments in pseudo-Wilson notation were converted to pseudo-Herzberg notation using Table 4.3.

b - Authors used the true Herzberg notation for 39 vibrations.

c - No notation was used.

d - Authors used the true Herzberg notation for 38 vibrations. See Section 4.4.

e - Authors used the true Herzberg notation for 30 ring vibrations.

f - Authors numbered all 39 vibrations in order of increasing wavenumber.

computed wavenumbers[18,19,26] of this vibration range from 965 to 979 cm^{-1}. The wavenumbers of the remaining two A_2 phenyl vibrations are in excellent agreement among the different experimental studies with the exception of Sverdlov's which are off by 6-8 cm^{-1}. The computed wavenumbers for these two vibrations are in very good agreement with the experimental values.

4.4.3 - Previous assignments of the 6 B_1 phenyl group vibrations of toluene

The wavenumbers and assignments of the B_1 vibrations are given in Table 4.13 which is arranged in a similar manner to Table 4.11. There are several disagreements about wavenumber assignments of the B_1 vibrations.

ν_{15} is assigned by Wilmshurst and Bernstein[15] at 966 cm^{-1}, while Fuson *et al.*[17], Varsanyi[23], Draeger[25] and Schrotter *et al.*[32] placed it around 977±3 cm^{-1}. Sverdlov *et al.*[22] placed it at 993 cm^{-1} based on Raman measurement. The computed wavenumbers[18,19,26] for this vibration range from 976 to 991 cm^{-1}.

In two other cases, one study disagrees with the remaining experimental studies. All experimental studies placed ν_{17} at 729±2 cm^{-1} with the exception of Sverdlov *et al.* who placed it at 716 cm^{-1}. All experimental studies assigned ν_{20} at 217±1 cm^{-1} with the exception of Draeger[25] who placed it at 205 cm^{-1}

The pseudo notations ν_4, ν_{11b}, ν_{19b} and ν_{20b} are often interchanged in different studies[15,17,18,23]. However these differences are minor as all of these displacements are essentially mixtures of out-of-plane H and out-of-plane C displacements.

4.4.4 - Previous assignments of the 10 B_2 phenyl group vibrations of toluene

The wavenumbers and assignments of the 10 B_2 vibrations are given in Table 4.14 which is arranged in a similar manner to Table 4.11. There are several disagreements on the wavenumbers of the B_2 vibrations. These disagreements cause a

Table 4.14 - Previous assignments of the 10 B_2 phenyl vibrations of toluene

		Experimental									Theoretical		
Herzberg notation		Wilmshurst[a] [Ref 15]		Fuson[a] [Ref 17]		Sverdlov[b] [Ref 22]	Varsanyi[a] [Ref 23]		Draeger[c] [Ref 25]	Schrotter[d] [Ref 32]	Schmid[e] [Ref 18]	Snyder[c] [Ref 19]	Boggs[f] [Ref 26]
true	pseudo	cm^{-1}		cm^{-1}		cm^{-1}	cm^{-1}		cm^{-1}	cm^{-1}	cm^{-1}	cm^{-1}	cm^{-1}
ν_{21}	ν_{12b}	3090	ν_{12b}	3039R	ν_{15b}	3074	3039	ν_{15b}	3056	3065R	3079	3055	3074
ν_{22}	ν_{15b}	3032	ν_{15b}	3029	ν_{12b}	3034	3029	ν_{12b}	3039	3034R	3044	3054	3052
ν_{23}	ν_{16b}	1600	ν_{16b}	1586	ν_{16b}	1581	1586	ν_{16b}	1585	1586R	1593	1589	1602
ν_{24}	ν_{13b}	1455	ν_{13b}	1494	ν_9	1439R	1468	ν_{13b}	1463	1441R	1444	1445	1468
ν_{25}	ν_3	1155	ν_9	1460	ν_{13b}	1330	1331	ν_3	1330	1332R	1308	1326	1338
ν_{26}	ν_9	1155	ν_{10}	1312	ν_3	1278R	1318	ν_9	1278	1308R	1280	1290	1192
ν_{27}	ν_{17b}	1105	ν_3	1154	ν_{17b}	1162	1154	ν_{17b}	1155	1156R	1147	1168	1123
ν_{28}	ν_{10}	1081	ν_{14b}	1080	ν_{14b}	1086	1080	ν_{14b}	1083	1082R	1092	1081	1082
ν_{29}	ν_{18b}	623	ν_{18b}	623R	ν_{18b}	623	623	ν_{18b}	623	623R	632	616	628
ν_{30}	ν_{14b}	345	ν_{17b}	344R	ν_{10}	347	344	ν_{10}	341	347R	388	341	341

a - Assignments in pseudo-Wilson notation were converted to pseudo-Herzberg notation using Table 4.3.

b - Authors used the true Herzberg notation for 39 vibrations.

c - No notation was used.

d - Authors used the true Herzberg notation for 38 vibrations. See Section 4.4.

e - Authors used the true Herzberg notation for 30 ring vibrations.

f - Authors numbered all 39 vibrations in order of increasing wavenumber.

different wavenumber ordering which leads to different true Herzberg notations for the same wavenumber in different studies. Thus, ~1155 cm^{-1} is ν_{26} (and ν_{25}) for Wilmshurst and Bernstein[15] but ν_{27} for most other works[17,22,23,25,32].

One of the two aromatic CH stretching B_2 vibrations, is generally agreed to be at

3032 ±3 cm^{-1} with the exception of Draeger[25] who placed it at 3039 cm^{-1}. There is no agreement on the assignment of ν_{21} which has been placed from 3090 to 3039 cm^{-1}.

ν_{23} was assigned by Wilmshurst and Bernstein[15] at 1600 cm^{-1}, while the other experimental studies[17,22,23,25,32] placed it at 1585±5 cm^{-1}. The two groups of authors interchanged the assignment of ν_{23} and ν_4 (A_1) vibration.

Different choices were made for the B_2 phenyl group vibrations between 1500 and 1100 cm^{-1}. Consequently, the wavenumbers and true Herzberg notation of ν_{24} to ν_{27} disagree in the different studies. The only agreement is that one fundamental is near 1155 cm^{-1} and a second is near 1455 cm^{-1}.

All authors agree on the assignment of ν_{28} to ν_{30}.

The differences in the pseudo notation are not serious. Under the pseudo-Herzberg notation, ν_{12b} and ν_{15b} are both CH stretching displacements, while ν_3, ν_9, ν_{10}, ν_{13b}, ν_{14}, ν_{17b} and ν_{18b} are HCC deformation and CC stretching displacements which mix in the normal vibration.

4.4.5 - Previous assignment of the 9 CH_3 group vibrations of toluene

The wavenumbers and assignments of the 9 CH_3 group vibrations are given in Table 4.15 which is arranged in a similar manner to Table 4.11. The vibrations are arranged in order of symmetry species, i.e. 2 A_1, 1 A_2, 3B_1 and 3 B_2, and are numbered 31 to 39 using the true Herzberg notation.

Table 4.15 - Previous assignments of the 9 CH_3 group vibrations of toluene

		Experimental										Theoretical	
True Herzberg	Sym.	Wilmshurst[a] [Ref 15] cm^{-1}		Fuson[a] [Ref 17] cm^{-1}		Sverdlov[b] [Ref 22] cm^{-1}	Varsanyi[a] [Ref 23] cm^{-1}		Draeger[c] [Ref 25] cm^{-1}	Schrotter[d] [Ref 32] cm^{-1}	Schmid[e] [Ref 18] cm^{-1}	Snyder[c] [Ref 19] cm^{-1}	Boggs[f] [Ref 26] cm^{-1}
ν_{31}	A_1	2923	ν_s	2921	ν_s	2910	2921	ν_s	2921	2920R		2900	2919
ν_{32}	A_1	1377	δ_s	1379	δ_s	1380	1379	δ_s	1384	1379R		1379	1384
ν_{33}	A_2				t				15			44	
ν_{34}	B_1	2930	ν	2979	ν_a'''	2976	2979	ν_{as}	2933			2949	2976
ν_{35}	B_1	1436	δ'	1460	δ_a''	1462	1460	$\delta_{as}+$	1453	1441R		1455	1454
ν_{36}	B_1	1041	r	1040	r_a''	1040			1043			1040	1043
ν_{37}	B_2	2952	ν	2952	ν_a'	2976	2952	ν_{as}	2933	2982R		2951	2990
ν_{38}	B_2	1460	δ'	1460	δ_a'	1462			1463			1463	1468
ν_{39}	B_2	1081	r	1040	r_a'	970R	1040	$\delta_{as}-$	980			976	983

a - Authors used their own notation.

b - Authors used the true Herzberg notation for 39 vibrations.

c - No notation was used.

d - Authors used the true Herzberg notation for 38 vibrations. See Section 4.4.

e - Authors used the true Herzberg notation for 30 ring vibrations.

f - Authors numbered all 39 vibrations in order of increasing wavenumber.

There is general agreement on the wavenumbers of the A_1 vibrations. Only Draeger[25] has assigned the A_2 CH_3 torsion. There are several disagreements in the wavenumbers of the B_1 and B_2 vibrations.

There is disagreement over the wavenumbers, particularly of the two antisymmetric CH_3 stretching vibrations, and over the wavenumber of ν_{35} (B_1), one of the two antisymmetric CH_3 deformations, and its proximity to ν_{38}, the B_2 deformation. The wavenumber of the CH_3 rocking modes is also not settled. The most reliable assignment appears to be that of Fuson et al[17] who found that some of Wilmshurst and Bernstein's doublet bands were actually due to noise, and who had the spectra of toluene-α-d_3 to guide their determination of the bands due to the CH_3 vibration.

4.5 - Assignment of the vibrations of toluene

The methods used to evaluate the assignment of the toluene vibrations are similar to those used for the chlorobenzene assignment. Thus, the infrared spectrum of the gas and the Raman spectrum of the liquid recorded under parallel and perpendicular polarizations with linearly polarized incident light were obtained and a simple normal coordinate calculation was performed for toluene.

There are however two minor differences. First, the CH_3 group was approximated in the calculation by an atom of mass 15. Therefore no wavenumbers, eigenvectors or PED calculations are available for the 9 CH_3 vibrations. Second, the difference between A-type and C-type contours is not as clear as for chlorobenzene because of smaller differences between the moments of inertia of toluene.

Although Wilmshurst and Bernstein[15] gave figures of the infrared spectra of the gas and liquid phases and tabulated, as did Fuson *et al.*[17], all of the observed features in their infrared and Raman spectra, the experimental data and the results of the calculations obtained for this thesis will be presented on expanded scales, so as to form a basis for the evaluation.

The liquid phase refractive index spectra of toluene reported in Chapter 2 were converted into the liquid phase molar polarizability spectra by use of Equations 1.3.33 and 1.3.28. The entire imaginary molar polarizability, α''_m, spectrum of toluene is shown in Figure 4.9. Figures 4.10 through 4.14 show the infrared absorbance spectrum of the gas, the α''_m spectrum, and the parallel and perpendicular Raman spectra of the liquid for smaller wavenumber ranges, and thus provide a better view of the features in these spectra.

Table 4.16 contains the information for every feature observed in the three different spectra of toluene for the regions where the fundamentals are expected, i.e. 3150 - 2850 cm^{-1} and 1700 - 200 cm^{-1}. The table is arranged in a similar manner to Table 4.8 of chlorobenzene.

The computed wavenumbers, eigenvectors and potential energy distribution (PED) for the 30 phenyl group vibrations are given in Table 4.17. The table is arranged in a similar manner to Table 4.9 of chlorobenzene.

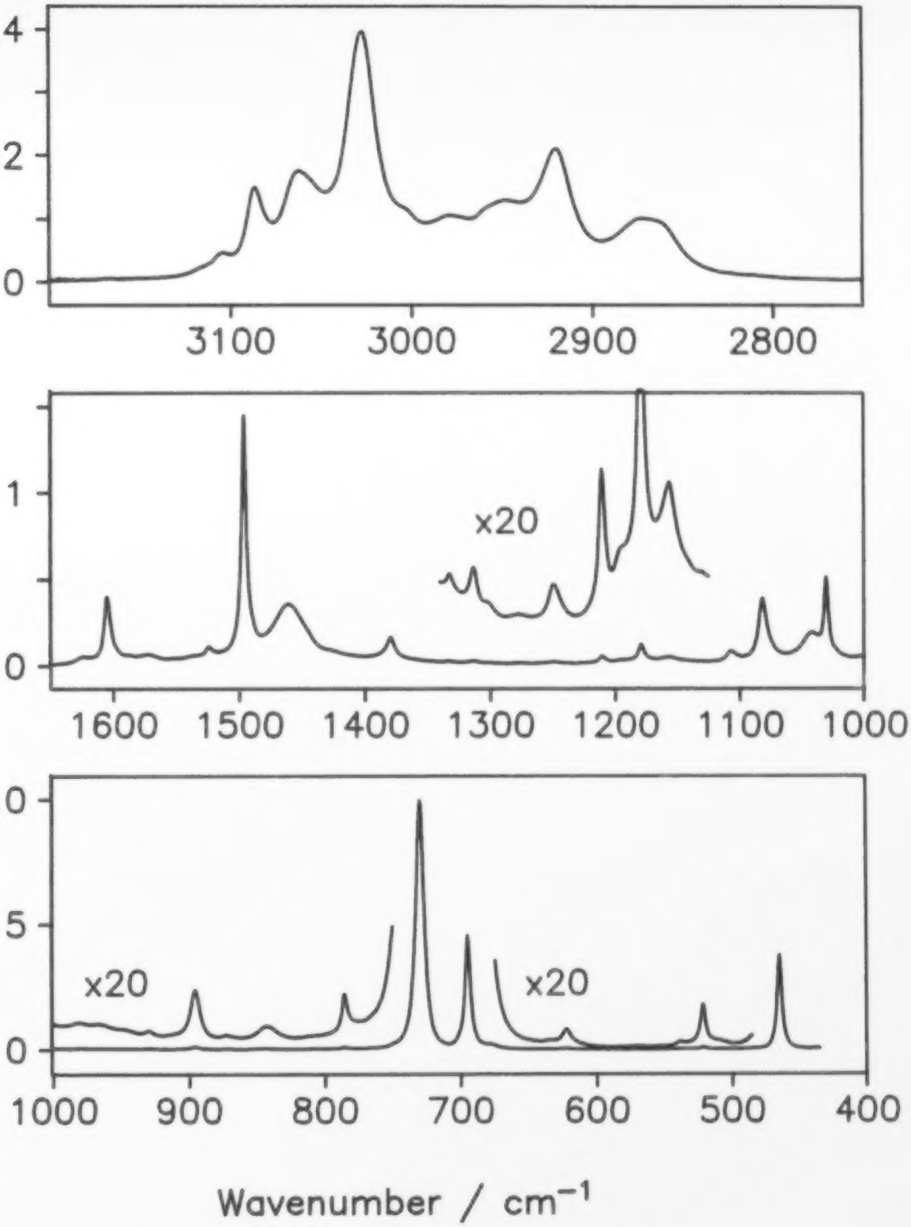

Figure 4.9 - Imaginary molar polarizability, α''_m, spectrum of liquid toluene. Units are cm^3 mol^{-1}. In each box, the ordinate scale is for the lower curve. It needs to be divided by 20 for the upper curve.

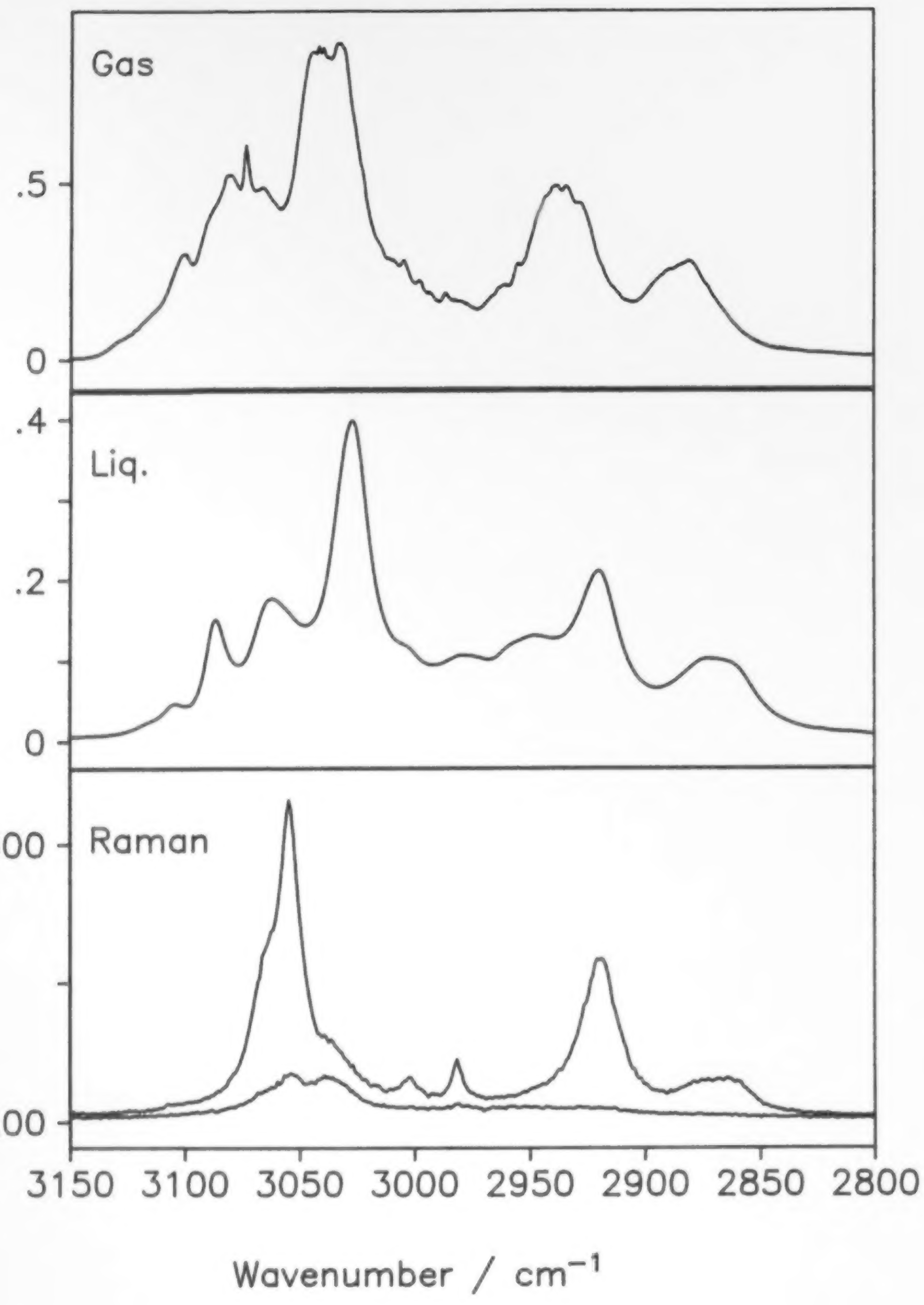

Figure 4.10 - Infrared spectra of gas and liquid toluene and Raman parallel (upper) and perpendicular (lower) spectra of the liquid between 3150 and 2800 cm^{-1}.

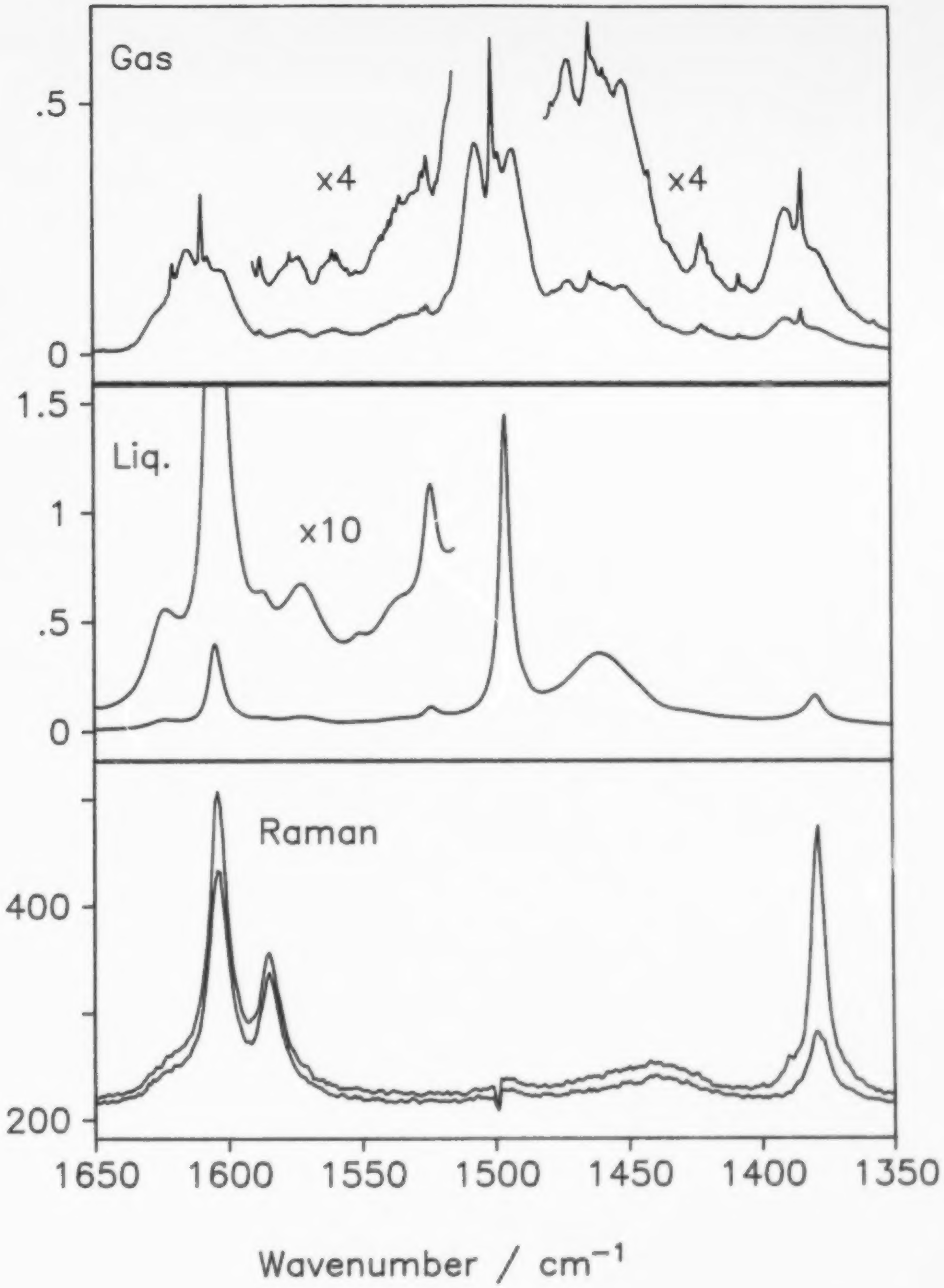

Figure 4.11 - Infrared spectra of gas and liquid toluene and Raman parallel (upper) and perpendicular (lower) spectra of the liquid between 1650 and 1350 cm^{-1}. In each box, the ordinate scale is for the lower curve. It needs to be divided by the multiplication factor for the upper curve.

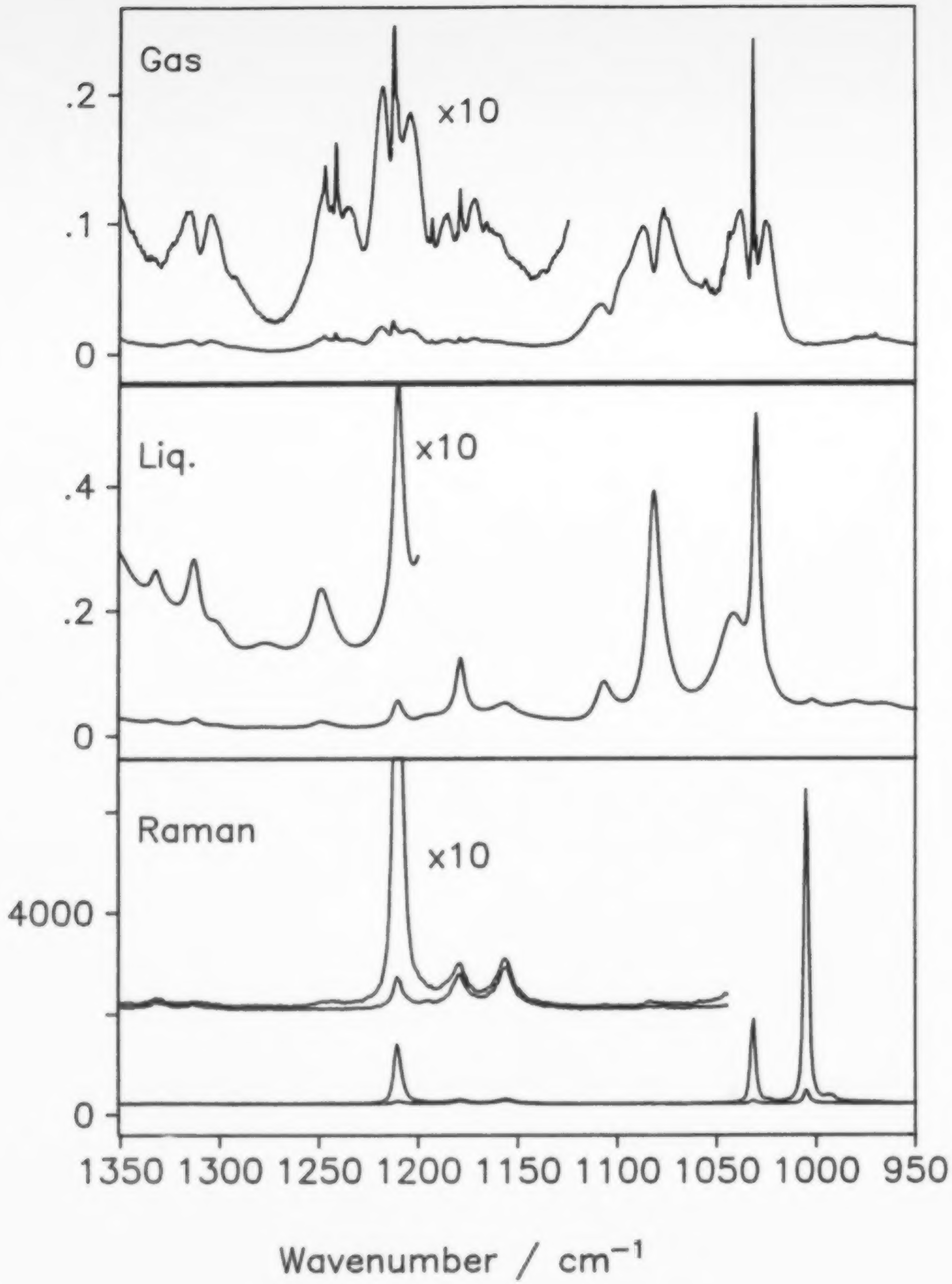

Figure 4.12 - Infrared spectra of gas and liquid toluene and Raman parallel (upper) and perpendicular (lower) spectra of the liquid between 1350 and 950 cm^{-1}. In each box, the ordinate scale is for the lower curve. It needs to be divided by the multiplication factor for the upper curve.

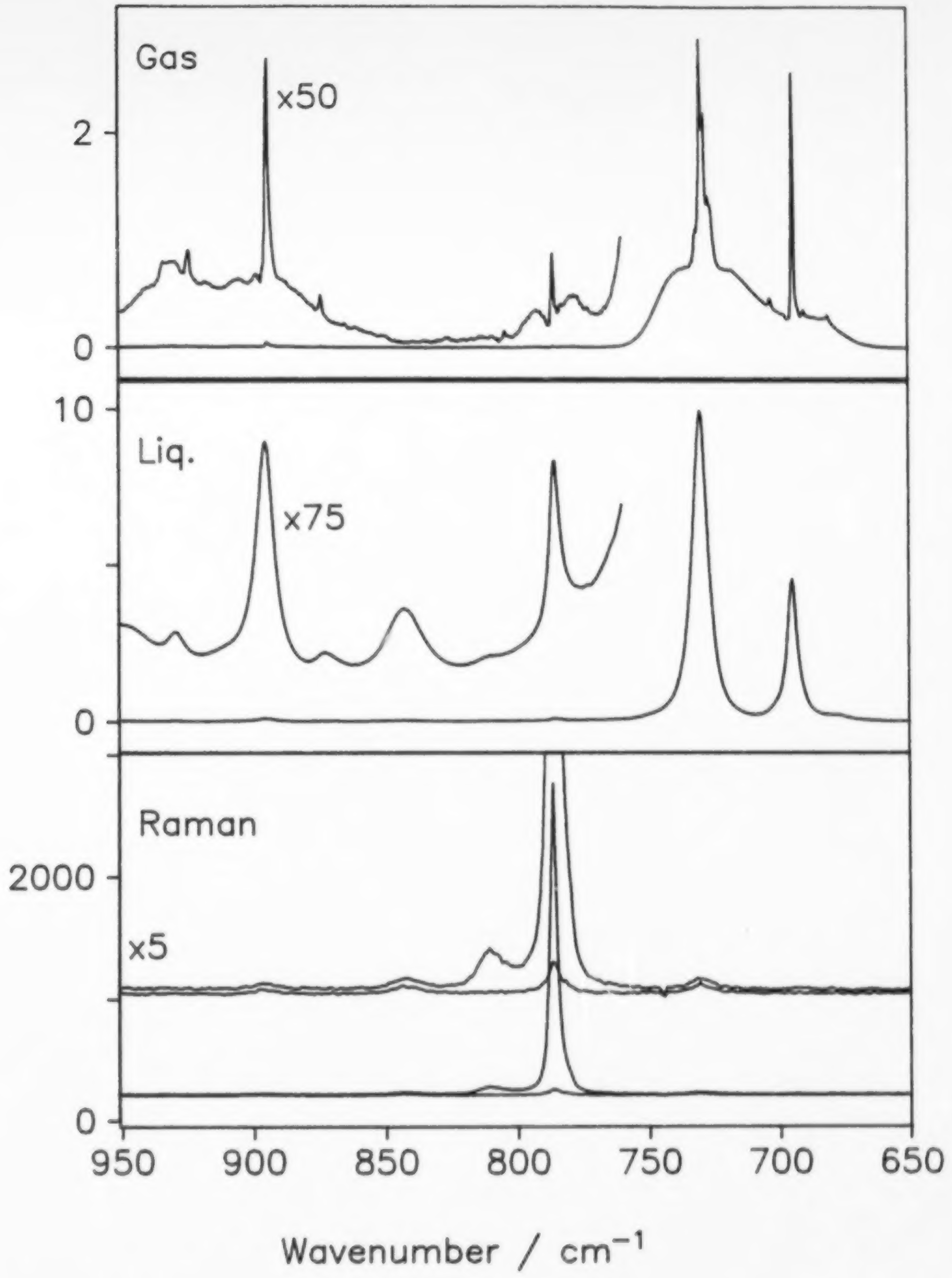

Figure 4.13 - Infrared spectra of gas and liquid toluene and Raman parallel (upper) and perpendicular (lower) spectra of the liquid between 950 and 650 cm^{-1}. In each box, the ordinate scale is for the lower curve. It needs to be divided by the multiplication factor for the upper curve.

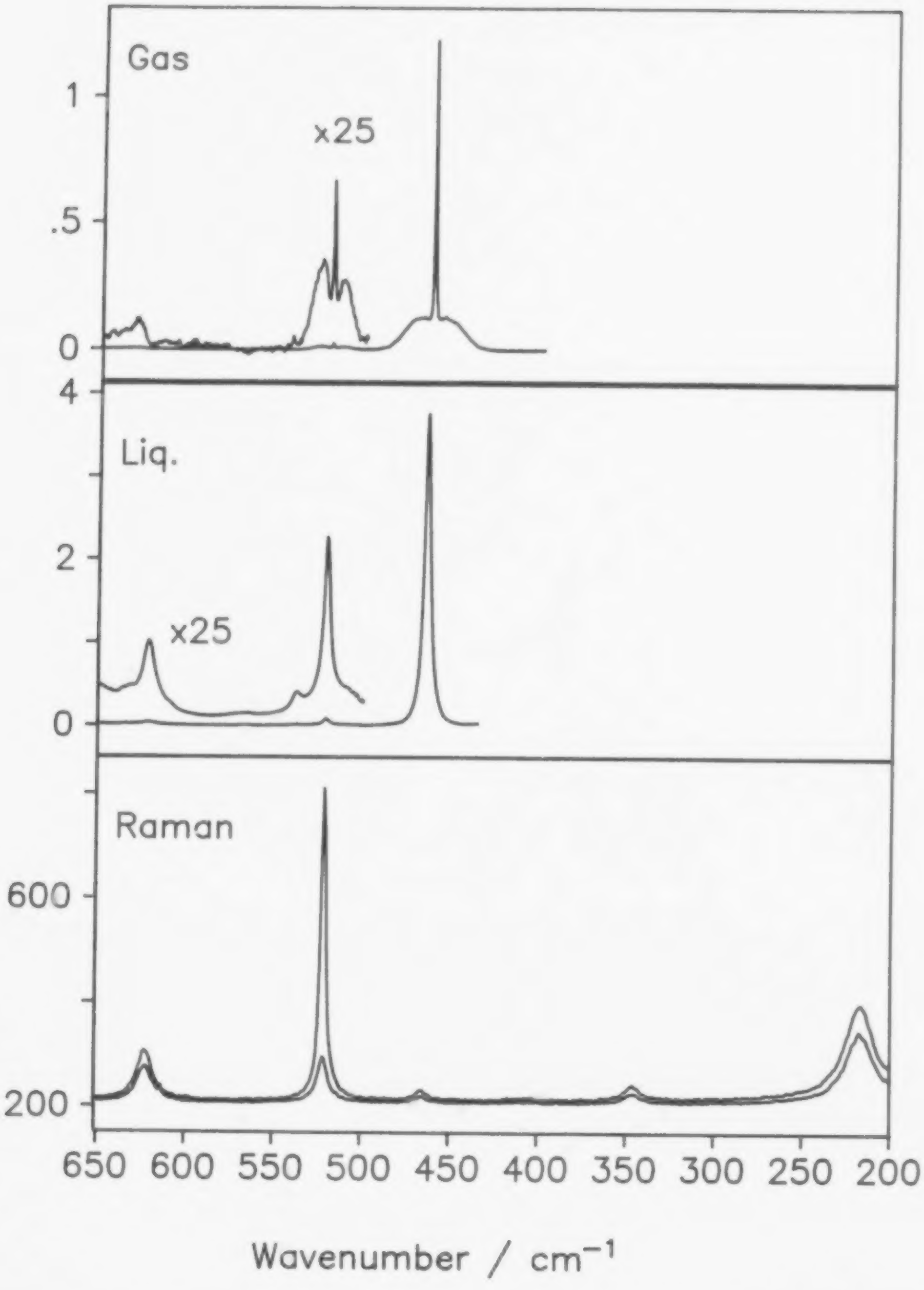

Figure 4.14 - Infrared spectra of gas and liquid toluene and Raman parallel (upper) and perpendicular (lower) spectra of the liquid between 650 and 200 cm^{-1}. In each box, the ordinate scale is for the lower curve. It needs to be divided by the multiplication factor for the upper curve.

Table 4.16 - Spectral features in infrared spectrum of gaseous toluene and infrared and spectra of the liquid

Infrared liquid[a]			Infrared gas[d]		Raman liquid[b]		
cm^{-1}	Desc.[b]	α_m^{nc}	cm^{-1}	Contour	cm^{-1}	ρ_l^e	comments
~3203	vw br sh	~0.0029			3205 vw	0.16	
3167.5	vw	0.00629	3175	??	3168 vw	p	
~3115	w br sh	~0.026	~3120	??			
3104.1	m	0.0478					
3086.4	s	0.152	3096	B			
3062.1	s br	0.177	3073	A	~3065 sh		
~3054	s br sh ?	0.157			3055 ms	0.08	
					~3038 vw	dp	
3027.0	s	0.398	~3040	B?			
~3003	s sh	0.118			3003 vw	p	
			2998	??			
			2993	??			
2979.1	s br	0.107	2986	C??	2981 vw	0.10	
~2950	s br	0.131	~2959	B ???			
2919.9	s	0.211	~2934	A ???	2920 m	p	
2872.3	s br	0.103	2881 br		2870 br vw	p	
1696.8	w	0.0106					
1676.7	w	0.0121					
1657.8	w br	0.0124					
1623.1	m br sh/p	0.056	1620	A? C?			
1604.6	s	0.402	1609	A	1604 m	0.82	
1586.7	m p/sh	0.0641			1585 w	dp	
1572.1	m	0.0674	1576	C??			
1550.3	m br sh/p	0.0452	~1560	??			
~1537	m br sh	~0.06					
1523.6	s br	0.113	1526	B??			
1495.7	vs	1.45	1500	A			
1460.3	s br	0.358	1467	B??			
			1463	C??			
			1454	B??	~1442 br vw	dp	

Table 4.16 - Continued

Infrared liquid[a]			Infrared gas[d]		Raman liquid[b]		
cm^{-1}	Desc.[b]	α_m''[c]	cm^{-1}	Contour	cm^{-1}	ρ_t[e]	comments
~1422	m sh	~0.08	1421	??			
1378.9	s	0.166	1384	A	1378 m	0.33	
1332.0	w	0.0266	1330	B?	1332 vw	0.73	
1312.7	w	0.0284	1310	B	1313 vw	dp	
~1302	w sh	0.0184					
1277.6	w br	0.0150					
1248.7	w	0.0236	1242	A?	~1245 vw	p	
			1247	C??			
1210.2	m	0.0569	1213	A	1210 s	0.05	
~1193	w br sh	0.0345	1193	A? C?			
1178.6	s	0.125	1179	A	1179 vw	0.70	
1155.9	m	0.0531			1156 vw	0.73	
~1130	w br sh/p	0.0272					
1106.5	m	0.088	1104	B			
1081.4	s	0.392	1082	B	1083 vw	p	
1041.4	s	0.196	~1043	??			
1030.1	s	0.516	1032	A	1031 s	0.02	
~1023	s sh	0.102			1023 vw	p	
1002.3	m	0.0581			1003 vs	0.02	
					~993 w	p	
980.7	m	0.0553					
966.4	m br	0.0519	970-5	??	~971 vw	p	
~947	w br sh	0.0211					
929.6	w	0.0383	~924-933	A??C??			
~910	w br sh ?	0.0107	913	B??			
895.4	s	0.120	894	C	896 vw	0.77	
872.9	w	0.0297	874	C			
842.7	m	0.0482			842 vw	dp	
810.4	w br sh	0.0282			810 vw	p	
785.6	s	0.111	786	A	786 vs	0.28	

Table 4.16 - Continued

Infrared liquid[a]			Infrared gas[d]		Raman liquid[b]		
cm^{-1}	Desc.[b]	$\alpha_m''^{c}$	cm^{-1}	Contour	cm^{-1}	ρ_ℓ^e	comments
729.9	vs	9.97	730	C	731 vw	0.78	
694.8	vs	4.56	694	C			
~678	s br p/sh	0.219	~681	??			
633.0	w sh	0.0195					
622.0	m	0.0411	~630	??	622 m-w	0.76	
565.2	vw br	0.0061					
537.8	w	0.0166					
521.0	m	0.091	520	A	521 m-s	0.22	
~508	vw sh	0.00342					
464.4	vs	3.77	462	C	465 vw	0.75	
					405 vvw	dp	
					346 w	0.73	
					217 mw	0.75	
<100							CH_3 torsion

a - Features are from the α_m'' spectrum.

b - Abbreviations used: v- very, w- weak, m- medium, s- strong, sh- shoulder, br- broad, sh/p- shoulder or a peak.

c - Peak heights in the α_m'' spectrum in cm^3 mol^{-1}.

d - Peak positions in the absorbance spectrum of the gas. B-type position is measured at the minimum between the R and P branches. ? and ?? indicate degrees of uncertainty in the determination of the band shape.

e - Depolarization ratio, $\rho_\ell = \frac{I_\perp}{I_\parallel}$. When the feature is too weak or noisy to obtain a reliable ratio, p or dp indicate polarized and depolarized, respectively.

Table 4.17 - Computed wavenumbers, eigenvectors and potential energy distributions for toluene.

ν_i	cm^{-1}	Eigenvectors[a]				PED[b]
ν_1	3177	S_5 -0.84	S_1 -0.59			CH
ν_2	3171	S_1 -0.73	S_{15a} -0.55	S_5 0.42		CH
ν_3	3158	S_{12a} 0.80	S_{15a} -0.62			CH
ν_4	1597	S_{18a} 0.80	S_{16a} 0.42	S_{17a} 0.39	S_{14a} -0.27	CC (75), HCC (25)
ν_5	1556	S_{14a} -1.08	S_{18a} 0.41	S_{13a} -0.25		HCC (50), CC (35), CX (15)
ν_6	1314	S_{14a} -0.73	S_{18a} 0.55	S_6 -0.26		HCC (55), CX (45)
ν_7	1157	S_{18a} 0.89	S_{14a} 0.23			HCC (60), CC (25), CX (15)
ν_8	1030	S_{14a} 0.50	S_6 -0.29	S_{13a} 0.21		CC (60), HCC (25), CCC (15)
ν_9	1001	S_6 -0.48	S_2 -0.19			CCC (55), CC (45)
ν_{10}	824	S_6 0.24	S_{17a} -0.24	S_2 -0.12		CCC (40), CC (40), CX (20)
ν_{11}	490	S_{17a} 0.29	S_{18a} -0.13			CCC (75), CX (25)
ν_{12}	971	S_{19a} 1.25	S_{20a} 0.44			oop H
ν_{13}	852	S_{11a} 1.03				oop H
ν_{14}	403	S_{20a} 0.70	S_{19a} 0.26			oop C (85), oop H (15)
ν_{15}	987	S_7 1.14	S_{19b} 0.64	S_8 -0.59		oop H (85), oop C (15)
ν_{16}	916	S_{19b} -0.85	S_{11b} -0.66	S_7 0.49		oop H
ν_{17}	749	S_8 0.71	S_4 0.60	S_{11b} -0.54	S_7 -0.45	oop H (67), oop C (33)
ν_{18}	698	S_8 1.04	S_4 -0.51	S_7 -0.41		oop C (67), oop H (33)
ν_{19}	489	S_{20b} 0.63	S_{19b} 0.39	S_4 -0.34		oop X (50), oop C (50)
ν_{20}	260	S_{20b} 0.30	S_4 0.14	S_{11b} 0.12		oop C (65), oop X (35)
ν_{21}	3157	S_{15b} 0.86	S_{12b} -0.57			CH
ν_{22}	3151	S_{12b} -0.87	S_{15b} -0.57			CH
ν_{23}	1584	S_{18b} -0.80	S_{16b} -0.43	S_{17b} -0.37		CC (75), HCC (25)
ν_{24}	1452	S_{14b} 1.10	S_3 -0.53			HCC (65), CC (35)
ν_{25}	1330	S_3 -1.09	S_{10} -0.65			HCC (70), CC (30)
ν_{26}	1294	S_3 0.58	S_{10} -0.50	S_9 0.40	S_{18b} -0.34	CC (75), HCC (25)
ν_{27}	1158	S_{10} -0.80	S_{18b} -0.61			HCC (65), CC (35)
ν_{28}	1073	S_{14b} 0.44	S_{10} 0.39	S_{18b} -0.38	S_{13b} 0.22	CC (55), HCC (45)
ν_{29}	617	S_{17b} 0.40				CCC
ν_{30}	399	S_{18b} 0.25	S_{14b} 0.22	S_{10} -0.18	S_3 0.13	XCC

a - The numbers are the $\partial S_i/\partial Q_j$ elements of the indicated symmetry coordinate in the particular vibration. Only the dominant terms are shown.

b - CH, CC or CX are stretches, HCC and XCC are bends, CCC is ring deformation. Out-of-plane vibrations are denoted by oop. Percent contributions are given in brackets..

4.5.1 - Assignments of the 11 A_1 phenyl group vibrations of toluene

Five aromatic CH stretching fundamentals are expected in toluene: three A_1 and two B_2 vibrations. As was the case for chlorobenzene, they are expected between 3100 and 3050 cm^{-1}.

One obvious A_1 vibration yields the A-type band at 3073 cm^{-1} in the infrared spectrum of the gas and the corresponding band at 3062 cm^{-1} in the infrared spectrum of the liquid and the polarized Raman shoulder at about 3065 cm^{-1}. A second A_1 vibration is observed as the polarized Raman band at 3055 cm^{-1}. There is a hint of a shoulder in the infrared spectrum of the liquid and a band centered at 3054 cm^{-1} was needed to obtain a good curvefit with CDHO bands.

The third A_1 CH vibration is not accounted for. Wilmshurst and Bernstein[15], Varsanyi[23] and Schrotter[32] assigned 3003 cm^{-1}. While a polarized Raman band is observed near 3003 cm^{-1}, the calculations suggest that this wavenumber is rather low as all of the aromatic CH stretching vibrations are expected within a 30 cm^{-1} range. Overall the band at 3003 cm^{-1} is probably due to combination or overtone transitions. Fuson et al[17] assigned this fundamental at 3087 cm^{-1}. However the corresponding gas-phase band is a B-type, so a B_2 vibration is assigned to it. Draeger[25] assigned it to a polarized Raman band at 3039 cm^{-1} but we find the band to be depolarized (Fig. 4.10).

ν_4 is expected near 1600 cm^{-1} and is assigned to the strong band in the infrared spectrum of the liquid at 1605 cm^{-1} which corresponds to the A-type band at 1609 cm^{-1} in the gas. A weak, depolarized Raman band is observed at 1604 cm^{-1} and this could be a case where the depolarization ratio of an A_1 band is equal to 0.75.

ν_5 is expected near 1550 cm^{-1} and is assigned as the very strong band in the infrared spectrum of the liquid at 1496 cm^{-1} which corresponds to the A-type band at 1500 cm^{-1} in the gas.

The remaining A_1 vibrations are predicted near 1310 cm^{-1} (ν_6), 1160 cm^{-1} (ν_7), 1030 cm^{-1} (ν_8), 1000 cm^{-1} (ν_9), 825 cm^{-1} (ν_{10}) and 490 cm^{-1} (ν_{11}). The assignment of ν_8, ν_9, ν_{10} and ν_{11} is clearly shown by the polarized Raman bands at 1031, 1003, 786 and 521 cm^{-1}. The assignments are confirmed by A-type bands in the spectrum of the gas at 1030 (s), 786 (vw) and 520 (w) cm^{-1} and strong or medium bands in the α''_m spectrum of the liquid at 1030, 1002, 786 and 521 cm^{-1}.

The assignment of ν_6 and ν_7 is less clear. They are expected near 1310 and 1160 cm^{-1} from the approximate normal coordinate calculation. A-type bands are observed in the spectrum of the gas at 1380, possibly 1242, 1213 and 1179 cm^{-1} (Figs. 4.11 and 4.12). Polarized Raman bands are at 1378 (m), ~1245 (vvw), 1210 (s) and (possibly polarized) 1179 (vw) cm^{-1}. The corresponding infrared bands of the liquid are at 1379 (s), 1249 (w), 1210 (m) and 1179 (s) cm^{-1}. Based on the infrared spectrum of the gas and the Raman spectrum, the most natural assignment is ν_6 at 1379 cm^{-1} and ν_7 at 1210 cm^{-1}. However, the spectrum of $C_6H_5CD_3$ shows[17] that the 1379 cm^{-1} band is due to the symmetric CH_3 deformation, so ν_6 and ν_7 are apparently both between 1250 and 1175 cm^{-1}. Accordingly, the assignment of previous authors is accepted, with ν_6 at 1210 cm^{-1} and ν_7 at 1179 cm^{-1}.

4.5.2 - Assignments of the 3 A_2 phenyl group vibrations of toluene

The three A_2 vibrations are expected near 970, 850 and 400 cm^{-1}. These vibrations are inactive in the infrared of the gas but may appear in the spectrum of the liquid. Usually the intensity in the liquid is very weak but as toluene is not a pure C_{2v} molecule, the A_2 modes may interact with the B_1 modes and their intensity might be stronger. The vibrations give depolarized Raman bands but these are usually very weak for A_2 vibration of C_{2v} molecules.

The assignments of ν_{13} and ν_{14} were in agreement among previous experimental studies and the present evidence is consistent with the assignments. Thus, the very weak, depolarized Raman band at 842 cm^{-1}, coincident with a medium band in the infrared spectrum, is assigned to ν_{13} and the very weak Raman band, probably depolarized, which is observed at about 405 cm^{-1}, is assigned to ν_{14}.

Fuson[17], Sverdlov[22], Varsanyi[23] and Draeger[25] assigned ν_{12} at 967±3 cm^{-1}. Wilmshurst and Bernstein[15] and Schrotter[32] assigned it as 992±2 cm^{-1}. While a weak Raman band is observed at 993 cm^{-1} it is clearly polarized and can not be assigned to ν_{12}. Therefore we assign ν_{12} to the medium, broad band at 966 cm^{-1} in the infrared spectrum of the liquid, which corresponds to a band of a complex contour at 975-970 cm^{-1} for the gas.

4.5.3 - Assignments of the 6 B_1 phenyl group vibrations of toluene

The computed wavenumbers for the six B_1 vibrations of toluene are: 987 cm^{-1} for ν_{15}, 916 cm^{-1} for ν_{16}, 749 cm^{-1} for ν_{17}, 698 cm^{-1} for ν_{18}, 489 cm^{-1} for ν_{19} and 260 cm^{-1} for ν_{20}. The fundamental bands should be depolarized in the Raman spectrum and should have a C-type contour in the infrared gas spectrum.

Three strong bands at 895, 730 and 464 cm^{-1} are observed in all experimental spectra with the appropriate contour and polarization and are assigned to ν_{16}, ν_{17} and ν_{19}, respectively. The band at 695 cm^{-1} in the liquid is very strong and exhibits a C-type contour in the gas spectrum. Although no Raman band is observed nearby, it is assigned to ν_{18}.

As the gas spectrum was not recorded below 400 cm^{-1}, the assignment of ν_{20} is based on the Raman bands and on the computed wavenumbers. Of the two depolarized Raman bands at 346 and 217 cm^{-1}, ν_{20} is assigned to the band at lower wavenumber, in agreement with its computed wavenumber being 140 cm^{-1} lower than that of ν_{30} (B_2).

ν_{15} was previously[15,17,22,23,25,32] assigned at 980±15 cm^{-1}. A band at 981 cm^{-1} is observed in the infrared spectrum of the liquid. A very weak band of undetermined shape is observed in the gas at about 980 cm^{-1}. The Raman band at 993 cm^{-1} is clearly polarized. For lack of better evidence, we follow the previous authors and assign ν_{15} to 981 cm^{-1}.

4.5.4 - Assignments of the 10 B_2 phenyl group vibrations of toluene

The computed wavenumbers of the two B_2 CH stretches are 3157 and 3151 cm^{-1}. Allowance for anharmonicity places the observed wavenumbers about 100 cm^{-1} lower. In this region, the strongest band in the spectrum of the gas has a B contour at about 3040 cm^{-1} and corresponds to the strongest band in the spectrum of the liquid, at 3027 cm^{-1}. It is assigned to ν_{22}.

A B-type contour is observed at 3096 cm^{-1} in the infrared spectrum of the gas, corresponding to 3086 cm^{-1} in the infrared spectrum of the liquid. A band at similar wavenumber for chlorobenzene was assigned to ν_{21} although the wavenumber is higher than expected. It is assigned as ν_{21}.

ν_{23} is expected near 1585 cm^{-1}. It is assigned to the depolarized Raman band observed at 1587 cm^{-1}, nearly coincident with a medium shoulder in the infrared spectrum of the liquid.

ν_{24} is expected near 1450 cm^{-1}. The B_1 and B_2 antisymmetric CH_3 deformations are also expected in this vicinity. A strong and very broad band at 1460 cm^{-1} is observed in the infrared spectrum of the liquid (Fig. 4.11). There is a corresponding possible B-type contour at 1467 cm^{-1} and a possible C-type band at 1463 cm^{-1} in the spectrum of the gas. Another possible B-type contour is at 1454 cm^{-1} which corresponds to the very weak and broad depolarized Raman band at about 1442 cm^{-1}. Balfour and Fried[30] gave in their figure 1, the transmittance spectra of liquid toluene, toluene-o-d, toluene-m-d, toluene-p-d and toluene-α-d. It is clear from their figure, that a broad band remains when the isotopic substitution is in the ring, suggesting it is due to the antisymmetric CH_3 deformations. When the isotope substitution is in the methyl group the broad band disappears and a sharp band appears at a slightly lower wavenumber, suggesting it is due to the phenyl B_2 fundamental. Therefore we conclude that the antisymmetric CH_3 deformations are at 1460 cm^{-1} and ν_{24} is within 20 cm^{-1} of them, perhaps at 1442 cm^{-1}.

The remaining B_2 vibrations ν_{25}, ν_{26}, ν_{27}, ν_{28}, ν_{29} and ν_{30} are expected near 1330, 1300, 1160, 1070, 620 and 400 cm^{-1}. Their assignment is fairly clear from depolarized Raman bands that are coincident with infrared bands of the liquid and, in several cases, B-type bands in the gas. ν_{30} is assigned at 346 cm^{-1} based solely on the Raman spectrum, while ν_{25}, ν_{26}, ν_{27}, ν_{28} and ν_{29} are assigned at 1332, 1313, 1156, 1081 and 622 cm^{-1} based on the infrared and Raman spectra of the liquid. B-type bands in the spectrum of the gas at 1330 (vw), 1310 (vw) and 1082 (s) cm^{-1} support the assignments of ν_{25}, ν_{26}, ν_{27} and ν_{28}. The clear B-type band at 1104 cm^{-1} (Fig. 4.12) is assigned to a combination band, following Fuson et al[17].

4.5.5 - Assignments of the 9 CH_3 vibrations of toluene

There are three methyl CH stretching vibrations in toluene. They are expected at about 100 cm^{-1} lower than the aromatic CH stretching vibrations. The symmetric stretch is expected about 50 cm^{-1} below the two antisymmetric stretching vibrations.

A strong band is observed at 2920 cm^{-1} in the infrared spectrum of the liquid coincident with a polarized Raman band (Figure 4.10). A complex band is located at about 2934 cm^{-1} in the spectrum of the gas and is perhaps related. As the Raman and infrared band of the liquid are the strongest bands in the region they are assigned to the A_1 fundamental, the symmetric CH_3 stretching vibration, ν_{31}.

The antisymmetric CH stretching vibrations, ν_{34} (B_1) and ν_{37} (B_2), are expected approximately 50 cm^{-1} higher than the symmetric stretch. Bands are observed in the spectrum of the liquid at 2950 cm^{-1} and 2979 cm^{-1}, both broad, and there is a shoulder at ~2965 cm^{-1}. In the spectrum of the gas, a Q branch may occur at 2986 cm^{-1} (Fig. 4.10) and an even more uncertain B-type band may be observed near 2959 cm^{-1}. The only Raman band in the vicinity is very weak and polarized at 2981 cm^{-1}, so it can not arise from a B_1 or a B_2 vibration. For lack of better evidence we tentatively assign both ν_{34} (B_1) and ν_{37} (B_1) at 2950 cm^{-1}.

ν_{32} (A_1), the symmetric CH_3 deformation, is assigned to the A-type band at 1384 cm^{-1} in the spectrum of the gas, the polarized Raman band at 1378 cm^{-1} and the band at 1379 cm^{-1} in the infrared spectrum of the liquid. It is clear from the spectra of Balfour and Fried[30] that the band remains when the phenyl ring is isotopically substituted, and almost disappears when the isotopic substitution occurs at the methyl group.

As discussed in the previous section, the antisymmetric CH_3 deformations are assigned to the very broad band at 1460 cm^{-1} in the liquid. In addition to the spectra provided by Balfour[30] which indicate that the band is due to a methyl vibration, a complex contour is observed in the spectrum of the gas with a possible B-type band at

1467 cm^{-1} and a possible C-type band at 1463 cm^{-1}. We are unable to separate the two vibrations and use the same wavenumber for both.

The methyl rocking vibrations, ν_{36} (B_1) and ν_{39} (B_2) are both assigned to the same wavenumber in the infrared spectrum of the liquid, at 1041 cm^{-1}. It is clear from the spectra of Balfour and Fried[30] that the band remains when the ring is isotopically substituted, and disappears when the isotopic substitution occurs at the methyl group. Furthermore, two CDHO bands at 1040 cm^{-1} and 1043 cm^{-1} are needed to obtain a good fit of the α''_m band of the liquid.

ν_{33}, the A_2 methyl torsion vibration was not observed in this study. Draeger[25] reported an observed and a calculated wavenumber for this vibration, both at 15 cm^{-1}. La Lau and Snyder[19] calculated the wavenumber at 44 cm^{-1}. In their calculations, the authors used a small value (1×10^{-4} mdyne-Å/rad) so that their calculated wavenumber is low enough to prevent it from coupling with other vibrations. Hameka and Jensen[34], based on La Lau and Snyder data, calculated it at 28.9 cm^{-1}. It is clear that the wavenumber for this vibration is well below 100 cm^{-1}.

4.5.6 - Summary of the assignments of toluene

The fundamental wavenumbers are collected in Table 4.18 which corresponds to Table 4.10. The table includes the pseudo-Herzberg assignments obtained from Table 4.17 by including all symmetry coordinates with eigenvectors at least half of the largest. It is clear that the pseudo-Herzberg assignment is complicated for most of the vibrations.

Table 4.18 - Assignments of the fundamental vibrations of liquid toluene

true Herzberg	cm^{-1} [a]	pseudo-Herzberg[b]	Description[c]
ν_1	3062.1	ν_5, ν_1	CH
ν_2	3055.0	ν_1, ν_{15a}, ν_5	CH
ν_3	3038 ???	ν_{12a}, ν_{15a}	CH
ν_4	1604.6	ν_{18a}, ν_{16a}, ν_{17a}	HCC, CC
ν_5	1495.7	ν_{14a}	HCC
ν_6	1210.2	ν_{14a}, ν_{18a}	HCC
ν_7	1178.6	ν_{18a}	HCC
ν_8	1030.1	ν_{14a}, ν_6	HCC, CCC
ν_9	1002.3	ν_6	CCC
ν_{10}	785.6	ν_6, ν_{17a}, ν_2	CCC, CC
ν_{11}	521.0	ν_{17a}	CCC, CC
ν_{12}	[illegible]66.4 ??	ν_{19a}	oop H
ν_{13}	842.7	ν_{11a}	oop H
ν_{14}	~ 405 ?	ν_{20a}	oop C
ν_{15}	980.7 ??	ν_7, ν_{19b}, ν_8	oop H, oop C
ν_{16}	895.4	ν_{19b}, ν_{11b}, ν_7	oop H, oop C
ν_{17}	729.9	ν_8, ν_4, ν_{11b}, ν_7	oop C, oop H
ν_{18}	694.8	ν_8, ν_4	oop C, oop H
ν_{19}	464.4	ν_{20b}, ν_{19b}, ν_4	oop C, oop H
ν_{20}	217	ν_{20b}, ν_4	oop C, oop H
ν_{21}	3086.4	ν_{15b}, ν_{12b}	CH
ν_{22}	3027.0	ν_{12b}, ν_{15b}	CH
ν_{23}	1586.7	ν_{18b}, ν_{16b}	HCC, CC, CCC
ν_{24}	~ 1442 ??	ν_{14b}	HCC, CC
ν_{25}	1332.0	ν_3, ν_{10}	HCC
ν_{26}	1312.7	ν_3, ν_{10}, ν_9, ν_{18b}	HCC, CC
ν_{27}	1155.9	ν_{10}, ν_{18b}	HCC
ν_{28}	1081.4	ν_{14b}, ν_{10}, ν_{18b}, ν_{13b}	HCC, CC
ν_{29}	622.0	ν_{17b}	CCC
ν_{30}	346	ν_{18b}, ν_{14b}, ν_{10}, ν_3	HCC, CC
ν_{31} (A_1)	2919.9		symmetric CH_3 stretch
ν_{32} (A_1)	1378.9		symmetric CH_3 deformation

Table 4.18 - Continued

true Herzberg	cm^{-1}[a]	pseudo-Herzberg[b]	Description[c]
ν_{33} (A_2)	< 100		CH$_3$ torsion
ν_{34} (B_1)	~2950 ??		antisymmetric CH$_3$ stretch
ν_{35} (B_1)	1460.3 ?		antisymmetric CH$_3$ deformation
ν_{36} (B_1)	1041.4 ?		CH$_3$ rock
ν_{37} (B_2)	~2950 ??		antisymmetric CH$_3$ stretch
ν_{38} (B_2)	1460.3 ?		antisymmetric CH$_3$ deformation
ν_{39} (B_2)	1041.4 ?		CH$_3$ rock

a - Peak wavenumbers of the imaginary molar polarizability spectrum of liquid toluene.

b - Contributions greater than 50% of the largest contribution.

c - CH, CC are stretches, HCC is CH bend, CCC is ring deformation and oop is out-of-plane.

Note that ν_{13a}, a C-C stretching displacement, does not appear in Table 4.18. It is a minor contributor to several vibrations.

A question arises from the table, where are the C-CH$_3$ stretch and the C-CH$_3$ in-plane and out-of-plane bends?

From the unsymmetrized eigenvectors, the C-CH$_3$ stretch contributes with HCC, CC and CCC to the following A_1 vibrations: ν_4 (1597), ν_5 (1556), ν_6 (1314), ν_7 (1157), ν_{10} (824) and ν_{11} (490). It does not make the major contribution to any of them. From the potential energy distribution, the C-CH$_3$ stretch is among the three main contributors to ν_5 (1556), ν_6 (1314), ν_7 (1157), ν_{10} (824) and ν_{11} (490) but is the major contributor to none of these. Therefore we conclude that no single vibration can be called to the C-CH$_3$ stretch.

The unsymmetrized eigenvectors and the PED agree that the CC- CH$_3$ in-plane bending displacement is the dominant contributor to ν_{30}, calculated at 399 cm^{-1} and observed at 346 cm^{-1} and is, therefore, the CC- CH_3 in-plane bend.

The unsymmetrized eigenvectors and the PED show that the out-of-plane CC-CH_3 bending displacement mixes with the CCC out-of-plane displacement to form ν_{19} and ν_{20}. ν_{19} is about an equal mixture of the two while the CCC deformation dominates by a factor of 2 in ν_{20}.

Chapter 5 - Infrared Integrated Intensities for Liquid Chlorobenzene and Toluene

In Chapter 4, the fundamental vibrations of chlorobenzene and toluene were assigned. While it is possible to determine infrared intensities without a complete assignment, it is far more meaningful to determine transition moments and dipole moment derivatives with some knowledge of the nature of the transition.

Bertie *et al.*[48] have shown that if the Lorentz local field is valid, molecular properties and behavior are more directly reflected in the imaginary molar polarizability spectrum, α''_{m}, than in the imaginary refractive index spectrum, k, the molar absorption coefficient spectrum, E_{m}, or the imaginary dielectric constant spectrum, ε''. Accordingly, the refractive indices of toluene and chlorobenzene, given in Chapters 2 and 3 respectively, were used to calculate the imaginary molar polarizability spectra of toluene and chlorobenzene using Eqs. 1.3.28a, 1.3.28b and 1.3.33b. The imaginary molar polarizability spectra are shown in Figs. 5.1 and 5.9 and the integrated intensities of chlorobenzene and toluene are presented in Sections 5.1 and 5.2, respectively.

In order to calculate the integrated intensities, the α''_{m} spectrum must be separated into contributions from the different transitions. The integration limits can be chosen arbitrarily so that the integrated intensity is taken as the area between these limits and is assumed to be solely due to a single specific transition. This approach can give good results in optimal circumstances, namely when the band is single, well defined, and fairly isolated from other bands. But even for such a band, the choice of integration limits can introduce large uncertainty to the intensity. To obtain 98% of the area under a

Lorentzian band one must integrate over 16 times the full-width at half-height on each side of the band. Further, when, as is usual, bands are close or actually overlap, any arbitrary separation could introduce considerable error into the integrated intensity value.

The alternative method is to fit the α_m'' spectrum with bands of appropriate and well-defined shape, and calculate the integrated intensities from the areas under the fitted bands. As discussed in Section 1.4, the general theory of infrared spectra of liquids[48], indicates that the bands in the α_m'' spectrum have the shapes of classical damped harmonic oscillator (CDHO) bands. Thus, the α_m'' spectra of chlorobenzene and toluene were fitted with CDHO bands.

The integrated intensities, C_j, (Eqs. 1.4.2 to 1.4.4) are the areas under the $\tilde{\nu}\alpha_m''$ spectra of the bands that fitted the original α_m'' spectra. The j^{th} CDHO band in the imaginary molar polarizability is described by

$$\alpha_m''(\tilde{\nu}) = \frac{S_j \Gamma_j \tilde{\nu}_j}{(\tilde{\nu}_j^2 - \tilde{\nu}^2)^2 + \Gamma_j^2 \tilde{\nu}_j^2} \qquad (5.1.1)$$

Program CURVEFIT yields the parameters, S_j, Γ_j and $\tilde{\nu}_j$. The area C_j under the corresponding $\tilde{\nu}\alpha_m''$ band is given by $C_j = S_j \pi/2$. Provided a good fit can be obtained, the uncertainty introduced by the choice of integration limits is, then, eliminated as the limits are effectively zero and infinity.

There are, however, two major disadvantages to curve fitting. First, the fit can be artificially improved by the addition of extra bands. Some of these extra bands may not be actually present in the original spectrum and they will affect the integrated intensity assigned to a particular band. Therefore care must be taken to ensure that addition of extra bands is limited and can be justified. In the curve fitting performed in this work, the minimum number of bands was used to obtain a good fit. Extra bands were added only when the observed band was clearly asymmetric. With the exception of two or three cases, all bands used for the fit could be justified based on band asymmetry or a distinct shoulder observed in the original spectrum.

Second, the fit within a region is heavily influenced by bands that are outside the region. The best solution for this problem would be to fit the entire spectrum. This solution, however, is often in conflict with available computer programs for curve fitting. These programs usually require large memory space and execution times increase manyfold with increase of the number of bands to be fitted. Therefore, the spectrum is usually divided into several regions and a fit is performed for each region. If the curve fitting procedure is done properly, the contributions from adjacent regions are included and taken into account during the fit.

Galactic Industries' program CURVEFIT was modified in our laboratory by C.D. Keefe and S.L. Zhang to use CDHO bands. It was also written in FORTRAN and compiled with Microway's NDP FORTRAN under OS/2 2.1 in order to provide access to 16 Megabyte of memory and to obtain a tenfold decrease in execution time[73]. The program was limited to 80 peaks in the fitted spectrum and the input spectrum was limited to 8192 points.

For benzene[73], chlorobenzene and toluene, each with well over 150 bands of various intensity in the spectrum, 80 peaks are not enough and the spectrum must be divided into two or three regions. Furthermore, at the start of this work, some of the 80 peaks, had to be reserved for bands outside the region that contributed more than 10^{-6} cm^3 $mole^{-1}$ to the fit inside the region. For benzene[73], the number of regions had to be increased to 10 to 15 as the number of required outside peaks increased as more regions were fitted. The fit in each region was refined iteratively until the bands in the entire spectrum were constant.

Thus, a serious drawback to this FORTRAN program at the start of this work was the need to include among the 80 peaks that would be refined an increasingly large number of peaks outside the region being fitted. An improvement was made for the work of this thesis.

In the improved program, once a region has been fitted, its bands are considered constant for the adjacent region. Therefore the contribution can be calculated first and then subtracted from the region of the spectrum to be fitted. This resulting region is then fitted with bands within the region. This allows all of the 80 peaks that can be refined by the program to be within the region. Each region is fitted in this way, then, the whole procedure is repeated several times, each time calculating the initial contribution from the last fit of the adjacent regions. Refinement of the fit is continued until all bands in all regions remain constant. The new program allows 80 bands within the region to be fitted and 200 constant bands outside of the region to be included. This allows larger regions to be fitted, and, to accommodate this, the number of points in the input spectrum was increased to 16384.

With this revised program only three regions were needed to fit an entire spectrum and, with the inclusion of all contributions from all of the outside bands, only three to four cycles of refinement were needed to fit the α_m'' spectra of chlorobenzene and toluene.

5.1 - Integrated intensities and dipole moment derivatives of liquid chlorobenzene

The imaginary molar polarizability, α_m'', spectrum of liquid chlorobenzene was fitted with 193 CDHO bands between 4475 and 350 cm^{-1}. An entire spectrum, called the fitted spectrum in this thesis, was obtained by adding the 193 bands, each of which extended from 4475 to 350 cm^{-1}. This fitted spectrum and the experimental α_m'' spectrum are shown in Figure 5.1.

The fit is very good and the two spectra nearly coincide. As can be seen from the magnified curves in Fig 5.1, the fit is not as good in the wings of sharp bands as elsewhere. The CDHO band does not fit the observed bandshape very well, and, the addition of extra CDHO bands did not improve the fit in these wings, and, consequently these extra bands were not used in the final fit.

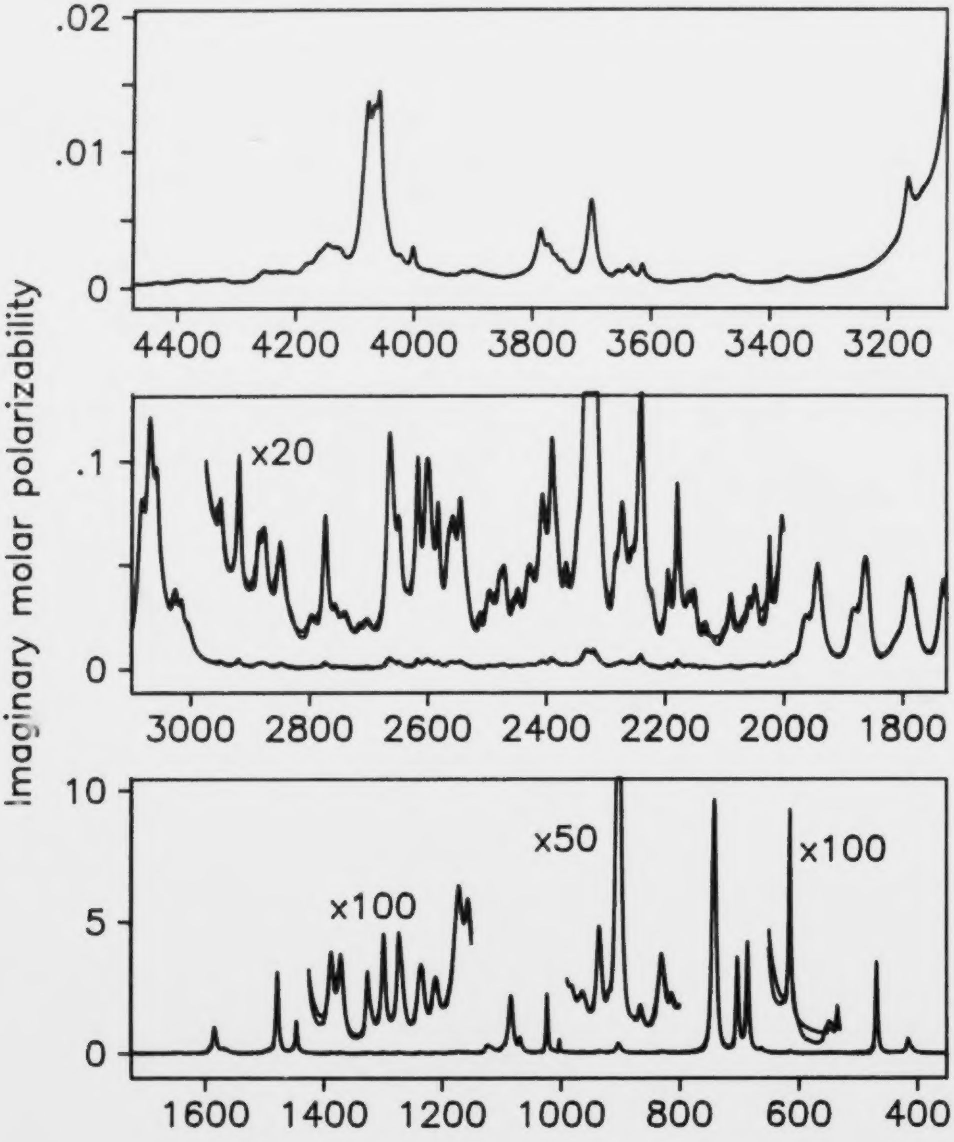

Figure 5.1 - Superimposed experimental imaginary molar polarizability, α''_m, and curve fitted α''_m spectra of liquid chlorobenzene. Units are cm^3 $mole^{-1}$. In each box, the ordinate scale is for the lower curves. The labels must be divided by the multiplication factor for the upper curves.

The overall average percent difference between the fitted and experimental α''_m peak heights is 2.5%. The difference is on average greater for weaker peaks and decreases for stronger peaks. For peak heights less than < 0.01 cm^3 mole^{-1}, between 0.01 and 0.1 cm^3 mole^{-1}, between 0.1 and 1 cm^3 mole^{-1}, and > 1 cm^3 mole^{-1}, the average percent differences are ~3%, 2.8%, 1.7% and 0.6%, respectively. Thus, the peak heights are fitted to 0.6% on average for the peaks that are usually observed in an infrared spectrum that is recorded to show the peak maxima.

An important check on the quality of the fit is to compare the total area under the experimental spectrum to that under the fitted spectrum over a wide wavenumber range. Between 4475 and 800 cm^{-1}, the area under the fitted spectrum is greater by 0.45% and between 800 and 350 cm^{-1}, it is greater by 2.6%. Overall, the area under the fitted spectrum is 1.7% greater than that under the experimental α''_m spectrum.

The parameters of the fitted CDHO bands are given in Table 5.1. In this table, the peak positions in the α''_m spectrum of the liquid and the band symmetry of the spectrum of the gas are given in the first two columns. The fitted peak positions are given in column 3, and the CDHO parameter Γ_j, which is essentially the full width at half height (FWHH) of the band, is given in column 4. It is followed by the integrated intensity, C_j, in km mole^{-1} in column 5 and by the dipole transition moment, $|\vec{R_j}|$, in Debye in column 6. The C_j values were calculated using Eq. 1.4.2 while the $|\vec{R_j}|$ values were calculated using Eq. 1.4.3.

Table 5.1 - Integrated intensities and dipole moment transitions of liquid chlorobenzene.

Exp α''_m [a,b] cm^{-1}	Gas[c]	Fitted cm^{-1}	Γ_j cm^{-1}	C_j km / mol	$\lvert\overrightarrow{R_j}\rvert$ Debye	Assignment[d]
4468.1 vw		4469.5	26.5	0.000225	0.00126	
4448.9 vw		4449.1	15.1	0.000091	0.00080	
4432.5 vw		4436.8	11.2	0.000054	0.00062	
		4432.1	8.7	0.000045	0.00057	
		4426.8	34.3	0.000367	0.00162	
4404.1 vw		4405.7	14.1	0.000141	0.00100	$\nu_{21}+\nu_{25}$ (4408)
4387.4 vw br		4384.9	36.4	0.00106	0.00276	$\nu_1+\nu_{25}$ (4395) or $\nu_3+\nu_{25}$ (4385)
4359.2 vw		4358.4	20.4	0.000272	0.00140	$\nu_{21}+\nu_{26}$ (4356)
4340.8 vw		4341.0	23.7	0.000318	0.00152	$\nu_1+\nu_{26}$ (4341)
4323.9 vw br		4323.2	26.0	0.000610	0.00211	$\nu_3+\nu_{26}$ (4331) or $\nu_{22}+\nu_{26}$ (4332)
~4295 vw br		4295.3	16.9	0.000078	0.00076	
4252.8 vw br		4254.5	18.2	0.000534	0.00199	$\nu_{21}+\nu_6$ (4255)
		4250.8	44.7	0.000698	0.00227	
4226.8 vw br		4223.6	59.4	0.00306	0.00478	
4178.6 vw		4180.8	21.6	0.00109	0.00287	
~4161 vw sh		4161.3	21.5	0.00126	0.00309	
4145.8 vw br		4145.8	26.7	0.00321	0.00494	$\nu_3+\nu_7$ (4142) or $\nu_{22}+\nu_7$ (4144) or $\nu_{21}+\nu_{28}$ (4151)
4131.4 vw br		4126.2	26.4	0.00257	0.00443	
4077.4 w	B	4082.6	20.4	0.00651	0.00709	
		4077.5	11.5	0.00433	0.00578	$\nu_{22}+\nu_8$ (4083) or $\nu_{21}+\nu_9$ (4085)
4066.5 w	A	4067.1	15.0	0.00701	0.00737	$\nu_1+\nu_9$ (4071)
4058.7 w	B	4057.8	11.2	0.00647	0.00709	$\nu_{22}+\nu_9$ (4062)
~4045 vw sh		4045.5	18.4	0.00205	0.00400	
4022.8 vw br		4021.9	19.6	0.00121	0.00308	$\nu_{22}+\nu_{12}$ (4024) or $\nu_3+\nu_{12}$ (4023)
4000.5 vw		4000.3	8.4	0.000921	0.00269	$4\nu_9$ (4008)
3968.9 vw br		3977.5	70.8	0.00320	0.00503	$\nu_1+\nu_{16}$ (3973)
~3950 vw sh						
3938.4 vw						
3917.7 vw		3917.8	11.3	0.000189	0.00123	$\nu_{21}+\nu_{13}$ (3913)

Table 5.1 - Continued

Exp α_m'' [a,b] cm^{-1}	Gas[c]	Fitted cm^{-1}	Γ_j cm^{-1}	C_j km / mol	$\lvert\overrightarrow{R_j}\rvert$ Debye	Assignment[d]
3899.5 vw br		3899.5	10.8	0.000148	0.00109	$\nu_1+\nu_{13}$ (3899)
		3894.3	75.0	0.00303	0.00495	$\nu_{21}+\nu_{13}$ (3890) or $\nu_3+\nu_{13}$ (3889)
~3878 vw sh						
~3867 vw sh						
~3804 vw sh		3796.6	73.1	0.00279	0.00481	$\nu_{1,2}+\nu_{17}$ (3810)
3785.1 vw		3785.2	15.3	0.00276	0.00479	$\nu_{21}+\nu_{10}$ (3786)
3772.2 vw br		3772.9	12.5	0.000331	0.00166	$\nu_1+\nu_{10}$ (3772)
		3768.3	8.9	0.000797	0.00258	$\nu_{21}+\nu_{18}$ (3768)
~3759 vw sh		3759.1	10.4	0.000421	0.00188	
3749.3 vw br		3747.8	17.0	0.000901	0.00275	
3699.4 vw		3699.5	16.6	0.00572	0.00698	$\nu_{21}+\nu_{29}$ (3697)
~3685 vw sh		3685.5	191.7	0.00178	0.00390	$\nu_1+\nu_{29}$ (3684)
3653.4 vw br		3654.3	12.0	0.000356	0.00175	
3636.9 vw		3636.8	16.8	0.00102	0.00297	
~3628 vw sh						
3613.6 vw		3613.3	9.0	0.000613	0.00231	$4\nu_{16}$ (3612)
~3602 vw sh		3601.8	10.9	0.000091	0.00089	
3583.9 vw		3583.7	5.3	0.000031	0.00052	
3546.9 vw br		3549.0	16.0	0.000089	0.00089	$\nu_{21}+\nu_{19}$ (3551)
3531.1 vw		3531.5	27.2	0.000254	0.00151	$\nu_1+\nu_{19}$ (3538) or $\nu_3+\nu_{19}$ (3527) or ? $\nu_{22}+\nu_{19}$ (3528)
3488.8 vw		3490.7	33.9	0.00109	0.00314	
3464.1 vw		3463.3	18.6	0.000463	0.00205	
~3445 vw sh		3446.1	9.9	0.000025	0.00048	
3420.4 vw						
3368.4 vw br		3369.7	17.2	0.000325	0.00174	$\nu_1+\nu_{30}$ (3367)
3297.5 vw br						
~3261 vw sh						$\nu_1+\nu_{20}$ (3265) or $\nu_3+\nu_{20}$ (3254)
3165.4 vw br		3165.9	11.7	0.00183	0.00427	$2\nu_{23}$ (3168) or $2\nu_4$ (3168) or $\nu_{23}+\nu_4$ (3168)
~3140 vw sh		3144.3	89.5	0.0153	0.0124	

Table 5.1 - Continued

Exp α''_m [a,b] cm^{-1}	Gas[c]	Fitted cm^{-1}	Γ_j cm^{-1}	C_j km / mol	$\lvert\overrightarrow{R_j}\rvert$ Debye	Assignment[d]
3083.1 m	B	3084.0	12.5	0.0319	0.0181	ν_{21}
3069.5 s	A	3069.5	12.4	0.0482	0.0222	ν_1 , ν_2 ??
3058.5 m br	A??	3057.9	9.0	0.0163	0.0130	ν_3 (3059), ν_{22} (3060??)
		3056.3	40.9	0.0703	0.0269	
3025.8 w		3025.8	10.6	0.00962	0.0100	ν_4+ν_{24} (3029) or ν_{23}+ν_{24} (3029)
3016.3 w		3015.7	9.1	0.00633	0.00813	
~3004 w sh		3003.7	19.5	0.0112	0.0108	3ν_9 (3006)
2949.8 vw		2949.9	12.9	0.000802	0.00293	2ν_5 (2956)
2919.0 vw	B	2918.8	7.9	0.00121	0.00361	ν_5+ν_{24} (2923)
~2906 vw sh						ν_4+ν_{25} (2909) or ν_{23}+ν_{25} (2909)
2885.6 vw db?	A	2882.8	20.1	0.00162	0.00421	2ν_{24} (2891)
2877.0 vw db?		2874.9	9.0	0.000433	0.00218	
2849.2 vw		2847.7	18.6	0.00166	0.00429	ν_4+ν_{26} (2856) or ν_{23}+ν_{26} (2856)
~2831 vw sh						
2795.2 vw br		2795.6	12.7	0.000275	0.00176	ν_5+ν_{25} (2803) ??
2772.9 vw		2772.7	9.9	0.00127	0.00380	ν_{24}+ν_{25} (2771)
2755.9 vw		2755.9	14.0	0.000348	0.00199	ν_4+ν_6 (2756) or ν_{23}+ν_6 (2756)
2738.9 vw br		2738.8	21.1	0.000607	0.00264	ν_4+ν_{27} (2740) or ν_{23}+ν_{27} (2740)
2714.2 vw		2714.7	9.0	0.000099	0.00107	ν_{24}+ν_{26} (2718)
2703.1 vw br		2701.9	16.7	0.000340	0.00630	3ν_{16} (2709)
2663.5 vw		2664.7	10.1	0.00146	0.00415	ν_4+ν_7 (2668) or ν_{23}+ν_7 (2668)
		2659.4	12.6	0.00108	0.00305	
2648.1 vw		2647.7	10.5	0.000838	0.00316	ν_5+ν_6 (2649) or 2ν_{25} (2650)
~2632 vw sh		2625.8	57.8	0.00185	0.00471	ν_5+ν_{27} (2634)
2616.2 vw		2616.4	7.9	0.00111	0.00366	ν_{24}+ν_6 (2517)
2599.8 vw br		2602.3	7.7	0.000576	0.00264	ν_{24}+ν_{27} (2602)
		2597.5	11.1	0.00119	0.00380	ν_{25}+ν_{26} (2598)
		2590.1	21.0	0.000542	0.00257	
2582.2 vw		2581.9	7.1	0.000648	0.00281	ν_{23}+ν_9 (2586) or ν_4+ν_9 (2586)
~2563 vw sh		2564.9	9.7	0.000461	0.00238	
2557.4 vw		2557.3	14.1	0.00122	0.00388	

Table 5.1 - Continued

Exp α''_m [a,b] cm^{-1}	Gas[c]	Fitted cm^{-1}	Γ_j cm^{-1}	C_j km / mol	$\lvert\overrightarrow{R_j}\rvert$ Debye	Assignment[d]
2544.3 vw asym		2544.1	11.4	0.00116	0.00379	
		2535.7	16.7	0.000604	0.00274	
2510.9 vw		2511.0	4.1	0.000064	0.00090	$\nu_{24}+\nu_{28}$ (2514)
2496.0 vw		2495.5	16.2	0.000709	0.00299	$\nu_{25}+\nu_{6}$ (2497) or $\nu_{5}+\nu_{8}$ (2501)
2477.5 vw br		2477.6	14.5	0.000656	0.00289	$\nu_{5}+\nu_{9}$ (2480) or $\nu_{25}+\nu_{27}$ (2482)
2471.3 vw		2469.7	10.7	0.000494	0.00251	$\nu_{24}+\nu_{8}$ (2468)
~2453 vw sh		2453.9	10.5	0.000215	0.00166	
2446.6 vw		2446.6	8.5	0.000246	0.00178	$\nu_{24}+\nu_{9}$ (2447) or $\nu_{26}+\nu_{6}$ (2444)
2427.3 vw br		2428.0	18.2	0.00110	0.00378	$\nu_{26}+\nu_{27}$ (2429)
2406.4 vw		2406.3	14.3	0.00162	0.00461	
2390.3 vw asym		2390.3	9.9	0.00133	0.00419	$\nu_{25}+\nu_{28}$ (2393)
		2382.9	14.2	0.000877	0.00340	$\nu_{5}+\nu_{16}$ (2381)
2365.6 vw		2365.7	9.7	0.000385	0.00226	
~2346 vw sh		2347.7	12.7	0.000475	0.00252	$\nu_{25}+\nu_{8}$ (2348) or $\nu_{24}+\nu_{16}$ (2349)
2331.0 vw		2331.8	15.6	0.00428	0.00760	
2319.8 vw		2319.1	12.1	0.00273	0.00609	
		2311.3	12.1	0.000724	0.00314	
~2282 vw sh		2283.1	6.0	0.000182	0.00158	
2271.8 vw		2271.8	15.1	0.00159	0.00470	
~2255 vw sh		2255.6	13.3	0.000488	0.00261	$\nu_{6}+\nu_{7}$ (2255) or $\nu_{26}+\nu_{15}$ (2256)
2240.5 vw	B?	2240.3	11.5	0.00244	0.00586	$\nu_{6}+\nu_{28}$ (2240) or $\nu_{27}+\nu_{7}$ (2240)
~2223 vw sh		2221.9	10.6	0.000251	0.00189	$3\nu_{17}$ (2224) or $\nu_{27}+\nu_{28}$ (2225)
2194.0 vw		2194.3	8.1	0.000423	0.00246	$\nu_{6}+\nu_{8}$ (2194)
2178.7 vw		2179.0	6.8	0.000712	0.00321	
		2176.1	7.8	0.000240	0.00186	
~2167 vw sh		2167.5	12.3	0.000151	0.00148	$2\nu_{7}$ (2167)
2159.7 vw		2159.3	9.3	0.000236	0.00186	$\nu_{27}+\nu_{9}$ (2158)
2150.5 vw		2150.1	9.6	0.000334	0.00221	
2132.5 vw		2131.3	9.9	0.000128	0.00138	$2\nu_{28}$ (2136) ?
~2123 vw sh						$\nu_{27}+\nu_{12}$ (2120)
~2100 vw sh		2098.7	3.9	0.000013	0.00044	$\nu_{16}+\nu_{13}$ (2103)

Table 5.1 - Continued

Exp α_m'' [a,b] cm^{-1}	Gas[c]	Fitted cm^{-1}	Γ_j cm^{-1}	C_j km / mol	$\lvert\overrightarrow{R_j}\rvert$ Debye	Assignment[d]
2089.1 vw		2088.6	9.4	0.000306	0.00215	$\nu_5+\nu_{29}$ (2092) or $\nu_{28}+\nu_8$ (2091) or $\nu_7+\nu_9$ (2086)
~2067 vw sh		2067.4	7.1	0.000044	0.00082	$\nu_{28}+\nu_9$ (2070) or $\nu_7+\nu_{15}$ (2067) or $\nu_{25}+\nu_{17}$ (2066)
2058.2 vw		2058.0	7.9	0.000152	0.00153	$\nu_{27}+\nu_{16}$ (2059) or $\nu_{24}+\nu_{29}$ (2060)
2045.5 vw db?		2047.8	7.8	0.000206	0.00178	
2023.7 vw		2023.7	3.1	0.000159	0.00157	$\nu_8+\nu_9$ (2025) or $\nu_{25}+\nu_{10}$ (2028)
2002.5 vw br		2003.3	6.1	0.000218	0.00185	$2\nu_9$ (2004) or $\nu_8+\nu_{15}$ (2006) or ? $\nu_6+\nu_{13}$ (2002)
~1989 vw sh		1989.2	5.3	0.000314	0.00223	
1983.0 vw		1984.8	3.6	0.000151	0.00155	$\nu_9+\nu_{15}$ (1985) or $\nu_{23}+\nu_{14}$ (1984) or ? $\nu_4+\nu_{14}$ (1984)
1962.2 w br	A	1963.9	16.7	0.00921	0.0122	$2\nu_{15}$ (1966)
1942.9 m	B	1942.5	17.4	0.0247	0.0200	$\nu_{15}+\nu_{12}$ (1947)
1881.4 w br	A	1885.4	11.5	0.00496	0.00910	$\nu_{23}+\nu_{30}$ (1881) or $\nu_{26}+\nu_{29}$ (1887) or $\nu_{15}+\nu_{16}$ (1886)
		1878.6	13.4	0.00508	0.00923	
1861.9 m	B	1865.3	12.4	0.0113	0.0138	$\nu_{24}+\nu_{11}$ (1861) or $\nu_{27}+\nu_{10}$ (1859)
		1859.0	10.6	0.00953	0.0127	
~1825 vw sh		1816.0	12.8	0.00141	0.00495	$\nu_7+\nu_{17}$ (1825) or $\nu_{15}+\nu_{13}$ (1813)
~1806 w sh		1806.4	15.5	0.00265	0.00680	$2\nu_{16}$ (1806) or ? $\nu_{28}+\nu_{17}$ (1809)
1787.8 m br	A	1789.4	17.1	0.0152	0.0164	$\nu_7+\nu_{10}$ (1786)
		1780.3	18.4	0.00841	0.0122	
1730.5 m br	B	1736.7	9.6	0.00288	0.00723	$\nu_{16}+\nu_{13}$ (1733)
		1731.1	9.8	0.00632	0.0107	
		1725.1	13.7	0.00699	0.0113	
~1703 vw sh		1703.3	14.7	0.00168	0.00557	$\nu_9+\nu_{10}$ (1704) or $\nu_{12}+\nu_{17}$ (1705)
1685.9 vw		1686.0	4.2	0.000270	0.00225	
		1682.1	2.0	0.000029	0.00074	
1645.5 w		1644.6	15.6	0.00891	0.0131	$\nu_{16}+\nu_{17}$ (1644) or $\nu_{12}+\nu_{18}$ (1649)
1636.9 w br						$\nu_8+\nu_{29}$ (1637)
1622.1 w br		1622.3	6.1	0.00301	0.00764	$\nu_{25}+\nu_{30}$ (1623) or $\nu_{27}+\nu_{19}$ (1625)

Table 5.1 - Continued

Exp α''_m [a,b] cm^{-1}	Gas[c]	Fitted cm^{-1}	Γ_j cm^{-1}	C_j km / mol	$\lvert \vec{R_j} \rvert$ Debye	Assignment[d]
~1591 s sh	A??	1592.0	4.0	0.00750	0.0122	$\nu_{16}+\nu_{18}$ (1588) or ν_4 ??
1583.9 vs	B??	1583.5	7.4	0.179	0.0597	ν_{23} and ν_4 ??
1566.1 s br sh		1566.1	11.7	0.0386	0.0279	$\nu_{26}+\nu_{30}$ (1570)
~1496 s sh		1494.4	13.8	0.0249	0.0229	$\nu_7+\nu_{11}$ (1499) or $\nu_8+\nu_{19}$ (1491)
1477.8 vs	A	1477.6	4.9	0.354	0.0869	ν_5
1445.5 vs	B	1446.0	11.6	0.0594	0.0360	ν_{24}
		1445.4	3.0	0.0677	0.0384	
1387.1 w		1386.7	9.6	0.00588	0.0116	$\nu_{10}+\nu_{18}$ (1387)
1370.7 w	A	1370.6	10.9	0.00696	0.0126	$\nu_{16}+\nu_{19}$ (1371) or $2\nu_{18}$ (1370)
1325.2 w	B?	1325.3	5.7	0.00270	0.00801	ν_{25}
		1319.1	9.9	0.00159	0.00616	$\nu_8+\nu_{30}$ (1320) or $\nu_{16}+\nu_{11}$ (1318)
1298.1 m	B	1298.2	8.0	0.00634	0.0124	$\nu_9+\nu_{30}$ (1299) or $\nu_{16}+\nu_{14}$ (1303) or $\nu_{13}+\nu_{19}$ (1298)
1272.5 m	B?	1273.0	5.0	0.00194	0.00693	ν_{26}
		1269.3	12.9	0.00698	0.0132	
1235.2 w	A	1237.7	10.0	0.00329	0.00915	$\nu_{13}+\nu_{14}$ (1230) ?
		1232.7	9.3	0.00272	0.00834	
1210.9 w	A	1210.6	13.5	0.00491	0.0113	$\nu_{17}+\nu_{19}$ (1209)
1171.6 m	A	1172.4	18.7	0.0167	0.0212	ν_6
		1171.1	1.5	0.000040	0.00104	$\nu_{10}+\nu_{19}$ (1171)
1156.4 m		1155.9	11.3	0.00632	0.0131	ν_{27}
1122.7 s	A?	1123.2	7.5	0.0336	0.0307	$\nu_{10}+\nu_{11}$ (1118)
~1116 s sh		1116.6	9.9	0.0244	0.0262	$\nu_4-\nu_{19}$ (1116)
~1093 s sh		1094.1	13.5	0.0282	0.0285	$\nu_{16}+\nu_{20}$ (1099)
1083.6 vs	A	1083.9	7.9	0.256	0.0863	ν_7
		1080.8	6.6	0.0417	0.0349	
1068.1 s	B	1068.0	3.7	0.0279	0.0287	ν_{28}
		1064.2	4.5	0.00796	0.0153	
1022.8 vs	A	1023.1	2.4	0.0382	0.0343	ν_8
		1022.3	3.3	0.0749	0.0480	
		1020.0	3.2	0.00360	0.0105	

Table 5.1 - Continued

Exp α''_m [a,b] cm^{-1}	Gas[c]	Fitted cm^{-1}	Γ_j cm^{-1}	C_j km / mol	$\lvert \vec{R_j} \rvert$ Debye	Assignment[d]
1012.6 s		1012.3	4.4	0.00486	0.0123	$\nu_{29}+\nu_{14}$ (1014)
1001.9 s	A?	1001.9	2.6	0.0206	0.0254	ν_{9}
990.5 m		990.6	11.4	0.00428	0.0117	$\nu_{10}+\nu_{30}$ (1000)
983.2 m br		980.7	13.4	0.00498	0.0126	ν_{15}
963.7 m br		963.0	18.7	0.00852	0.0167	ν_{12}
935.0 m	A	935.0	10.6	0.0125	0.0205	$\nu_{17}+\nu_{20}$ (937) or $2\nu_{19}$ (936)
~919 m sh		919.4	5.6	0.000896	0.00554	$\nu_{29}+\nu_{30}$ (912)
903.0 s asym	C	903.5	6.9	0.0293	0.0320	ν_{16}
		900.1	8.5	0.0153	0.0231	
~880 w sh ?		878.5	7.5	0.000495	0.00421	$\nu_{18}+\nu_{20}$ (881)
866.3 w		865.4	9.9	0.00270	0.00991	$\nu_{19}+\nu_{14}$ (868)
830.0 m		830.2	12.8	0.00968	0.0192	ν_{13}
812.2 m	??	813.0	6.7	0.00132	0.00715	$\nu_{11}+\nu_{14}$ (815) or $\nu_{29}+\nu_{20}$ (810)
741.2 vs	C	743.9	5.6	0.259	0.105	ν_{17}
		741.2	4.9	0.329	0.118	
		738.6	5.6	0.221	0.0971	
702.5 vs	A	702.9	4.0	0.122	0.0739	ν_{10}
		701.0	4.7	0.0647	0.0539	
685.2 vs	C	685.1	4.8	0.217	0.100	ν_{18}
662.1 s	??	661.9	6.3	0.00847	0.0201	$\nu_{19}+\nu_{20}$ (664)
614.1 m	B	614.0	3.7	0.00280	0.0120	ν_{29}
547.7 w		549.2	2.8	0.000103	0.00243	$\nu_{17}-\nu_{20}$ (545)
		544.9	2.8	0.000095	0.00234	
533.4 w		533.8	2.5	0.000222	0.00362	$\nu_{13}-\nu_{30}$ (533)
468.1 vs	C	468.0	3.9	0.0983	0.0813	ν_{19}
~434 m br sh		433.9	3.3	0.000549	0.00631	$\nu_{16}-\nu_{19}$ (435)
415.0 s	A	415.1	5.5	0.0185	0.0375	ν_{11}
~400 m sh		408.8	7.3	0.00621	0.0219	ν_{14}

a - Wavenumbers of peaks in the imaginary molar polarizability spectrum of liquid chlorobenzene.

b - Abbreviations used: v-very, w-weak, m-medium, s-strong, br-broad, sh-shoulder and db-doublet.

c - Band contours in the infrared spectrum of the gas.

d - Calculated wavenumbers are given in brackets.

In the last column of Table 5.1, an assignment is given. The assignments of the fundamentals were discussed in Chapter 4. The remaining peaks were assigned as overtone or combination transitions based on the band shape of the gas spectrum when observed, and on the agreement of the observed wavenumber with sums or differences of fundamental wavenumbers.

The accuracy of the C_j values is estimated from the sum of the accuracy of the fit and the accuracy of the real and imaginary refractive indices, n and k, that are used in the calculation of α''_{m}. The accuracy for the refractive indices was reported in Chapter 3 and is 0.2% for n and on the order of 2 to 3% for k. The accuracy of the fit is estimated from the accuracies of peak heights and areas under the α''_{m} spectrum, and is about 0.6 to 3% depending on the intensity of the band. Therefore, we estimate that the C_j values are accurate to better than 3-5% for strong peaks and to better than 5-10% for weak peaks.

5.1.1 - Integrated intensities and dipole moment derivatives of the fundamental vibrations of liquid chlorobenzene.

The integrated intensities, C_j, and the absolute values of the dipole moment derivatives with respect to normal coordinates, $|\mu_j|$, of the fundamental vibrations of liquid chlorobenzene are given in Table 5.2. The $|\mu_j|$ were calculated from the C_j using Eq. 1.4.4. As discussed earlier, the accuracy of C_j for strong fundamentals is estimated to be 3-5% and 5-10% for weak bands. Thus, in general, the percent accuracy of $|\mu_j|$ for

Table 5.2 - Dipole moment derivatives of liquid chlorobenzene

				$A_{j,gas}$ [b]	
ν_j	Fitted cm^{-1} [a]	$C_{j,liq}$ [b]	$\lvert\mu_j\rvert$ [c]	This work[d]	Pulay [Ref. 47][e]
ν_1	3069.5 [f]	0.0482 [f]	0.300 [f]	3.81 [f]	2.51
ν_2	3069.5 [f]	--- [f]	--- [f]	--- [f]	15.89
ν_3	3057.9	0.0163	0.175	1.29	0.00
ν_4	1592.0 [g]	0.0075 [g]	0.118 [g]	0.59 [g]	2.12
ν_5	1477.6	0.354	0.813	27.95	44.83
ν_6	1172.4	0.0167	0.177	1.32	0.05
ν_7 [h]	1083.9	0.298	0.971	23.50	40.23
ν_8 [h]	1022.3	0.117	0.723	9.21	10.98
ν_9	1001.9	0.0206	0.196	1.63	2.06
ν_{10} [h]	702.9	0.187	0.825	14.74	22.76
ν_{11}	415.1	0.0185	0.186	1.46	3.46
ν_{12}	963.0	0.00852	0.126	0.67 [i]	--- [i]
ν_{13}	830.2	0.00968	0.134	0.76 [i]	--- [i]
ν_{14}	408.8	0.00621	0.108	0.49 [i]	--- [i]
ν_{15}	980.7	0.00498	0.096	0.39	0.08
ν_{16} [h]	903.5	0.0446	0.403	3.52	3.94
ν_{17} [h]	741.2	0.809	2.123	63.88	46.75
ν_{18}	685.1	0.217	0.637	17.13	42.45
ν_{19}	468.0	0.0983	0.429	7.76	8.99
ν_{20}	(196.0)				0.09
ν_{21}	3084.0	0.0319	0.244	2.52	8.80
ν_{22}	(3060.0 ??) [j]				8.77
ν_{23}	1583.5 [g]	0.179 [g]	0.578 [g]	14.13 [g]	19.07
ν_{24} [h]	1445.4	0.127	0.689	10.04	10.79
ν_{25}	1325.3	0.00270	0.071	0.21	0.58
ν_{26} [h]	1269.3	0.00892	0.174	0.70	0.34
ν_{27}	1155.9	0.00632	0.109	0.50	0.00
ν_{28} [h]	1068.0	0.0359	0.350	2.83	2.03
ν_{29}	614.0	0.0028	0.072	0.22	0.17
ν_{30}	(297.5)				0.18

a - Integrated intensities were not obtained for ν_{20} and ν_{30} which are below the experimental wavenumber range of this work.

b - Units are km mole^{-1}.

c - Units are Debye Å^{-1} $\text{amu}^{-1/2}$.

d - Integrated intensities for the gas, $A_{j,gas}$ were calculated as $A_{j,gas} = 8\pi^2 C_{j,liq}$ with the assumption that $\mu_{j,liq}{}^2 = \mu_{j,gas}{}^2$.

e - $A_{j,ab\ in}$ values obtained from *ab initio* calculations reported in Ref. 47.

f - The same wavenumber was assigned to ν_1 and ν_2. All quantities are assigned to ν_1 in the table.

g - 1584 cm^{-1} was assigned to both ν_4 and ν_{23} although the evidence for ν_4 is less conclusive. The intensity of the fitted band at 1583.5 cm^{-1} was assigned in the table to ν_{23}. The reported values for ν_4 are those of the much weaker band at 1592 cm^{-1} which may possibly be ν_4.

h - Several CDHO bands were used to fit the observed band. The wavenumber reported is that of the prominent contributing band. All related quantities for this vibration are the sums from all contributing bands as shown in Table 5.1.

i - A_2 vibrations in chlorobenzene are infrared inactive in the spectrum of the gas, i.e $A_{j,gas}$=0 and were not calculated in Ref. 47. Our values are derived from $C_{j,liq}$ as described in footnote d.

j - The wavenumber was assigned based on Raman spectra.

strong fundamentals is about 1.5-2.5% and about 2.5-5% for weak fundamentals.

The only integrated intensities for chlorobenzene in the literature are those reported by Pulay *et al.*[47]. In their study the authors used scaled ab initio calculations to obtain wavenumbers and infrared integrated intensities of the fundamental vibrations of chlorobenzene. In order to compare our results with Pulay's, our integrated intensities of the liquid are converted to the integrated intensities the corresponding band would have in the gas phase if the dipole moment derivative were the same in the liquid and gas phases.

Equations 1.4.4 and 1.4.5 relate the square of the dipole moment derivative to the integrated intensities C_j and A_j. For a gas $\underline{n}$ is 1 and Equation 1.4.5 simplifies to

$$A_{j,\text{gas}} = \frac{N_A \pi}{3c^2} g_j \, \mu_j^2 \tag{5.1.2}$$

This equation and Equation 1.4.4 give

$$\frac{A_{j\,gas}}{C_{j\,liq}} = 8\pi^2 \left(\frac{\mu_{j\,gas}}{\mu_{j\,liq}}\right)^2 \tag{5.1.3}$$

Thus, if the dipole moment derivative is the same in the gas and liquid phases, $A_{j,gas}$ can be calculated from our measured C_j values by

$$A_{j,gas} = 8\pi^2 \, C_j = 78.96 \, C_j \tag{5.1.4}$$

The resulting $A_{j,gas}$ are included in Table 5.2 under the heading "$A_{j,gas}$ this work". The integrated intensities, $A_{j,ab\ in}$, obtained from *ab initio* calculation by Pulay *et al.*[47] are given in column 6 of Table 5.2 under the heading "$A_{j,gas}$ Pulay".

In the following subsections, figures of the curve fitted and experimental α_m'' spectra and the CDHO bands required in the fit, are given for regions of small wavenumber range. The intensities of fundamentals in these regions will be discussed and compared with Pulay's *ab initio* intensities.

5.1.1a - Intensities of the CH stretching vibrations

The experimental and curve fitted α_m'' spectra of liquid chlorobenzene for the region of the CH stretching vibrations are shown in Figure 5.2. There are seven bands required to fit this region, centred at 3084, 3069.5, 3057.9, 3056.3, 3025.8, 3015.7 and 3003.7 cm^{-1}. The fit in this region is very good. The area under the $\tilde{\nu}\alpha_m''$ spectrum of

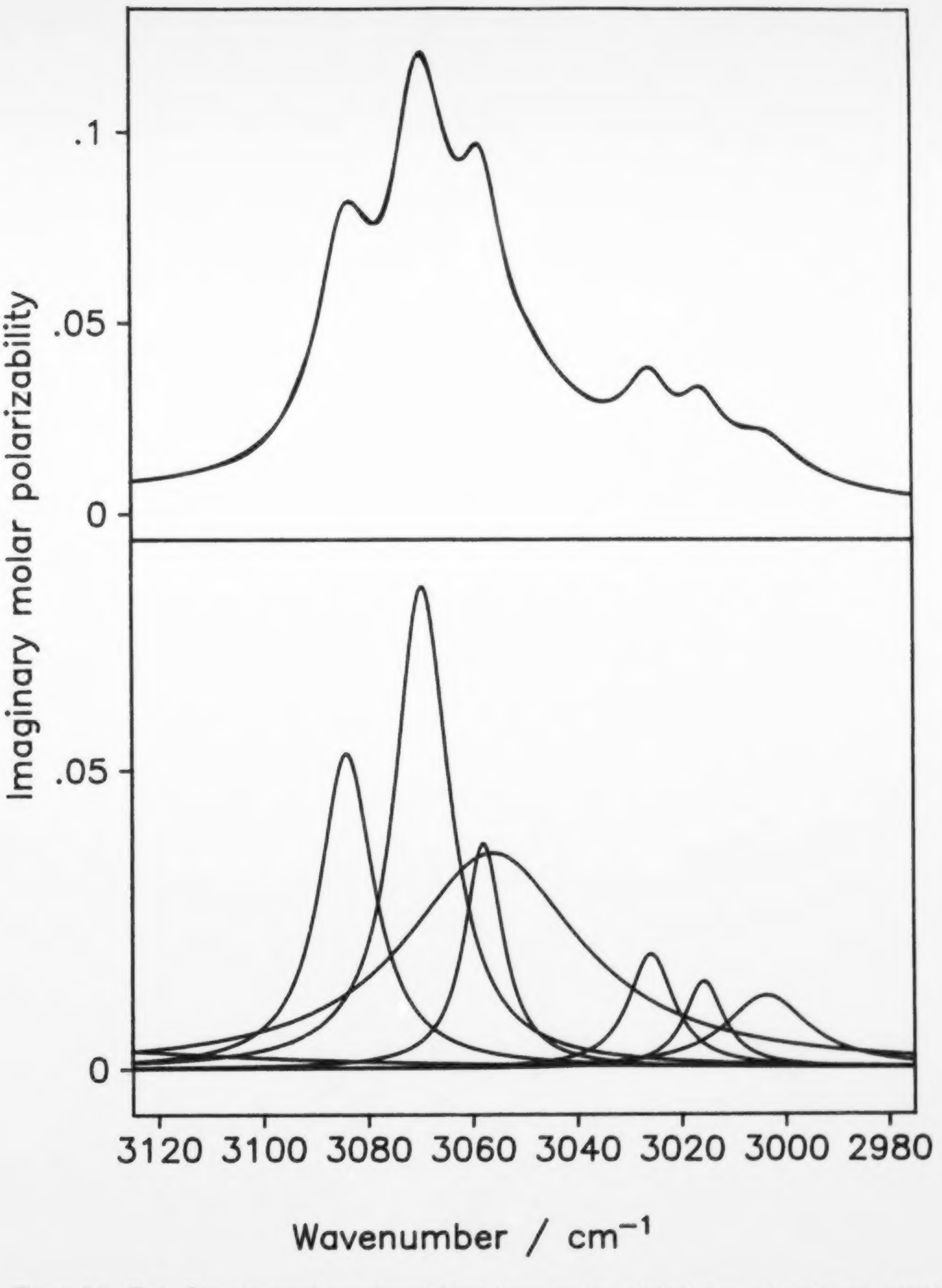

Figure 5.2 - Top - Superimposed experimental imaginary molar polarizability, α''_m, and curve fitted α''_m spectra of liquid chlorobenzene between 3125 and 2975 cm^{-1}. Bottom - The prominent CDHO bands in this region that were used to fit the experimental α''_m spectrum. Contribution from the 3140 cm^{-1} band can be seen as a tail inside the shown region from 3125 to ~3060 cm^{-1}. Units for both boxes are cm^3 mole^{-1}.

the fitted bands is 0.1% greater than the area under the $\tilde{\nu}\alpha''_m$ experimental spectrum. The peak heights are fitted on average to 0.3% and to within 0.7%.

In Chapter 4, three of the five CH stretching fundamentals were assigned to bands in the infrared spectrum, ν_1, ν_3 and ν_{21}, and ν_2 and ν_{22} were assigned to features in the Raman spectrum. It is not clear whether ν_2 and ν_{22} contribute to the infrared spectrum, although they well may do so. It is also not clear whether all of the intensity in the CH stretching region should be assigned to the active fundamentals, or just the intensity in the band required to fit the prominent features that were assigned to the fundamentals. It is probable that all of the intensity in the region should be so assigned, on the grounds that some of the fundamental intensity is lent to the many overtone and combination transitions that contribute to the extensive absorption in this region, through Fermi resonance between the fundamental state and the various overtone and combination states. The intensity of the weak overtone and combination bands near the CH stretching fundamentals is noticeably greater than the intensity of the weak features further removed, such as those between 2900 and 2000 cm^{-1}.

Accordingly, the intensity is assigned in two ways. First, the intensities of the fitted bands at 3084, 3069.5 and 3058 cm^{-1} are assigned to ν_{21}, ν_1, and ν_3, respectively, and no infrared intensity is assigned to ν_2 and ν_{22}. The total intensity assigned to the fundamentals in this way is, from Table 5.1, $\Sigma C_{CH} = 0.0964$ km mole^{-1}. The intensity left to be assigned to overtone and combination bands in this region is 0.0974 km mol^{-1}, greater than that assigned to the fundamentals.

As a consequence, an alternative assignment of the intensity is considered, namely that the total intensity of the bands between 3125 and 2975 cm^{-1}, $\Sigma C_j = 0.194$ km mole^{-1} is assigned to the CH stretching fundamentals as a group. With this assignment it is recognized that the harmonic and anharmonic interactions are sufficiently complex that assignment of the intensity to individual normal vibrations is not possible, and possibly not even meaningful.

The equivalent intensity $A_{j\,gas}$ of the fundamentals in these two assignments is 7.61 km mol^{-1} and 15.32 km mol^{-1}, respectively. The sum of the intensity of the fundamentals calculated by Pulay[47] is 35.97 km mol^{-1}. Unfortunately, Pulay did not calculate the intrinsic intensity of overtone and combination bands. Clearly, Pulay's calculated intensities are 4.7 or 2.4 times those found for the liquid, depending on the assignment used. For benzene[73] the ratio between the actual intensities of the gas and those of the liquid, both expressed as $A_{j\,gas}$, is 1.72. Thus, part of the difference between Pulay's calculations and our results may be a significant difference between the intensities of the CH stretching bands of chlorobenzene in the gas and liquid phases.

5.1.1b - Intensities of the ν_4, ν_5, ν_{23} and ν_{24} vibrations

The experimental α_m'' and curve fitted α_m'' spectra of liquid chlorobenzene between 1650 and 1400 cm^{-1} are shown in Figure 5.3. The fit in this region is good. The area

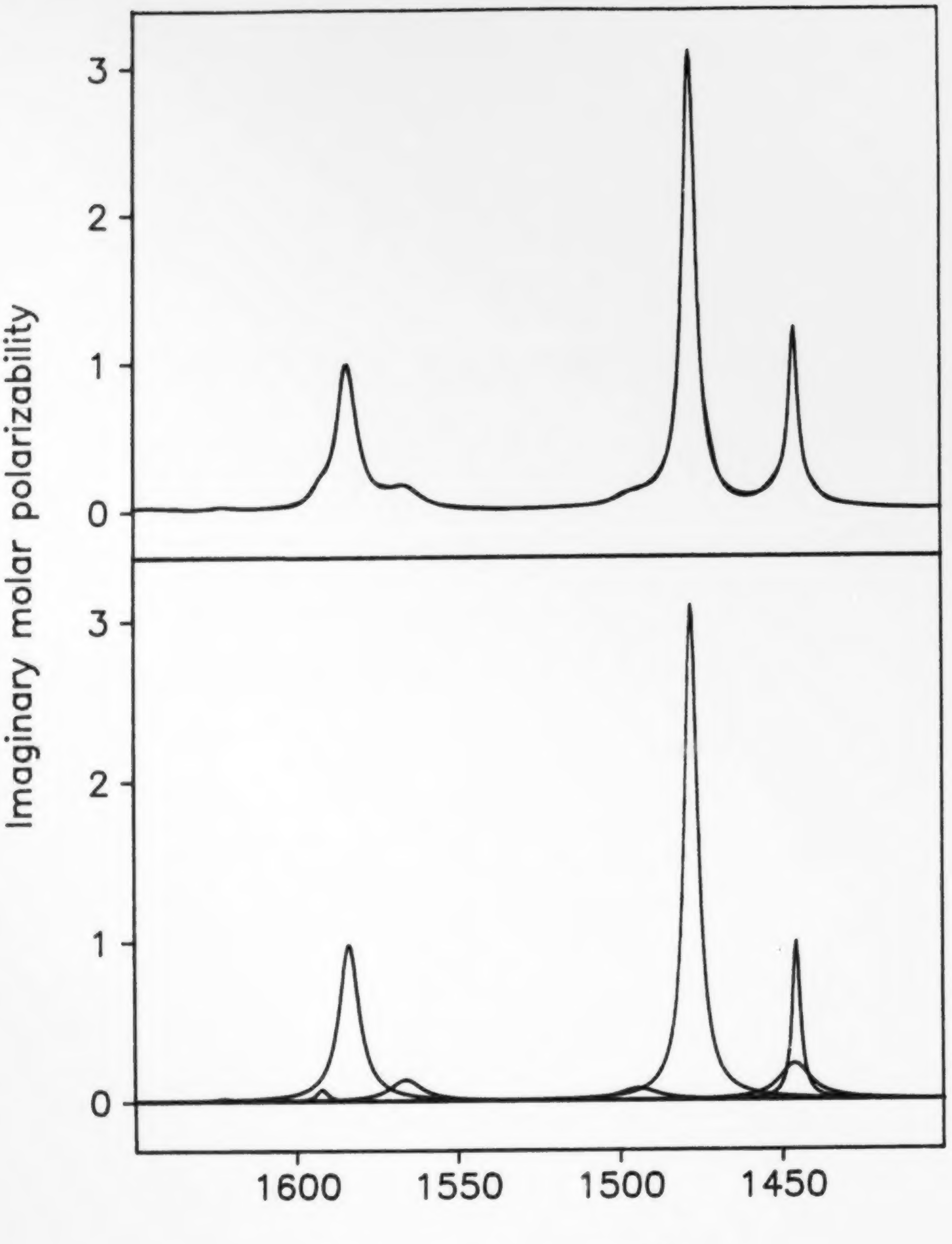

Figure 5.3 - Top - Superimposed experimental imaginary molar polarizability, α''_m, and curve fitted α''_m spectra of liquid chlorobenzene between 1650 and 1400 cm^{-1}. Bottom - The prominent CDHO bands in this region that were used to fit the experimental α''_m spectrum. Units for both boxes are cm^3 mole^{-1}.

under the curve fitted α''_m spectrum is greater by 0.75% than the area under the experimental α''_m spectrum. The peak heights of the fundamentals are reproduced to better than 0.32%. Those of the weak band at 1622 cm^{-1} and the shoulders at 1566 and 1496 cm^{-1} are reproduced to 5-6%. All of these three bands are due to combination transitions.

In Chapter 4, ν_{23} and ν_4 were assigned at the same wavenumber, 1584 cm^{-1}. The assignment of ν_{23} was supported by the various experimental data. On the other hand, the assignment of ν_4 was less conclusive and relied on a possible Q branch at 1589 cm^{-1} in the spectrum of the gas phase. Therefore, we assign the intensity of the strong CDHO band at 1583.5 cm^{-1} to ν_{23}. A weak CDHO band centered at 1592 cm^{-1} was needed to fit the 1591 cm^{-1} shoulder. We tentatively assign its intensity to ν_4.

The intensity of the CDHO band at 1477.6 cm^{-1} is assigned to ν_5 while those of the two CDHO bands at 1446.0 and 1445.4 cm^{-1} which were required to fit the 1445.5 cm^{-1} peak are assigned to ν_{24}.

The *ab initio* calculated $A_{j,ab\ in}$ of Pulay et al[47] is greater by 7% for ν_{24}, 60% for ν_5 and 35% for ν_{23}. They are 3.6 times larger for ν_4. However, if the intensities of ν_4 and ν_{23} are combined, since the assignment of ν_4 is not as clear as that of the others, Pulay's value is only 45% greater than $A_{j,gas}$.

5.1.1c - Intensities of the ν_6, ν_{25}, ν_{26} and ν_{27} vibrations

The experimental α_m'' and curve fitted α_m'' spectra of liquid chlorobenzene between 1400 and 1140 cm^{-1} are shown in Figure 5.4. The absorption is weak and, as a consequence, the fit in this region is not good as in the previous regions. Large contributions from the strong bands at 1123 and 1084 cm^{-1} influenced the fitting in this region and the addition of more CDHO bands didn't improve the fit significantly. Thus, the fit presented involves the minimum number of bands needed to obtain a decent, but far from perfect, fit. The area under the curve fitted α_m'' is smaller by 0.44% than the area under the experimental α_m'' spectrum. The peak heights of the 9 peaks in the region are reproduced on average to 2.5%. The reproduction of only one fundamental, ν_{27} at 1156 cm^{-1}, exceeds this average with 4.25%.

The intensity of the CDHO band at 1325.3 cm^{-1} was assigned to ν_{25} while that of the close band at 1319.1 cm^{-1} that is needed to fit the distinct shoulder in the α_m'' spectrum is assigned as a combination transition. Similarly, the intensity of the CDHO band at 1172.4 cm^{-1} is assigned to ν_6 while that of the hardly visible (Fig. 5.2), much weaker band at 1171.1 cm^{-1} is assigned to a combination transition.

The intensities of the two CDHO bands at 1273.0 and 1269.3 cm^{-1} are assigned to ν_{26} while that of the band at 1155.9 cm^{-1} is assigned to ν_{27}.

For ν_{25}, Pulay's[47] reported $A_{j,ab\,in}$ equals 0.58 km mole^{-1}, greater by a factor of 2.8 than our value of 0.21 km mole^{-1}. Pulay's reported values for the other three fundamentals in this region are much smaller than the values obtained in this work. For

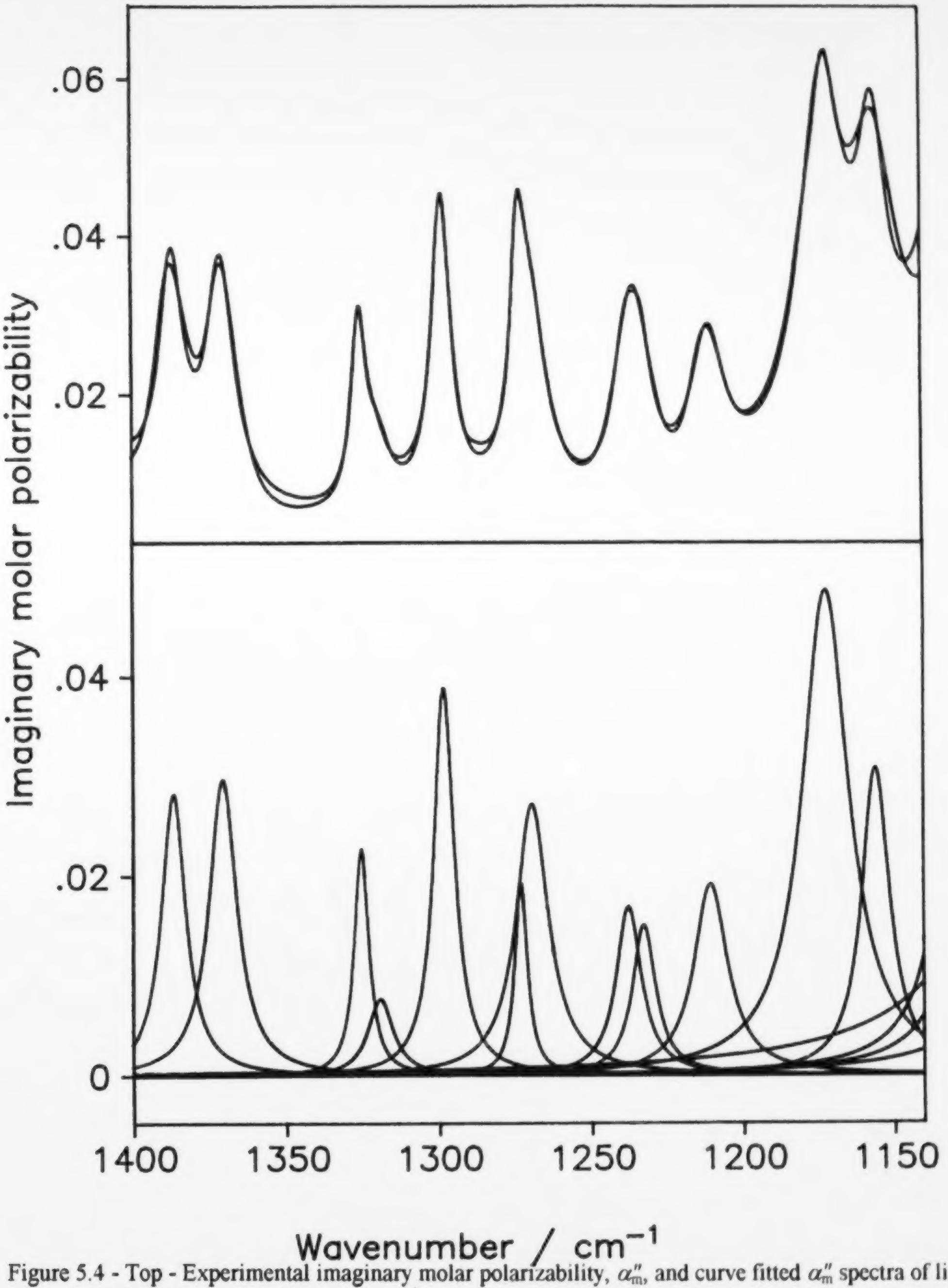

Figure 5.4 - Top - Experimental imaginary molar polarizability, α''_m, and curve fitted α''_m spectra of liquid chlorobenzene between 1400 and 1140 cm^{-1}. Bottom - The prominent CDHO bands in this region that were used to fit the experimental α''_m spectrum. Strong contributions from 4 bands at lower wavenumbers are clearly seen as tails from 1140 to about 1300 cm^{-1}. Units for both boxes are cm^3 mole^{-1}.

ν_{26}, Pulay's value is about half of ours, 0.34 versus 0.70 km mole^{-1}. For ν_6, Pulay's value is about 4% of our value, and for ν_{27} Pulay's reported value is zero while our value is 0.50 km mole^{-1}.

The fact that for ν_6, ν_{26} and ν_{27}, our A_j values for the gas are much greater than those reported by Pulay is perhaps an indication that for these three weak vibrations, the small dipole moment derivatives are influenced by the liquid forces and are greater in the liquid than in the gas.

5.1.1d - Intensities of the ν_7, ν_8, ν_9 and ν_{28} vibrations

The experimental α_m'' and curve fitted α_m'' spectra of liquid chlorobenzene between 1140 and 990 cm^{-1} are shown in Figure 5.5. The fit in this region is very good. 12 bands were needed to fit the nine features visible in the spectrum. Two of the three unsuspected bands were needed to fit the 1022.8 cm^{-1} peak and the third was needed to fit the 1084 cm^{-1}. The area under the curve fitted α_m'' is greater by 0.49% than the area under the experimental α_m'' spectrum. Peak heights in this region are reproduced on average to better than 1%.

Two CDHO bands at 1083.9 and at 1080.8 cm^{-1} were needed to obtain a good fit of the very strong band observed at 1083.6 cm^{-1} in the α_m'' spectrum of the liquid. Their combined intensities are assigned to ν_7. Similarly the intensities of the two CDHO bands at 1068.0 and at 1064.1 cm^{-1} are assigned to ν_{28} and those of the bands at 1023.1,

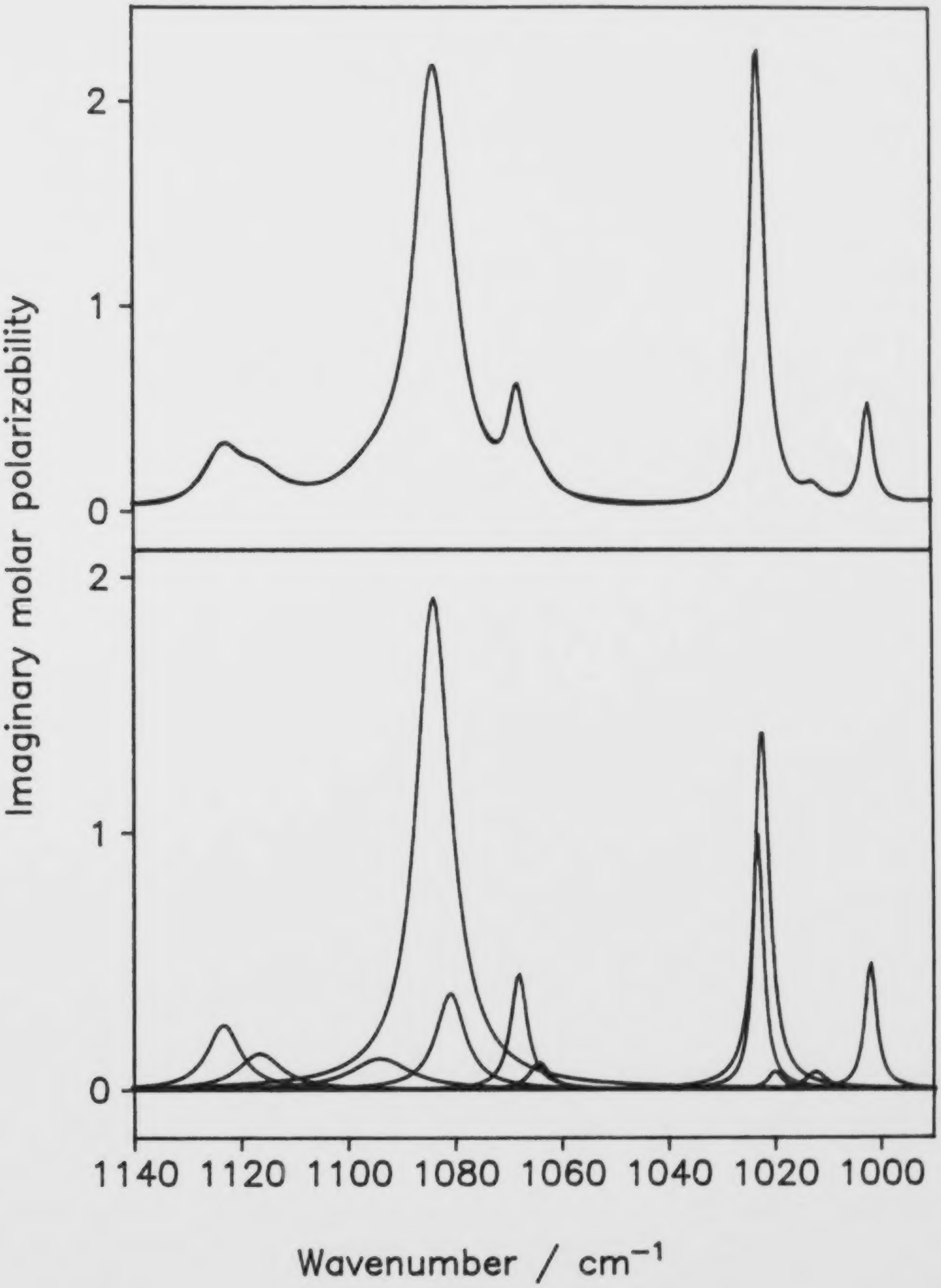

Figure 5.5 - Top - Superimposed experimental imaginary molar polarizability, α''_m, and curve fitted α''_m spectra of liquid chlorobenzene between 1140 and 990 cm^{-1}. Bottom - The prominent CDHO bands in this region that were used to fit the experimental α''_m spectrum. Units for both boxes are cm^3 mole^{-1}.

1022.3 and 1020.0 cm^{-1} are assigned to ν_8. The ν_9 band at 1001.9 cm^{-1} was fitted nearly perfectly by a single fitted band

Pulay's[47] reported $A_{j,ab\ in}$ values for ν_7, ν_8 and ν_9 are greater than the assigned $A_{j,gas}$ values by 71%, 19% and 26%, respectively (Table 5.2). Pulay's reported $A_{j,ab\ in}$ for ν_{28}, is smaller than the assigned value by about 18%.

5.1.1e - Intensities of the ν_{12}, ν_{13}, ν_{15} and ν_{16} vibrations

The experimental α''_m and curve fitted α''_m spectra of liquid chlorobenzene between 990 and 800 cm^{-1} are shown in Figure 5.6. The fit between 950 and 850 cm^{-1} is very good but in the remaining, weak, regions it is not good. At the low wavenumber end this is partly because the spectrum is influenced by strong bands outside the region, the tails of which can be clearly seen in Fig 5.6. The area under the curve fitted α''_m is smaller by 1.32% than the area under the experimental α''_m spectrum. Peak heights in this region are reproduced on average to 2.5%.

Two CDHO bands at 903.5 and at 900.1 cm^{-1} were needed to obtain a good fit of the strong asymmetric band observed at 903.0 cm^{-1} in the α''_m spectrum of the liquid. Their combined intensities were assigned to ν_{16}.

ν_{12} and ν_{13} are A_2 vibrations and as such are infrared inactive in the spectrum of the gas and their intensities were not calculated by Pulay[47]. The values reported by us in Table 5.2 for the $A_{j,gas}$ of the A_2 vibrations were calculated from the $C_{j,liq}$ following

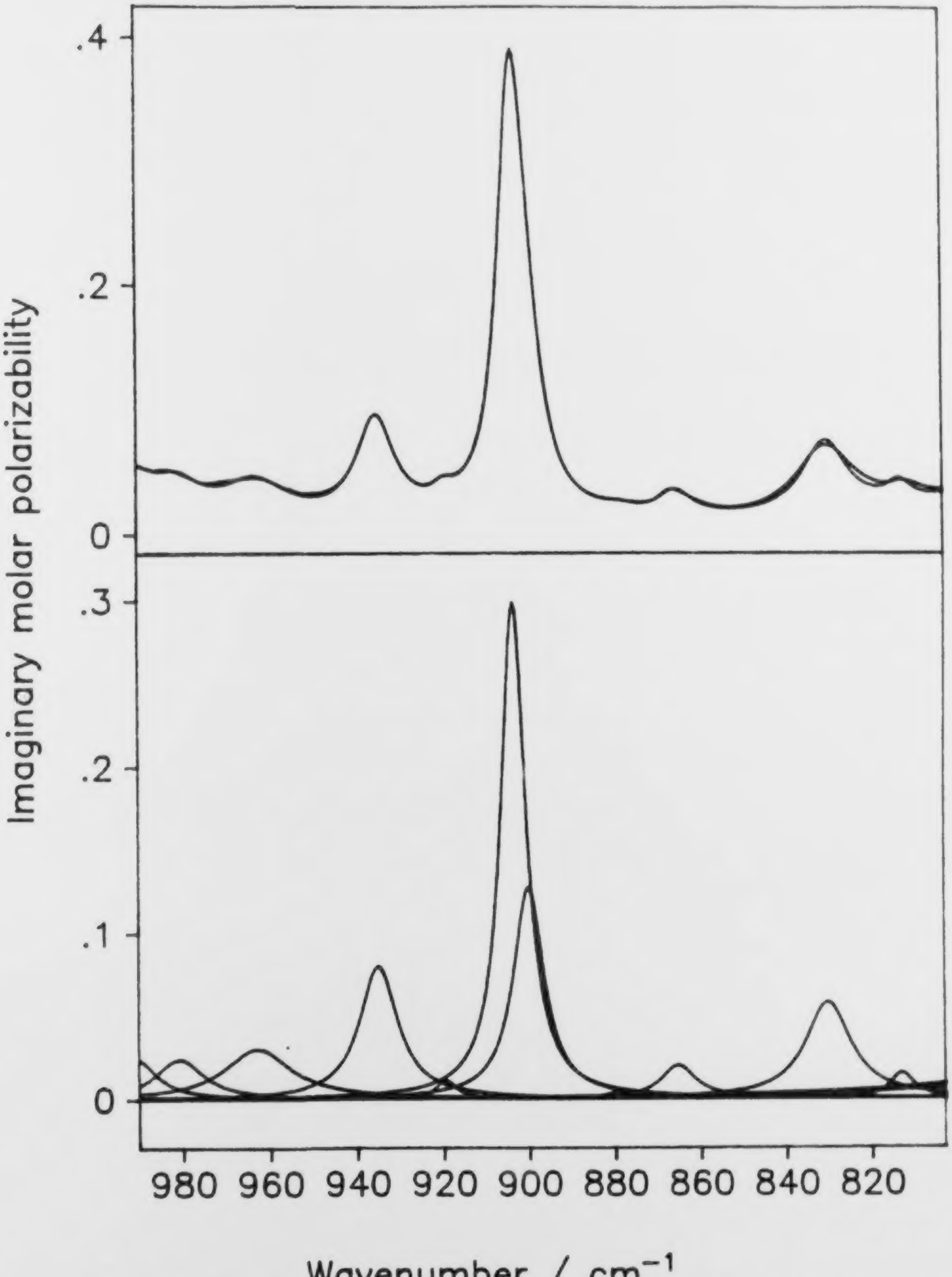

Figure 5.6 - Top - Superimposed experimental imaginary molar polarizability, α''_m, and curve fitted α''_m spectra of liquid chlorobenzene between 990 and 800 cm^{-1}. Bottom - The prominent CDHO bands in this region that were used to fit the experimental α''_m spectrum. Strong contributions from bands outside the shown region can be seen as tails on either sides of the region. Units for both boxes are cm^3 mole^{-1}.

the same procedure as for the other modes.

For the two B_1 vibrations in this region, ν_{15} and ν_{16}, Pulay's reported $A_{j,ab\ in}$ is smaller than our assigned value for ν_{15} by 79% (0.05 vs. 0.39 km mole^{-1}) and for ν_{16} is greater by 12% (3.94 vs. 3.52 km mole^{-1}). Pulay's calculated relative intensities support the assignment of these two modes, particularly that of ν_{15} to an extremely weak infrared feature.

5.1.1f - Intensities of the ν_{10}, ν_{17} and ν_{18} vibrations

The experimental α''_m and curve fitted α''_m spectra of liquid chlorobenzene between 800 and 650 cm^{-1} are shown in Figure 5.7. The area under the curve fitted α''_m is greater by 1.66% than the area under the experimental α''_m spectrum. The peak height of ν_{17} at 741 cm^{-1} is reproduced to 1.55% while those of ν_{10} and ν_{18} at 703 and 685 cm^{-1}, respectively, are reproduced to better than 0.15%.

Three CDHO bands at 743.9, 741.2 and 738.6 cm^{-1} were needed to obtain a good fit of the very strong band observed at 741.2 cm^{-1} in the α''_m spectrum of the liquid. Their combined intensities were assigned to ν_{17}. Pulay's[47] reported $A_{j,ab\ in}$ of 46.75 km mole^{-1} is lower by 27% the assigned intensity of 63.88 km mole^{-1}.

Two CDHO bands at 702.9 and 701.0 cm^{-1} were needed to obtain fit the ν_{10} band at 702.5 cm^{-1} and their combined intensities were assigned to ν_{10}. Pulay's[47] reported $A_{j,ab\ in}$ of 22.76 km mole^{-1} is 55% greater than the assigned value of 14.74 km mole^{-1}.

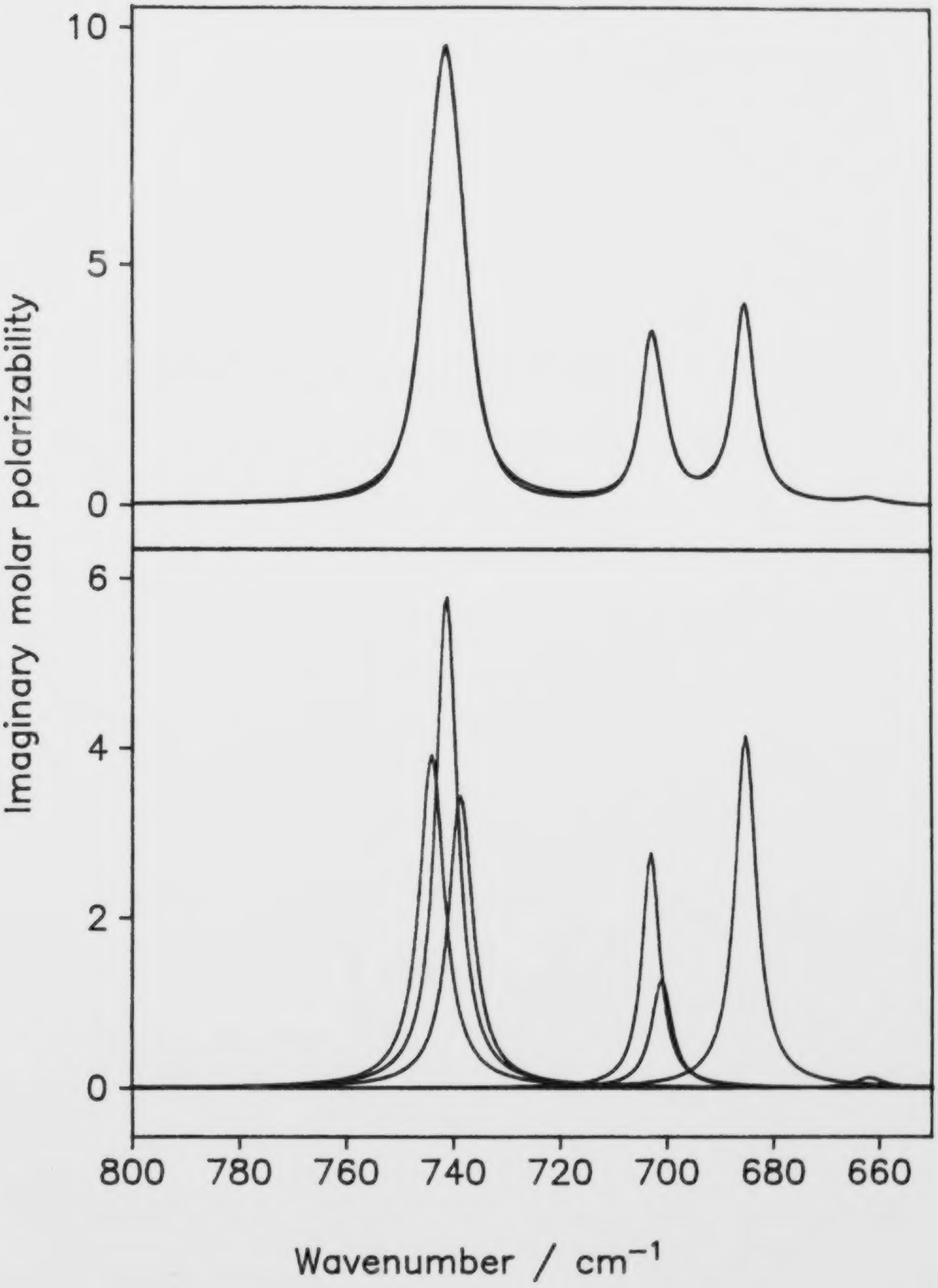

Figure 5.7 - Top - Superimposed experimental imaginary molar polarizability, α''_m, and curve fitted α''_m spectra of liquid chlorobenzene between 800 and 650 cm^{-1}. Bottom - The prominent CDHO bands in this region that were used to fit the experimental α''_m spectrum. Units for both boxes are cm^3 mole^{-1}.

ν_{18} at 685 cm^{-1} was fitted by a single of C_j=0.217 km mole^{-1} and corresponding $A_{j,gas}$= 17.13 km mole^{-1}. Pulay's value 42.45 km mole^{-1}, greater by a factor of 2.5

5.1.1g - Intensities of the ν_{11}, ν_{14}, ν_{19}, ν_{20}, ν_{29} and ν_{30} vibrations

The experimental α''_m and curve fitted α''_m spectra of liquid chlorobenzene between 650 and 350 cm^{-1} are shown in Figure 5.8. The fit in this region is not as good as in other regions. The area under the curve fitted α''_m is greater by 7.8% than the area under the experimental α''_m spectrum. Peak heights are reproduced to 2-4%. The poor fit is due partly to the curve fitted wings of the band at 468 cm^{-1} being higher than the wings of that band in the experimental spectrum, and partly to poorer experimental data between 521 and 484.5 cm^{-1} for which k was set to zero (Table 3.5).

The bands at 614 cm^{-1}, due to ν_{29}, and 468 cm^{-1}, due to ν_{19}, were each fitted by a single CDHO band. The two fitted bands at 415.1 and 408.8 cm^{-1} were assigned to ν_{11} and ν_{14}, respectively, the latter very tentatively.

No comparison is made for three vibrations. The wavenumbers of two fundamentals, ν_{20} and ν_{30}, are below the experimental range so their intensities were not measured. The intensity of ν_{14}, an A_2 vibration, is zero for the gas, so was not calculated by Pulay *et al.*[47].

Pulay's[47] reported intensities, $A_{j,ab\ in}$, for ν_{11}, ν_{19} and ν_{29} are greater by a factor of 2.4, greater by 16% and smaller by 23%, respectively, than our assigned intensities, $A_{j,gas}$,

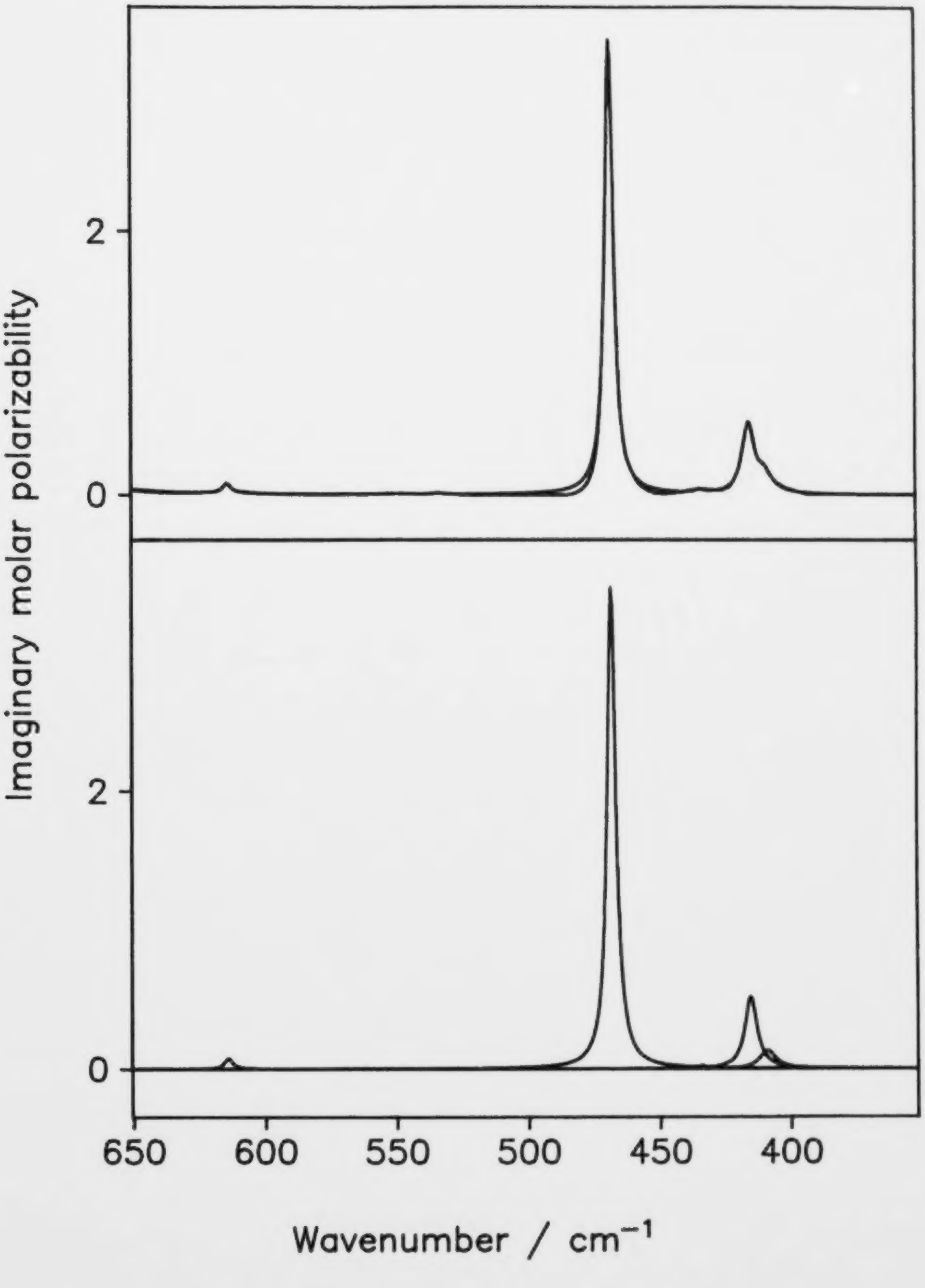

Figure 5.8 - Top - Superimposed experimental imaginary molar polarizability, α''_m, and curve fitted α''_m spectra of liquid chlorobenzene between 650 and 350 cm^{-1}. Bottom - The prominent CDHO bands in this region that were used to fit the experimental α''_m spectrum. Units for both boxes are cm^3 mole^{-1}.

for these vibrations. However, the magnitude of Pulay's intensities clearly support the assignments.

5.1.2 - Summary of intensity assignment of chlorobenzene

The assignment of the fundamental vibrations to the experimentally observed infrared bands of liquid chlorobenzene is given in Table 4.10, and the assignment of the intensity of the fitted bands is summarized in Table 5.2.

The comparison of the $A_{j,gas}$ values, which were calculated from the C_j values of the liquid under the assumption that the dipole moment derivatives are the same in the gas and liquid phases, with the $A_{j,ab\ in}$ values, which were calculated by Pulay[47] by *ab initio* quantum mechanics is of interest. The agreement is extremely good in the sense that Pulay's calculations reproduce the pattern of intensities extremely well. He calculates weak bands to be weak and intense bands to be intense. The numerical agreement is within a factor of two for most cases, which is remarkably good. In principle there is no reason for agreement between intensities calculated for the gas and those observed for the liquid. The agreement observed must mean that the vibrations in question have very similar intensities in the two phases, and that the *ab initio* calculations do a remarkably good job of calculating them.

There are notable exceptions. As discussed in Section 5.1.1a, the CH stretching intensities in Table 5.2 were obtained by assigning the intensity of the fitted band to a specific fundamental, and the total is nearly 5 times smaller than Pulay calculated. If the total intensity in the region is assigned to the CH stretching fundamentals collectively, the measured intensities are smaller than Pulay's by a factor of 2.4. This can be compared with a factor of 1.7 between the intensities measured for gaseous and liquid benzene, to suggest that the CH stretching vibrations of chlorobenzene may also be much weaker in the liquid than in the gas phase. However, firm conclusions must await the measurement of the gas phase intensities.

Another exception to the factor of two generality is for ν_{18} at 685 cm^{-1}, which is ~2.5 times weaker than calculated. But the experimental intensity of ν_{17} and ν_{18} combined is ~81 km mol^{-1}, just 9% smaller than Pulay's calculated value, 89.2 km mole^{-1}. Thus, with reference to Table 4.10, the difference probably arises because the calculations for the gas gave different contributions to these two vibrations from the two sets of out-of-plane displacements, the CCCC torsion and the oop hydrogen motion, than actually occur in the liquid. A similar explanation may well be correct for the weaker example of ν_{25} and ν_{26} for which the total intensity calculated is within 2% of that observed, but the distribution between the two vibrations is different.

Thus, the experimental study and assignment of the liquid and the *ab initio* calculations of Pulay are thought to support each other strongly.

The assignment of nearly all of the other fitted bands that are classified as "weak" or stronger was made from the sums of the fundamental wavenumbers with little difficulty. They will provide experimental evidence against which to compare calculations of the intensities of the overtone and combination bands, which are only active through the anharmonic parts of the potential energy and the non-linearity of the dipole moment with respect to internuclear distance.

Many of the very weak bands above 2000 cm^{-1} have not been assigned in this way, mainly because there are frequently many possible assignments for them.

5.2 - Integrated intensities and dipole moment derivatives of liquid toluene

The imaginary molar polarizability, α_m'', spectrum of liquid toluene was fitted with 166 CDHO bands between 4800 and 442 cm^{-1}. An entire spectrum, called the fitted spectrum, was computed through the summation of all the 166 band spectra, each of which expanded over the full range, 4800-442 cm^{-1}. This fitted spectrum and the α_m'' spectrum are shown in Figure 5.9.

The two spectra almost coincide and, in general, the fit is very good, especially for peak heights and areas under the spectra. As can be seen from the magnified curves in Fig 5.9, the fit is not as good at the wings of sharp bands.

For peak of heights < 0.01 cm^3 mole^{-1}, between 0.01 and 0.1 cm^3 mole^{-1}, between 0.1 and 1 cm^3 mole^{-1}, and greater than 1 cm^3 mole^{-1}, the average percent difference between the fitted and measured spectra are ±3%, ±2.3%, ±1.1% and ±0.5%, respectively.

For the region between 4800 and 800 cm^{-1}, the area under the fitted spectrum is smaller than the area under the α_m'' spectrum by 0.45% and for the region between 800

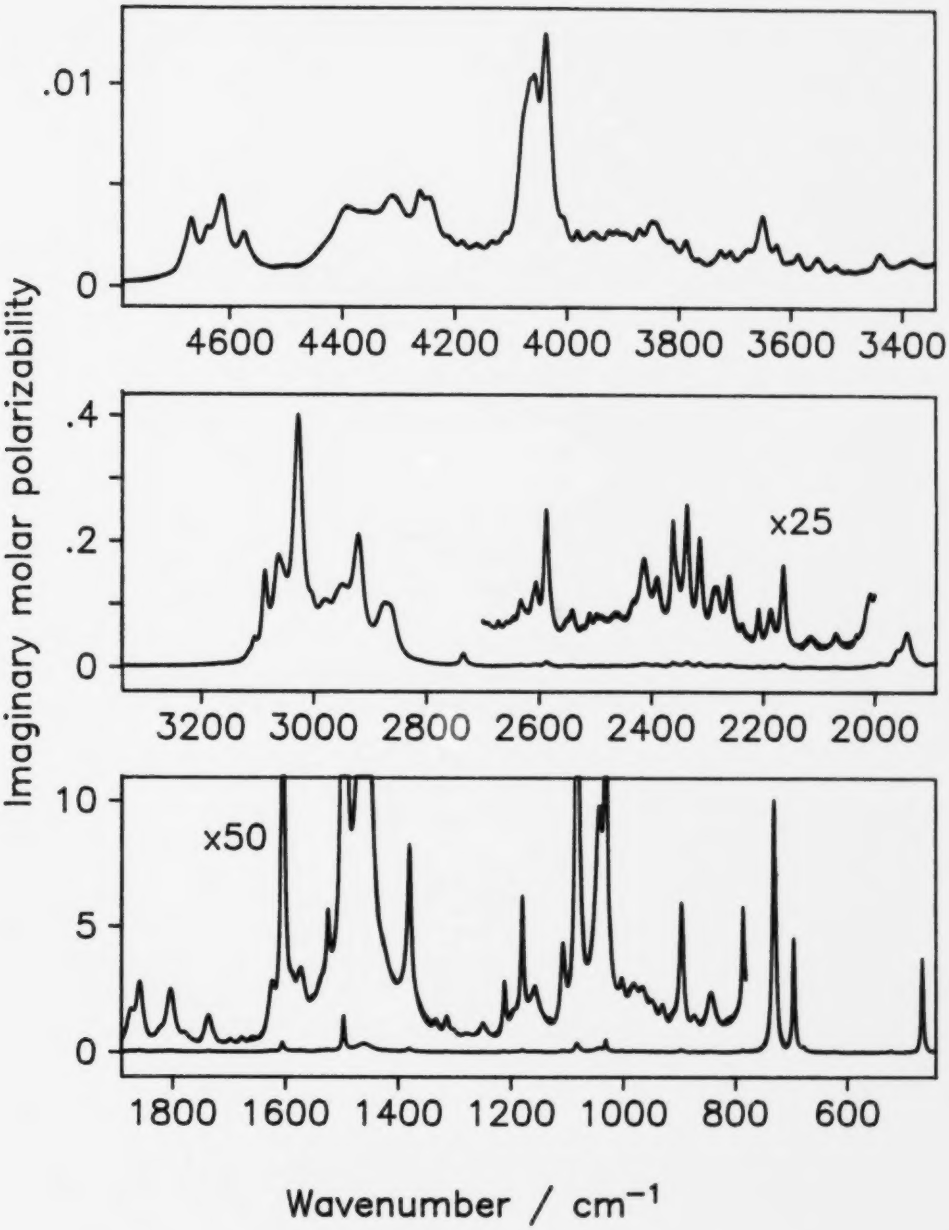

Figure 5.9 - The experimental imaginary molar polarizability, α''_m, spectrum and curve fitted α''_m spectrum of liquid toluene. Units are cm^3 $mole^{-1}$. In each box, the ordinate scale is for the lower curves. It needs to be divided by the multiplication factor for the upper curves. The two spectra coincide over most of the range.

Table 5.3 - Integrated intensities of toluene.

Exp α''_m [a,b] cm^{-1}	Gas[c]	Fitted cm^{-1}	Γ_j cm^{-1}	C_j km / mol	$\lvert\overrightarrow{R_j}\rvert$ Debye	Assignment[d]
~4716 vw br sh		4713.9	95.4	0.00867	0.00761	
~4682vw br sh		4681.4	18.4	0.000568	0.00195	$\nu_{21}+\nu_4$ (4691)
4667.0 vw		4667.2	20.8	0.00378	0.00505	$\nu_1+\nu_4$ (4667) or $\nu_{21}+\nu_{23}$ (4673)
4637.1 vw		4639.0	21.7	0.00234	0.00399	$\nu_3+\nu_4$ (4643) or $\nu_2+\nu_{23}$ (4642)
~4623 vw sh		4622.9	20.9	0.00138	0.00307	$\nu_3+\nu_{23}$ (4625)
4612.1 vw		4611.3	21.6	0.00481	0.00573	$\nu_{22}+\nu_{23}$ (4614)
4573.6 vw br		4573.5	18.2	0.00153	0.00325	$\nu_{21}+\nu_5$ (4582) ?
		4570.2	61.2	0.00348	0.00490	
~4536 vw br sh						
~4495 vw br sh		4501.9	59.0	0.00120	0.00290	
~4435vw br sh		4434.7	53.1	0.00198	0.00375	$\nu_2+\nu_{32}$ (4434) or $\nu_1+\nu_{32}$ (4441)
4388.7 vw		4393.3	57.1	0.0101	0.00851	
~4357 vw		4356.0	51.8	0.00474	0.00585	
4311.0 vw br		4308.1	63.4	0.0141	0.0102	
4261.3 vw		4261.9	21.6	0.00293	0.00465	
4244.3 vw br		4241.0	33.1	0.00583	0.00658	
~4211 vw sh		4208.6	27.3	0.00155	0.00341	
4186.3 vw		4185.4	20.5	0.00108	0.00285	$\nu_{22}+\nu_{27}$ (4183)
4161.3 vw br		4160.2	32.2	0.00202	0.00391	
4132.3 vw		4132.9	25.4	0.00144	0.00331	
4106.7 vw br sh		4110.7	22.5	0.00129	0.00314	
		4078.3	22.0	0.00635	0.0070	
~4065 w vvbr		4065.4	21.3	0.00681	0.00726	
		4055.2	15.9	0.00397	0.00555	
4036.3 w		4035.7	21.8	0.0144	0.0106	
~4007 vw sh		4003.7	19.1	0.00149	0.00342	
3980.3 vw		3980.0	15.8	0.000979	0.00278	
3951.2 vw br		3951.7	41.7	0.00460	0.00606	
3923.8 vw		3923.6	19.6	0.00142	0.00338	$\nu_{31}+\nu_9$ (3922) or $\nu_{22}+\nu_{16}$ (3922)
3909.9 vw		3909.5	15.6	0.000938	0.00275	

Table 5.3 - Continued

Exp α''_m [a,b] cm^{-1}	Gas[c]	Fitted cm^{-1}	Γ_j cm^{-1}	C_j km / mol	$\lvert\vec{R}_j\rvert$ Debye	Assignment[d]
3895.9 vw br db ?		3897.7	17.9	0.000898	0.00269	$\nu_{31}+\nu_{15}$ (3901) or $\nu_2+\nu_{13}$ (3898)
		3888.1	19.9	0.00102	0.00287	$\nu_{31}+\nu_{12}$ (3886)
3869.7 vw		3870.0	19.3	0.00167	0.00369	$\nu_{22}+\nu_{13}$ (3870) or $\nu_{21}+\nu_{10}$ (3872)
3847.2 vw br db		3850.5	20.6	0.00149	0.00349	
		3838.0	29.1	0.00302	0.00498	
3812.2 vw br		3811.6	29.1	0.00203	0.00410	
3786.3 vw		3785.7	17.1	0.00133	0.00333	$\nu_2+\nu_{17}$ (3785)
3763.9 vw		3762.3	23.1	0.000717	0.00245	$\nu_{31}+\nu_{13}$ (3763)
~3738 vw br sh		3738.0	22.9	0.000461	0.00197	
3724.1 vw		3724.4	16.7	0.00867	0.00856	$\nu_{22}+\nu_{18}$ (3722)
3707.0 vw		3706.7	16.2	0.000797	0.00260	$\nu_{21}+\nu_{29}$ (3708) or $\nu_{31}+\nu_{10}$ (3705)
3675.0 vw		3678.2	28.8	0.00162	0.00372	$\nu_2+\nu_{29}$ (3677)
3649.0 vw		3649.1	21.9	0.00344	0.00545	$\nu_{31}+\nu_{17}$ (3650) or $\nu_{22}+\nu_{29}$ (3649)
3624.0 vw		3623.1	15.0	0.000935	0.00285	
3598.9 vw br		3600.6	17.9	0.00346	0.00550	$\nu_{21}+\nu_{11}$ (3607)
3584.6 vw		3585.1	15.1	0.000744	0.00256	$\nu_1+\nu_{11}$ (3583)
3549.8 vw br		3550.5	21.1	0.00963	0.00924	
3519.3 vw		3518.5	13.6	0.00305	0.00523	$\nu_2+\nu_{19}$ (3519)
3494.7 vw br		3494.9	14.4	0.000099	0.00094	
~3472 vw br sh		3471.4	14.2	0.000057	0.00072	$\nu_{34,37}+\nu_{11}$ (3471)
3439.7 vw		3439.4	21.6	0.00105	0.00310	$\nu_{31} + \nu_{11}$ (3441)
~3404 vw sh		3397.5	20.1	0.000280	0.00161	$\nu_2+\nu_{30}$ (3401) or $\nu_1+\nu_{30}$ (3408)
3385.3 vw br		3381.3	17.9	0.000376	0.00187	$\nu_3+\nu_{30}$ (3384) or $\nu_{31}+\nu_{19}$ (3384)
~3325 vw br sh		3330.0	10.2	0.000127	0.00110	$\nu_{31}+\nu_{14}$ (3325)
3306.5 vw		3317.5	9.0	0.000079	0.00087	$\nu_{22}+\nu_{20}$ (3303)
~3203 vw br sh						$2\nu_4$ (3209)
3167.5 vw		3168.0	3.1	0.000184	0.00135	$2\nu_{23}$ (3173) or $\nu_{34}+\nu_{20}$ (~3167)
~3115 w br sh		3114.4	9.3	0.00335	0.00582	
3104.1 m		3105.3	8.2	0.00878	0.00944	$\nu_4+\nu_5$ (3100)
3086.4 s	B	3086.3	10.9	0.0617	0.0251	ν_{21}
3062.1 s br	A	3063.8	18.4	0.0982	0.0318	ν_1

Table 5.3 - Continued

Exp α_m'' [a,b] cm^{-1}	Gas[c]	Fitted cm^{-1}	Γ_j cm^{-1}	C_j km / mol	$\lvert\overrightarrow{R_j}\rvert$ Debye	Assignment[d]
~3055 s br sh		3054.0	19.9	0.0510	0.0229	ν_2 and ?? ν_3
3027.0 s	B	3027.3	19.0	0.335	0.0590	ν_{22}
~3003 s sh		3002.4	15.0	0.0234	0.0157	$3\nu_9$ (3007)
2979.1 s br		2980.6	29.1	0.0709	0.0274	$\nu_4+\nu_{32}$ (2984)
~2950 s sh		2950.1	39.4	0.167	0.0422	? ν_{34} and ?? ν_{37}
2919.9 s	A??	2920.7	21.8	0.149	0.0401	ν_{31}
		2916.1	11.5	0.0139	0.0123	
2872.3 s vbr		2875.4	27.7	0.0825	0.0301	$\nu_5+\nu_{32}$ (2875)
		2860.2	21.4	0.0503	0.0235	
~2824 w br sh						
~2811w br sh		2808.9	8.5	0.000599	0.00259	
~2780 vw br sh						$\nu_4+\nu_7$ (2783)
2734.1w	A?	2734.0	10.8	0.00897	0.0102	$\nu_{34}-\nu_{20}$ (2733) ??
~2692 vw br sh		2689.1	6.8	0.000051	0.00077	$\nu_{32}+\nu_{26}$ (2692)
2671.7 vw		2671.6	6.5	0.000155	0.00135	
~2657 vw br sh		2656.0	10.6	0.000232	0.00166	$2\nu_{25}$ (2664)
~2644 vw br sh		2644.4	15.7	0.000578	0.00262	$\nu_4+\nu_{36,39}$ (2646)
2631.9 vw		2632.0	10.2	0.000687	0.00287	
~2624 vw br sh		2624.1	14.1	0.000463	0.00236	$\nu_{23}+\nu_{36,39}$ (2628) or $2\nu_{26}$ (2625)
~2609 vw br sh		2609.3	15.9	0.00125	0.00388	
2604.7 vw		2603.9	8.0	0.000585	0.00266	$\nu_4+\nu_9$ (2607)
2585.9 vw	A?	2586.0	10.2	0.00331	0.00636	
~2576 vw		2576.4	17.5	0.000400	0.00221	$\nu_5+\nu_{28}$ (2577)
2548.2 vw		2550.6	19.2	0.000819	0.00318	$\nu_{23}+\nu_{12}$ (2553)
2540.4 vw		2539.6	12.5	0.000795	0.00314	$\nu_{38}+\nu_{28}$ (2542) or $\nu_{25}+\nu_6$ (2542)
~2521 vw br sh		2521.8	15.4	0.000415	0.00228	
2509.2 vw		2509.4	10.5	0.000558	0.00837	$\nu_{25}+\nu_7$ (2511)
2496.7 vw		2497.2	12.0	0.000434	0.00233	
~2490 vw br sh		2487.5	22.1	0.000918	0.00341	
2465.4 vw br db		2462.2	36.9	0.00277	0.00595	
2431.2 vw br		2432.6	19.4	0.00113	0.00383	$\nu_{23}+\nu_{13}$ (2429)

Table 5.3 - Continued

Exp α''_m [a,b] cm^{-1}	Gas[c]	Fitted cm^{-1}	Γ_j cm^{-1}	C_j km / mol	$\lvert \vec{R_j} \rvert$ Debye	Assignment[d]
2412.4 vw		2412.5	20.4	0.00382	0.00706	
2389.0 vw		2388.8	17.1	0.00216	0.00534	
2360.6 vw		2360.7	6.3	0.00106	0.00376	$\nu_{25}+\nu_8$ (2362) or $\nu_6+\nu_{27}$ (2366)
~2354 vw br sh		2355.6	24.2	0.00319	0.00653	
2335.3 w		2335.5	10.3	0.00298	0.00634	
2312.6 vw	A?	2312.6	10.4	0.00233	0.00563	
2286.1 vw db		2287.6	18.4	0.00175	0.00491	
2280.7 vw db		2279.6	12.5	0.000716	0.00315	
2260.5 vw	B	2260.3	13.3	0.00176	0.00495	$\nu_7+\nu_{28}$ (2260)
~2240 vw		2240.4	63.6	0.00214	0.00549	$\nu_6+\nu_8$ (2240)
2237.3 vw		2236.6	6.8	0.000121	0.00131	$\nu_{27}+\nu_{28}$ (2237)
~2225 vw br sh						
2207.5 vw		2207.7	7.1	0.000507	0.00269	
2185.3 vw br	B	2186.0	13.4	0.00105	0.00389	$\nu_{27}+\nu_8$ (2186)
2163.7 vw	A	2163.4	10.1	0.00178	0.00509	$\nu_{32}+\nu_{10}$ (2165)
~2138 vw sh						
~2123 vw sh						
2116.6 vw		2114.9	24.3	0.000698	0.00322	
~2111 vw sh						
2068.5 vw		2069.5	12.3	0.000356	0.00233	
2032.0 vw						$\nu_8+\nu_9$ (2032)
~2014 vw sh		2014.6	7.7	0.000222	0.00186	$\nu_5+\nu_{11}$ (2017)
2008.5 vw br	C?	2008.2	8.9	0.000469	0.00271	$\nu_8+\nu_{15}$ (2011)
1991.1 vw	A	1991.6	9.4	0.00157	0.00498	$\nu_6+\nu_{10}$ (1996)
1983.6 vw br	C?	1983.8	5.2	0.000334	0.00230	$\nu_9+\nu_{15}$ (1983)
~1958 w sh	A	1959.4	14.6	0.00812	0.0114	$\nu_7+\nu_{10}$ (1964) or $2\nu_{15}$ (1960)
1942.1m	B	1942.1	16.7	0.0267	0.0208	$\nu_{15}+\nu_{12}$ (1947) or $\nu_{27}+\nu_{10}$ (1942)
1897.9 vw br		1899.9	4.0	0.000147	0.00156	$\nu_9+\nu_{16}$ (1898) or $\nu_{32}+\nu_{11}$ (1900)
1872.0 w br	A	1873.7	15.9	0.0108	0.0135	$\nu_{15}+\nu_{16}$ (1876)
1857.6 m	B	1857.3	14.3	0.0201	0.0185	$\nu_{12}+\nu_{16}$ (1862) or $\nu_{25}+\nu_{11}$ (1853)
~1820 w sh	B?	1822.1	17.0	0.00367	0.00797	$\nu_{15}+\nu_{13}$ (1823)

Table 5.3 - Continued

Exp α''_m [a,b] cm^{-1}	Gas[c]	Fitted cm^{-1}	Γ_j cm^{-1}	C_j km / mol	$\lvert\overrightarrow{R_j}\rvert$ Debye	Assignment[d]
1802.6 m	A	1802.5	17.0	0.0215	0.0194	
1778.5 w br		1776.1	18.0	0.00358	0.00797	$\nu_{27}+\nu_{29}$ (1778) or 3A_2 options
1735.6 w		1735.3	16.2	0.0110	0.0141	$\nu_{16}+\nu_{13}$ (1738)
1696.8 w		1697.4	9.3	0.000968	0.00424	
1676.7 w		1675.8	18.3	0.00197	0.00609	
1657.8 w br						
1623.1 m br	Q?	1623.6	12.7	0.0117	0.0151	$\nu_{16}+\nu_{17}$ (1625) ?
1604.6 s	A	1604.9	4.7	0.0319	0.0250	ν_4
		1602.8	7.4	0.0249	0.0221	
1586.7 m br		1590.0	26.9	0.0207	0.0203	ν_{23}
1572.1 m	Q?	1571.4	16.2	0.0141	0.0168	2ν_{10} (1571) or $\nu_{13}+\nu_{17}$ (1573)
1550.3 m br	Q?					$\nu_8+\nu_{11}$ (1551) or $\nu_6+\nu_{30}$ (1556)
~1537 m br sh		1530.0	45.1	0.0358	0.0271	$\nu_{13}+\nu_{18}$ (1538)
1523.6 s br	B??	1523.5	5.2	0.00571	0.0109	$\nu_7+\nu_{30}$ (1525)
1495.7 vs	A	1495.7	4.0	0.113	0.0488	ν_5
		1494.3	10.5	0.0467	0.0314	
1460.3 s br		1459.8	31.9	0.250	0.0734	ν_{35} ??, ν_{38} ?? and ν_{24} ??
~1422 m sh		1419.7	18.8	0.00653	0.0120	$\nu_{17}+\nu_{18}$ (1425) or $\nu_6+\nu_{20}$ (1427) or $\nu_{28}+\nu_{20}$ (1427)
1378.9 s	A	1382.3	44.4	0.0356	0.0285	ν_{32}
		1379.0	7.1	0.0170	0.0197	
1332.0 w	B?	1332.0	10.0	0.00174	0.00641	ν_{25}
1312.7 w	B	1312.7	10.0	0.00331	0.00891	ν_{26}
~1302 w sh		1300.7	12.2	0.00127	0.00555	$\nu_{16}+\nu_{14}$ (1300)
1277.6 w br		1277.6	22.6	0.00236	0.00763	$\nu_5-\nu_{20}$ (1279)
1248.7 w		1248.2	22.0	0.00593	0.0122	
1210.2 m	A	1210.1	6.3	0.00480	0.0112	ν_6
~1193 w br sh	Q?	1193.4	18.7	0.00602	0.0126	$\nu_{17}+\nu_{19}$ (1194) or $\nu_{15}+\nu_{20}$ (1198)
1178.6 s		1178.6	5.7	0.0103	0.0166	ν_7
1155.9 m		1156.8	31.5	0.0219	0.0244	ν_{27}
~1130 w br sh						$\nu_{10}+\nu_{30}$ (1132) or $\nu_{17}+\nu_{14}$ (1135)

Table 5.3 - Continued

Exp α''_m [a,b] cm^{-1}	Gas[c]	Fitted cm^{-1}	Γ_j cm^{-1}	C_j km / mol	$\lvert \vec{R_j} \rvert$ Debye	Assignment[d]
1106.5 m	B	1106.5	9.4	0.0102	0.0170	$\nu_{18}+\nu_{14}$ (1100)
1081.4 s	B	1081.1	8.6	0.0521	0.0390	ν_{28}
1041.4 s	??	1042.6	11.4	0.0145	0.0209	ν_{36} ?? and ν_{39} ??
		1040.2	37.2	0.0604	0.0428	
1030.1 s	A	1030.0	3.9	0.0261	0.0283	ν_8
1002.3 m		1001.5	10.8	0.00394	0.0111	ν_9
980.7 m		980.9	23.2	0.0115	0.0192	ν_{15} ??
966.4 m br		964.2	15.7	0.00591	0.0139	ν_{12} ??
~947 w br sh		947.4	17.7	0.00559	0.0136	$\nu_{17}+\nu_{20}$ (947)
929.6w		929.0	12.1	0.00366	0.0111	$2\nu_{19}$ (929) or $\nu_{11}+\nu_{14}$ (926)
~910 w br sh		910.4	13.9	0.00211	0.00854	$\nu_{18}+\nu_{20}$ (912)
895.4 s	C	895.4	8.6	0.0126	0.0211	ν_{16}
872.9 w		872.3	14.2	0.00264	0.00976	$\nu_{19}+\nu_{14}$ (869) or $4\nu_{20}$ (868)
842.7 m		842.8	17.4	0.00783	0.0171	ν_{13}
810.4 w br sh						$\nu_{19}+\nu_{30}$ (810) or $2\nu_{14}$ (811)
785.6 s	A	785.5	3.7	0.00337	0.0116	ν_{10}
729.9 vs	C	729.9	6.7	0.777	0.183	ν_{17}
694.8 vs	C	694.9	4.1	0.189	0.0926	ν_{18}
		693.1	3.2	0.0151	0.0262	
		690.9	4.2	0.0115	0.0229	
~678 s br sh		677.5	6.8	0.00857	0.0200	$\nu_{19}+\nu_{20}$ (681)
633.0 w sh						
622.0 m		621.9	6.6	0.00161	0.00903	ν_{29}
565.2 vw br						$\nu_{30}+\nu_{20}$ (563)
537.8 w		537.5	4.5	0.000342	0.00448	
521.0 m	A	521.0	4.4	0.00297	0.0134	ν_{11}
~508 vw sh		509.6	12.7	0.000341	0.00459	
464.4 vs	C	464.4	4.1	0.110	0.0864	ν_{19}

a - Wavenumbers of peaks in the imaginary molar polarizability spectrum of liquid toluene.

b - Abbreviations used: v-very, w-weak, m-medium, s-strong, br-broad, sh-shoulder and db-doublet.

c - Band contours in the infrared spectrum of the gas.

d - Calculated wavenumbers are given in brackets.

and 440 cm^{-1}, it is greater by 2.8% than that of the α''_{m} spectrum. Overall, the area under the fitted spectrum is greater by 1.5% than that under the α''_{m} spectrum.

The parameters of the 166 CDHO bands required to fit the α''_{m} spectrum of toluene are given in Table 5.3. The table is arranged similarly to Table 5.1 of chlorobenzene. The accuracy of the integrated intensities, C_j, is estimated from the sum of the accuracy of the fit and the accuracy of the real and imaginary refractive indices, n and k, that are used in the calculation of the α''_{m} spectrum of toluene. The accuracy of the refractive indices was reported in Chapter 2 and is 0.2% for n and on the order of 2 to 3% for k. The accuracy of the fit is about 0.5 to 3% depending on the intensity of the band. Therefore, the accuracy of C_j is estimated to be better than 3-5% for strong peaks and 5-10% for weak peaks.

5.2.1 - Integrated intensities and dipole moment derivatives of the fundamental vibrations of liquid toluene

The intensities of the bands fitted to the experimental α''_{m} spectrum are assigned in the following sub-sections to the fundamental vibrations of toluene. Table 5.4 summarizes the integrated intensities, C_j, of the fundamental vibrations and the dipole moment derivatives with respect to the normal coordinates, $|\mu_j|$, calculated from them through Eq. 1.4.4. The estimated errors in the intensities are discussed above, and the errors in the dipole moment derivatives are estimated to be about 2% for strong fundamentals and about 4% or more for weak ones. In some cases it will be clear that the uncertainty in the assignment is considerable, making the estimated error in the values potentially very large.

The only integrated intensities of toluene reported in the literature are those published by Boggs[26] and by Galabov[29]. Boggs *et al.* used scaled *ab initio* calculations to obtain wavenumbers and infrared integrated intensities, $A_{j,ab\ in}$, of the fundamental vibrations of toluene. The latter are given in column 6 of Table 5.4. Galabov *et al.* used *ab initio* calculation to obtain the sign of the dipole moment derivatives with respect to symmetry coordinates but refined their calculated intensities through a least squares refinement procedure using experimental integrated intensity data for 4 bands of benzene, 12 bands of toluene and 16 bands of toluene-d_8. Galabov used an empirical force field developed for methyl benzenes by La Lau and Snyder[19], so, in contrast to Boggs, their wavenumbers and eigenvectors were not determined from *ab initio* calculations. The problems of separating the contributions of overlapping bands to the total intensity are more severe for the generally broader gas-phase bands than for the liquid-phase bands. Galabov *et al.* acknowledged the problem, but gave no information that allows the error of their experimental intensities to be estimated. Galabov's computed, $A_{j,ab\ in}$, and experimental, $A_{j,exp}$, intensities are given in columns 7 and 8 of Table 5.4. For comparison, our integrated intensities of the gas, $A_{j,gas}$, were calculated from the C_j of the liquid using Eq. 1.5.4 under the assumption that the $|\mu_j|$ values are the same in the gas and in the liquid phases, and are given in column 5 of Table 5.4.

Table 5.4 - Dipole moment derivatives and integrated intensities of toluene

	This work				Boggs[26]	Galabov[29]	
ν_j	Fitted cm^{-1} [a]	$C_{j,liq}$ [b]	$\lvert\mu_j\rvert$ [c]	$A_{j,gas}$ [b,d]	$A_{j,ab\ in}$ [b,e]	$A_{j,ab\ in}$ [b,f]	$A_{j,exp}$ [b]
ν_1	3063.8	0.0982	0.428	7.75	14.52	0.49	[g]
ν_2	3054.0	0.0510	0.309	4.03	14.62	4.03	26.45 [g]
ν_3	(3038 ???) [h]	0.0	0.0	0.0	5.57	3.40	[g]
ν_4	1604.9 [i]	0.0568	0.460	4.49	6.31	0.61	7.26 [j]
ν_5	1495.7 [i]	0.160	0.755	12.61	15.95	11.50	14.87
ν_6	1210.1	0.00480	0.095	0.38	0.03		
ν_7	1178.6	0.0103	0.139	0.81	0.22		
ν_8	1030.0	0.0261	0.221	2.06	1.41	2.30	
ν_9	1001.5	0.00394	0.086	0.31	0.13		
ν_{10}	785.5	0.00337	0.079	0.27	0.35	0.72	[k]
ν_{11}	521.0	0.00297	0.074	0.23	0.77	0.08	[ℓ]
ν_{12}	964.2	0.00591	0.105	0.47 [m]	0.00		
ν_{13}	842.7	0.00783	0.121	0.62 [m]	0.00		
ν_{14}	(405 ?)				0.00		
ν_{15}	980.9	0.0115	0.147	0.91	0.22		
ν_{16}	895.4	0.0126	0.153	0.99	0.39		
ν_{17}	729.9	0.777	1.205	61.35	47.18	34.48	40.96 [k]
ν_{18}	694.9 [i]	0.216	0.909	17.02	27.99	18.18	[k]
ν_{19}	464.4	0.110	0.453	8.69	8.47	6.00	6.24 [ℓ]
ν_{20}	(217)				2.48		
ν_{21}	3086.3	0.0617	0.340	4.87	43.01	19.16	38.18 [g]
ν_{22}	3027.3	0.335	0.791	26.45	3.61	31.85	[g]
ν_{23}	1590.0	0.0207	0.197	1.63	0.83	0.95	[j]
ν_{24}	1459.8 [n]	0.250 [n]	0.683 [n]	19.74 [n]	14.56	1.16	6.54 [o]
ν_{25}	1332.0	0.00174	0.057	0.14	0.00	0.02	[p]
ν_{26}	1312.7	0.00331	0.079	0.26	0.03		
ν_{27}	1156.8	0.0219	0.202	1.73	0.20		
ν_{28}	1081.1	0.0521	0.312	4.11	3.70	3.52	4.30
ν_{29}	621.9	0.00161	0.055	0.13	0.09	0.01	[k]
ν_{30}	(346)				0.42		

Table 5.4 - Continued

	This work				Boggs[26]	Galabov[29]	
ν_j	Fitted cm^{-1} [a]	$C_{j,liq}$ [b]	$\lvert\mu_j\rvert$ [c]	$A_{j,gas}$ [b,d]	$A_{j,ab\ in}$ [b,e]	$A_{j,ab\ in}$ [b,f]	$A_{j,exp}$ [b]
ν_{31}	2920.7	0.149	0.528	11.76	27.05	10.42	11.05
ν_{32}	1382.3 [i]	0.0526	0.436	4.15	0.39	3.26	3.08 [p]
ν_{33}	(<100)						
ν_{34}	2950.1 [q]	--- [q]	--- [q]	--- [q]	28.25	5.50	18.52 [r]
ν_{35}	1459.8 [n]	--- [n]	--- [n]	--- [n]	5.15	2.45	[o]
ν_{36}	1042.6 [s]	0.0145 [s]	0.165 [s]	1.14 [s]	9.24		
ν_{37}	2950.1 [q]	0.167 [q]	0.559 [q]	13.19 [q]	18.46	12.94	[r]
ν_{38}	1459.8 [n]	--- [n]	--- [n]	--- [n]	0.15	3.78	[o]
ν_{39}	1040.2 [s]	0.064 [s]	0.336 [s]	4.77 [s]	0.02		

a - Integrated intensities were not obtained for ν_{14}, ν_{20}, ν_{30} and ν_{33} which are below the experimental wavenumber range for this work.

b - Units are km mole^{-1}.

c - Units are Debye Å^{-1} amu$^{-1/2}$.

d - Integrated intensities for the gas, $A_{j,gas}$ were calculated as $A_{j,gas} = 8\pi^2 C_{j,liq}$ with the assumption that $\mu_{j,liq}{}^2 = \mu_{j,gas}{}^2$.

e - $A_{j,gas}$ values obtained from *ab initio* calculations reported in Ref. 26.

f - $A_{j,gas}$ values reported in Ref. 29. Intensities were obtained from *ab initio* calculations refined with experimental intensities of 4 bands of benzene, 12 bands in toluene and 16 bands in toluene-d_8.

g - Total aromatic CH stretching intensity is 64.63 km mole^{-1}. Galabov gave the two values 26.45 and 38.18 given in the table but did not say how the separation was achieved.

h - This vibration has not been assigned with confidence.

i - More than one CDHO band was used in the fit. The wavenumber listed is that of the prominent contributing band. All related quantities for this vibration are the sums from all contributing bands.

j - Experimental $A_{j,gas}$ was given for ν_4 and ν_{23} collectively.

k - Experimental $A_{j,gas}$ was given for ν_{10}, ν_{17}, ν_{18} and ν_{29} collectively.

ℓ - Experimental $A_{j,gas}$ was given for ν_{11} and ν_{19} collectively.

m - A_2 vibrations in chlorobenzene are infrared inactive in the spectrum of the gas, i.e $A_{j,gas} = 0$. Our values are derived from $C_{j,liq}$ as described in footnote d.

n - The same wavenumber was assigned to ν_{24}, ν_{35} and ν_{38}. All quantities are assigned in this table to ν_{24}.

o - Experimental $A_{j,gas}$ was given for ν_{24}, ν_{35} and ν_{38} collectively.

p - Experimental $A_{j,gas}$ was given for ν_{25} and ν_{32} collectively.

q - The same wavenumber was assigned to ν_{37} and ν_{34}. All quantities are assigned to ν_{37} in this table.

r - The value given for ν_{34} includes the intensity of and ν_{37}.

s - 1041 cm^{-1} was assigned to both ν_{36} and ν_{39}. The intensities of the fitted bands at 1042.6 and 1040.2 cm^{-1} were assigned arbitrarily to ν_{36} and ν_{39} respectively.

5.2.1a - Integrated intensities of the CH stretching vibrations

The experimental α''_m and curve fitted α''_m spectra of liquid toluene in the region of the CH stretching vibrations are shown in Figure 5.10. The fit in this region is very good. The area under the curve fitted α''_m is smaller by 0.1% than the area under the experimental α''_m spectrum. Peak heights are reproduced on average to 0.6% and no fundamental exceeds 1.1%.

The existence of many relatively intense overtone and combination bands in the CH stretch region again makes it impossible to make a unique assignment of the intensity to the different normal vibrations. The possible assignments are presented and discussed below, starting with the assignment of the intensity of specific fitted bands to specific fundamentals.

The intensity assignments of four of the five aromatic CH stretching vibrations, ν_{21}, ν_1, ν_2 and ν_{22} are straightforward. The intensities of the single CDHO bands at 3086, 3064, 3055 and 3027 cm^{-1}, are assigned to these vibrations, respectively. In section 4.5.1, ν_3 was assigned to a Raman band at 3038 cm^{-1} with no infrared counterpart identified. No additional CDHO band was needed to improve the fit in this region, and no integrated intensity is assigned to this vibration.

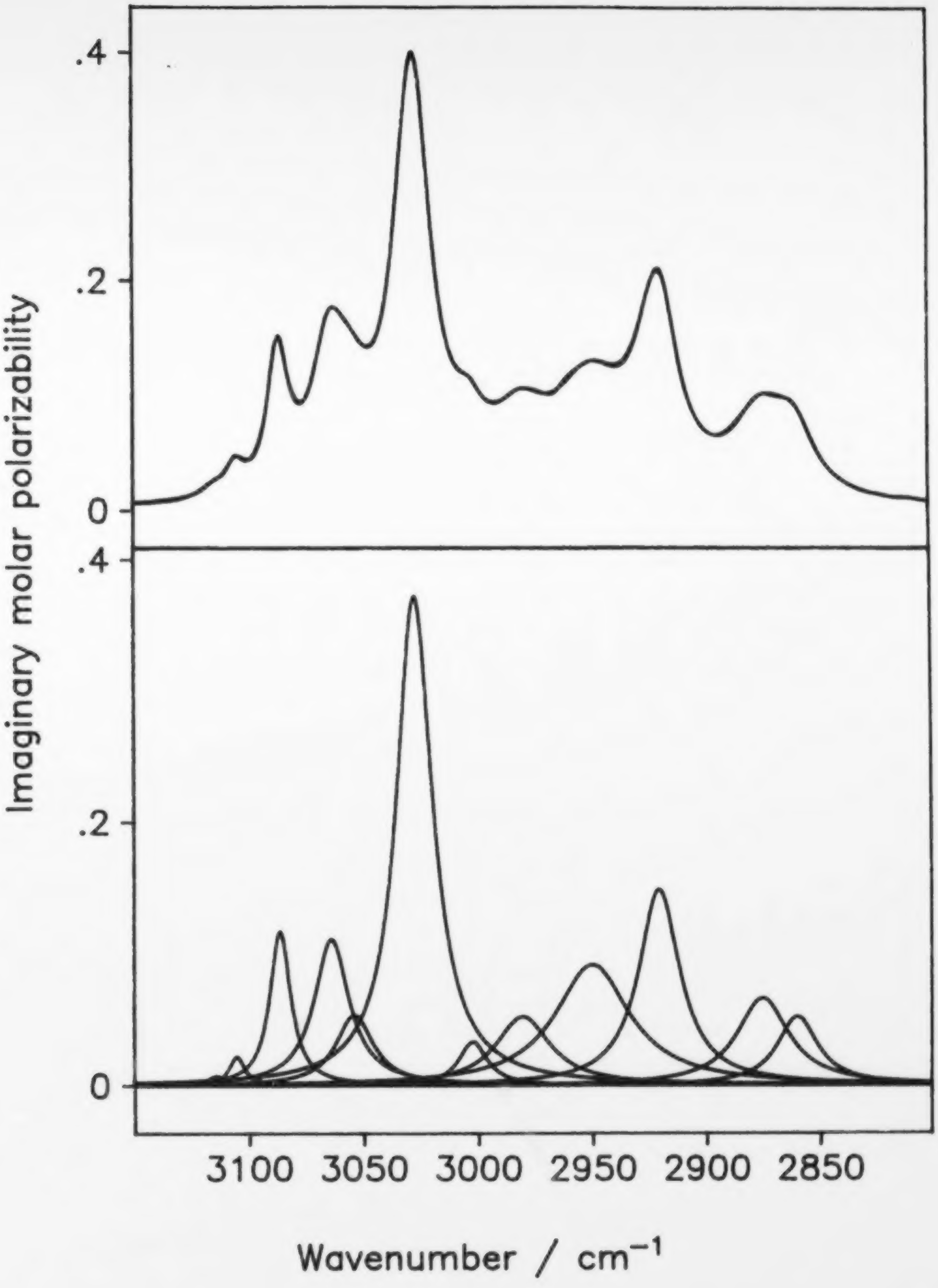

Figure 5.10 - Top - Superimposed experimental imaginary molar polarizability, α''_m, and curve fitted α''_m spectra of liquid toluene between 3150 and 2800 cm^{-1}. Bottom - The prominent CDHO bands in this region that were used to fit the experimental α''_m spectrum. Units for both boxes are cm^3 mole^{-1}.

The combined intensities, $A_{j,gas}$, of the aromatic CH stretching vibrations, calculated from the assigned $C_{j,liq}$ is 43.1 km mole^{-1}. Galabov's[29] combined experimental value, $A_{j,exp}$, is 64.6 km mole^{-1}, about 50% greater than our value. Boggs'[26] value, $A_{j,ab\ in}$, of 81.3 km mole^{-1} is about a factor of 2 larger than our value.

The intensity of the fitted band at 2920.7 cm^{-1} is assigned to the symmetric CH_3 stretching vibration. This yields an $A_{j,gas}$ value of 11.76 km mole^{-1} which is within 6% of Galabov's experimental value for the gas, 11.05 km mole^{-1}. Boggs' calculated value[26], $A_{j,ab\ in}$ is 27.05 km mole^{-1}, 2.3 times greater than either of these experimental values.

The assignment of the antisymmetric CH_3 stretching vibrations ν_{34} and ν_{37} is very uncertain. They were both tentatively assigned in section 4.5.5 to the broad peak at 2950 cm^{-1}. This peak was fitted by a single band of intensity C_j = 0.167 km mole^{-1}, which is equivalent to $A_{j,gas}$ = 13.2 km mole^{-1}. Galabov's combined experimental value for these two vibrations is 18.5 km mole^{-1} and Boggs' combined *ab initio* value is 46.7 km mole^{-1}. These values are greater than our value by 40% and by a factor of 3.5, respectively. Under this assignment the intensities $A_{j,gas}$ of the aromatic and aliphatic CH stretching vibrations are 43.1 and 25.0 km mole^{-1}, respectively, while those of Galabov are 64.6 and 29.5 km mole^{-1} and those of Boggs 81.3 and 73.7 km mole^{-1}. The agreement is not impressive.

A second assignment is to note that the CDHO band at 2980.6 cm^{-1} is assigned in Table 5.3 to the combination transition $\nu_4+\nu_{32}$ because the polarized band in the Raman spectrum excludes it from being assigned as a B_1 or a B_2 vibration (section 4.5.5). If, however, its intensity is added to that of the 2950 cm^{-1} band, the combined $A_{j,gas}$ is then 18.78 km mole^{-1}, within 1% of Galabov's experimental value. Boggs' value is then greater by a factor of 2.5 than our value, which is similar to the discrepancy observed in the aromatic CH stretching vibrations.

A third alternative assignment, and possibly the most probable, is to assign to the CH stretching fundamentals all of the intensity in the region where the overtone and combination bands are unusually strong, namely between 3200 and 2775 cm^{-1}. This intensity is C_j = 1.08 km mole^{-1} which transforms to $A_{j,gas}$ = 84.1 km mole^{-1}. The sum of all of the intensity in this region reported by Galabov or Boggs is 94.2 or 155 km mole^{-1}, respectively, but there is no indication in the case of Galabov whether he has removed any of the experimental intensity as due to overtone or combination bands.

In a somewhat arbitrary attempt to refine this assignment by separating the aromatic and aliphatic CH stretching intensities, the total area under the spectrum was divided at 3000 cm^{-1} to obtain ΣC_j = 0.581 km mole^{-1} between 3200 and 3000 cm^{-1} and 0.498 km mole^{-1} between 3000 and 2775 cm^{-1}. These values convert to ΣA_j = 45.9 km mole^{-1} for the aromatic CH and 39.3 km mole^{-1} for the aliphatic CH, which compares with 43.1 for the aromatic and 25.0 for the aliphatic under the first assignment. Clearly, the first and third assignments are not very different for the aromatic CH stretching vibrations but the third assignment increases the intensity of the aliphatic CH stretches by 56%.

These assignments of the CH stretching vibrations are discussed again later in a comparison of the intensities of different molecules.

5.2.1b - Integrated intensities of the ν_4, ν_5, ν_{23}, ν_{24}, ν_{32}, ν_{35} and ν_{38} vibrations

The experimental α_m'' and curve fitted α_m'' spectra of liquid toluene between 1650 and 1350 cm^{-1} are shown in Figure 5.11. The fit in this region is very good. The area under the curve fitted α_m'' is smaller by 0.36% than the area under the experimental α_m'' spectrum. Peak heights are reproduced on average to 0.8% and no fundamental exceeds 1.0%.

The intensities of the two CDHO bands at 1604.9 and 1602.8 cm^{-1} are assigned to ν_4, while that of the CDHO band at 1590.0 cm^{-1} is assigned to ν_{23}. The combined intensity, $A_{j,gas}$, of ν_4 and ν_{23} is 6.12 km mole^{-1}. Galabov's[29] combined experimental value, $A_{j,exp}$, is 7.26 km mole^{-1}, about 19% greater than our value, while Boggs'[26] value, $A_{j,ab\ in}$, of 7.14 km mole^{-1} is about 17% greater than our value.

The intensities of the two CDHO bands at 1495.7 and 1494.3 cm^{-1} are assigned to ν_5 and combine to give $A_{j,gas}$ = 12.61 km mole^{-1}. It is smaller by 18% than Galabov's reported experimental value of 14.87 km mole^{-1}, and 26% smaller than Boggs'[26] computed $A_{j,ab\ in}$ of 15.95 km mole^{-1}.

In sections 4.5.4 and 4.5.5, ν_{35} and ν_{38} were both tentatively assigned at 1460 cm^{-1}, with ν_{24} in their proximity, perhaps at 1442 cm^{-1}. Only one CDHO band was required to obtain a good fit of the strong broad band at 1460 cm^{-1} in the α_m'' spectrum, and its intensity is assigned to these three vibrations. Our calculated, $A_{j,gas}$, is 19.74 km

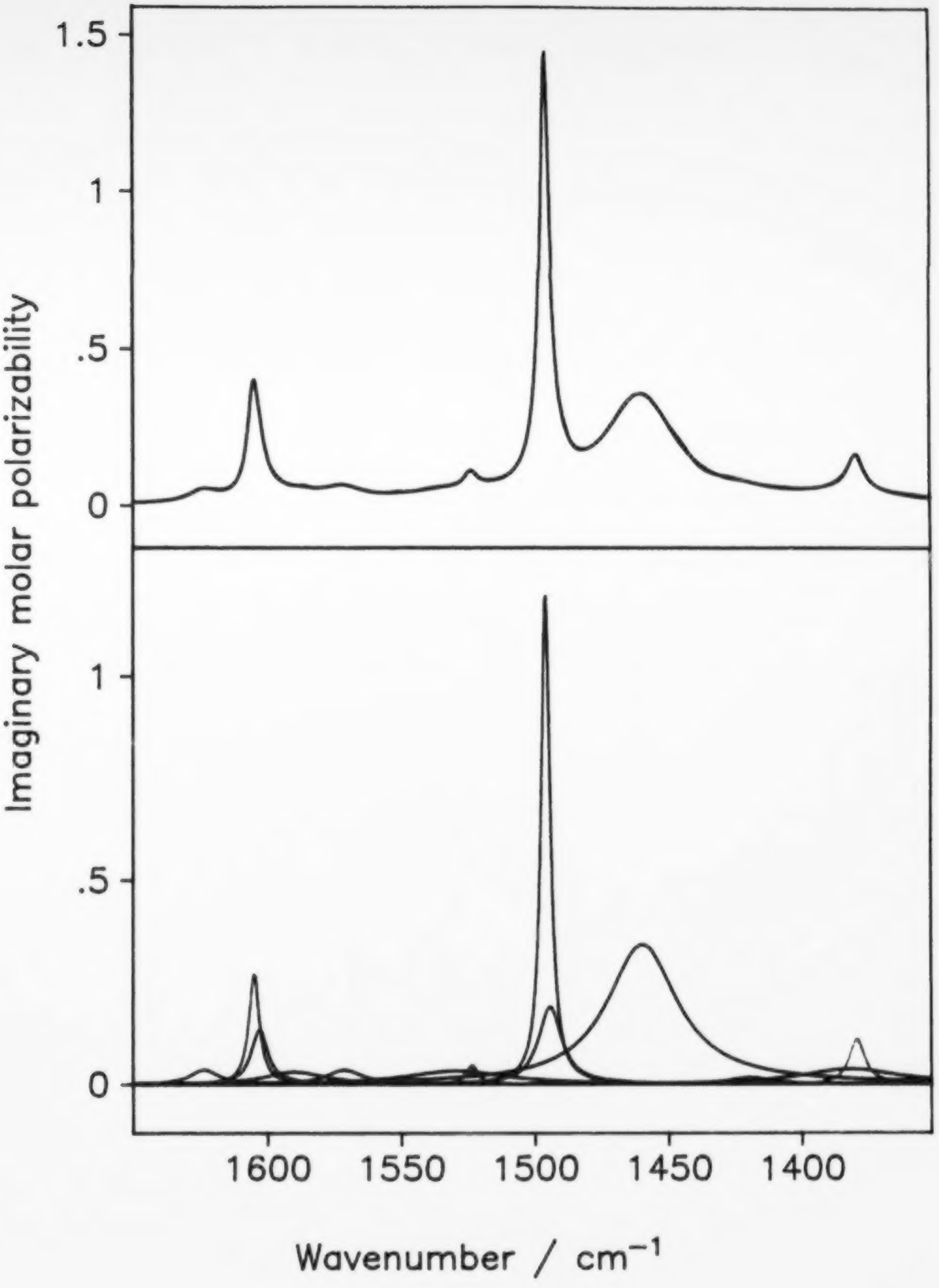

Figure 5.11 - Top - Superimposed experimental imaginary molar polarizability, α''_m, and curve fitted α''_m spectra of liquid toluene between 1650 and 1350 cm^{-1}. Bottom - The prominent CDHO bands in this region that were used to fit the experimental α''_m spectrum. Units for both boxes are cm^3 mole^{-1}.

km mole^{-1}, in good agreement with Boggs'[26] computed value of 20.08 km mole^{-1}, but far larger than Galabov's[29] experimental value, 6.54 km mole^{-1}.

The intensities of the two CDHO bands at 1382.3 and 1379.0 cm^{-1} are assigned to the symmetric CH_3 deformation ν_{32}. Galabov[29] reported the combined experimental intensity, $A_{j,exp}$, of ν_{32} and ν_{25} (1332 cm^{-1}) as 3.08 km mole^{-1}. Boggs'[26] computed intensities for these vibrations are 0.39 and 0.00 km mole^{-1}. The intensity assigned to ν_{25} is (next section) $C_j = 0.00174$ km mole^{-1}, i.e. $A_{j,gas} = 0.14$ km mole^{-1}. Thus, for ν_{32} and ν_{25} combined we find $A_{j,gas} = 4.29$ km mole^{-1}, which is 40% greater than Galabov's experimental value and 11 times greater than Boggs' reported values. It is noteworthy that based on our work and the theoretical values of Boggs and Galabov, the intensity of ν_{32} is much greater than that of ν_{25}, and therefore Galabov's $A_{j,exp}$ of 3.08 km mole^{-1} is largely due to ν_{32} rather than to ν_{25}.

5.2.1c - Integrated intensities of the ν_6, ν_7, ν_8, ν_9, ν_{25}, ν_{26}, ν_{27}, ν_{28}, ν_{36} and ν_{39} vibrations

The experimental α''_m and curve fitted α''_m spectra of liquid toluene between 1350 and 990 cm^{-1} are shown in Figure 5.12. The fit in this region of weak absorption is not as good as in other regions. The area under the curve fitted α''_m is smaller by 1.6% than the area under the experimental α''_m spectrum. Peak heights are reproduced on average to 3.1%.

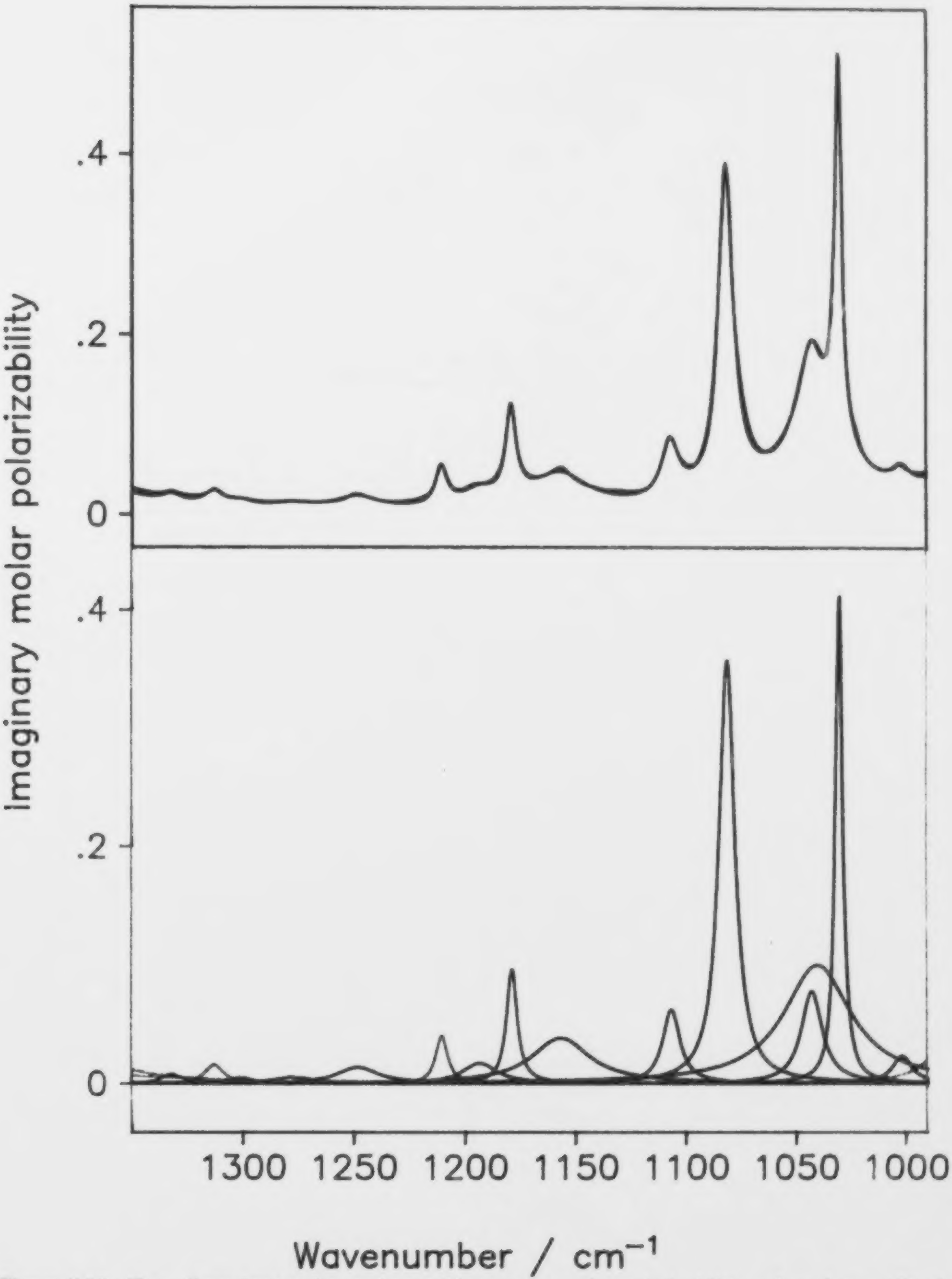

Figure 5.12 - Top - Superimposed experimental imaginary molar polarizability, α_m'', and curve fitted α_m'' spectra of liquid toluene between 1350 and 990 cm^{-1}. Bottom - The prominent CDHO bands in this region that were used to fit the experimental α_m'' spectrum. Strong contributions from bands outside the region can be seen as tails on both ends of the region. Units for both boxes are cm^3 mole^{-1}.

The intensity assignments of ν_{25}, ν_{26}, ν_6, ν_7, ν_{27}, ν_{28}, ν_8 and ν_9 are straightforward. They are assigned the intensities of the single CDHO bands at 1332, 1313, 1210, 1179, 1156, 1081, 1030 and 1002 cm^{-1}, respectively. In section 4.5.5, ν_{36} and ν_{39} were both assigned to the same wavenumber at 1040 cm^{-1}. Two CDHO bands were used in the fit, one at 1042.6 and a sharper band at 1040.2 cm^{-1}. Their intensities are arbitrarily assigned to ν_{36} and ν_{39}, respectively. Their combined intensity will be compared with literature values.

The experimental intensity of ν_{25} was discussed with that of ν_{32} in section 5.2.1b. Galabov gave No experimental $A_{j,exp}$ are given for ν_6, ν_7, ν_9, ν_{26}, and ν_{27}. Boggs'[26] reported *ab initio* values are smaller than our $A_{j,gas}$ by factors of 12.7, 3.7, 2.4, 8.7 and 8.7, respectively for these weak vibrations.

$A_{j,gas}$ of ν_{28}, is 4.11 km mole^{-1} and is in good agreement with Galabov's[29] $A_{j,exp}$ of 4.30 km mole^{-1}. Boggs'[26] calculated value is 3.70 km mole^{-1}, about 11% smaller than our value.

Galabov[29] gives the combined intensity of ν_{36}, ν_{39} and ν_8 as 2.67 km mole^{-1}. Our $A_{j,gas}$ values are 5.91 km mole^{-1} for ν_{36} and ν_{39} combined and 2.06 for ν_8, for a total of 7.97 km mole^{-1}. Boggs'[26] *ab initio* values for these vibrations are 9.26 and 1.41 km mole^{-1} for a total of 10.67 km mole^{-1}, about 35% greater than our total value.

5.2.1d - Integrated intensities of the ν_{10}, ν_{12}, ν_{13}, ν_{15} and ν_{16} vibrations

The experimental α_m'' and curve fitted α_m'' spectra of liquid toluene between 990 and 750 cm^{-1} are shown in Figure 5.13. The fit in this region is not as good as in other regions probably because the absorption is extremely weak. The area under the curve fitted α_m'' is greater by 3.8% than the area under the experimental α_m'' spectrum. The large difference which can be seen in Fig 5.13 at the low wavenumber edge of the region, is mainly due to the strong bands at 730 and 695 cm^{-1}. Peak heights are reproduced on average to 1.5% with only one peak, that of ν_{10} at 786 cm^{-1}, exceeding this value with 4.3%.

The intensities of the single CDHO bands at 981, 964, 895, 843 and 786 cm^{-1}, are assigned to ν_{15}, ν_{12}, ν_{16}, ν_{13} and ν_{10}, respectively. ν_{12} and ν_{13} are A_2 vibrations and as such are inactive in the infrared spectrum of the gas, so their intensities were not given by Galabov[29] and were given as 0.00 by Boggs[26].

The $A_{j,gas}$ values for the two B_1 vibrations, ν_{15} and ν_{16}, are about equal at 0.91 and 0.99 km mole^{-1}. Boggs reported *ab initio* values that are much smaller and less equal, namely 0.02 and 0.39 km mole^{-1} for ν_{15} and ν_{16}.

$A_{j,gas}$ for ν_{10} is 0.27 km mole^{-1} and, considering the weakness and the far from perfect fit of this band (FIg. 5.13) is in good agreement with Boggs' $A_{j,ab\ in}$ value, 0.35 km mole^{-1}.

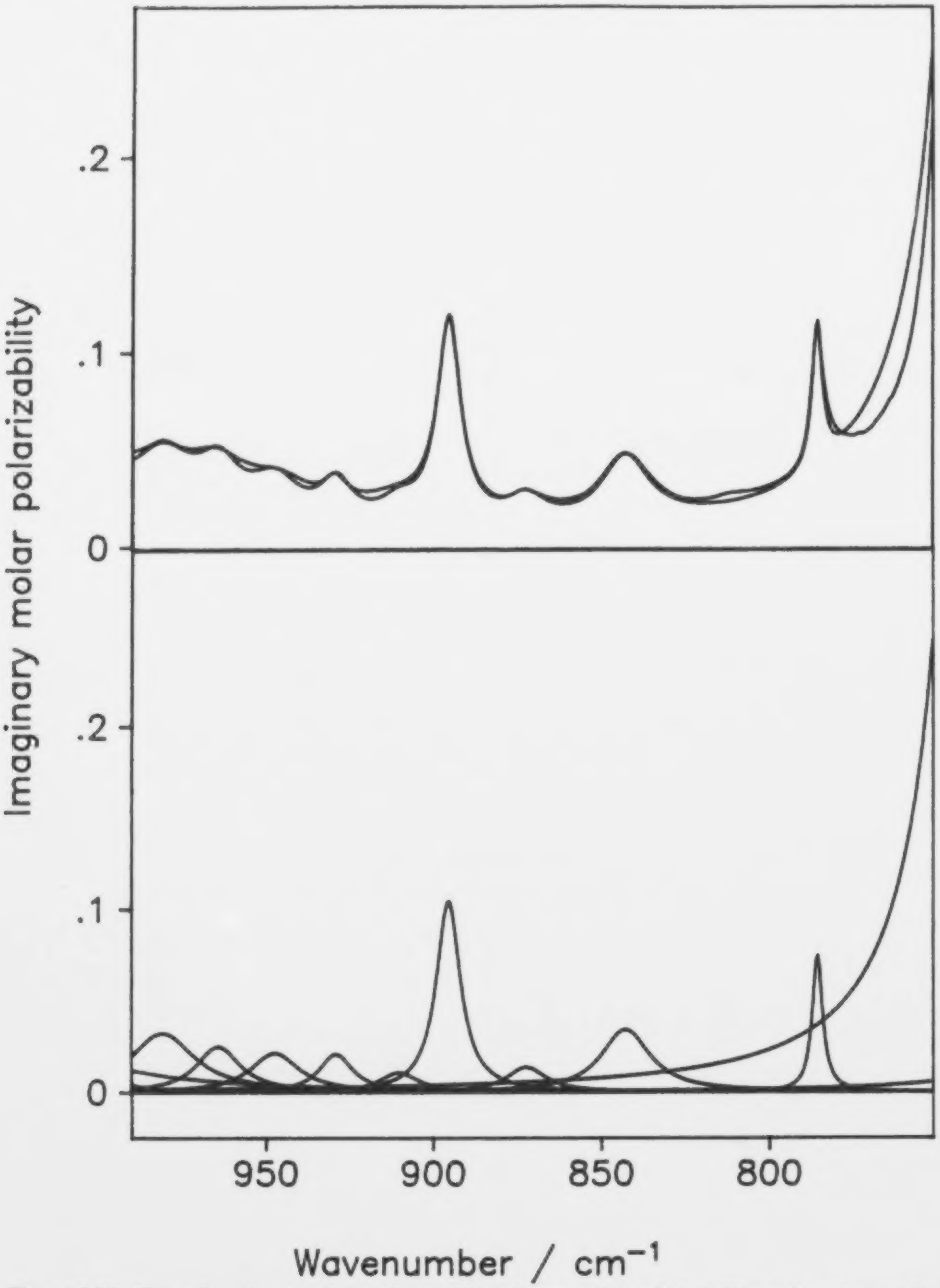

Figure 5.13 - Top - Superimposed experimental imaginary molar polarizability, α''_m, and curve fitted α''_m spectra of liquid toluene between 990 and 750 cm^{-1}. Bottom - The prominent CDHO bands in this region that were used to fit the experimental α''_m spectrum. Strong contributions from the strong bands at 730 and 695 cm^{-1} is clearly visible. Units for both boxes are cm^3 mole^{-1}.

5.2.1e - Integrated intensities of the ν_{17} and ν_{18} vibrations

The experimental α''_m and curve fitted α''_m spectra of liquid toluene between 750 and 650 cm^{-1} are shown in Figure 5.14. The fit in this region is good except for the wings of the strong band at 730 cm^{-1}. Here, and elsewhere, the experimental bands fall off slightly faster than the CDHO bands, undoubtedly due to a small Gaussian contributions. This accounts for the area under the fitted curve being greater by 2.1% than the area under the experimental α''_m spectrum. The peak height of ν_{17} is reproduced to 1.2% and that of ν_{18} to 0.1%.

Three CDHO bands, all within 5 cm^{-1}, were needed to fit the strong band at 695 cm^{-1} and their combined intensity is assigned to ν_{18}. Only one CDHO band was needed for the stronger band at 730 cm^{-1}. The fit in the wings was not improved by the addition of extra CDHO bands.

$A_{j,gas}$ for ν_{17} is 61.35 km mole^{-1} and for ν_{18} is 17.02 km mole^{-1} (Table 5.4). Boggs'[26] *ab initio* intensities for these two vibrations are 47.18 and 27.99 km mole^{-1}, respectively. Although the values for each vibration are different the combined intensities differ by less than 5% (78.37 to 75.17 km mole^{-1}). Galabov's[29] experimental value is 40.96 km mole^{-1} for ν_{17} and ν_{18} combined and also includes the intensities of ν_{10} (at 785 cm^{-1}) and ν_{29} (at 622 cm^{-1}) as well, although according to his theoretical calculations the calculated results of his fitting procedure indicated that their contributions are small.

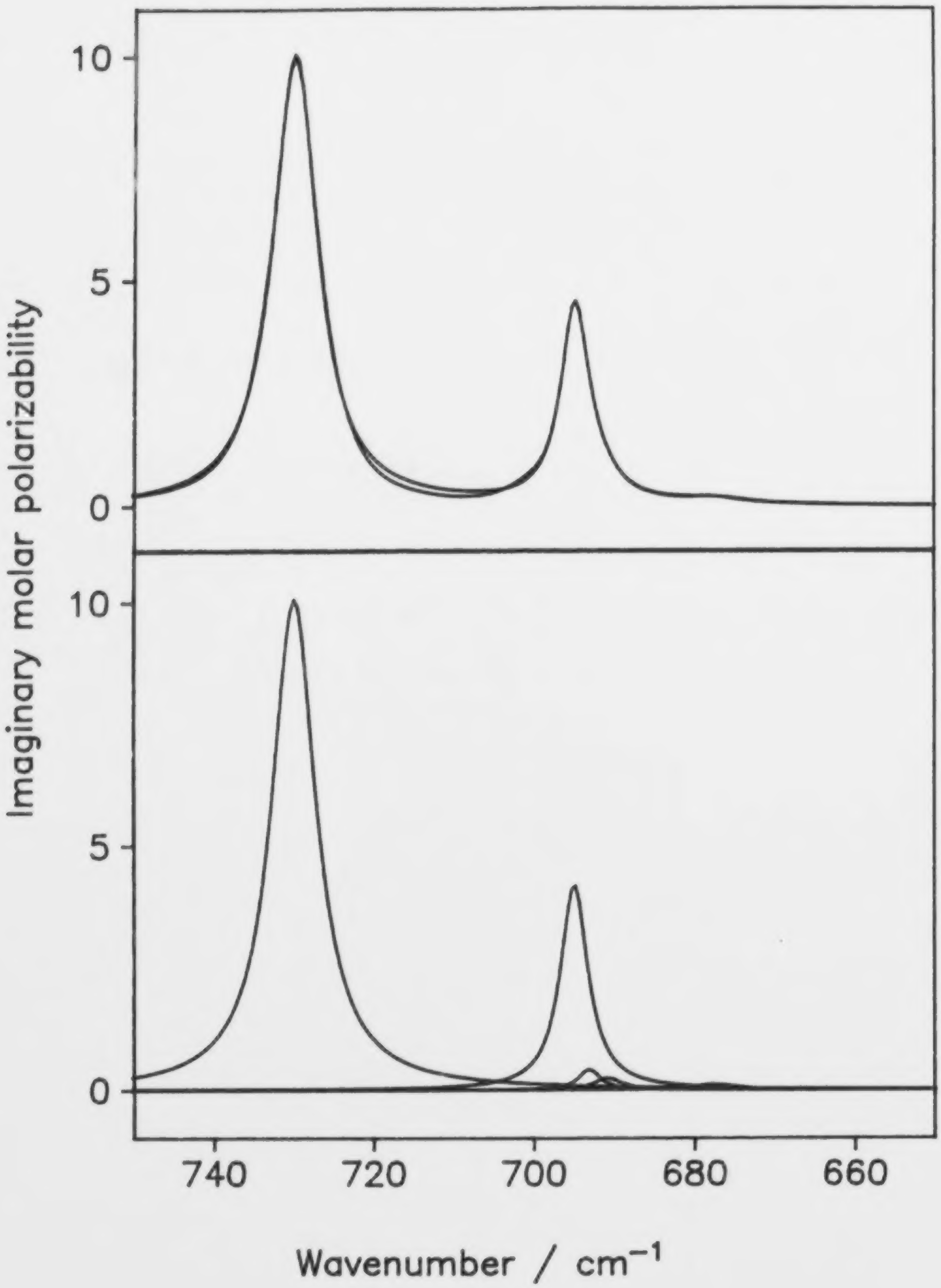

Figure 5.14 - Top - Superimposed experimental imaginary molar polarizability, α''_m, and curve fitted α''_m spectra of liquid toluene between 750 and 650 cm^{-1}. Bottom - The prominent CDHO bands in this region that were used to fit the experimental α''_m spectrum. Units for both boxes are cm^3 mole^{-1}.

5.2.1f - Integrated intensities of the ν_{11}, ν_{14}, ν_{19}, ν_{20}, ν_{29}, ν_{30} and ν_{33} vibrations

The experimental α_m'' and curve fitted α_m'' spectra of liquid toluene between 650 and 440 cm^{-1} are shown in Figure 5.15. The area under the curve fitted α_m'' is greater by 3.8% than the area under the experimental α_m'' spectrum. Peak heights of fundamentals are reproduced on average to 1.05%.

The wavenumbers of ν_{14}, ν_{20}, ν_{30} and ν_{33} are below the experimental range studied in this work, and, thus, no intensities were obtained for them.

The intensity of the CDHO band at 621.9 cm^{-1} is assigned to ν_{29}. Its $A_{j,gas}$ is 0.13 km mole^{-1}, which is small but in good agreement with Boggs'[26] *ab initio* value of 0.09 km mole^{-1}.

The intensity of the CDHO band at 521.0 cm^{-1} is assigned to ν_{11}. Its $A_{j,gas}$ value of 0.23 km mole^{-1} is about 3 times smaller than Boggs'[26] value 0.77 km mole^{-1}. The intensity of the CDHO band at 464.4 cm^{-1} is assigned to ν_{19}. Its $A_{j,gas}$ of 8.69 km mol^{-1} is in good agreement with Boggs' reported $A_{j,ab\ in}$ of 8.47 km mole^{-1}. Galabov[29] gives the combined experimental intensity of ν_{11} and ν_{19} as 6.24 km mole^{-1}.

5.2.2 - Summary of intensity assignments of toluene

The assignments in the previous sections are summarized in Table 5.4, with the intensities from the literature. As noted previously, in order to compare our results for the liquid with the computed, fitted or measured values for the gas, the C_j values (Eq.

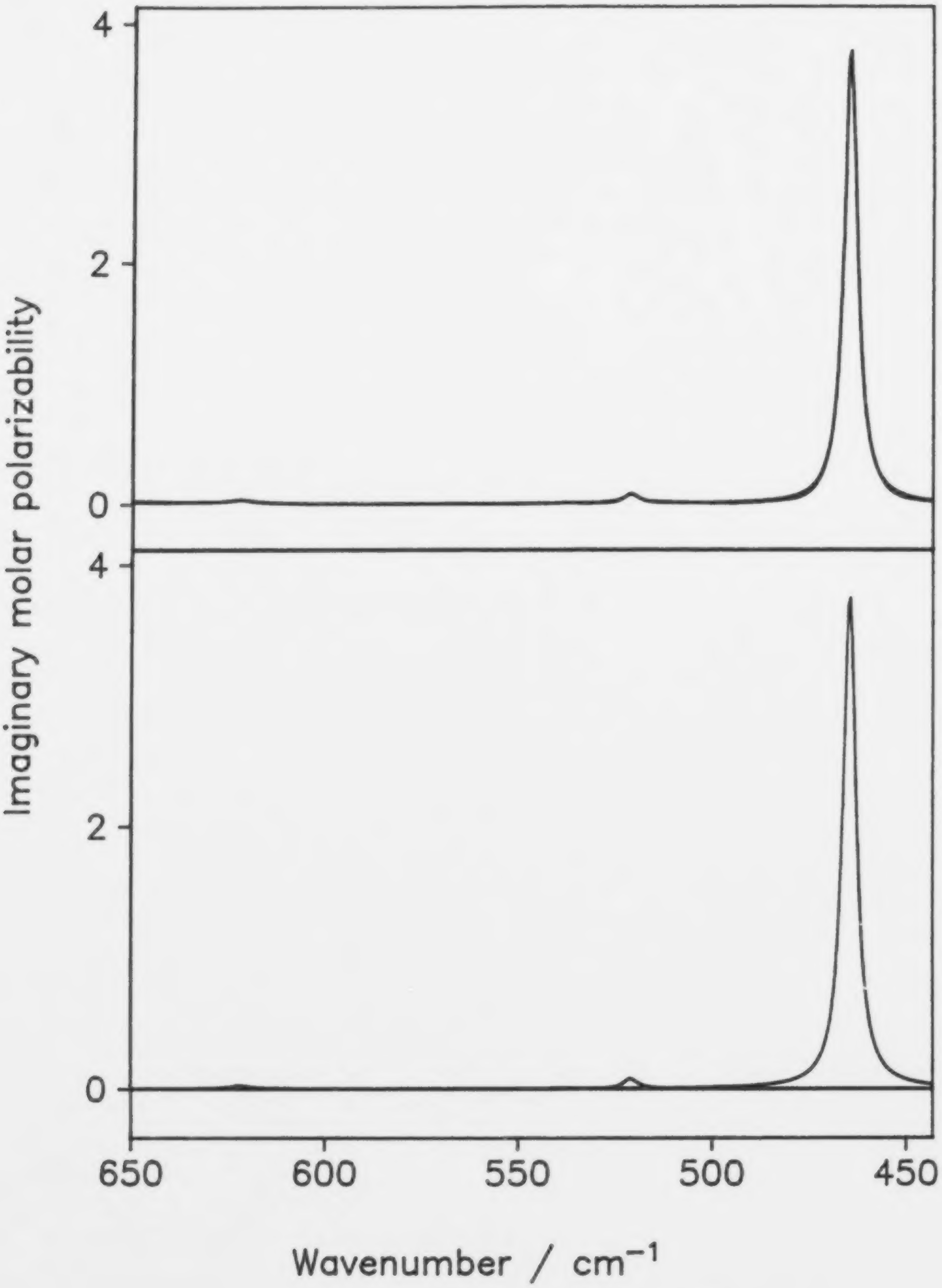

Figure 5.15 - Top - Superimposed experimental imaginary molar polarizability, α''_m, and curve fitted α''_m spectra of liquid toluene between 650 and 442 cm^{-1}. Bottom - The prominent CDHO bands in this region that were used to fit the experimental α''_m spectrum. Units for both boxes are cm^3 mole^{-1}.

1.4.2) assigned for the liquid were converted to A_j values (Eq. 1.4.1) for the gas by multiplying them by $8\pi^2$, i.e, by 78.96 (Eq. 5.1.4). This conversion gives the A_j intensity the gas molecules would have if the intrinsic intensity of the vibration were the same in the gas and liquid phases.

In this section, the A_j values are used to compare the present and literature measurements. Boggs' values[26] are from *ab initio* calculations of isolated molecules, and it is of interest to observe how well such calculations agree with the values measured for the liquid. Galabov[29] gives two sets of values, those measured for gaseous molecules and those calculated through the eigenvectors obtained from normal coordinate calculations from the dipole moment parameters calculated by fitting the measured intensities. His experimental values are the most fundamentally valuable. Unfortunately, the many studies of the intensities of gaseous benzene have shown that experimental gas phase intensities are difficult to measure and are frequently not very reproducible between laboratories. In the case of benzene, the agreement between $A_{j,gas}$ values of the four infrared active fundamentals from different laboratories of is within ±15% for each band.[84]

The vibrations of the phenyl group are considered first. Four of these, ν_3, ν_{14}, ν_{20} and ν_{30} were not measured in this work, and ν_{12}, ν_{13} and ν_{14} have A_2 symmetry and are not infrared active in the gas. Of the remaining 24 vibrations, 12 have intensity $A_{j,gas}$ greater than 2.0 km mole^{-1} and 12 have intensity less than 2.0 km mole^{-1}.

Of the 12 more intense bands, the *ab initio* calculated intensities agree with the observed intensities for the liquid to better than a factor of 2 for all except ν_2, ν_{21} and ν_{22}. In the case of the B_1 CH stretching modes, ν_{21} and ν_{22}, the sum of their intensities agrees with the sum calculated by Boggs to well within a factor of 2, and in fact the individual intensities agree within a factor of 2 if the assignments are reversed. It seems most probable that this difference is due to differences in the calculated wavenumbers or eigenvectors, rather than to a difference in the simplest molecular intensity quantities, the dipole moment derivatives. ν_2 is also a CH stretching mode, of symmetry A_1. However, neither the addition of the intensities of ν_1, ν_2 and ν_3, nor any interchange of assignments, improves the agreement with the *ab initio* values to within a factor of 2 for these A_1 CH stretching modes.

There are 12 vibrations with $A_{j,gas}$ intensities less than 2 km mole^{-1}, and 10 of them differ by a factor of 2 or more from the *ab initio* results. This is not a surprising result, given the weakness of the bands and the imperfection of the experiments, assignments, and calculations.

Overall, the agreement between the experimental and *ab initio* results is very good, sufficiently good to indicate fairly clearly that the liquid forces do not cause the gas phase intensities to change in a major way for these liquids which do not interact strongly in solution.

The question of the extent to which the individual vibrational intensities actually do change between the gas and liquid phase is a more detailed question that requires a

Table 5.5 - Experimental integrated intensities of toluene

ν_j	A_j [a,b] This work	A_j [a,b] Galabov et al[29]
ν_1, ν_2, ν_3	11.8	26.5
ν_{21}, ν_{22}	31.3	38.2
ν_{31}	11.8	11.1
ν_{34}, ν_{37}	13.2	18.5
ν_4, ν_{23}	6.1	7.3
ν_5	12.6	14.9
$\nu_{24}, \nu_{35}, \nu_{38}$	19.7	6.5
ν_{25}, ν_{32}	4.3	3.1
ν_{28}	4.1	4.3
$\nu_{10}, \nu_{17}, \nu_{18}, \nu_{29}$	79	41
ν_{11}, ν_{19}	8.9	6.2

a- $A_{j,gas}$ values for this work are taken from column 5 of Table 5.4, and Galabov's experimental values are taken from column 8 of Table 5.4.

b- Units are km mole^{-1}.

comparison of actual measured intensities. For this we compare our $A_{j,gas}$ values in column 5 of Table 5.4 with Galabov's 11 measured values in column 8. Because many of Galabov's values are for the sum of several vibrations, Table 5.5 conveniently compares them with appropriate sums of our $A_{j,gas}$ values. It is clear that there are cases of excellent agreement, that in the majority of cases the values lie within a factor of 2, and that there are many cases of significant disagreement.

As noted above, there are uncertainties in our intensity assignments, but the intensities of the major bands are believed to be accurate to a few percent. Although there is no intention to question the care with which Galabov *et al.* did their measurements, it must be noted that they provided no spectra or other evidence to allow readers to judge the probable accuracy of their experimental values. The fact that there are many factors that can introduce error into the measurement of intensities of gases suggests that it is wisest to await other measurements of the gas phase intensities before any attempt is made to interpret these differences.

5.3 - Comparison of integrated intensities of liquid chlorobenzene and liquid toluene

As discussed in Chapter 4, it is not possible to describe the fundamental vibrations of chlorobenzene and toluene as arising from a single symmetry coordinate of benzene. The majority of the vibrations are rather due to mixture of coordinates. Nevertheless, as the wavenumbers of many fundamentals of the two compounds do not differ by more than 15 cm^{-1}, it is interesting to compare the integrated intensities of liquid chlorobenzene and toluene because the two compounds have the same molecular skeleton with the exception of the chlorine atom and the methyl group.

Table 5.6 lists the integrated intensities, $C_{j,liq}$, of the fundamentals of chlorobenzene, the 30 phenyl group fundamentals of toluene and some of the fundamentals of benzene. The values for the first two liquids are from Tables 5.2 and 5.4, and those of benzene are taken from Ref. 73. The assignment for chlorobenzene and toluene is given first, followed by the wavenumber and intensities $C_{j,liq}$ for these liquids. This is followed by the ratio of the $C_{j,liq}$ of the two liquids, and the

Table 5.6 - Integrated intensities of liquid chlorobenzene, toluene and benzene

	Chlorobenzene		Toluene			Benzene [Ref. 73]		
ν_j [a]	cm^{-1} [b]	$C_{j,liq}$ [c]	cm^{-1} [b]	$C_{j,liq}$ [c]	$\frac{C_{j\ C6H5Cl}}{C_{j\ C6H5CH3}}$	cm^{-1} [b]	ν_j [d]	$C_{j,liq}$ [c]
ν_1, ν_2, ν_3, ν_{21}, ν_{22} [e]	~3070 [e]	0.119 [e]	~3060 [e]	0.546 [e]	0.22 [e]	~3040 [e]	ν_{12} [e]	0.539 [e]
ν_4	~1592 [f]	0.187 [g]	1605	0.0775 [g]	2.4	1586	ν_{16}	0.00782
ν_{23}	1584		1587					
ν_5	1478	0.354	1496	0.160	2.2	~1475	ν_{13}	~0.25 [i]
ν_{24}	1445	0.127	1460 [h]	0.250 [h]	0.51			
ν_5 and ν_{24}		0.481		0.410	1.17			
ν_{25}	1325	0.00270	1332	0.00174	1.55	~1345 [j]	ν_3	
ν_6 [k]	1172	0.0167	1179	0.0103	1.62	1177	ν_{17}	0.0233
ν_{27}	1156	0.00632	1156	0.0219	0.29			
ν_6 and ν_{27}		0.0230		0.0322	0.71			
ν_{28}	1068	0.0359	1081	0.0521	0.69	1037	ν_{14}	0.130
ν_8	1023	0.117	1030	0.0261	4.5			
ν_{28} and ν_8		0.153		0.0782	2.0			
ν_9	1002	0.0206	1002	0.00394	5.2	1010	ν_6	0.00500
ν_{15}	983	0.00498	981	0.0115	0.43	971	ν_{19}	0.0163
ν_{12}	964	0.00852	966	0.00591	1.44			
ν_{15} and ν_{12}		0.0135		0.0174	0.78			
ν_{16}	903	0.0446	895	0.0126	3.5	850	ν_{11}	0.0155
ν_{13}	830	0.00968	843	0.00783	1.24			
ν_{16} and ν_{13}		0.0543		0.0204	2.7			
ν_{17}	741	0.809	730	0.777	1.04	703 [j]	ν_8	
ν_{18}	685	0.217	695	0.216	1.00	675	ν_4	1.275
ν_{29}	614	0.00280	622	0.00161	1.74	606 [j]	ν_{18} [l]	
ν_{19}	468	0.0983	464	0.110	0.89	403	ν_{20}	0.00087
ν_{14}	~400	0.00621	~405	----- [m]				

Table 5.6 - Continued

	Chlorobenzene		Toluene			Benzene [Ref. 73]		
ν_j [a]	cm^{-1} [b]	$C_{j,liq}$ [c]	cm^{-1} [b]	$C_{j,liq}$ [c]	$\frac{C_{j\ C6H5Cl}}{C_{j\ C6H5CH3}}$	cm^{-1} [b]	ν_j [d]	$C_{j,liq}$ [c]
x-sensitive								
ν_{26}	1270	0.00892	1312	0.00331	2.7	1310	ν_9 ? [n]	0.00342
ν_7 [k]	1084	0.298	1210	0.00480	62.1		? [n]	
ν_{10}	702	0.187	786	0.00337	55.5	993	ν_2 ? [n]	0.00642
ν_{11}	415	0.0185	521	0.00297	6.2	606 [i]	ν_{18} [ℓ]	
ν_{30}	297	----- [m]	345	----- [m]		1148	ν_{10} ? [n]	
ν_{20}	196	----- [m]	217	----- [m]		994	ν_7 ? [n]	

a - Assignments for chlorobenzene and toluene.

b - Observed wavenumber in the imaginary molar polarizability spectrum of the liquid.

c - Units are km mole^{-1}.

d - Assignments were taken from Ref. 73. Correlation between vibrations of benzene and those of chlorobenzene and toluene is based on wavenumber proximity and symmetry species.

e - The integrated intensities of the aromatic CH stretching vibrations are taken collectively. In benzene, $C_{j,liq}$ is assigned to the active vibration ν_{12}. 3 inactive vibrations, ν_1, ν_5 and ν_{15} are also assigned wavenumbers in the proximity of ν_{12}.

f - The wavenumber of the CDHO band assigned to ν_4.

g - Combined intensity for ν_4 and ν_{23}.

h - The same wavenumber was assigned to ν_{24}, ν_{35} and ν_{38}. $C_{j,liq}$ of the CDHO band at 1460 cm^{-1} is given.

i - Average value of the two values given in Ref. 73.

j - Wavenumber not observed in the spectrum and taken from Painter and Koening[85].

k - ν_6 in chlorobenzene is ν_7 in toluene and vice versa.

ℓ - The degenerate ν_{18} vibration in benzene was correlated with ν_{29} and ν_{11} in chlorobenzene and toluene.

m - Wavenumber below the experimental range of this study. thus, no integrated intensity is available.

n - Uncertain correlation between the benzene vibration and those of chlorobenzene and toluene.

wavenumber, assignment and $C_{j,liq}$ for benzene are given in the last three columns. It should be noted that ν_{11} to ν_{20} are degenerate vibrations in gaseous benzene that are each split in C_{2v} molecules into two vibrations. A tentative correlation between the vibrations of benzene and those of chlorobenzene and toluene has been made in Table 5.6 based on wavenumbers and symmetry species of the fundamentals of the three compounds.

Of the 30 vibrations, the wavenumbers of 24 vibrations are not sensitive to the different group substitution, in that their wavenumbers in chlorobenzene and toluene differ by less than 15 cm^{-1}. The integrated intensities of these vibrations are listed in order of decreasing wavenumber. Six vibrations can be considered X-sensitive[37], in that the different substitutions cause the wavenumbers to be more than 15 cm^{-1} apart. The integrated intensities for these six vibrations are given at the end of the table.

The ratio, $\frac{C_{j\,C6H5Cl}}{C_{j\,C6H5CH3}}$, gives an indication whether the intensity of a fundamental vibration in liquid chlorobenzene is significantly different from that in liquid toluene. For qualitative evaluation, a difference is not considered significant if the ratio of the integrated intensities is $0.5 < \frac{C_{j\,C6H5Cl}}{C_{j\,C6H5CH3}} < 2.0$, i.e. the intensities differ by less than a factor of 2.

For the vibrations under 990 cm^{-1} that are not sensitive to substitution, it is found that for 6 out of 8 vibrations $0.5 < \frac{C_{j\,C6H5Cl}}{C_{j\,C6H5CH3}} < 2.0$. Thus, for these 6 vibrations, the change in intensity between the two molecules is not significant.

The two exceptions are ν_{15} and ν_{16}, where the ratios are 0.43 and 3.5. The difference in ν_{15} can be explained when the splitting of the degenerate ν_{19} in benzene is considered. ν_{19} in benzene is assigned to 971 cm^{-1} and is split in C_{2v} molecules into ν_{15} (~982 cm^{-1}) and ν_{12} (~965 cm^{-1}). The ratio for the combined intensities for these vibrations in chlorobenzene and toluene is 0.78. Thus, it appears that a different distribution of intensities occurs in chlorobenzene and toluene but the total intensity does not change significantly.

The ratio for the combined intensities of ν_{16} and ν_{13} which result from the split of ν_{11} in benzene is 2.7. The total intensity increases from 0.0155 km $mole^{-1}$ in benzene to 0.0204 km $mole^{-1}$ in toluene to 0.0543 km $mole^{-1}$ in chlorobenzene. The individual ratios for ν_{16} and ν_{13} are 3.5 and 1.24. Thus, the intensity of ν_{16} changes significantly upon substitution.

The non sensitive vibrations above 990 cm^{-1}, largely derive from the splitting of degenerate modes in benzene, except ν_{25} and ν_9. The intensity of ν_{25} does not change significantly between chlorobenzene and toluene, while that of ν_9 in chlorobenzene is 5.2 times more intense than in toluene and 4.1 times more intense than the corresponding intensity in benzene (ν_6).

There are three pairs of vibrations, in which the intensity distribution among the two vibrations that result from the splitting of a degenerate vibration in benzene is significantly different in chlorobenzene and toluene. Yet, the ratio of the combined intensities does not indicate a significant difference. These vibration pairs are: ν_5 and

ν_{24}, which arise from ν_{13} in benzene, ν_6 and ν_{27}, which arise from ν_{17} in benzene and ν_{28} and ν_8, which arise from ν_{14} in benzene.

A fourth pair, ν_4 and ν_{23}, shows significant change, as $C_{j,liq}$ of chlorobenzene is 2.4 greater than that of toluene which is itself about 10 times greater than the intensity of ν_{16} the corresponding degenerate vibration in benzene.

The combined intensities $C_{j,liq}$ of the aromatic CH stretching vibrations in toluene, ν_1, ν_2, ν_3, ν_{21} and ν_{22}, is 0.546 km mole^{-1} which is very similar to the intensity assigned to the infrared active vibration in benzene[73], ν_{12}, at 0.539 km mole^{-1}. It is greater by a factor of 4.6 than the corresponding intensity of chlorobenzene. It appears that the chlorine substitution shifts intensity from the CH stretching vibrations to other vibrations.

Of the six X-sensitive vibrations which have wavenumbers that differ by more than 15 cm^{-1} in chlorobenzene and toluene, ν_{30} and ν_{20}, are below the experimental range of the study, so no integrated intensities are available. The ratios $\frac{C_{j\,C6H5Cl}}{C_{j\,C6H5CH3}}$ were calculated for the other four vibrations, ν_{26}, ν_7, ν_{10} and ν_{11} and all showed integrated intensities in liquid chlorobenzene that are significantly greater than those in toluene, by factors of 2.7, 62.1, 55.5 and 6.2, respectively. It is quite possible that the gain in intensity in these vibrations, and in particular ν_7 and ν_{10}, is associated with the presence of the electronegative chlorine and with the loss of intensity of the CH stretching vibrations.

A satisfactory further analysis of these intensity differences between benzene, chlorobenzene and toluene requires a combination of *ab initio* calculations and a simple normal coordinate analysis for these molecules. These calculations will allow proper account to be taken of the different combinations of atomic displacements that occur in the normal vibrations of the different molecules, i.e., of the different eigenvectors in the different molecules, which, in turn, will allow the intensities to be analysed in terms of more basic properties such as the change in molecular dipole moment during a particular symmetry coordinate or a particular bond or angle displacement. Such calculations are not ideal for the interpretation of such data but, when guided by *ab initio* calculations, are the best that is available.

In order to understand the change caused by the reduction of symmetry from the D_{6h} of benzene to the C_{2v} of chlorobenzene and toluene without the added complication of the different chemical nature of the substituent, the intensities of C_6H_5D have been measured in this laboratory. Thus, a further analysis of the data presented in this thesis will be made in the future with the wavenumber and intensity values of liquid C_6H_6, C_6D_6, C_6H_5D, C_6H_5Cl, and $C_6H_5CH_3$.

Chapter 6 - A simple and effective approximate method for the calculation of infrared optical constant spectra of liquids from transmission measurements*

6.1 - Introduction

Earlier papers from this laboratory reported the absolute infrared absorption intensities of four liquids, benzene[1], toluene[2], chlorobenzene[3] and dichloromethane[4], obtained from transmission measurements. Intensities from this work were accepted by the International Union of Pure and Applied Chemistry (IUPAC) as secondary absorption intensity standards[5]. The purpose of this paper is to describe a much simpler but approximate computational procedure for obtaining such quantitative intensities from transmission spectra of liquids. This approximate procedure yields results of very nearly the same accuracy as the more complex but exact procedure used to date, although we recommend caution if the refractive index of the sample in non-absorbing infrared regions differs from that of the windows by more than ~0.15.

The primary result of transmission spectroscopy is the transmittance of the cell plus sample, $\frac{I_t}{I_o}$, where I_o is the intensity incident on the cell and I_t is the intensity which leaves the cell, both measured outside of the cell. For quantitative studies this is always converted to the "absorbance", by taking $-\log_{10}\{\frac{I_t}{I_o}\}$. The term "absorbance" is given in quotation marks here, because it is not the quantity that is equated with E_mCd, the product of the molar absorption coefficient, E_m, the concentration, C, and the path length through the liquid, d, in the Beer-Lambert law. The absorbance, A_{10}, as defined by IUPAC[6] and as equated with E_mCd, is a measure of energy lost from the radiation beam due solely to absorption by the sample, a liquid in our case. In contrast, the "absorbance" that is calculated as described above, and reported by the spectrometer in most transmission experiments, is a measure of the energy lost due to absorption by the sample, *plus* the energy lost due to reflection from the interfaces of the cell, *plus* the energy lost due to unexplained baseline errors.

---

* A version of this chapter has been accepted for publication. Bertie and Apelblat, Appl. Spectrosc., 1996.

The IUPAC definition[6] of absorbance, A_{10}, is used in this laboratory. The term *experimental absorbance*[7] is used for the "absorbance" calculated as described above, and the term *apparent absorbance*[7] is used for the contributions to the experimental absorbance from processes other than absorption by the sample. Thus the experimental absorbance is the sum of the absorbance, A_{10}, *plus* the apparent absorbance due to reflection *plus* the apparent absorbance due to baseline errors. It should be noted that the latter may be positive or negative.

In Refs. 1 to 4, the imaginary refractive index spectrum, $k(\tilde{\nu})$, of the liquid was calculated by an iterative procedure that fully corrects the experimental absorbance, EA, spectrum for the non-absorption processes. The real refractive index spectrum, $n(\tilde{\nu})$, and the molar absorption coefficient spectrum $E_m(\tilde{\nu})$ were calculated from the $k(\tilde{\nu})$ spectrum.

The method used previously[1-4] to correct the experimental absorbance spectrum for the apparent absorbance due to reflection losses is exact for an ideal experiment[7-9]. Thus Fresnel's equations are applied to each interface, specifically, the interface between the air and the first window, the interface between the first window and the thin liquid film, the interface between the liquid film and the second window, and the interface between the second window and the air. The interference fringes generated by multiple reflections within the liquid layer are calculated. In contrast, the calculation averages over the multiple reflections within the windows and, thus, averages over the interference fringes generated in the windows, as is appropriate for ~5mm alkali halide windows and 1 cm^{-1} resolution. Further, the calculation corrects for the convergence and polarization of the incident beam. It is a calculation that is exact in the ideal case, but is sufficiently complex to discourage new users.

In the present paper, a very simple calculation of the apparent absorbance due to reflection is presented. This greatly simplifies the correction of the experimental absorbance spectrum for the apparent absorbance due to reflection and, thus, greatly simplifies the calculation of optical constant spectra from transmission spectra. Although simpler, the method gives imaginary refractive index, *k,* values which agree within 1% with those from the exact calculation for all but the strongest infrared absorptions, provided that the real refractive indices of the sample and windows are not too different.

6.2 - Method

The *EA* spectrum of a cell full of liquid is obtained by dividing the intensity spectrum through the full cell by that through the empty sample compartment and taking the negative logarithm of the result.

$$EA = -\log_{10} T = -\log_{10} \frac{I_t(\tilde{\nu})}{I_o(\tilde{\nu})} \qquad (6.1)$$

In the method used previously[1-4], the refractive index spectra are calculated from the *EA* spectrum by program RNJ46A. The program was developed by Jones and his coworkers in the National Research Council of Canada and was later improved in this laboratory. It is described elsewhere[7-10], the algorithm is outlined in the appendix, and the salient features for the present purpose are given briefly next.

Experimental absorbance spectra are used in two parts of the procedure. In the first part, *EA* spectra of samples with several different very long path lengths are used to determine the linear absorption coefficients, $K(\tilde{\nu})$, at so-called *anchor points* in the regions of baseline absorption. $K(\tilde{\nu}) = \ell^{-1} A_{10}$, where ℓ is the path length through the liquid[6] and A_{10} is the absorbance of the sample. The K values are calculated from the *EA* spectra by program ANCHORPT.FOR which is outlined in the appendix. The baseline error is assumed to be zero in this calculation, which is a good approximation if the experimental absorbance is about 0.3 or greater and which is evaluated later by the agreement seen in the K values calculated from cells with different path lengths. With this assumption, $EA = A_{10} + AA_R$, where AA_R is the apparent absorbance due to reflection. At each anchor point AA_R is calculated exactly, by applying Fresnel's equations to each interface and using the known real refractive index of the windows, for an approximately correct value of the real refractive index of the sample.

The K values thus produced are then used in the second part of the procedure to remove the apparent absorbance due to baseline errors in spectra of samples with normal path lengths. This is done by calculating where the baseline should be at each anchor point, through $EA = K\ell + AA_R$, and shifting the spectrum to move the baseline to that correct place. Linear interpolation of the required shift is used between the anchor points.

In the second part of the procedure, the EA spectrum is used in program RNJ46A to calculate the refractive index spectra by an iterative procedure, after the baseline is corrected. During this part, the apparent absorbance due to reflection is recalculated in each iteration cycle.

In the first calculation cycle, a first approximation to the imaginary refractive index, k, spectrum is calculated. For this purpose, the reflection loss is calculated, for all wavenumbers in the EA spectrum, from the known refractive index spectrum of the windows and a constant value of the real refractive index of the sample. From the approximate k spectrum thus generated, a real refractive index spectrum, n, is calculated by a Kramers-Kronig (KK) transform. In subsequent iteration cycles, the wavenumber-dependent real refractive index spectrum of the sample is used in the calculation of the reflection losses and of the baseline-correction of the EA spectrum.

In the second part of the procedure, the n and k spectra of the sample are used with the n spectrum of the windows, to calculate the EA spectrum. The calculated and the baseline-corrected experimental EA spectra are compared, the k spectrum is adjusted to improve the fit and the n spectrum is recalculated. This cycle is repeated as the k and n spectra are refined by iteration[7-9] to convergence. The current n spectrum is used in the calculation of AA_R and the baseline correction. The convergence of the radiation beam can be included in the calculation, as can be the polarization of the beam. The latter two factors are not significant for the beam convergence and polarization in the Bruker IFS 113V spectrometer in this laboratory.

In the approximate method presented here, the reflection losses are calculated by considering that the cell is simply a single window. The transmittance of the window is given by $T(\tilde{\nu}) = \dfrac{2n(\tilde{\nu})}{n^2(\tilde{\nu})+1}$,where n is the real refractive index of the window. Thus, the apparent absorbance due to reflection losses at wavenumber $\tilde{\nu}$, $AA_R(\tilde{\nu})$ is simply

$$AA_R(\tilde{\nu}) = -\log_{10} \frac{2n(\tilde{\nu})}{n^2(\tilde{\nu})+1} \qquad (6.2)$$

The approximate method uses this simple formula in both parts of the procedure outlined above, which eliminates the need for an iterative calculation in the second part. The method is implemented in the program WIND8.FOR. The program incorporates the functions of both ANCHORPT and RNJ46A. Program WIND8 is outlined in the appendix, where its relation to ANCHORPT and RNJ46A is emphasized.

It is convenient to consider here the approximation made in this simple procedure. The discontinuity in the real refractive index at the window-liquid boundary is neglected. Fig, 6.1 shows an absorption band in the *k* spectrum and the anomalous dispersion[11] in the real refractive index, *n*, that accompanies it. The real refractive index of the liquid is not constant near an absorption band, so the neglected reflection losses are not constant. Whether these losses are greater to high or to low wavenumber of the absorption band depends on whether the (nearly constant) refractive index of the window is larger or smaller than the average *n* value of the sample through the absorption band. The size of the deviations of *n* from the average value is directly proportional to the height of the absorption band in the *k* spectrum. Thus, the simple procedure is expected to be most accurate for weak absorptions, and the largest deviations from the correct procedure are expected for strong absorptions.

The approximation involved in the simpler procedure can be seen directly in Figure 6.2, in which the bottom box shows the standard real refractive index spectrum of chlorobenzene[3,5] between 1700 and 1100 cm^{-1}, and the top and middle boxes show the apparent absorbance due to reflection that is calculated by the approximate and exact methods for two different cases.

The top box shows the case of 100 μm thick chlorobenzene between KBr windows. The refractive indices of the window and sample are very close in this case, with $n \sim 1.51$ for chlorobenzene between strong absorptions and $n \sim 1.52$ for KBr. The smooth bottom curve is that calculated from Eq. 6.2. The top curve is the result of the exact calculation, which used the standard *n* spectrum of chlorobenzene[3,5]. The

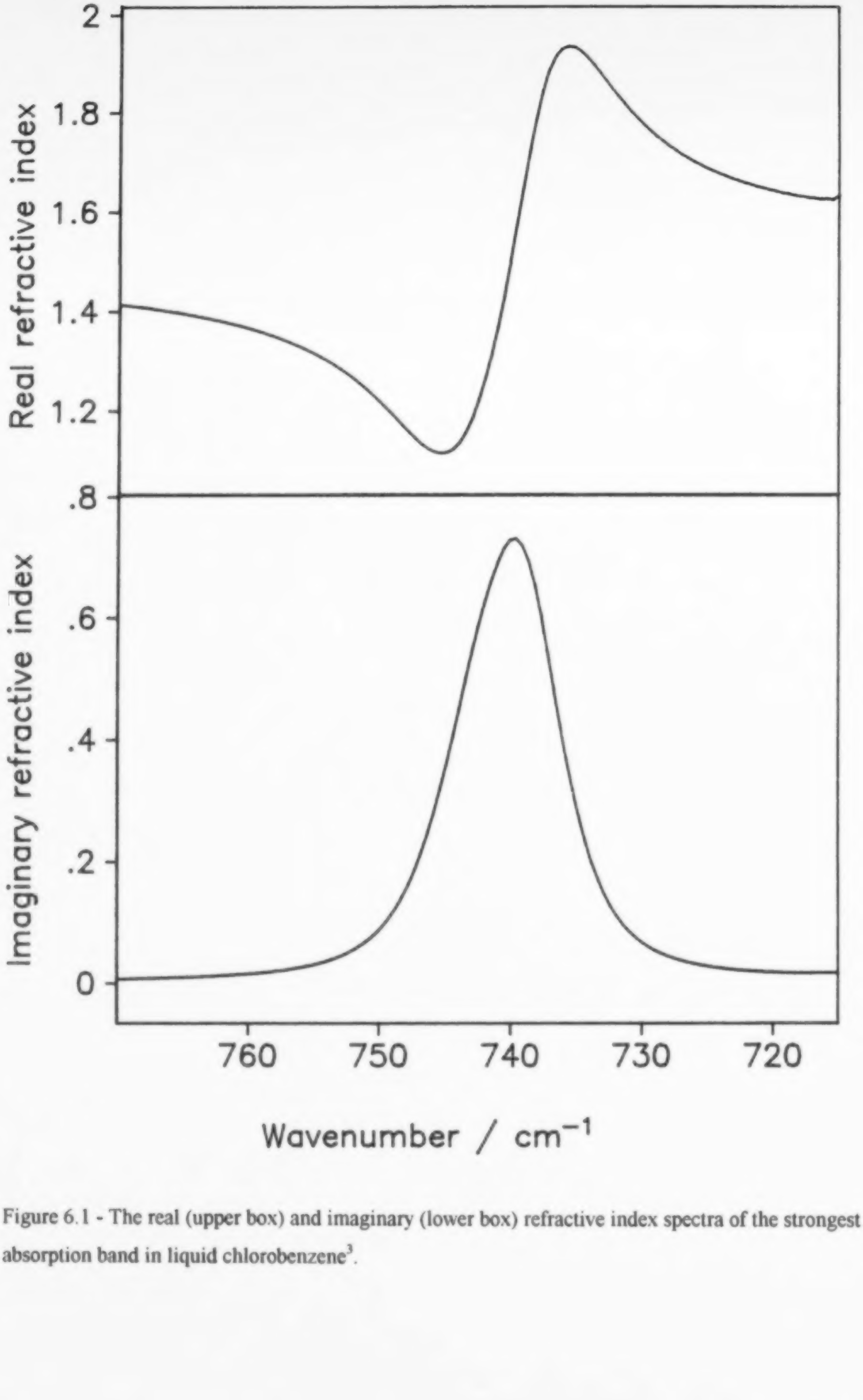

Figure 6.1 - The real (upper box) and imaginary (lower box) refractive index spectra of the strongest absorption band in liquid chlorobenzene[3].

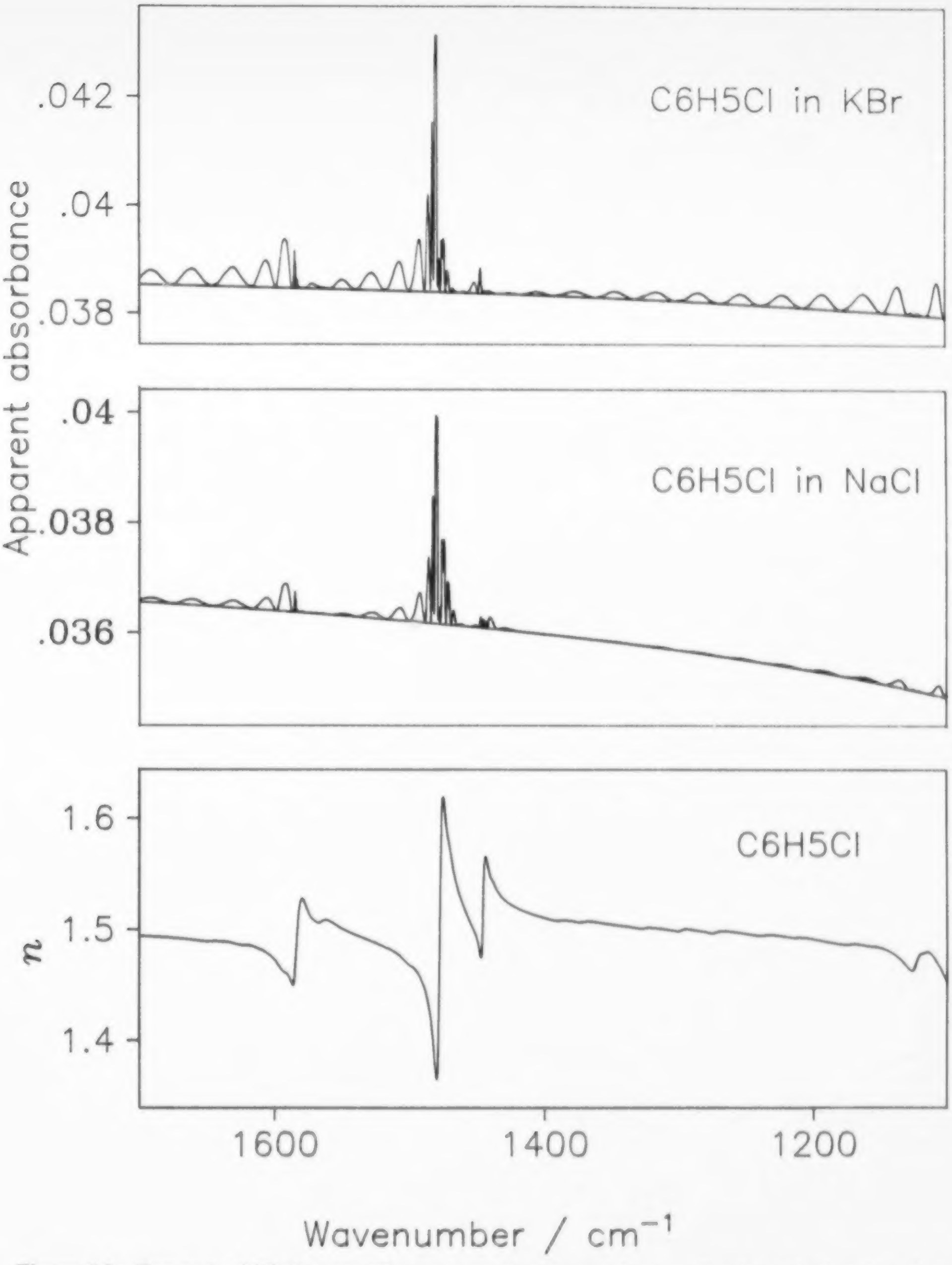

Figure 6.2 - Top and middle boxes: The apparent absorbance due to reflection calculated by the exact method (upper, featured curve) and the approximate method (lower unfeatured curve) for 100 μm of chlorobenzene(ℓ) between KBr windows (top box) and NaCl windows (middle box). Bottom box: The real refractive index spectrum of liquid chlorobenzene[3,5] at 25°C.

interference fringes arise from the multiple reflections that are ignored in the approximate method. The middle box shows the case of 100 μm thick chlorobenzene between NaCl window, for which $n \sim 1.50$, again with the smooth bottom curve being that from the approximate calculation. The effect of the refractive index of the windows is evident in the lower apparent absorbance and in the different shape of the apparent absorbance spectrum from the exact calculation. The effect of the wavenumber dependence of the refractive index of the sample is also evident, in that no interference fringes are visible in regions where the refractive indices of sample and window are very close, but fringes are visible in other regions where the refractive index of the sample is different because of the anomalous dispersion.

6.3 - Results

The *EA* spectra were processed with programs ANCHORPT and RNJ46A to calculate *k* spectra by the exact method. The same *EA* spectra were processed with program WIND8 to calculate *k* spectra by the approximate method. The *K* values at anchor points in the baseline were calculated and used to adjust the baseline in both cases; it is essential to do this for the best quantitative results. In the exact method the molar absorption coefficient, E_m, spectrum is calculated from the final, converged, *k* spectrum through

$$E_m = \frac{4\pi \tilde{\nu} k}{2.303C} \qquad (6.3)$$

where C = the molar concentration. In the approximate method the E_m spectrum is calculated directly from the absorbance spectrum (after correction for the apparent absorbance due to baseline errors and reflection losses) through

$$E_m = \frac{A_{10}}{C\ell} \qquad (6.4).$$

The approximate method was tested with spectra of chlorobenzene, several mixtures of chlorobenzene and toluene, and, to a limited extent, with spectra of acetonitrile. To demonstrate its value, results are first presented for four regions of the spectrum of liquid chlorobenzene. These are the region between 805 and 715 cm^{-1} which contains a single band of very strong absorption, and three regions which contain multiple bands of strong (1635 - 1400 cm^{-1}), medium (3200 - 2930 cm^{-1}) and weak (1405 - 1140 cm^{-1}) absorption. In Figs. 6.3 and 6.4 these regions are labeled A, B, C and D, respectively. Comparison is made of the peak heights, the areas under the $E_m(\tilde{\nu})$ spectrum, and the K values at the anchor points, that are calculated by the two methods. The peak heights and areas are compared for E_m spectra instead of for k spectra, because the molar absorption coefficient is more familiar to chemists, and because the two quantities are related by Eq. 6.3 so the percent differences are essentially the same in both cases. Note that regions B and D are in the range of Fig. 6.2, but these figures can not be compared directly because the two path lengths, and hence the interference fringe patterns, are different.

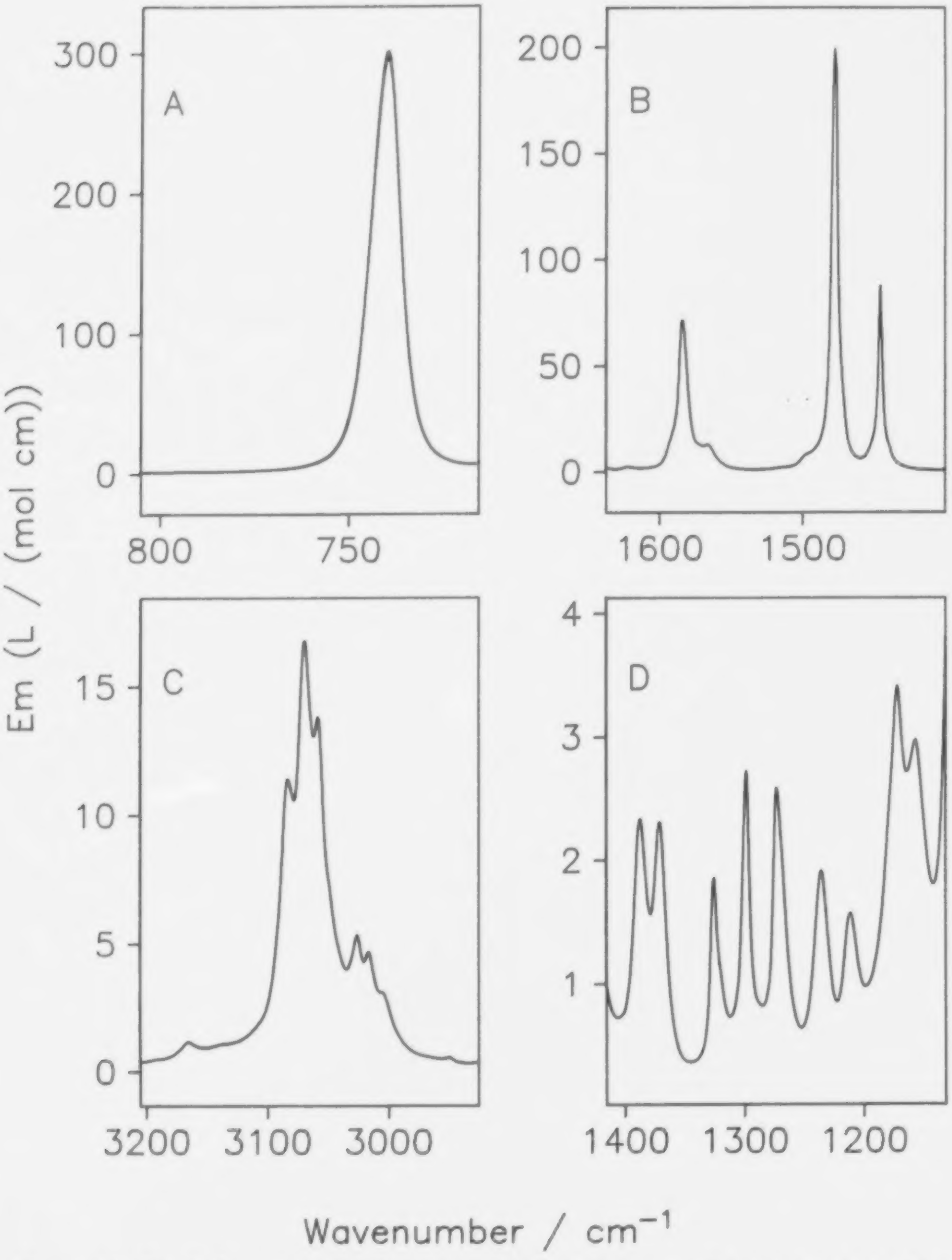

Figure 6.3 - The $E_m(\tilde{\nu})$ spectrum of chlorobenzene(ℓ) in four regions. The spectra calculated by the correct and approximate methods are shown in each box, and essentially coincide. The transmission spectra, from which these E_m spectra were calculated, were recorded with KBr windows and chlorobenzene thicknesses of: Box A 8.70 μm; Box B 11.02 μm; Box C 34.39 μm; Box D 533.0 μm.

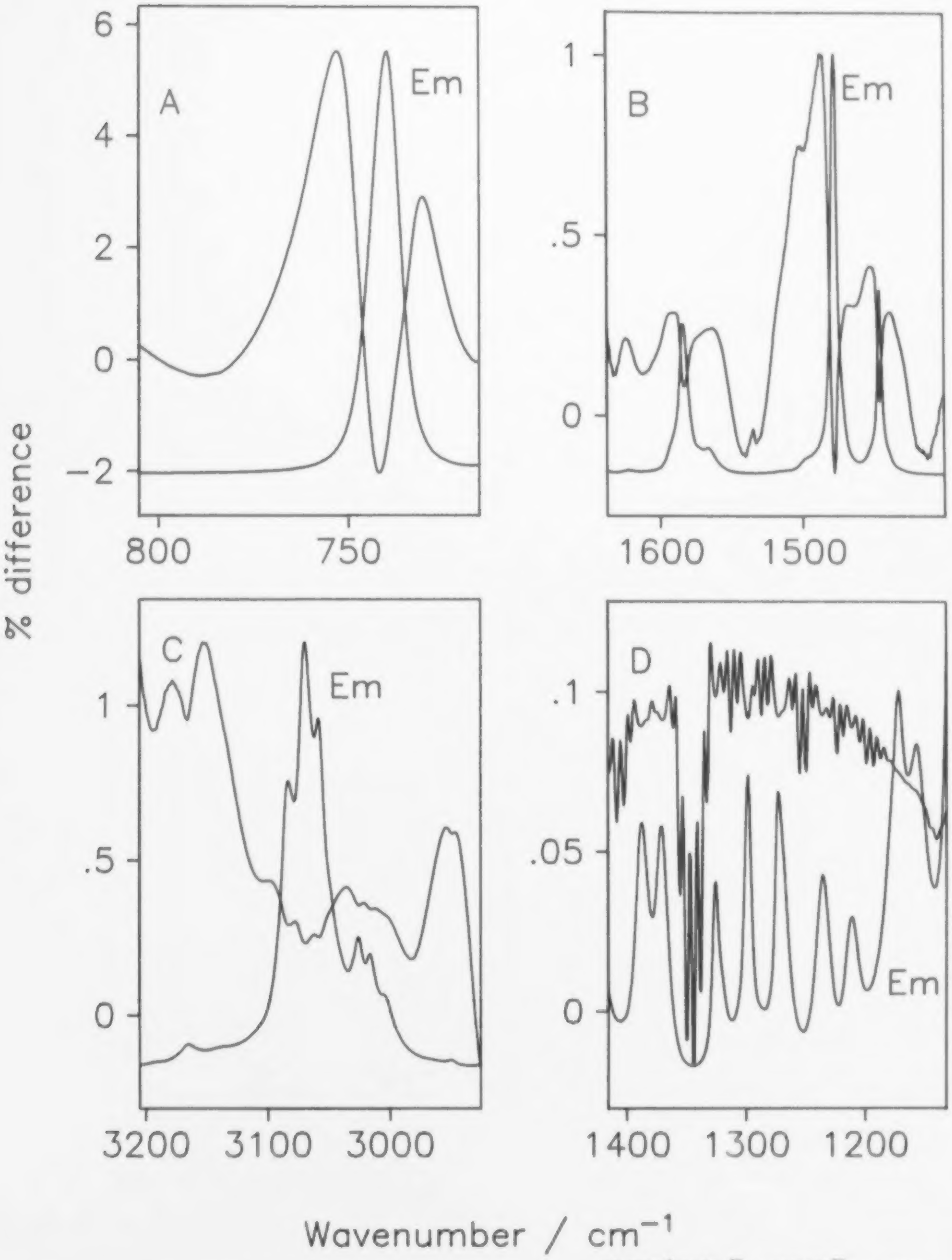

Figure 6.4 - The percent difference between the E_m spectra, $\frac{\text{approximate } E_m - \text{exact } E_m}{\text{exact } E_m} \times 100\%$, of chlorobenzene($\ell$) in the four regions of Fig. 6.3. For reference, the exact E_m spectrum is included, on an arbitrary scale, in each box.

Figure 6.3 shows the approximate and correct molar absorption coefficient spectra in the four regions. The spectra are essentially coincident. This shows that the band shapes are not much distorted by the approximate calculation. Bandshape distortion is seen more clearly in the spectra of the % difference, defined as $\frac{\text{approximate } E_m \text{ - exact } E_m}{\text{exact } E_m} * 100$. These spectra are shown in Figure 6.4 for the four regions. For reference, the exact E_m spectrum is included in each box of Fig. 6.4, on an arbitrary scale. The % difference spectra show that the line shape is slightly distorted, but the distortion is ~1% or less for all but the strong band at 740 cm^{-1}, for which the distortion reaches several percent in the wings of the band.

Values of the linear absorption coefficients at the anchor points, K, computed by the two methods are given in Table 6.1. They are averages from several spectra and their 95% confidence limits are given in parentheses. The values from the approximate method agree with those from the correct method to within 0.05%, well within the 95% confidence limits of the values. The two sets of 95% confidence limits also agree. The one exception is for the highest anchor point K value, at 717.4 cm^{-1}, which is less precise from the approximate method although its precision is still 1.2%.

The peak heights calculated by the two methods, and their percent differences, are given in Table 6.2. The peak heights agree to better than 1%, except for 1.5% for the very strong 740 cm^{-1} band.

As noted above, small changes in band shape result from the approximate

Table 6.1 - Linear absorption coefficients, $K(\tilde{\nu})$, of liquid chlorobenzene at anchor points in the baseline.

Region	Wavenumber (cm^{-1})	Approximate $K(\tilde{\nu})^a$	Exact $K(\tilde{\nu})^a$	% difference[b]
A	801.3	12.66 (8)	12.66(8)	+0.05
	717.4	65.9(8)	65.9(6)	-0.002
B	1630.5	11.65(3)	11.64 (3)	+0.03
	1534.0	9.08 (3)	9.08 (3)	+0.04
	1404.8	7.06(3)	7.06(3)	+0.05
C	3200.3	3.98(2)	3.98(2)	+0.01
	2931.2	3.15 (2)	3.15 (2)	+0.02
D	1404.8	7.06(3)	7.06(3)	+0.05
	1345.1	3.53(2)	3.53(2)	+0.01
	1251.5	6.24(3)	6.24(3)	+0.02
	1197.5	9.55(2)	9.55(2)	+0.02
	1141.6	17.7(1)	17.6 (1)	+0.04

a - The number in parentheses is the 95% confidence limit in the last digit.

b - The % difference is $\frac{\text{approximate } K\text{ - exact } K}{\text{exact } K}$ *100, calculated before the values were truncated for presentation.

method, most noticeably for the strong peak in region A, for which the anomalous dispersion in the real refractive index is large (Fig. 6.1). For this band, deviations of ~5% and ~2.5% occur on the high- and low- wavenumber sides of the band (Fig. 6.4). For lineshape studies of strong bands, the exact method is clearly preferred. The bands in region B are weaker but are still quite intense for organic compounds. For these bands the distortion is of the order of 1%, which is probably too small to be significant at the present time. The bands in groups C and D are much weaker, and the distortion within the band is well below 1%, although the error is ~1% in the baseline near 3200

Table 6.2 - Peak heights in the molar absorption coefficient spectrum, $E_m(\tilde{\nu})$, of liquid chlorobenzene.

Region	Wavenumber (cm^{-1})	Approximate $E_m(\tilde{\nu})^a$	Exact $E_m(\tilde{\nu})^a$	% difference^b
A	739.7	297.7	302.3	-1.52
B	1622.0	2.428	2.423	+0.21
	1583.8	72.89	72.82	+0.10
	1566.1	12.93	12.90	+0.23
	1477.1	199.5	199.8	-0.15
	1445.4	87.89	87.85	+0.05
C	3165.2	1.193	1.182	+0.93
	3083.2	11.46	11.43	+0.26
	3069.5	16.82	16.78	+0.24
	3058.4	13.84	13.81	+0.22
	3025.7	5.358	5.339	+0.36
	3016.3	4.699	4.683	+0.34
	2949.7	0.561	0.558	+0.54
D	1386.9	2.341	2.339	+0.09
	1370.6	2.318	2.315	+0.13
	1325.2	1.870	1.868	+0.11
	1298.0	2.733	2.731	+0.07
	1272.5	2.605	2.603	+0.08
	1235.1	1.918	1.916	+0.10
	1210.8	1.575	1.574	+0.06
	1171.5	3.413	3.411	+0.06
	1156.4	2.980	2.978	+0.07

a - The unit of E_m is L mol^{-1} cm^{-1}.

b - $\frac{\text{approximate } E_m - \text{exact } E_m}{\text{exact } E_m} * 100$.

cm^{-1} for the bands in region C.

The areas under bands in the exact and approximate $E_m(\tilde{\nu})$ spectra are given in Table 6.3. Two areas are given for each band, the area above zero ordinate and the area

Table 6.3 - Areas under the molar absorption coefficient spectrum, $E_m(\tilde{\nu})$, of chlorobenzene.

		AREA					
	Integration	Above zero ordinate[a]			Above baseline[a]		
Region	range (cm^{-1})	Approximate	Exact	% difference[b]	Approximate	Exact	% difference[b]
A	801.3-717.9	3430	3433	-0.09	3093	3096	-0.10
B	1605.4-1410.7	3226	3220	+0.20	2939	2933	+0.22
	1605.4-1545.7	949	947	+0.18	844	842	+0.20
	1530.2-1410.7	2261	2257	+0.22	2158	2153	+0.23
C	3200.3-2931.2	909	906	+0.37	810	808	+0.34
D	1405.9-1345.1	77.9	77.8	+0.09	44.9	44.8	+0.11
	1345.1-1252.5	107.3	107.2	+0.10	60.7	60.6	+0.12
	1252.5-1198.5	65.1	65.0	+0.09	21.1	21.1	+0.11
	1198.5-1141.7	127.7	127.6	+0.07	47.9	47.9	+0.08

a - The unit of area is L mol^{-1} cm^{-2}. Multiply the area by 100 to change the unit to km mol^{-1}.

b - $\frac{\text{approximate area - exact area}}{\text{exact area}}$ *100, calculated before the values were truncated for presentation.

above a linear baseline drawn between the ordinates at the integration limits. The latter is useful when the baseline intensities are not of interest. Table 6.3 shows that the exact and approximate methods yield the same areas to better than 0.4% in all ranges, and to better than 0.25% for all except the CH stretching region, 3200.3 to 2931.2 cm^{-1}. It is noteworthy that region A shows the largest differences for the peak heights and lineshapes but shows nearly the smallest difference for the areas.

Most transmission measurements in this laboratory have been made with KBr and NaCl windows. Thus the refractive index mismatch between sample and windows is usually small, because most liquids have refractive indices near 1.5. Exceptions exist, however, and the probable effect of refractive index mismatch on the usefulness of the approximate method has been explored by applying both methods to spectra of 23.26 μm of acetonitrile, n ~1.32, between KBr windows. The top box of Figure 6.5 shows the apparent absorbance due to reflection calculated by the approximate and exact methods. The approximate method fails to calculate interference fringes that are ~0.006 absorbance units peak-to-peak, about 10 times larger than for chlorobenzene between KBr. The impact of this on the molar absorption coefficients calculated by the two methods is shown in the middle and lower boxes of Fig. 6.5. The approximate method gives E_m values that are smaller than the exact values in this case, and fails to correct for the interference fringes that are visible in the *EA* spectrum but are correctly eliminated by the exact calculation. The percent difference between the E_m values from the two methods is ≤~2% near the peaks and rises to 30% in the baseline due to the neglect of the fringes. The percent difference between the areas under the peaks is 2% between 1700 and 1200 cm^{-1} and 4% between 1200 and 900 cm^{-1}.

We have not explored the effect of refractive index mismatch to a much greater extent than this, because in practice it is not common. It is clear that the effect is significant, but that acceptable accuracy in peak heights and areas for peaks of medium intensity can be obtained when, as for CH_3CN between KBr, the refractive index mismatch is ~0.2. It is recommended that results calculated with the approximate method be regarded with caution if the refractive indices of the sample and windows differ by more than 0.15.

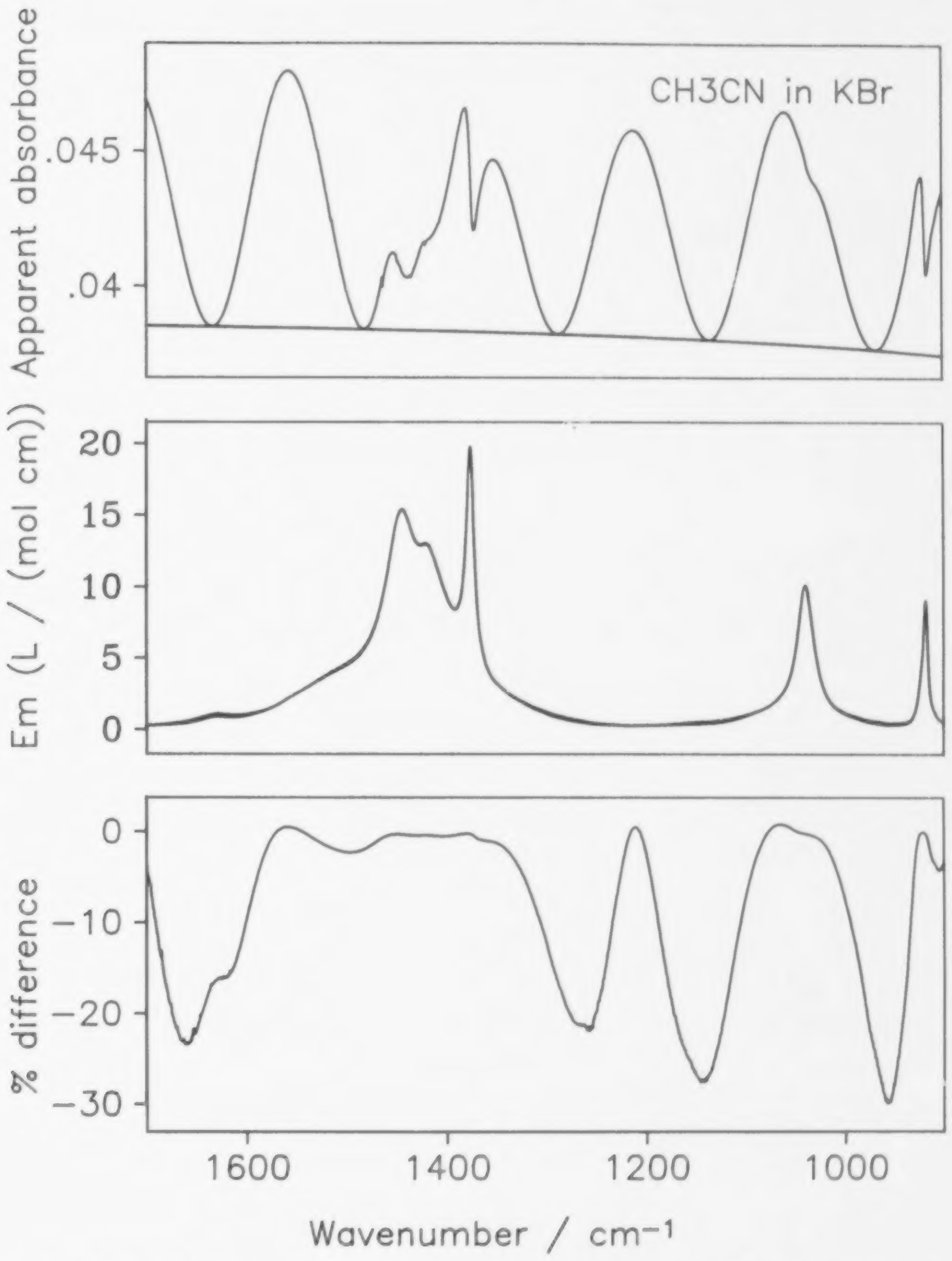

Figure 6.5 - Top box: The apparent absorbance due to reflection calculated by the exact method (upper, featured curve) and the approximate method (lower unfeatured curve) for 23.26 μm of $CH_3CN(\ell)$ between KBr windows. Middle box: The E_m spectra of $CH_3CN(\ell)$ calculated by the exact and approximate methods. Lower box: The % difference between the E_m spectra, defined as for Fig. 6.4, of CH_3CN between KBr windows. The refractive indices of $CH_3CN(\ell)$ and KBr in this spectral region are ~1.32 and ~1.52.

6.4 - Conclusions

An approximate method for the calculation of the optical constant spectra of liquids from transmission spectra is presented in this paper. The method calculates the reflection losses by treating the cell as a single window, instead of applying Fresnel's equations to each interface. In spite of this drastic approximation the method yields, for all but the strongest bands, imaginary refractive index and molar absorption coefficient values that are within ~1% of those calculated by the exact method. The line shape distortion is minimal for all but the strongest bands, and the integrated intensities agree with those from the exact method to better than 0.4% throughout. The agreement is excellent in regions of very weak baseline absorption, with the K values at the anchor points within 0.05% of those from the exact method.

This approximate method is much easier to understand and program than the more complex method, and a well written program runs much faster. It is clearly the method of choice except when one needs to obtain the exact bandshapes and peak heights without risk of distortion, and except when the spectrum contains bands whose intensities are comparable to or greater than that of the 740 cm^{-1} band of chlorobenzene. The effect of the size of the refractive index mismatch has been explored to some extent with CH_3CN between KBr windows, for which the mismatch is $\Delta n \sim 0.2$. It is recommended that results from the approximate method be regarded with caution if the refractive indices of the sample and windows differ by more than 0.15.

6.5 - Appendix I

6.5.1. - Program ANCHORPT

ANCHORPT calculates the linear absorption coefficient, $K(\tilde{\nu})$, at anchor points in the baseline from the experimental absorbance, EA, spectrum of the liquid in a cell with long path length. Usually several EA spectra recorded with different path lengths are provided, so that an average value of K can be calculated, with its precision, for each anchor point. The program contains equations from which the real refractive indices of the common window materials can be calculated at infrared wavenumbers. Other required input is: the approximate real refractive index spectrum of the liquid; the number of anchor points and their wavenumbers; for each EA spectrum, the path length and the window material.

Procedure

1. For the first anchor point wavenumber, the real refractive indices of the liquid and the windows are used to calculate the transmission of the cell full of liquid, T_{abc}, and hence the apparent absorbance due to reflection, $AA_{\mathrm{R}} = -\log_{10}(T_{\mathrm{abc}})$. T_{abc}, is calculated as in Ref. 9, corrected as described by Ohta and Ishida[12]. The equations are given in Appendix II. For this calculation it is assumed that the liquid does not absorb at the anchor point wave number.

2. K at this wave number is calculated by subtracting AA_{R} from the EA value at this wave number in the first EA spectrum, and dividing the result by the path length.

3. Steps 1 and 2 are repeated for each anchor point.

4. Steps 1 to 3 are repeated for each *EA* spectrum.

5. The average value of *K* at each anchor point is calculated, with its standard deviation and 95% confidence limit.

6.5.2 - Program RNJ46A

RNJ46A is a modified version of the National Research Council of Canada program[8] XLVI. The modifications have been described[7], and the general procedure has been outlined[1,10]. RNJ46A calculates the real, *n*, and imaginary, *k*, refractive index spectra of a liquid from an experimental absorbance spectrum. The program contains equations from which the real refractive indices of the common window materials can be calculated at infrared wavenumbers. Other required input is: the anchor point wavenumbers and linear absorption coefficients, *K*, the window material, the path length of the cell, ℓ, and the real refractive index of the liquid at the high-wavenumber limit of the *EA* spectrum, $n(\tilde{\nu}_{max})$. The half-cone angle of the non-parallel beam and the polarization discrimination, i.e., the relative intensities in the two polarizations of the incident beam, can be supplied if desired.

Procedure

1. The transmittance spectrum, T_{abc}, of the cell full of liquid is calculated as in Ref. 9, corrected as described by Ohta and Ishida[12]. The equations are given in Appendix II. If

the half-cone angle of the beam and the polarization discrimination are supplied, the calculation uses these factors. Then $-\log_{10} T_{abc}$ is calculated.

2. The first requirement is to calculate the approximate transmission spectrum that results solely from reflection losses. It is, therefore, first assumed that the imaginary refractive index is zero at all wavenumbers and the real refractive index of the liquid is constant. The value $n(\tilde{\nu}_{max})$ is used. With these assumptions, step 1 yields an approximate apparent absorbance due to reflection, AA_R. AA_R is subtracted from the EA spectrum to yield the approximate absorbance spectrum, AS.

3. The absorbance at the anchor points is calculated as $A_{AP} = K \times \ell$.

4. The baseline correction to be applied to the AS spectrum at the anchor points is calculated as $A_{AP} - AS$, and the corrections required between the anchor points are found by linear interpolation. The AS spectrum is corrected to give the AS_I spectrum.

5. The baseline of the EA spectrum is corrected by calculating the correct EA at the anchor points, as $EA_c = AA_R + A_{AP}$, calculating the correction to EA at the anchor points as $EA_c - EA$, calculating the correction to EA between the anchor points by linear interpolation, and adding the corrections to the EA spectrum. The resulting baseline-corrected EA spectrum has been called the ideal experimental absorbance spectrum[7]. It is here denoted EA_I. The EA_I spectrum is used in step 9.

6. An approximate k spectrum is calculated from the corrected AS spectrum from step 4

as $k = \dfrac{2.303}{4\pi \ell \tilde{\nu}} AS_I$.

7. An approximate n spectrum is calculated from the k spectrum and $n(\tilde{\nu}_{\max})$ by the Kramers-Kronig transformation.

{The k spectrum from a given EA spectrum is not seriously influenced by the n spectrum. Thus, in this step one need not take the usual care to ensure that all the bands in the k spectrum are on scale and that all absorption beyond the ends of the EA spectrum is included in the transform. The n spectrum that is reported for the liquid is calculated later from a k spectrum that is assembled from many different EA spectra.}

8. Step 1 is repeated, but this time using the k and n spectra calculated in steps 6 and 7. The result of this calculation is the calculated ideal experimental absorbance spectrum, EA_C.

9. The calculated, EA_C and experimental, EA_I, ideal experimental absorbance spectra are compared, and the k spectrum is adjusted by the addition of $\Delta k = \dfrac{2.303}{4\pi \ell \tilde{\nu}} \{EA_I - EA_C\}$.

Here k, EA_I and EA_C are at wavenumber $\tilde{\nu}$.

10. The original baseline correction was not accurate, because the n spectrum of the liquid was assumed constant in step 1. Accordingly, the K values at the anchor points are used to correct the new k spectrum, where $K = 4\pi \tilde{\nu} k / 2.303$, again using linear interpolation of the correction between the anchor points. Further, the experimental EA spectrum is again baseline corrected, as in step 5 except that now the AA_R values at the anchor points are calculated using the n spectrum calculated in step 7.

11. A new n spectrum is calculated from the new, corrected, k spectrum and $n(\tilde{\nu}_{max})$, as in step 7.

12. Steps 8 to 11 are repeated until the magnitude of the correction in step 9 averaged over all spectral points is less than 2×10^{-5}.

6.5.3 - Program WIND8

WIND8 combines the functions of ANCHORPT and RNJ46A except that the n spectrum of the liquid is not calculated. The program makes a simplified calculation of the reflection losses in which Eq. 6.2, is used instead of the equations in Appendix II. The program contains equations from which the real refractive indices of the common window materials can be calculated at infrared wavenumbers.

Thus, WIND8 calculates the values of K at the anchor points in the baseline from EA spectra of cells with long path lengths, and calculates the imaginary refractive index, k, and molar absorption coefficient, E_m, spectra of a liquid from an experimental absorbance spectrum in a cell of normal path length. Usually a large number of EA spectra in long path length cells are supplied.

The following input is required: EA spectra in long path length cells, an EA spectrum in a cell of normal path length, the window material and path lengths of these cells, the molar volume of the liquid, the number of anchor points and their wavenumbers.

Procedure

1. The K values at the anchor points are calculated exactly as in program ANCHORPT except that Eq. 6.2 is used to calculate AA_R instead of the equations in appendix II.

2. The calculation of the k spectrum from the EA spectrum in a cell of normal length is started by following steps 2 to 4 of program RNJ46A, except that AA_R is calculated by Eq. 6.2. The result is the baseline-corrected absorbance spectrum, AS_I, which is the approximation to A_{10} given by this method.

3. The k spectrum is calculated, as in step 6 of program RNJ46A, as $k = \dfrac{2.303}{4\pi\,\ell\,\tilde{\nu}} AS_I$.

4. The E_m spectrum is calculated as $E_m = \dfrac{AS_I}{C\ell}$, where C is the molar concentration and ℓ is the path length of the cell.

Comments about the use of the programs

Both RNJ46A and WIND8 yield useful k values in those regions of the EA spectrum in which $0.2 \le EA \le 2.0$. Other regions of the EA spectrum are processed by the programs but do not yield useful values of k. The final k spectrum is assembled by averaging and merging results from EA spectra in cells of sufficiently different lengths to give useful k values throughout. The final n spectrum is calculated from the final k spectrum by Kramers-Kronig transformation and the value of n at the high-wavenumber limit of the k spectrum or, ideally, when it is known[13], the value of n_{el} at each wave number, where n_{el}

is due solely to electronic absorption[13].

6.6 - Appendix II

$$T_{abc} = \frac{T_a\,T_{ba}}{1\text{-}R_a\,R_{ba}}$$

Where: $T_{ba} = \dfrac{T_aT_b}{1\text{-}R_aR_b}$ $\quad R_{ba} = R_b + \dfrac{R_a\,T_b^{\,2}}{1\text{-}R_aR_b}$

$$T_a = \frac{4n_w}{(1+n_w)^2} \qquad R_a = \left\{\frac{1\text{-}n_w}{1+n_w}\right\}^2$$

$$R_b = \left|\frac{r_{12}\,(1\text{-}e^{-i\delta})}{1\text{-}r_{12}^{\,2}\,e^{i\delta}}\right|^2 \qquad \delta = 4\pi\tilde{\nu}\ell\hat{n}_s \qquad r_{12} = \frac{\hat{n}_s - n_w}{\hat{n}_s + n_w}$$

$$T_b = \left|\frac{t_{12}\,t_{21}}{1\text{-}r_{12}^{\,2}\,e^{i\delta}}\right|^2 \qquad t_{12} = \frac{2\hat{n}_s}{\hat{n}_s + n_w} \qquad t_{21} = \frac{2n_w}{n_w + \hat{n}_s}$$

$\hat{n}_s$ and n_w are the complex refractive index of the sample liquid and the real refractive index of the window, respectively. ℓ is the path length of the cell.

6.7 - References

1. J. E. Bertie, R. N. Jones and C. D. Keefe, Appl. Spectrosc. **47**, 891 (1993).
2. J. E. Bertie, R. N. Jones, Y. Apelblat and C. D. Keefe, Appl. Spectrosc. **48**, 127 (1994).

3. J. E. Bertie, R. N. Jones and Y. Apelblat, Appl. Spectrosc. **48**, 144 (1994).
4. J. E. Bertie, Z. Lan, R. N. Jones and Y. Apelblat, Appl. Spectrosc. **49**, 840 (1995)
5. J. E. Bertie, C. D. Keefe and R. N. Jones, Tables of Intensities for the Calibration of Infrared Spectroscopic Measurements in the Liquid Phase. International Union of Pure and Applied Chemistry Chemical Data Series No. 40 (Blackwell Science 1995).
6. I. Mills, T. Cvitas, K. Homann, N. Kallay and K. Kuchitsu, Quantities, Units and Symbols in Physical Chemistry. International Union of Pure and Applied Chemistry (Blackwell Scientific Publications, Oxford, 1988).
7. J. E. Bertie, C. D. Keefe and R. N. Jones, Can. J. Chem. **69**, 1609 (1991).
8. D. G. Cameron, J. P. Hawranek, P. Neelakantan, R. P. Young and R. N. Jones, Computer programs for infrared spectrophotometry XLII to XLVII. National Research Council of Canada bulletin 16, 1977.
9. J. P. Hawranek, P. Neelakantan, R. P. Young and R. N. Jones, Spectrochim. Acta, **32A**, 75 (1976).
10. J. E. Bertie, S. L. Zhang and C. D. Keefe, Vib. Spectr. **8**, 215 (1995).
11. *Fundamentals of Optics*, F. A. Jenkins and H. E. White, Third edition, McGraw-Hill, New York, 1957, page 469.
12. K. Ohta and H. Ishida. Appl. Opt. **29**, 2466 (1990).
13. J. E. Bertie and Z. Lan, J. Chem. Phys., **103**, 10152 (1995).

Chapter 7 - A Compact Table for the Publication of Infrared Spectra That Are Quantitative on Both Intensity and Wavenumber Axes*

7.1 - Introduction

Infrared spectroscopists have traditionally reported their results as a spectrum in graphical form and as a table of the wavenumbers of the peaks and other spectral features with their assignment and points of interest. The ordinate values are usually measures of the percentage of the incident light that is transmitted or reflected, or the logarithmic forms of these quantities, such as the absorbance. These ordinate values have typically been put on record simply by noting, next to the wavenumber, that a feature is strong (s) or weak (w), etc. This approach has usually been employed because accurate knowledge of the wavenumber axis has been possible since the publication of the IUPAC "green"[1] and "blue" books[2] but the ordinate axis has been trusted only to give a qualitative indication of the relative intensities. The ordinate axis could not be trusted to give an accurate measure of the amount of radiation absorbed or reflected.

Several workers have made quantitative intensity measurements. Even in these cases it has been usual for the results to be presented as figures of the spectra and tables of the wavenumber and intensity values at the peaks and other spectral features[3], and sometimes tables of the areas under the bands in the spectra[4]. Although some authors have presented tables of pairs of wavenumber and intensity values over specific bands in the spectrum[5], and several authors[6] have presented such data over the entire spectrum at relatively large intervals, it has not been the practice to do so. The graphs are needed to allow one to see the form of the spectrum quickly, but quantitative values can only be recovered with much labour and very limited accuracy unless they are tabulated.

---

* A version of this chapter has been published. Bertie, Jones and Apelblat, Appl. Spectrosc., 47, 1989 (1993).

As long as the accuracy of the intensity information was low, these practices were acceptable, if annoying, to those who wanted to recover and use quantitative information that was available only as graphs. However, today it is possible to measure intensities with an estimated accuracy of 1 or 2%. To place such information on the record for future use requires that both wavenumber and intensity information be given numerically throughout the spectrum. This is particularly the case if the real and imaginary refractive index spectra are measured. These are fundamental physical properties of the sample, and all other optical properties, such as the dielectric constants of the sample, or the result of any spectroscopic experiment on the sample, can be calculated if these two refractive index spectra are available in numeric form.

Clearly the most compact way of presenting spectra numerically is in digital form, either on diskettes or on a generally accessible data base. However, the organization of and confidence in long-term storage by such digital means have not reached the state that the scientific record can dispense with the paper copy.

The difficulty with paper copy is that a spectrum that is digitized at 0.5 cm^{-1}

intervals from 5000 to 500 cm^{-1} contains 9000 spectral points, i.e. 9000 wavenumber, $\tilde{\nu}$, and intensity, $Y(\tilde{\nu})$, pairs. Scientific journals can print sixty lines on each page, and six double columns $\tilde{\nu}$ and $Y(\tilde{\nu})$ can be put on each line, to give 360 spectral points per page. The table for each spectrum thus requires 25 journal pages. If real, $n(\tilde{\nu})$, and imaginary, $k(\tilde{\nu})$, refractive index spectra are both to be presented, four triple columns $\tilde{\nu}$, $k(\tilde{\nu})$, and $n(\tilde{\nu})$ can be put on each line, to give 240 data triplets per page. The table then requires 38 journal pages. These tables are clearly too large to be published in a spectroscopic journal. For publication in a journal for the scientific record, the spectral information must be compacted in such a way that the table is short and readable but allows the original spectrum to be recovered with at least its experimental accuracy.

We describe in this paper a procedure that enables quantitative spectroscopic data to be published over the entire spectrum, by compressing spectral data into a Compact Table. This table contains sufficient information to allow the spectrum to be recovered without loss of accuracy, yet is sufficiently concise that journals can realistically be expected to print it. Further, the table is readable, so that individual numerical values can be recovered from it with minimal effort. We also present a Fortran program for creating the table from a digital spectrum, and a Fortran program that reads the tabulated data and recreates the original spectrum. The creation of the Compact Table, and the recovery of the spectrum from it, is demonstrated for the real and imaginary refractive index spectra, $n(\tilde{\nu})$ vs. $\tilde{\nu}$ and $k(\tilde{\nu})$ vs. $\tilde{\nu}$ and the molar absorption coefficient spectrum, $E_m(\tilde{\nu})$ vs. $\tilde{\nu}$, of liquid chlorobenzene[7]. Compact Tables have been used recently to present spectra of the refractive indices and molar absorption coefficient of liquid benzene[8] and the refractive indices of liquid methanol[9]. The effectiveness of the Compact Table is particularly well illustrated by Table 2 of reference 9. The one-page table contains all of the information needed to recover the absorption intensities of liquid methanol at 1 cm^{-1} intervals between 8000 and 2 cm^{-1}, accurate to about 2%.

7.2 - Construction of a Compact Table

There are two aspects to the procedure. First, the number of spectral points that are reported is reduced and, second, a very compressed format is used for the table which contains the reduced spectrum.

The major consideration in reducing the number of spectral points is to ensure that the tabulated information allows recovery of the original spectrum without reducing the accuracy below that of the measurements. Our experimental values of the imaginary refractive index or molar absorption coefficient are believed accurate within ~±2.5%, so that the original spectrum must be recovered from the tabulated data within ±2.5%. In fact a stricter criterion is applied which ensures recovery of nearly all of the spectrum to ≤±1%.

In the construction of the table, the number of spectral points is first reduced by a factor of two by ignoring every second point[10]. The ordinate values are truncated to the appropriate number of significant figures and are tabulated. The tabulated values are then read into the recovery program, interpolated back to the original wavenumber spacing and compared with the original spectrum. The same procedure is repeated for reduction factors of 4, 8, 16, 32, etc.. Then the spectrum is divided into regions of constant wavenumber spacing in such a way that the number of spectral points in each region is reduced by the largest factor that allows recovery to $\leq 1\%$.

The original real and imaginary refractive index spectra and the original molar absorption coefficient spectrum of chlorobenzene[7] each contains 9024 points between 4800 and 450 cm^{-1}. The method described above allows each spectrum to be reduced to 2437 points, in 35 regions with different spacing in adjacent regions. Even after such a reduction of the number of spectral points by a factor of almost four, seven pages are needed for a normal ($\tilde{\nu}$ Y) table with 60 lines per page and 6 $\tilde{\nu}$-Y pairs per line. Such tables are still too long to be published in most journals. In Table 7.1, we present a small part of such a table, from 2008.49 to 1352.82 cm^{-1} which contains 360 spectral points.

When the spectral points are known to be uniformly spaced, it is wasteful in Table 7.1 to give the wavenumber every time an ordinate value is given. Instead of giving all of the wavenumber values in the spectrum, we divide the table into regions of constant wavenumber spacing, and give the first wavenumber of each line and the wavenumber spacing for that line. A similar procedure with just one region per spectrum has been used for digital data files for nearly two decades, e.g. in files in the

Table 7.1 - Reduced data of imaginary refractive index of chlorobenzene in XY format.

cm^{-1}	*k*	cm^{-1}	*k*	cm^{-1}	*k*	cm^{-1}	*k*	cm^{-1}	*k*	cm^{-1}	*k*
2008.49	.0001953	1924.61	.0009501	1706.69	.0008392	1610.27	.0017846	1533.13	.0011030	1451.17	.0196166
2007.53	.0002144	1922.68	.0008343	1702.83	.0008091	1609.30	.0018416	1531.20	.0011635	1450.21	.0224716
2006.57	.0002344	1920.75	.0007323	1698.98	.0007158	1608.34	.0019065	1529.27	.0012259	1449.24	.0265342
2005.60	.0002531	1918.82	.0006468	1695.12	.0006164	1607.38	.0019961	1527.34	.0012960	1448.28	.0337179
2004.64	.0002683	1916.89	.0005778	1691.26	.0005305	1606.41	.0021089	1525.42	.0013976	1447.31	.0493102
2003.68	.0002791	1914.97	.0005273	1689.34	.0005373	1605.45	.0022471	1523.49	.0015155	1446.35	.0800344
2002.71	.0002838	1913.04	.0004955	1687.41	.0006090	1604.48	.0024248	1521.56	.0017051	1445.38	.1033189
2001.75	.0002822	1911.11	.0004722	1685.48	.0006452	1603.52	.0026442	1519.63	.0019199	1444.42	.0783155
2000.78	.0002773	1907.25	.0004558	1683.55	.0005664	1602.55	.0029069	1517.70	.0021886	1443.46	.0503902
1999.82	.0002727	1903.40	.0005119	1681.62	.0005313	1601.59	.0032295	1515.77	.0024605	1442.49	.0339685
1998.85	.0002697	1899.54	.0006196	1679.69	.0004872	1600.63	.0036169	1513.85	.0026776	1441.53	.0244790
1997.89	.0002690	1895.68	.0008208	1677.76	.0004494	1599.66	.0041135	1511.92	.0028190	1440.56	.0191549
1996.93	.0002719	1891.82	.0011981	1675.84	.0004521	1598.70	.0047675	1509.99	.0029493	1439.60	.0163045
1995.96	.0002790	1887.97	.0017996	1673.91	.0004698	1597.73	.0056709	1508.06	.0031955	1438.63	.0137411
1995.00	.0002915	1884.11	.0022907	1671.98	.0005026	1596.77	.0069249	1506.13	.0036336	1437.67	.0108982
1994.03	.0003113	1880.25	.0023773	1670.05	.0005349	1595.81	.0086147	1504.20	.0044065	1436.71	.0085718
1993.07	.0003400	1876.40	.0022514	1668.12	.0005584	1594.84	.0107694	1502.27	.0056930	1435.74	.0069902
1992.10	.0003784	1872.54	.0024329	1666.19	.0005784	1593.88	.0133269	1500.35	.0074933	1433.81	.0051557
1991.14	.0004231	1868.68	.0031992	1664.27	.0006082	1592.91	.0160376	1498.42	.0093099	1431.89	.0041926
1990.18	.0004645	1864.83	.0041122	1662.34	.0006509	1591.95	.0186616	1496.49	.0104603	1429.96	.0035584
1989.21	.0004927	1860.97	.0043739	1660.41	.0007049	1590.98	.0211753	1494.56	.0111881	1428.03	.0030469
1988.25	.0005080	1857.11	.0034551	1658.48	.0007916	1590.02	.0238395	1492.63	.0122996	1426.10	.0026083
1987.28	.0005192	1853.26	.0021042	1656.55	.0009286	1589.06	.0270981	1490.70	.0141691	1424.17	.0022237
1986.32	.0005330	1849.40	.0012062	1654.62	.0011378	1588.09	.0316606	1488.78	.0167832	1422.24	.0018924
1985.36	.0005481	1845.54	.0007463	1652.69	.0014265	1587.12	.0388300	1486.85	.0206693	1420.31	.0016236
1984.39	.0005594	1841.68	.0005319	1650.77	.0017320	1586.16	.0511551	1484.92	.0274626	1418.39	.0014137
1983.43	.0005642	1837.83	.0004480	1648.84	.0020280	1585.20	.0686019	1483.95	.0330786	1416.46	.0012710
1982.46	.0005639	1833.97	.0004555	1646.91	.0022225	1584.23	.0803482	1482.99	.0414312	1414.53	.0011619
1981.50	.0005629	1830.11	.0005505	1644.98	.0022633	1583.27	.0801655	1482.03	.0543342	1412.60	.0010560
1980.53	.0005661	1826.26	.0006608	1643.05	.0021739	1582.31	.0734641	1481.06	.0755927	1410.67	.0009829
1979.57	.0005771	1822.40	.0007380	1641.12	.0020225	1581.34	.0628704	1480.10	.1121719	1408.74	.0009406
1978.61	.0005994	1818.54	.0008833	1639.20	.0019179	1580.38	.0511596	1479.13	.1712698	1406.82	.0009162
1977.64	.0006344	1814.69	.0010684	1637.27	.0019527	1579.41	.0405318	1478.17	.2365395	1404.89	.0009192
1976.68	.0006842	1810.83	.0012481	1636.30	.0019380	1578.45	.0319523	1477.20	.2466504	1402.96	.0009400
1974.75	.0008319	1806.97	.0013892	1635.34	.0018158	1577.48	.0255474	1476.24	.2134474	1401.03	.0009762
1972.82	.0010416	1803.12	.0015481	1634.37	.0016314	1576.52	.0210303	1475.28	.1490597	1399.10	.0010468
1970.89	.0012972	1799.26	.0018692	1633.41	.0014709	1575.56	.0180213	1474.31	.1012828	1397.17	.0011805
1968.96	.0015670	1795.40	.0024781	1632.45	.0013624	1574.59	.0161671	1473.35	.0734671	1395.24	.0014104
1967.04	.0018091	1791.54	.0032260	1631.48	.0013055	1573.63	.0151757	1472.38	.0576492	1393.32	.0017663
1965.11	.0019811	1787.69	.0035527	1630.52	.0013077	1572.66	.0147124	1471.42	.0463420	1391.39	.0022515
1963.18	.0020625	1783.83	.0032802	1629.55	.0013453	1571.70	.0143540	1470.45	.0363176	1389.46	.0027548
1961.25	.0020640	1779.97	.0027101	1628.59	.0014313	1569.77	.0137425	1469.49	.0273849	1387.53	.0030219
1959.32	.0020284	1776.11	.0020662	1627.62	.0015765	1567.84	.0141497	1468.53	.0208967	1385.60	.0029408
1957.39	.0020023	1772.26	.0016335	1626.66	.0017782	1565.91	.0147272	1467.56	.0166134	1383.67	.0026547
1955.46	.0020277	1768.40	.0011537	1625.70	.0020285	1563.99	.0134075	1466.60	.0137121	1381.75	.0023349
1953.54	.0021407	1764.55	.0008596	1624.73	.0022934	1562.06	.0107829	1465.63	.0117276	1379.82	.0021122
1951.61	.0023646	1760.69	.0006972	1623.77	.0025175	1560.13	.0082193	1464.67	.0103099	1377.89	.0020582
1949.68	.0027306	1756.83	.0006177	1622.80	.0026380	1558.20	.0062247	1463.71	.0092746	1375.96	.0022140
1947.75	.0032198	1752.98	.0006227	1621.84	.0026583	1556.27	.0046822	1462.74	.0085466	1374.03	.0025594
1945.82	.0037111	1749.12	.0007161	1620.88	.0025862	1554.34	.0035677	1461.78	.0080684	1372.10	.0029269
1943.89	.0040454	1745.26	.0009533	1619.91	.0024562	1552.41	.0027762	1460.81	.0078293	1370.17	.0030159
1941.96	.0040582	1741.40	.0014245	1618.95	.0023009	1550.49	.0022425	1459.85	.0077828	1368.24	.0027181
1940.04	.0037969	1737.55	.0022052	1617.98	.0021390	1548.56	.0018639	1458.88	.0079636	1366.32	.0022235
1938.11	.0033506	1733.69	.0031242	1617.02	.0020018	1546.63	.0016132	1457.92	.0083674	1364.39	.0017392
1936.18	.0028268	1729.83	.0034346	1616.05	.0018928	1544.70	.0014374	1456.96	.0090407	1362.46	.0013388
1934.25	.0023159	1725.98	.0029111	1615.09	.0017998	1542.77	.0013195	1455.99	.0099930	1360.53	.0010424
1932.32	.0018723	1722.12	.0021053	1614.13	.0017440	1540.84	.0012203	1455.03	.0112685	1358.60	.0008373
1930.39	.0015193	1718.26	.0014449	1613.16	.0017242	1538.92	.0011566	1454.06	.0129105	1356.68	.0007026
1928.47	.0012618	1714.41	.0010508	1612.20	.0017166	1536.99	.0010871	1453.10	.0148860	1354.75	.0006146
1926.54	.0010844	1710.55	.0008674	1611.23	.0017394	1535.06	.0010687	1452.13	.0171278	1352.82	.0005569

Table 7.2 - The Compact Table of the imaginary refractive index of chlorobenzene.[a]

cm^{-1}	*XE*	*YE*	0	1	2	3	4	5	6	7	8	9	10	11	12	13	14	15	16
2008.49	0	-7	1953	2144	2344	2531	2683	2791	2838	2822	2773	2727	2697	2690	2719	2790	2915	3113	3400
1992.10	0	-7	3784	4231	4645	4927	5080	5192	5329	5481	5594	5642	5639	5629	5661	5771	5994	6344	6842
1974.75	1	-6	832	1042	1297	1567	1809	1981	2062	2064	2028	2002	2028	2141	2365	2731	3220	3711	4045
1941.96	1	-6	4058	3797	3351	2827	2316	1872	1519	1262	1084	950	834	732	647	578	527	496	472
1907.25	2	-6	456	512	620	821	1198	1800	2291	2377	2251	2433	3199	4112	4374	3455	2104	1206	746
1841.68	2	-6	532	448	456	550	661	738	883	1068	1248	1389	1548	1869	2478	3226	3553	3280	2710
1776.11	2	-6	2066	1634	1154	860	697	618	623	716	953	1425	2205	3124	3435	2911	2105	1445	1051
1710.55	2	-7	8674	8392	8090	7157	6164	5304											
1689.33	1	-7	5373	6090	6452	5664	5313	4872	4494	4521	4698	5026	5348	5584	5784	6082	6509	7049	7916
1656.55	1	-6	929	1138	1426	1732	2028	2223	2263	2174	2023	1918	1953						
1636.30	0	-6	1938	1816	1631	1471	1362	1306	1308	1345	1431	1576	1778	2028	2293	2517	2638	2658	2586
1619.91	0	-6	2456	2301	2139	2002	1893	1800	1744	1724	1717	1739	1785	1842	1906	1996	2109	2247	2425
1603.52	0	-5	264	291	323	362	411	477	567	692	861	1077	1333	1604	1866	2118	2384	2710	3166
1587.12	0	-5	3883	5116	6860	8035	8017	7346	6287	5116	4053	3195	2555	2103	1802	1617	1518	1471	1435
1569.77	1	-5	1374	1415	1473	1341	1078	822	622	468	357	278	224	186	161	144	132	122	116
1536.98	1	-6	1087	1069	1103	1163	1226	1296	1398	1516	1705	1920	2189	2460	2678	2819	2949	3195	3634
1504.20	1	-5	441	569	749	931	1046	1119	1230	1417	1678	2067	2746						
1483.95	0	-4	331	414	543	756	1122	1713	2365	2467	2134	1491	1013	735	576	463	363	274	209
1467.56	0	-5	1661	1371	1173	1031	927	855	807	783	778	796	837	904	999	1127	1291	1489	1713
1451.17	0	-4	196	225	265	337	493	800	1033	783	504	340	245	192	163	137	109	86	70
1433.81	1	-6	5156	4193	3558	3047	2608	2224	1892	1624	1414	1271	1162	1056	983	941	916	919	940
1401.03	1	-6	976	1047	1181	1410	1766	2252	2755	3022	2941	2655	2335	2112	2058	2214	2559	2927	3016
1368.24	1	-6	2718	2224	1739	1339	1042	837	703	615	557								

a - The column headed cm^{-1} contains the wavenumber of the first $k(\tilde{\nu})$ value in the row. The columns headed *XE* and *YE* contain the X-exponent and the Y-exponent, respectively, for the row. The columns headed 0,1,2,$\cdots$16, contain the ordinate values, and the headings give the indices of the ordinate values in the row. In a row which starts with $\tilde{\nu}(0)$, the wavenumber corresponding to the ordinate indexed J is $\tilde{\nu}(J) = \tilde{\nu}(0) - \dfrac{15798.002}{16384} \cdot J \cdot 2^{XE}$. The $k(\tilde{\nu})$ values in that row are the ordinate value shown times 10^{YE}. Thus the entry indexed 16 in the first row of the table shows that $k = 3400 \times 10^{-7} = 3.40 \times 10^{-4}$ at $\tilde{\nu} = 2008.49 - \dfrac{15798.002}{16384} \cdot 16 \cdot 2^{0} = 1993.06\ \text{cm}^{-1}$.

JCAMP[11] format.

We achieve further reduction in space by multiplying each ordinate value on a line by 10^{-YE}, to create integer ordinate values with the appropriate number of significant figures, and reporting these integer values and the Y-exponent, *YE*, for the line.

We call the resulting table a Compact Table. It contains the 2437 *Y* values and the minimal but complete information needed to obtain the $\tilde{\nu}$ values. The Compact Table for chlorobenzene occupies 2.5 pages. The complete Compact Table for the imaginary refractive index of chlorobenzene is given elsewhere[7]. Table 7.2 presents the small part of it that contains all of the information given in Table 7.1.

In Table 7.2, the first column is labeled "cm^{-1}" and in each row it contains the wavenumber, $\tilde{\nu}(0)$, of the first ordinate value in the row. This ordinate value is in the column labeled "0". The second column is labeled "XE" for X-exponent, and in each row contains the exponent that is used to calculate the wavenumber spacing between the ordinate values in that row. The third column contains YE, the Y-exponent used to calculate the ordinate values in the row. The remaining column headings, 0, 1, 2, 3, through 16, are the indices, J, of the ordinate values in that row. Under these seventeen columns are the seventeen Y values, each presented as an integer of three or four digits with leading zeros omitted.

The ordinate values in a row are obtained from the entries by $Y(J)$ = (entry under J)x 10^{YE}. In any row, the first entry is $\tilde{\nu}(0)$, and the wavenumber corresponding to the ordinate value under the column heading "J" is given by

$$\tilde{\nu}(J) = \tilde{\nu}(0) - \frac{15798.002}{16384} \times J \times 2^{XE} = \tilde{\nu}(0) - 0.964233 \times J \times 2^{XE}. \quad (7.1)$$

The factor 15798.002 / 16384 comes from the use of a He/Ne laser in vacuum, wavenumber 15798.002 cm^{-1}, the fact that fast Fourier transforms yield 2^N spectral points, and a decision that the wavenumber spacing for XE=0 should be near 1 cm^{-1}.

Table 7.3 - The Compact Table of the molar absorption coefficient of chlorobenzene.[a,b]

cm^{-1}	*XE*	*YE*	0	1	2	3	4	5	6	7	8	9	10	11	12	13	14	15	16
2008.49	0	-4	2187	2400	2623	2831	2999	3119	3170	3151	3095	3042	3007	2998	3028	3105	3244	3462	3779
1992.10	0	-4	4204	4698	5156	5466	5633	5755	5904	6069	6191	6241	6235	6221	6253	6372	6615	6998	7543
1974.75	1	-3	916	1146	1426	1721	1985	2171	2258	2258	2217	2186	2212	2332	2574	2969	3498	4028	4386
1941.96	1	-3	4396	4108	3622	3053	2498	2018	1636	1357	1165	1020	895	784	692	618	563	529	503
1907.25	2	-3	485	543	656	868	1264	1895	2407	2493	2356	2541	3334	4277	4540	3579	2175	1244	768
1841.68	2	-3	546	459	466	562	673	750	896	1081	1261	1400	1557	1876	2481	3223	3542	3264	2691
1776.11	2	-3	2047	1615	1138	846	685	605	609	699	928	1384	2137	3021	3314	2802	2022	1385	1005
1710.55	2	-4	8276	7988	7684	6782	5827	5004											
1689.33	1	-4	5063	5731	6065	5318	4983	4564	4205	4225	4386	4687	4982	5195	5376	5645	6035	6528	7323
1656.55	1	-3	858	1050	1315	1595	1865	2042	2077	1992	1851	1753	1783						
1636.30	0	-3	1769	1656	1487	1340	1240	1188	1189	1223	1300	1431	1613	1839	2078	2280	2388	2405	2338
1619.91	0	-3	2219	2078	1930	1805	1706	1621	1570	1551	1544	1563	1603	1653	1710	1790	1890	2012	2170
1603.52	0	-2	236	260	288	323	367	425	505	617	767	958	1185	1425	1657	1879	2114	2402	2804
1587.12	0	-2	3437	4526	6065	7100	7079	6483	5545	4509	3570	2813	2248	1849	1584	1420	1332	1290	1258
1569.77	1	-2	1203	1237	1286	1170	939	715	541	406	309	240	194	161	139	124	114	105	99
1536.98	1	-3	932	915	943	994	1046	1104	1189	1288	1447	1627	1853	2080	2261	2377	2484	2688	3052
1504.20	1	-2	370	477	627	778	873	933	1024	1178	1394	1714	2274						
1483.95	0	-1	274	343	449	624	926	1413	1950	2032	1757	1227	833	604	473	380	298	224	171
1467.56	0	-2	1360	1122	959	842	757	697	658	638	634	648	680	735	812	914	1047	1206	1387
1451.17	0	-2	1588	1818	2145	2724	3980	6456	8329	6309	4057	2733	1968	1539	1309	1103	874	687	560
1433.81	1	-3	4123	3348	2838	2427	2075	1766	1501	1286	1118	1004	917	832	773	739	719	720	736
1401.03	1	-3	763	817	920	1098	1373	1747	2135	2339	2273	2049	1799	1626	1582	1699	1961	2240	2305
1368.24	1	-3	2074	1694	1324	1017	791	634	532	464	420								

a - The column headed cm^{-1} contains the wavenumber of the first $E_m(\tilde{\nu})$ value in the row. The columns headed *XE* and *YE* contain the X-exponent and the Y-exponent, respectively, for the row. The columns headed 0,1,2,$\cdots$16, contain the ordinate values, and the headings give the indices of the ordinate values in the row. In a row which starts with $\tilde{\nu}(0)$, the wavenumber corresponding to the ordinate indexed J is $\tilde{\nu}(J) = \tilde{\nu}(0) - \frac{15798.002}{16384} \cdot J \cdot 2^{XE}$. The $E_m(\tilde{\nu})$ values in that row are the ordinate value shown times 10^{YE}. Thus the entry indexed 16 in the first row of the table shows that $E_m = 3779 \times 10^{-4} = 3.779 \times 10^{-1}$ at $\tilde{\nu} = 2008.49 - \frac{15798.002}{16384} \cdot 16 \cdot 2^0 = 1993.06\ \mathrm{cm}^{-1}$.

b - The units of the E_m values are L mole^{-1} cm^{-1}.

When the point spacings in two consecutive rows are different, the two rows have different *XE* values and the spacing between the last point of the first row and the first point of the second row is given by the *XE* value of the second row.

To observe the procedure for obtaining the $\tilde{\nu}$ and *Y* values from the Table 7.2, consider the entry in the first row under the column labeled 4. The wavenumber, $\tilde{\nu}$, corresponding to that entry is given by:

$$\tilde{\nu}(J) = \tilde{\nu}(0) - 0.964233 \times J \times 2^{XE} = 2008.49 - 0.964233 \times 4 \times 2^{0} =$$

$$= 2005.63 \text{ cm}^{-1}. \qquad (7.2)$$

The k value corresponding to 2005.63 cm^{-1} is 2683 x10^{-7} , i.e. $k(2005.63) = 0.0002683$.

Table 7.3 shows the corresponding table for the decadic molar absorption coefficient which was calculated from $k(\tilde{\nu})$ by the equation

$$E_m(\tilde{\nu}) = \frac{-\log_{10}[I_t(\tilde{\nu})/I_o(\tilde{\nu})]}{C\,d} = \frac{4\pi\tilde{\nu}}{2.303C}k(\tilde{\nu}) \qquad (7.3)$$

where C is the concentration, d is the pathlength and $-\log_{10}[I_t(\tilde{\nu})/I_o(\tilde{\nu})]$ is the absorbance. Note that I_t and I_o must be fully corrected for losses other than by absorption[10]. We follow the practice of analytical spectroscopists, by taking C in mol L^{-1}, d in cm and reporting $E_m(\tilde{\nu})$ in the units L mole^{-1} cm^{-1}.

The format of the table for the real refractive index is slightly modified. The common exponent YE is not used because real refractive index values are usually smaller than 9.999. Thus, 5 digits are used and it is implicit that the decimal point comes after the first digit of each entry, e.g. 1.5345 is given as 15345 and 0.8976 is given with a leading zero 08976. In Table 7.4 the values of the real refractive index of chlorobenzene are given for the same wavenumber range as in the previous two tables.

A Fortran program for creating the Compact Table and an input file are given in appendix A. Although the program is given with parameters and features to suit the

Table 7.4 - The Compact Table of the real refractive indices of chlorobenzene.[a]

cm^{-1}	*XE*	0	1	2	3	4	5	6	7	8	9	10	11	12	13	14	15	16
2008.49	0	14978	14978	14978	14977	14977	14977	14977	14977	14977	14976	14976	14976	14975	14975	14974	14974	14973
1992.10	0	14973	14973	14972	14972	14972	14972	14972	14972	14971	14971	14971	14970	14970	14969	14968	14967	14967
1974.75	1	14965	14964	14963	14963	14964	14966	14967	14969	14969	14969	14968	14967	14965	14965	14966	14969	14975
1941.96	1	14983	14989	14994	14996	14997	14996	14995	14993	14991	14989	14988	14986	14985	14983	14981	14980	14978
1907.25	2	14975	14972	14968	14965	14961	14960	14963	14966	14966	14963	14962	14968	14982	14995	14997	14992	14986
1841.68	2	14981	14977	14973	14969	14967	14964	14962	14960	14958	14957	14955	14952	14951	14954	14962	14970	14975
1776.11	2	14975	14974	14971	14967	14963	14959	14954	14950	14945	14940	14938	14942	14952	14960	14963	14960	14956
1710.55	2	14952	14948	14946	14943	14940	14936											
1689.33	1	14934	14933	14932	14931	14929	14927	14925	14923	14921	14919	14916	14914	14912	14910	14907	14905	14902
1656.55	1	14898	14895	14893	14891	14891	14892	14893	14893	14892	14889	14887						
1636.30	0	14887	14887	14885	14883	14880	14877	14874	14871	14867	14864	14861	14859	14858	14857	14857	14858	14858
1619.91	0	14857	14855	14853	14849	14846	14842	14837	14833	14828	14823	14817	14812	14806	14799	14792	14785	14776
1603.52	0	14768	14758	14747	14736	14723	14708	14691	14673	14655	14638	14625	14615	14608	14600	14588	14570	14544
1587.12	0	14512	14495	14562	14743	14941	15099	15208	15264	15278	15265	15238	15206	15174	15145	15121	15103	15091
1569.77	1	15071	15057	15064	15080	15086	15079	15067	15052	15037	15022	15008	14995	14983	14972	14962	14952	14943
1536.98	1	14934	14924	14915	14906	14897	14887	14878	14868	14857	14847	14836	14825	14814	14802	14787	14770	14749
1504.20	1	14726	14702	14680	14663	14646	14620	14581	14532	14469	14383	14258						
1483.95	0	14173	14070	13943	13794	13663	13713	14237	15138	15853	16190	16153	16023	15912	15834	15771	15700	15624
1467.56	0	15553	15490	15436	15389	15346	15308	15272	15239	15207	15177	15147	15118	15090	15063	15036	15011	14986
1451.17	0	14961	14929	14885	14821	14749	14809	15215	15593	15656	15609	15551	15497	15460	15438	15416	15390	15365
1433.81	1	15322	15290	15266	15246	15229	15214	15201	15188	15177	15167	15157	15148	15140	15132	15125	15118	15111
1401.03	1	15105	15098	15092	15086	15080	15077	15076	15078	15080	15080	15078	15075	15070	15066	15063	15064	15067
1368.24	1	15071	15071	15069	15066	15062	15058	15054	15051	15047								

a. The column headed cm^{-1} contains the wavenumber of the first $n(\tilde{\nu})$ value in the row. The column headed *XE* contains the X-exponent for the row. The columns headed 0,1,2,$\cdots$16, contain the $n(\tilde{\nu})$ values with the decimal point implicitly after the first digit in each value, and the headings give the indices of the $n(\tilde{\nu})$ values in the row. In a row which starts with $\tilde{\nu}(0)$, the wavenumber corresponding to the ordinate indexed J is $\tilde{\nu}(J) = \tilde{\nu}(0) - \frac{15798.002}{16384} \cdot J \cdot 2^{XE}$. Thus the entry indexed 16 in the first row of the table shows that $n = 1.4973$ at $\tilde{\nu} = 2008.49 - \frac{15798.002}{16384} \cdot 16 \cdot 2^{0} =$ $= 1993.06$ cm^{-1}, and the entry indexed 4 in the row which starts with 1368.24 cm^{-1} shows that $n = 1.5062$ at $\tilde{\nu} = 1360.53$ cm^{-1}.

format of our spectral files[10], it can be easily modified for other file formats.

Before we leave the construction of the Compact Table, a few words about significant figures are appropriate. If ordinate values are known to 1% they should be tabulated with three significant figures. If such numbers are later plotted, however, they frequently cause steps in the graph which were not present in the original spectrum.

The steps arise because information was lost in the truncation to three significant figures, in that the relative accuracy from point to point is much better than the absolute accuracy that can be assigned to each ordinate. (the wavenumbers are taken to be essentially exact, as they are from a Fourier transform spectrometer after proper calibration). Accordingly, we use a number of significant figures that is acceptable in relation to the ordinate accuracy but yields a plotted spectrum free of steps.

7.3 - Recovery of a spectrum from a Compact Table

The tabulated spectrum consists of ordinate values at wavenumbers that are equally spaced in each region but have different spacings in different regions. To recover the spectrum at a uniform spacing throughout, piecewise cubic spline interpolation[12] is used to interpolate between intensity values at equal wavenumber spacing, $\Delta\tilde{\nu} = \tilde{\nu}_1 - \tilde{\nu}_2$. Specifically the intensity values between two tabulated points, Y_1 at wavenumber $\tilde{\nu}_1$ and Y_2 at wavenumber $\tilde{\nu}_2$, are obtained from a polynomial function $P(\tilde{\nu}) = a_3\tilde{\nu}^3 + a_2\tilde{\nu}^2 + a_1\tilde{\nu} + a_0$ which is made to satisfy the position conditions $P(\tilde{\nu}_1) = Y_1$, $P(\tilde{\nu}_2) = Y_2$, and the slope conditions $P'(\tilde{\nu}_1) = S_1$ and $P'(\tilde{\nu}_2) = S_2$. We have chosen the free parameters[12], S_1 and S_2, as the first derivatives at $\tilde{\nu}_1$ and $\tilde{\nu}_2$ because they give better interpolation than the second derivatives. The first derivatives were calculated by $P'(\tilde{\nu}_1) = \dfrac{Y_2 - Y_0}{2\Delta\tilde{\nu}}$ and $P'(\tilde{\nu}_2) = \dfrac{Y_3 - Y_1}{2\Delta\tilde{\nu}}$, where Y_0 and Y_3 are the neighboring tabulated points of Y_1 and Y_2. Obtaining the 4 coefficients for the cubic polynomial from the values of

$P(\tilde{\nu}_1)$, $P(\tilde{\nu}_2)$, $P'(\tilde{\nu}_1)$ and $P'(\tilde{\nu}_2)$ is straightforward, as is the interpolation between points 1 and 2 from these coefficients.

In order to proceed, one needs to recognize 3 problematic areas for the interpolation: 1) the first point in the spectrum, 2) the last point in the spectrum , and 3) the boundaries between different regions.

When $\tilde{\nu}_1$ is the first point in the spectrum, Y_0 at $\tilde{\nu}_0$ is not known. We assume $Y_0 = Y_1$. This is usually the case for absorption index spectra, because the values at the highest wavenumber are close to or equal to zero, and it is also usually true for real refractive index spectra because n is almost constant at the highest wavenumber.

When $\tilde{\nu}_2$ is the last point in the spectrum, Y_3 at $\tilde{\nu}_3$ is not known. No generally useful assumption is evident. Values beyond the last point can not be assumed to be constant because the end point is usually determined by the limitations of the spectrometer or sample cell, and many samples absorb significantly at low wavenumbers. Therefore we do not interpolate to the last point, but only to the penultimate point in the table. In most cases the wavenumber spacing in the last region is increased one to four times when the table is constructed, so this practice typically reduces the length of the recovered spectrum by only one to four points.

The interpolation between adjacent regions is not straightforward because the spacing in the two regions is different and the two points used to calculate the slope are not equidistant from the central point. For simplicity, Figure 7.1 shows only 35 points in the middle of the original spectrum, and all Y values are shown equal. These 35

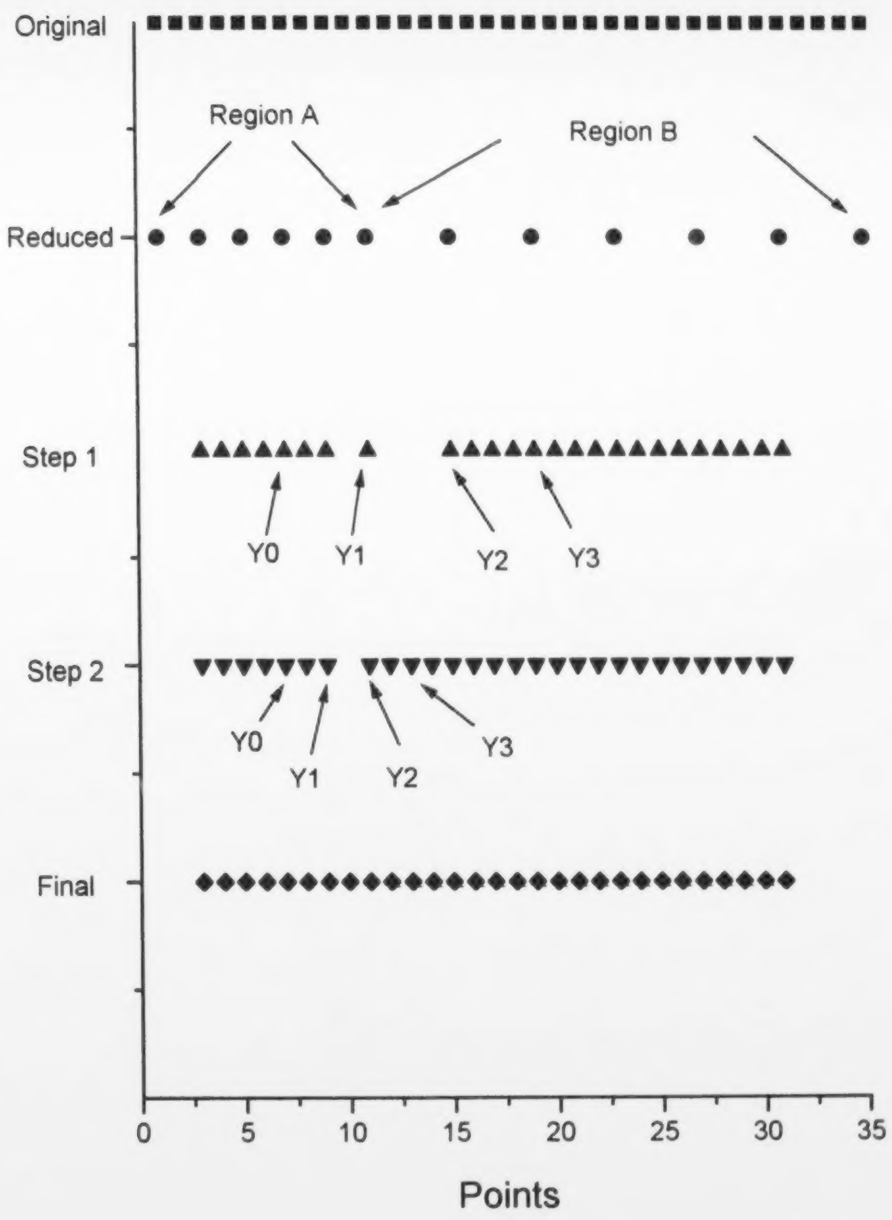

Figure 7.1 - Illustration of the step-wise procedure for interpolating to the original wavenumber spacing at the boundary between regions of different spacings, as described in the text.

points were reduced into two regions, A with 2-point reduction and B with 4-point reduction. Note that the spacing between the last point in region A and the first point in region B is the same as in region B. The interpolation between the two regions A and B is described below. A similar procedure would be followed at the other ends of the two regions to join this 35-point section to the remainder of the original spectrum

The interpolation is first completed in each region from its second point to its next-to-last point. This procedure is straightforward because the first and last points of the region can be used to find the required slopes at the second and next-to-last points, respectively. The result is labeled "Step 1" in Figure 7.1. Then, to interpolate between the two regions, one interpolates the region with the higher reducing factor, region B in the example, to its first point, which is also the last point of region A. As shown in "Step 1" in Fig. 7.1, all values of Y_0, Y_1, Y_2 and Y_3 at an equal spacing are known and the interpolation is straightforward between the points denoted by Y_1 and Y_2. The result is labeled "Step 2" in Figure 7.1. Then, the interpolation of the remaining part of region A can be completed since, again, all values of Y_0, Y_1, Y_2 and Y_3 at an equal spacing are known. Note that the interpolation of the more closely spaced region A can not be completed before the interpolation of the less closely spaced region B is completed. The required value labeled Y_3 in "Step 2" is not available before the completion of "Step 2".

The same procedure is followed at all other boundaries to yield the recovered spectrum at the same wavenumbers as the original spectrum, except that it stops at the last tabulated wavenumber instead of the last wavenumber in the spectrum. The interpolation program and its input file are given in appendix B and can easily be modified to suit any user.

7.4 - The accuracy in the recovered spectrum

Figure 7.2 shows the superimposed original and the recovered absorption index spectra of liquid chlorobenzene[7]. Both spectra are also enlarged to show weak bands. Even with magnification, differences between the original and recovered spectra are not observable. In the lower boxes of Figure 7.3, two bands from this spectrum are expanded, a weak band at high wavenumber and a relatively strong band at low wavenumber. Again, no differences between the original and recovered spectra are visible. To show these differences, the upper boxes of Figure 7.3 show the percent differences between the original and the recovered spectra in these ranges, i.e. the percent inaccuracies of recovery for these bands. Figure 7.4a shows the percent inaccuracies of recovery over the whole spectrum. The magnitudes of the inaccuracies of recovery average 0.2%. Nearly all points in the spectrum are recovered to 1% or better, and the few points that are recovered less accurately are not consecutive.

If the tabulated ordinate values were not truncated to the number of significant figures appropriate to their accuracy, the points in the recovered spectrum would be identical to the points in the original spectrum at the wavenumbers included in the table. To explore the effect of the truncation on the chlorobenzene $k(\tilde{\nu})$ spectrum, we

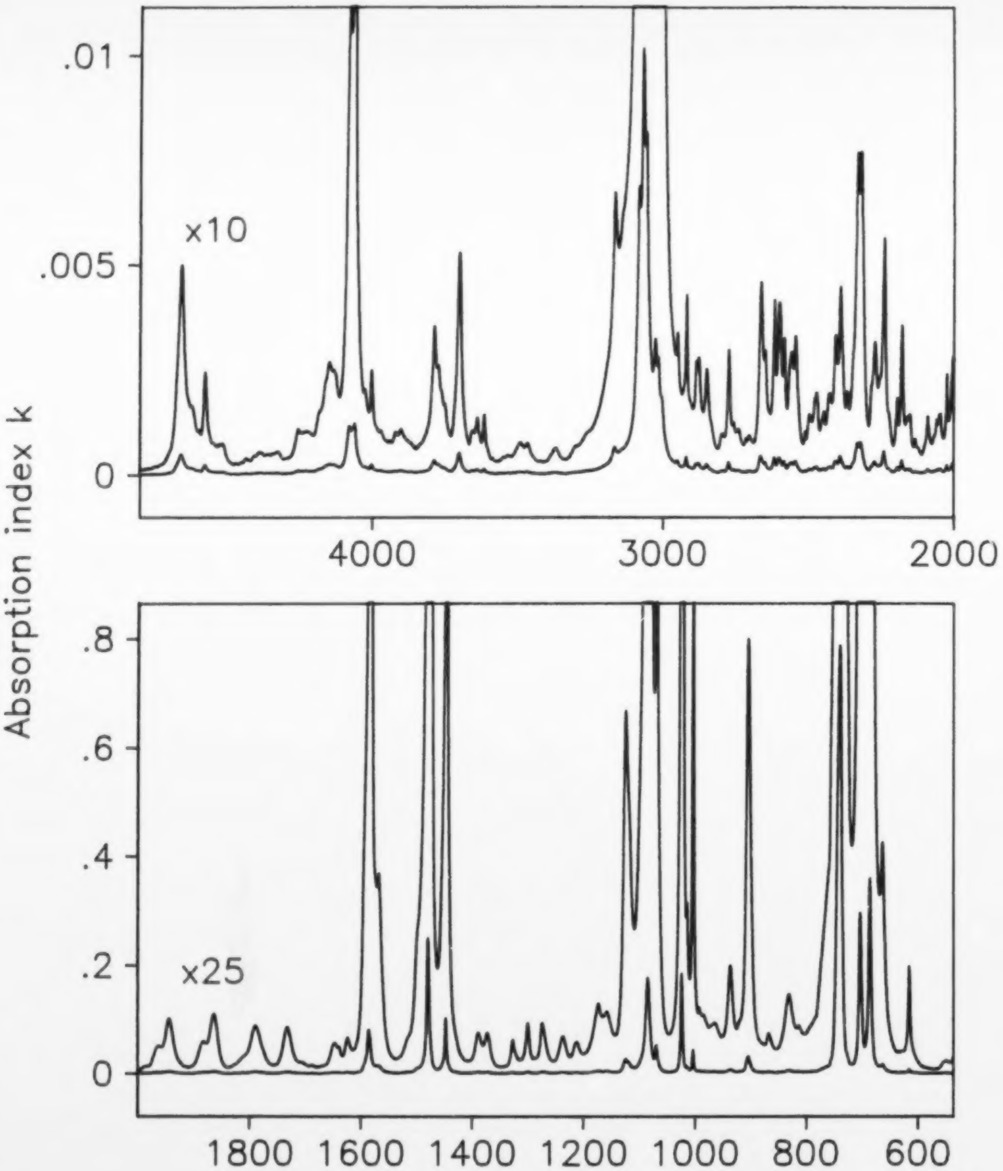

Figure 7.2 - The absorption index, $k(\tilde{\nu})$, spectrum of chlorobenzene at 25°C. In each box, the ordinate scale describes the lower spectrum. For the upper spectra, the ordinate labels must be divided by 10 (upper box) or 25 (lower box). Each curve is the superposition of the original spectrum and that recovered from a Compact Table.

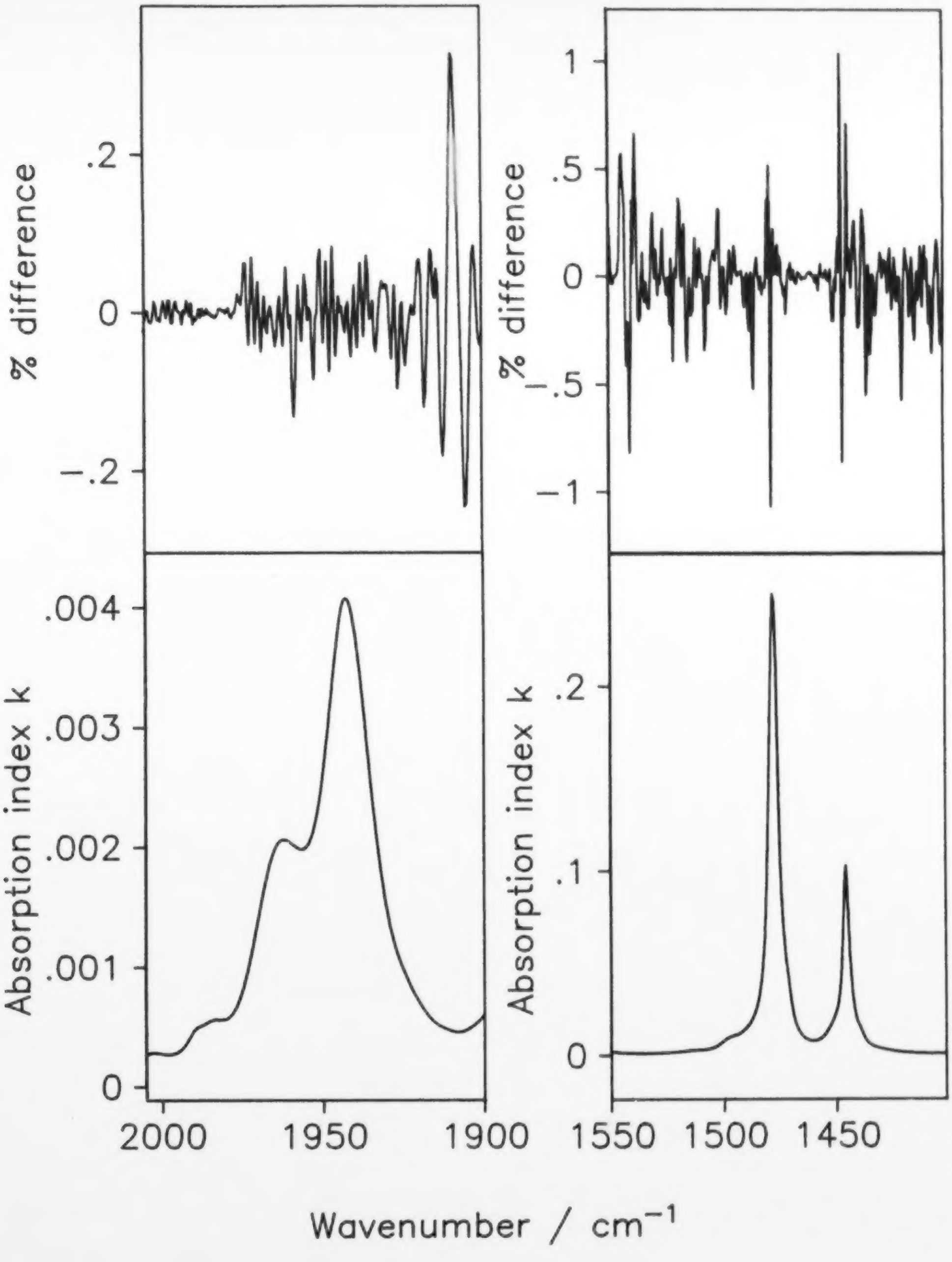

Figure 7.3 - Lower boxes: Two of the bands in Fig. 7.2, with the original spectrum superimposed on that recovered from a Compact Table. Upper boxes: The percent difference between the recovered and original spectra.

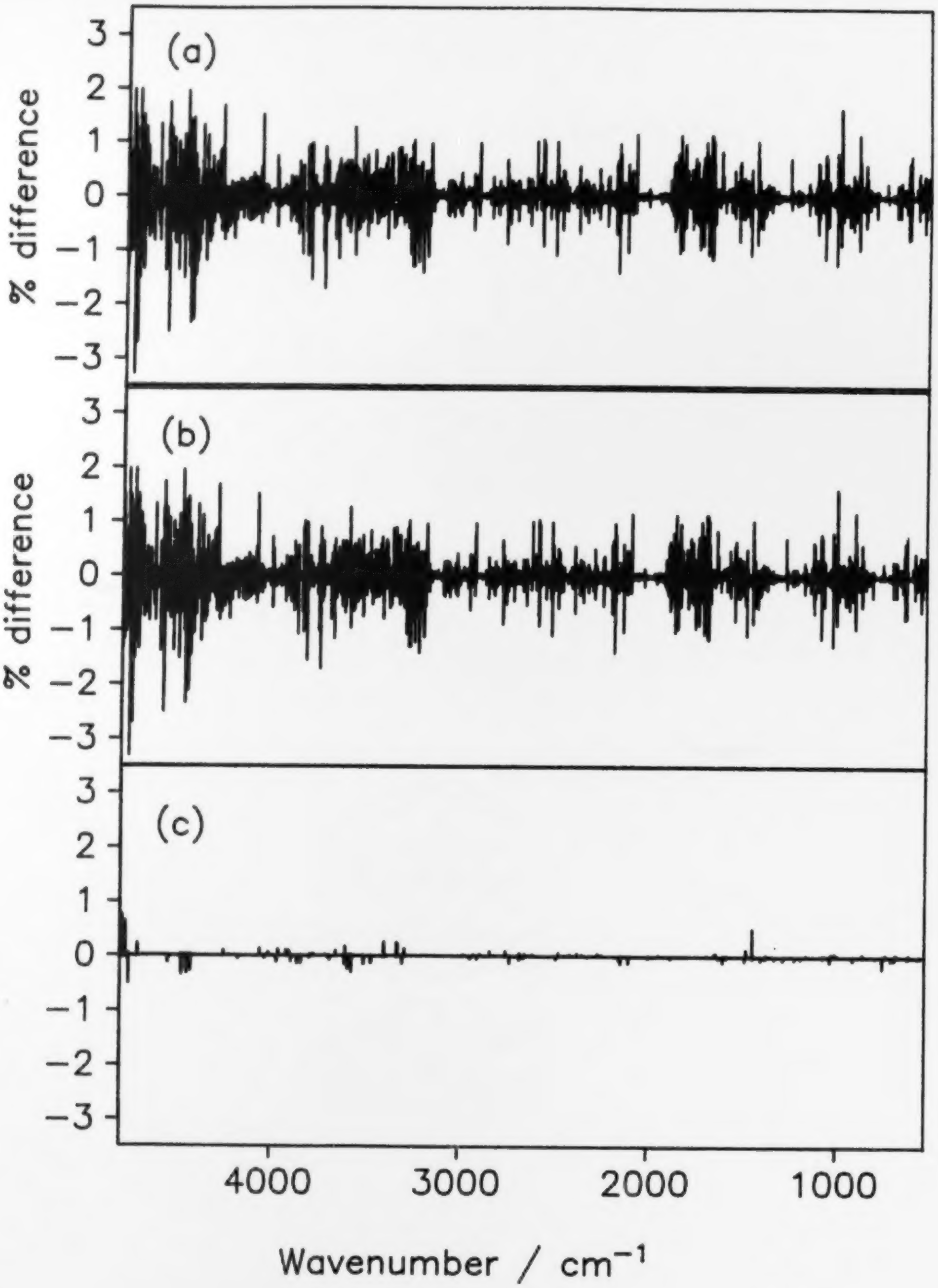

Figure 7.4 - The percent difference between the recovered and original $k(\tilde{\nu})$ spectra when (a) 4 digits or (b) 6 digits were retained in the Compact Table. (c) The difference between the percent differences in the upper two boxes.

constructed Compact Tables with integer ordinate values given to first four and then six significant figures, and recovered the spectrum from each. The accuracies of recovery are shown in Figures 7.4a and 7.4b respectively. The difference between the two is given in Figure 7.4c. In most cases the effect of truncation is less than ±0.1%. Again the few disagreements above 0.1% are not in consecutive points.

In addition to the imaginary refractive index spectrum, the real refractive index, $n(\tilde{\nu})$, and the molar absorption coefficient, $E_m(\tilde{\nu})$, spectra are of common interest. Figure 7.5 shows the recovery of the real refractive index spectrum by two different methods, by interpolation of the tabulated n values (middle box) and by Kramers-Kronig[13] transformation of the recovered absorption index spectrum (upper box). It is evident that the best method of recovering n values is through the Kramers-Kronig transformation of the recovered k values. However, in both cases the accuracy of recovery is better than ±0.02% at most wavenumbers, and the few larger disagreements are not in consecutive points. Thus, while the Kramers-Kronig transformation of the recovered imaginary refractive index is the best procedure (average accuracy of ±0.005%), the $n(\tilde{\nu})$ values can be recovered with good accuracy by interpolating the values in a compact $n(\tilde{\nu})$ table.

The molar absorption coefficient spectrum, $E_m(\tilde{\nu})$, can be calculated from the imaginary refractive index, as noted earlier. The accuracy of recovery of E_m values was tested by two methods. First, the E_m spectrum was calculated from the k spectrum, a Compact Table of E_m values was created, the E_m spectrum was recovered from the table

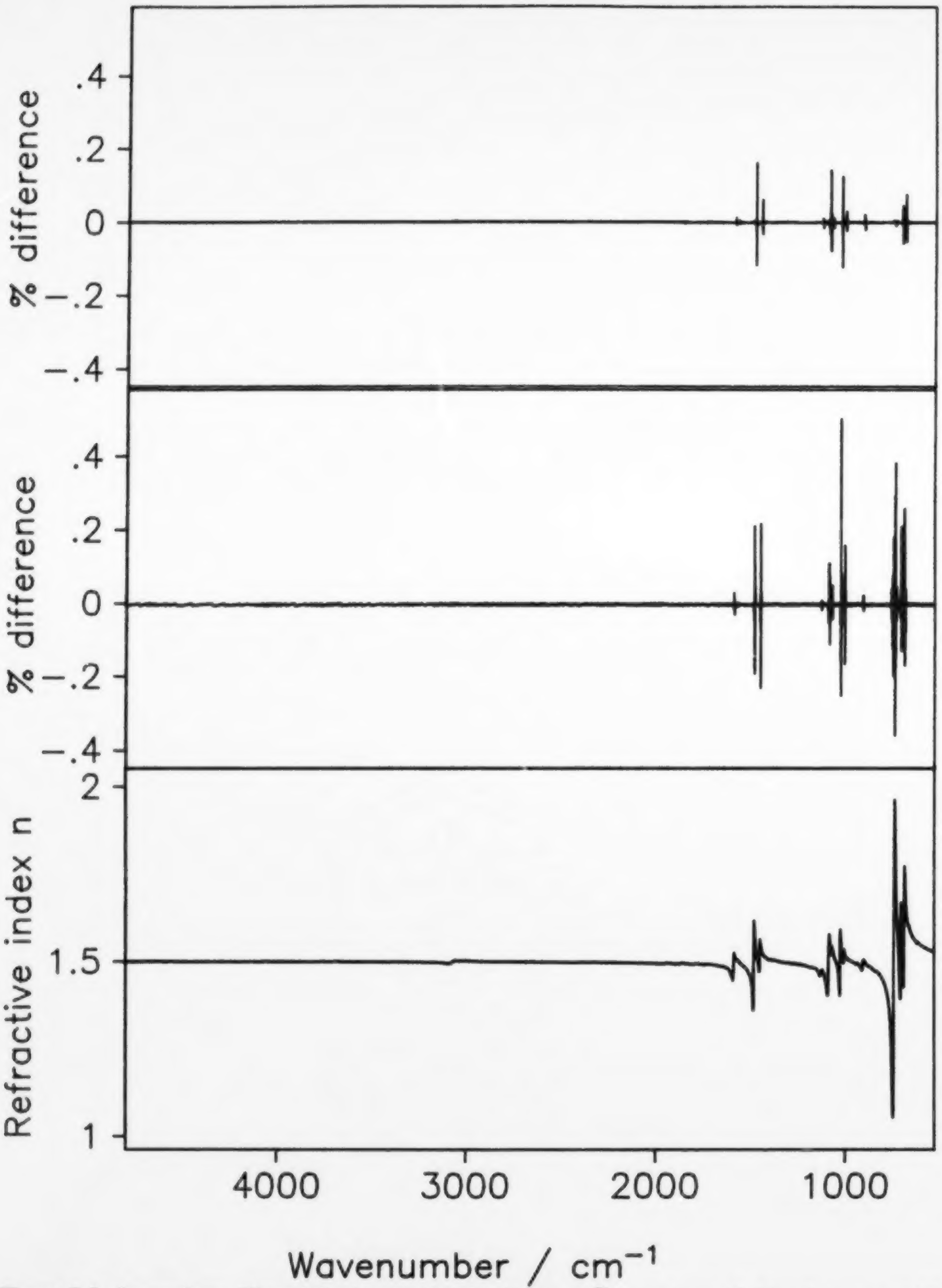

Figure 7.5 - Lower box: The original real refractive index, $n(\tilde{\nu})$, spectrum of chlorobenzene at 25°C superimposed on that recovered from a Compact Table of $n(\tilde{\nu})$ values. Middle box: The percentdifference between the recovered and original spectra in the lower box. Upper box: The percent difference between the original $n(\tilde{\nu})$ spectrum and that calculated by Kramers-Kronig transform of the $k(\tilde{\nu})$ spectrum recovered from a Compact Table of $k(\tilde{\nu})$ values.

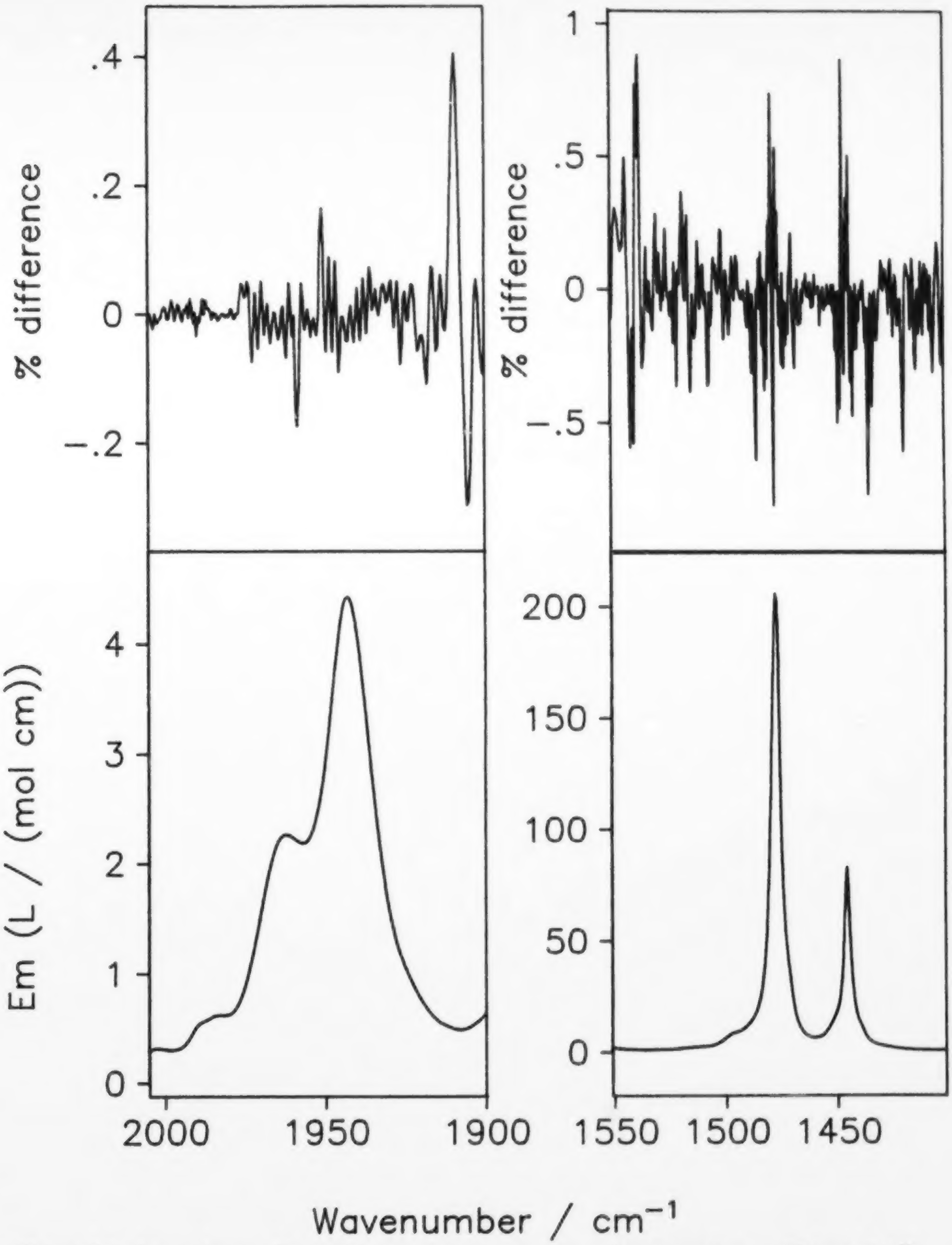

Figure 7.6 - Lower boxes: Two of the bands in the decadic molar absorption coefficient, $E_m(\tilde{\nu})$, spectrum of chlorobenzene at 25°C. The original spectrum is superimposed on that recovered from a Compact Table of $E_m(\tilde{\nu})$ values. Upper boxes: The percent difference between the recovered and original spectra.

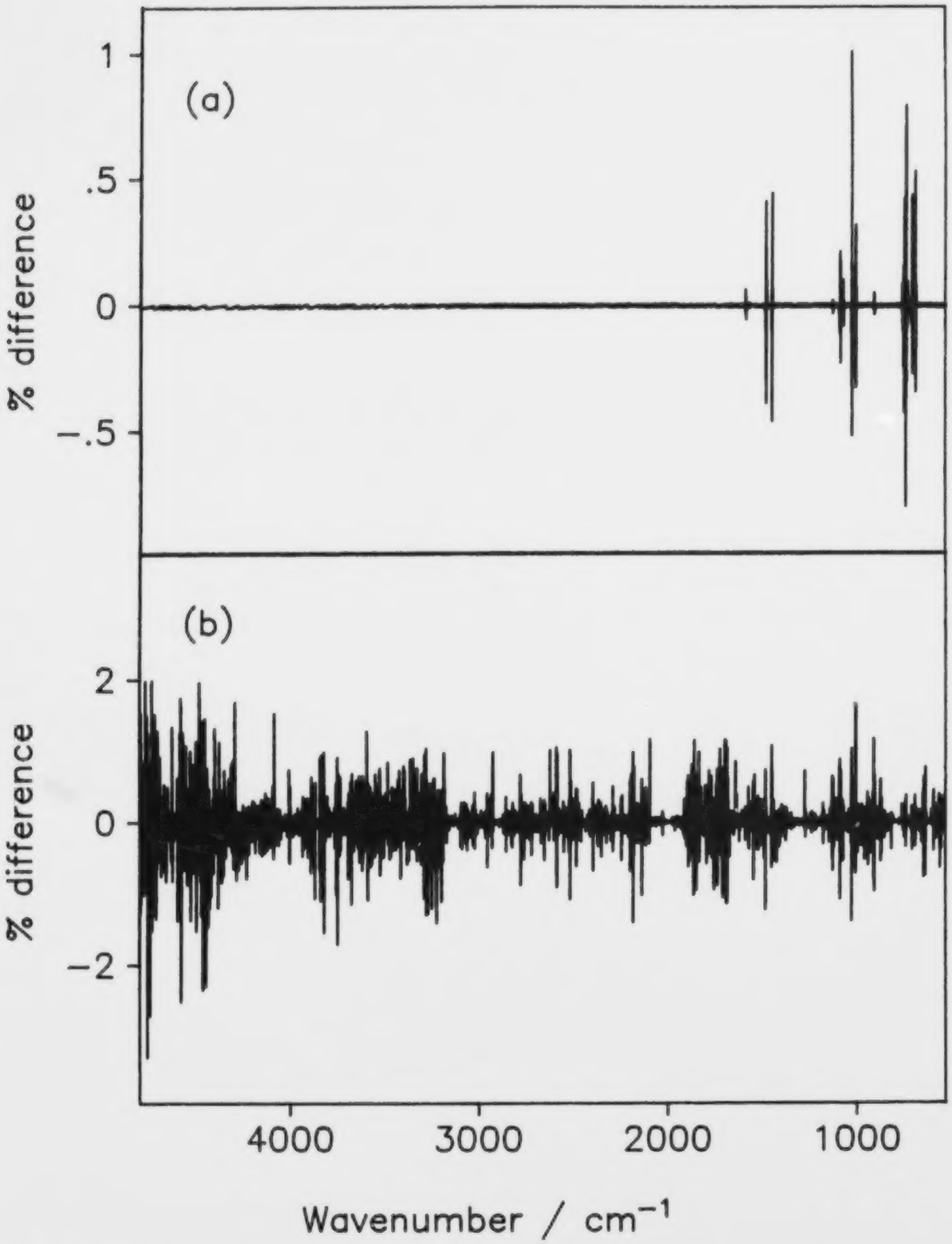

Figure 7.7 - The percent differences between the real (a) and imaginary (b) dielectric constants calculated from the original real and imaginary refractive index spectra and from real and imaginary refractive index spectra recovered from Compact Tables.

by interpolation as described above, and the recovered spectrum was compared with the original. Second, the E_m spectrum was calculated from the original k spectrum and also from the k spectrum recovered from a Compact Table, and the two E_m spectra were compared. The same level of accuracy in the recovered spectrum was obtained from both methods. The lower boxes of Figure 7.6 show two bands of the original molar absorption coefficient spectrum superimposed onto the two bands recovered by the first method. The accuracy of the recovery for these bands is shown in the upper boxes as the percent difference between the original and recovered spectra. The accuracy is expected to be of the same order as the accuracy of the imaginary refractive index, with slight differences because the molar absorption coefficient values are weighted by $\tilde{\nu}$. Comparison of Fig. 7.6 with Fig. 7.2, which shows the same information for the same bands in the imaginary refractive index spectrum, confirms this expectation.

The dielectric constants can be calculated from the refractive indices. The real dielectric constant, $\varepsilon'(\tilde{\nu})$, is given by $\varepsilon'(\tilde{\nu}) = n^2(\tilde{\nu}) - k^2(\tilde{\nu})$, while the imaginary part, $\varepsilon''(\tilde{\nu})$, also called the dielectric loss, is given by $\varepsilon''(\tilde{\nu}) = 2n(\tilde{\nu})k(\tilde{\nu})$. Figure 7.7 shows the percent differences between the real (a) and imaginary (b) dielectric constants calculated from original and recovered refractive index spectra. For the real dielectric constant, since $n > 10k$ for most of the spectral range, the accuracy of recovery should be that of the n^2 spectrum, i.e. the percent differences should be twice those of the recovered n spectrum. Comparison of Fig. 7.7a and 7.5 shows that this is the case. For the dielectric loss, the recovery should be accurate to the sum of the percent accuracies of recovery of the real and imaginary refractive indices. Since the percent accuracy of recovery of the *k* spectrum is much worse than that of the *n* spectrum, it follows that the accuracy of recovery of the imaginary dielectric constant spectrum (Fig. 7.7b) is essentially that of the *k* spectrum (Fig. 7.2).

7.5 - Summary

A Compact Table is described to allow numerical reporting of accurate spectral intensity values over the entire infrared spectrum. The table is about one tenth of the size required to report the spectrum in conventional XY format, and allows the intensity values to be recovered with no loss of the experimental accuracy.

The imaginary refractive index and the molar absorption coefficient values can be recovered with average accuracy of about 0.2% and better accuracy than 1% for nearly all points of the spectrum. The real refractive index values can be recovered with average accuracy 0.005%, with most spectral points recovered to better than 0.02%. When the recovered data are used to calculate the dielectric constants, the real dielectric constants have about half of the accuracy of the recovered real refractive index values, and the imaginary dielectric constants have the same degree of accuracy as the imaginary refractive index.

If one has the value of the real refractive index at the highest wavenumber in the spectrum and an accurate program for the Kramers-Kronig transform from $k(\tilde{\nu})$ to $n(\tilde{\nu})$, the $n(\tilde{\nu})$ spectrum can be recovered from a Compact Table of the absorption index values, $k(\tilde{\nu})$, to better accuracy than it can be recovered from a Compact Table of $n(\tilde{\nu})$ values. Thus the intensity properties can be recovered from a single Compact Table of $k(\tilde{\nu})$ values to at least the accuracies given above. This means, for example, that for liquid methanol a one-page Compact Table contains all of the information needed to recover the complete quantitative intensity information needed to calculate any spectroscopic property between 8000 and 2 cm^{-1} within the experimental accuracy[9].

7.6 - Appendix A

7.6.1 - Input file - Comptab.asc

nruns / no. of spectra, each one to be converted to a table
and then for each run
head(1) / comment
head(2) / comment
filein,fileout / input and output filenames
spectype / allowed entries: k or n or e
wl / laser wavenumber in cm^{-1}
nregion / no. of regions
xsreg(i),xfreg(i),factor(i) / starting cm^{-1}, final cm^{-1}, desired spacing in region. one line for each region.

7.6.2 - Summary of variables used in program:

y - a vector containing y values.
xs and xe - starting and ending wavenumbers.
zy(i) - vector zy contains y values after the reduction of the number of points.
z(i,j) - array z contains zy values arranged in rows (i) and columns (j).

nptsreg(i) - number of points in region i.

expo(i) - vector expo contains the Y-exponents.

jz(i,j) - array jz contains values of z(i,j)*10**(-expo(i)) stored as integers.

actspace - the wavenumber spacing in the original file.

nredstep - the reduction factor for the number of points in the region.

newnpts - number of points in the region after reduction.

indl - number of lines in the region.

ncorect - correction to the index in the original spectral file of the next starting wavenumber, xsreg(i+1), to ensure that each point is presented only once and the spacing between xfreg(i) and xsreg(i+1) is that of factor(i+1).

7.6.3. - Program listings

```
program Compact Table
implicit real*8(a-h,o-z)
dimension xsreg(35),xfreg(35),factor(35)
real*4 y(16384),xs,xe,res
dimension z(975,17),zy(16384)
integer*4 nptsreg(35),jz(975,17),expo(975)
integer*2 npts,ier
character*12 filein,fileout
character*192 comm
integer*1 xt,yt
character*1 spectype
character*76 head(2)
open(6,file='comptab.asc')
read(6,*)nruns
do 10 i=1,nruns
read(6,900)head(1)
read(6,900)head(2)
read(6,*)filein,fileout
```

```
        read(6,905)spectype
        read(6,*)wl
        if(spectype.eq.'k') nkflag=0
        if(spectype.eq.'n') nkflag=1
        if(spectype.eq.'e') nkflag=2
        read(6,*)nregion
        do 20 j=1,nregion
20      read(6,*)xsreg(j),xfreg(j),factor(j)
        open(8,file=fileout)
c       write table header according to nkflag
        if(nkflag.ne.1) write(8,895)
        if(nkflag.eq.1) write(8,896)
c       read data. the following part is for use with files in the .SPC format of Galactic
c       Industries' SpectraCalc software.  modification is needed for a different format of
c       input data
        call readsc(filein,y,npts,xs,xe,xt,yt,res,comm,ier)
c       calculate actual spacing
        actspace=(xs-xe)/(npts-1)
c       start a loop to calculate everything for each region
        j=1
c       calculate no. of pts in region, the reduction step and finally the new no. of pts in
c       that region
        if((factor(j)/actspace).lt.1) then
        write(*,*)' reduction is impossible. cannot create points'
        stop
        endif
        nredstep=idnint(factor(j)*(wl/16384.d0)/actspace)
40      nptsreg(j)=idnint((xsreg(j)-xfreg(j))/actspace+1.0)
        newnpts=idnint((nptsreg(j)-1.0)/nredstep)+1
        xfreg(j)=xsreg(j)-actspace*nredstep*(newnpts-1)
c       recalculate nptsreg and newnpts
```

```
      nptsreg(j)=idnint((xsreg(j)-xfreg(j))/actspace+1.0)
      newnpts=idnint((nptsreg(j)-1.0)/nredstep)+1
      ntype=nint(dlog(factor(j))/dlog(2.0))
c     create a zy array to store the reduced y data
      if(j.eq.1)ncorect=nint((xs-xsreg(1))/actspace+1)
      do 50 l=1,newnpts
50    zy(l)=y((l-1)*nredstep+ncorect)
c     calculate number of lines in region j
      inline=17
      indl=newnpts/inline
      if((indl*inline).ne.newnpts)indl=indl+1
      iflag=0
c     create a matrix, z, to store the zy data
      do 60 m=1,indl
      do 70 k=1,inline
70    z(m,k)=zy((m-1)*inline+k)
c     find 10^n exponent factor for the line
      if(m.eq.indl) iflag=1
      if(nkflag.ne.1) then
      call findexpo(z,m,expo,iflag,newnpts)
c     multiply by the exponent factor for the line expo(m)
      do 80 k=1,inline
80    jz(m,k)=ifix(z(m,k)*10.**(-expo(m))+0.5)
      else
      do 81 k=1,inline
81    jz(m,k)=ifix(z(m,k)*10000)
      endif
c     write line to file
85    zxline=xsreg(j)-actspace*((m-1)*inline)*nredstep
      if(nkflag.ne.1) then
      if(m.ne.indl)  write(8,925)zxline,ntype,expo(m),(jz(m,k),k=1,inline)
      if(m.eq.indl)   write(8,925)zxline,ntype,expo(m), (jz(m,k),k=1,newnpts-(m-1)*inline)
        else
        if(m.ne.indl) write(8,935)zxline,ntype,(jz(m,k),k=1,inline)
        if(m.eq.indl) write(8,935)zxline,ntype,(jz(m,k),k=1,newnpts-(m-1)*inline)
        endif
60      continue
c       calculate the reduction step for the next region, adjust the starting wavenumber for
c       that region and go back to statement 40 to redo the whole process for the next
c       region
        j=j+1
        if(j.le.nregion) then
        nredstep=idnint(factor(j)*(wl/16384.d0)/actspace)
        ncorect=ncorect+nptsreg(j-1)+nredstep-1
        xsreg(j)=xfreg(j-1)-nredstep*actspace
        goto 40
        endif
c       end of loop to calculate everything for each region
10      continue
895 format(1x,'cm-1 ',2x,'xe',1x,'ye',3x,'0',4x,'1',4x,'2',4x,'3',4x,'4',4x,'5',4x,'6',4x,'7',4x,
     + '8',4x,'9',3x,'10',3x,'11',3x,'12',3x,'13',3x,'14',3x,'15',3x,'16')
896 format(1x,'cm-1',4x,'xe',4x,'0',5x,'1',5x,'2',5x,'3',5x,'4',5x,'5',5x,'6',5x,'7',5x, '8',5x,
     +  '9',4x,'10',4x,'11',4x,'12',4x,'13',4x,'14',4x,'15',4x,'16')
900     format(a76)
905     format(a1)
925     format(f7.2,1x,i2,1x,i2,17(1x,i4))
935     format(1x,f7.2,1x,i2,17(1x,i5.5))
        stop
        end

        subroutine findexpo(z,m,expo,iflag,newnpts)
c       Suboutine to find the maximum value of z(j,k) in row j. Then to calculate expo(j),
c    such that the entries within that line are multiplied by 10**(-expo(j)) when the
c    table is created.
     implicit real*8(a-h,o-z)
     dimension z(975,17)
     integer*4 expo(975)
c    Find the largest entry within a row. Use iflag to deal with the last row, which may
c    contain fewer entries than  inline=17.
     zmax=0.e0
     if(iflag.ne.1) then
     do 200 i=1,17
200  zmax=amax1(zmax,z(m,i))
     else
     do 210 i=1,newnpts-(m-1)*17
210  zmax=amax1(zmax,z(m,i))
     endif
c    compute the exponential factor
     if(zmax.ge.10000.0)  then
     expo(m)=1
     elseif(zmax.ge.1000.0)  then
     expo(m)=0
     elseif(zmax.ge.100.0) then
     expo(m)=-1
     elseif(zmax.ge.10.0)  then
     expo(m)=-2
     elseif(zmax.ge.1.0) then
     expo(m)=-3
     elseif(zmax.ge.1.d-1) then
     expo(m)=-4
     elseif(zmax.ge.1d-2) then
     expo(m)=-5
     elseif(zmax.ge.1d-3) then
```

```
expo(m)=-6
elseif(zmax.ge.1d-4) then
expo(m)=-7
elseif(zmax.ge.1d-5) then
expo(m)=-7
elseif(zmax.ge.1d-6) then
expo(m)=-7
else
expo(m)=0
endif
return
end
```

7.7 - Appendix B

7.7.1 - Input file - Trecover.asc

nruns	/ no. of tables, each one to be converted to a spectrum
and then for each run	
head(1)	/ comment
head(2)	/ comment
filein,fileout	/ input and output filenames
xs,wl,idespace	/ first wavenumber in Compact Table, laser wavenumber, and the x-exponent, XE, to give the desired spacing in output spectrum (smallest XE in Compact Table)
spectype	/ allowed values: k or n or e
nregion	/ number of regions
nptsreg(i),nfactor(i)	/ number of points in region, reduction factor in the region. one line for each region.

7.7.2 - Summary of variables used in program

y - a vector created to contain the ordinate values calculated from the table.

z - a vector with the values of the current line in the table.

t (i) - the value of the i th point of the 4 points that are needed for the interpolation.

nfactor(j) - the interpolation factor in region j.

nptsreg (j) - the number of points in the table for region j.

indxhreg(j) - the high wavenumber index for the straightforward interpolation in region j.

indxlreg(j) - the low wavenumber index for the straightforward interpolation in region j.

nonhreg(m,k), nonlreg(m,k)

Boundary interpolation is defined by the four indices nonhreg(m,1), nonlreg(m,1), nonhreg(m,2) and nonlreg(m,2). m=1 to nregion-1 = index of high wavenumber region at the boundary. k=1 if the point indexed is in region m and k=2 if it is in region m+1.

idumnon - a dummy vector used in the interpolation (inter1) routine.

7.7.3 - Program listings

```
program  trecover
implicit real*8(a-h,o-z)
character*12 filein,fileout
dimension y(16384),z(17),t(4)
integer*4 indxhreg(35),indxlreg(35),nonhreg(35,2),nonlreg(35,2), nptsreg(35),
integer*4 nfactor(35), left(975),idumnon(35)
real*4 r(16384)
integer*1 xt,yt
integer*2 npt
character*76 head(2)
character*80 tablhead
character*192 comm
character*1 spectype
data  xt /1/, yt /0/, res /0/, ier /0/
open(6,file='trecover.asc')
```

```
      read(6,*)nruns
      do 10 i=1,nruns
      read(6,900)head(1)
      read(6,900)head(2)
      read(6,*)filein,fileout
      read(6,*)xs,wl,idespace
      read(6,901)spectype
      if(spectype.eq.'k')  nkflag=0
      if(spectype.eq.'n')  nkflag=1
      if(spectype.eq.'e')  nkflag=2
      read(6,*)nregion
      do 20 j=1,nregion
20    read(6,*)nptsreg(j),nfactor(j)
c     calculate total no. of points (npts), indices of straightforward and boundary
c     interpolation regions.
      npts=1+(nptsreg(1)-1)*nfactor(1)
      indxhreg(1)=1
      indxlreg(1)=1+(nptsreg(1)-2)*nfactor(1)
      if(nregion.gt.1) then
      do 30 j=2,nregion
      nonhreg(j-1,1)=indxlreg(j-1)
      nonlreg(j-1,1)=nonhreg(j-1,1)+nfactor(j-1)
      nonhreg(j-1,2)=nonlreg(j-1,1)
      nonlreg(j-1,2)=nonhreg(j-1,2)+nfactor(j)
      indxhreg(j)=npts+nfactor(j)
      npts=npts+nptsreg(j)*nfactor(j)
      indxlreg(j)=npts-nfactor(j)
30    continue
      endif
c     calculate the original end point xe and the final end point xe1
      xe=xs-(npts-1)*(wl/16384.d0)*2.**(idespace)
```

```
        xe1=xs-(indxlreg(nregion)-1)*(wl/16384.d0)*2.**(idespace)
c       read table values
        open(9,file=filein)
        read(9,910)tablhead
        do 40 k=1,nregion
c       calculate no. of lines in region k (lines) and no. of pts in the last line of region k
c       (left)
        lines=nptsreg(k)/17
        do 45 m=1,lines
        left(m)=17
45      continue
        if(lines*17.ne.nptsreg(k)) then
        lines=lines+1
        left(lines)=nptsreg(k)-(lines-1)*17
        endif
c       start reading region by region, one line at a time and create a temporary array, z,
c       for the line.  Then put the values of the line  into the correct position in the y array
        do 50 k1=1,lines
        if(nkflag.ne.1)  read(9,*)wvjunk,njunk,xn,(z(k2),k2=1,left(k1))
        if(nkflag.eq.1)  read(9,*)wvjunk,njunk,(z(k2),k2=1,left(k1))
        do 55 k3=1,left(k1)
   if(nkflag.ne.1) y(indxhreg(k)+(k1-1)*nfactor(k)*17+(k3-1)*nfactor(k))=z(k3)*10**xn
   if(nkflag.eq.1) y(indxhreg(k)+(k1-1)*nfactor(k)*17+(k3-1)*nfactor(k))=z(k3)/10000.
55      continue
50      continue
40      continue
c       start interpolating in regions that are straightforward.
        do 60 l=1,nregion
        if(l.eq.1) t(1)=y(1)
        if(l.ne.1)  t(1)=y(nonhreg(l-1,2))
        t(2)=y(indxhreg(l))
```

```
      t(3)=y(indxhreg(l)+nfactor(l))
      t(4)=y(indxhreg(l)+2*nfactor(l))
      ind=indxhreg(l)+2*nfactor(l)
      do 70 m=1,nptsreg(l)-2
      call inter1(y,t,l,m,nfactor,indxhreg)
c     adjust t
      ind=ind+nfactor(l)
      t(1)=t(2)
      t(2)=t(3)
      t(3)=t(4)
      t(4)=y(ind)
70    continue
60    continue
c     interpolate in boundary regions. In each boundary do the region with bigger
c     nfactor first.
      do 80 l1=2,nregion
      if(nfactor(l1-1).gt.nfactor(l1)) then
      t(1)=y(nonhreg(l1-1,1)-nfactor(l1-1))
      t(2)=y(nonhreg(l1-1,1))
      t(3)=y(nonlreg(l1-1,1))
      t(4)=y(nonlreg(l1-1,1)+nfactor(l1-1))
      idumnon(l1-1)=nonhreg(l1-1,1)
      call inter1(y,t,l1-1,1,nfactor,idumnon)
      t(1)=y(nonhreg(l1-1,2)-nfactor(l1))
      t(2)=y(nonhreg(l1-1,2))
      t(3)=y(nonlreg(l1-1,2))
      t(4)=y(nonlreg(l1-1,2)+nfactor(l1))
      idumnon(l1)=nonhreg(l1-1,2)
      call inter1(y,t,l1,1,nfactor,idumnon)
      else
      t(1)=y(nonhreg(l1-1,2)-nfactor(l1))
      t(2)=y(nonhreg(l1-1,2))
      t(3)=y(nonlreg(l1-1,2))
      t(4)=y(nonlreg(l1-1,2)+nfactor(l1))
      idumnon(l1)=nonhreg(l1-1,2)
      call inter1(y,t,l1,1,nfactor,idumnon)
      t(1)=y(nonhreg(l1-1,1)-nfactor(l1-1))
      t(2)=y(nonhreg(l1-1,1))
      t(3)=y(nonlreg(l1-1,1))
      t(4)=y(nonlreg(l1-1,1)+nfactor(l1-1))
      idumnon(l1-1)=nonhreg(l1-1,1)
      call inter1(y,t,l1-1,1,nfactor,idumnon)
      endif
80    continue
c     Write output file.  This section to statement 10 assumes Galactic Industries .SPC
c     ile format, as used by SpectraCalc and GRAMS softwares.  Y values are
c     converted to single precision and sent to the .SPC write subroutine.  Wavenumber
c     information is sent by the starting wavenumber, the ending wavenumber and the
c     number of points.
      npt=indxlreg(nregion)
      do 90 l=1,indxlreg(nregion)
90    r(l)=y(l)
      comm=head(2)
      call writesc(fileout,r,npt,real(xs),real(xe1),xt,yt,res,comm,ier)
10    continue
900   format(1x,a76)
901   format(a1)
910   format(a80)
      stop
      end

      subroutine inter1(y,t,l,m,nfactor,indxh)
      implicit real*8(a-h,o-z)
      dimension y(16384),t(4)
      integer*4 indxh(35), nfactor(35)
c     calculate slopes and coefficients
      s1=(t(3)-t(1))/2.0d0
      s2=(t(4)-t(2))/2.0d0
      a=2*t(2)-2*t(3)+s1+s2
      b=3*t(3)-3*t(2)-2*s1-s2
      do 700 kindx=1,nfactor(l)-1
      ratio=dble(kindx)/dble(nfactor(l))
      y(indxh(l)+(m-1)*nfactor(l)+kindx)=a*ratio**3+b*ratio**2+s1*ratio+t(2)
700   continue
      return
      end
```

7.8 - References

1. *"Tables of Wavenumbers for the Calibration of Infra-red Spectrometers"*, I.U.P.A.C. , Butterworths Scientific Publications, London, 1961.

2. A.R.H. Cole, *"Tables of Wavenumbers for the Calibration of Infrared Spectrometers"*, 2nd Ed. , Pergamon Press 1977.

3. T.G. Goplen, D.G. Cameron and R.N. Jones, Appl. Spectrosc., **34**, 657 (1980)

4. a) I.M. Nyquist, I.M. Mills, W.B. Person and B. Crawford, Jr., J. Chem. Phys., **26**, 552 (1957), b) A.D. Dickson, I.M. Mills and B. Crawford, Jr., J. Chem. Phys., **27**, 445 (1957).

5. a) A.C. Gilby, J. Burr, Jr., W. Krueger and B. Crawford, Jr., J. Phys. Chem., **70**,

1525 (1966), b) C.E. Favelukes, A.A. Clifford and B. Crawford, Jr., J. Phys. Chem., **72**, 962 (1968), c) T. Fujiyama and B. Crawford, Jr., J. Phys. Chem., **72**, 2174 (1968).

6. a) J.E. Bertie, H.J. Labbe and E. Whalley, J. Chem. Phys., **50**, 4501 (1969), b) G.M. Hale and M.R. Querry, Appl. Opt., **12**, 555 (1973), c) H.D. Downing and D. Williams, J. Geophys. Res., **80**, 1656 (1975), d) V.M. Zolotarev and A.V. Demin, Opt. Spectrosc. (USSR), **43**, 157 (1977).

7. J.E. Bertie, R.N. Jones and Y. Apelblat, Appl. Spectrosc., **48**, 144 (1994).

8. J.E. Bertie, R.N. Jones and C.D. Keefe, Appl. Spectrosc., **47**, 891 (1993).

9. J.E. Bertie, S.L. Zhang, H.H. Eysel, S. Baluja and M.K. Ahmed, Appl. Spectrosc., **47**, August (1993).

10. J.E. Bertie, C.D. Keefe and R.N. Jones, Can. J. Chem. **69**, 1607 (1991).

11. R.S. McDonald and P. A. Wilks, Jr., Appl. Spectrosc., **42**, 151 (1988).

12. C. de Boor, *"A practical guide to splines"* in Applied Mathematical Sciences **27**, 49-57, Springer-Verlag New York 1978.

13. J.E. Bertie and S.L. Zhang , Can. J. Chem. **70**, 520 (1992).

Chapter 8 - Summary

In this work the real and imaginary refractive index spectra of liquid chlorobenzene and toluene were measured across the entire mid-infrared region at 25°C. To evaluate the systematic errors, a comparison was made with spectra measured by other spectroscopists in different laboratories with different instruments. From this comparison, it was estimated that the accuracy is ±0.2% for the real refractive index and ±2-3% for the imaginary refractive index. The real and imaginary refractive indices are fundamental physical quantities. They were used to calculate other measures of infrared absorption intensities of these liquids such as the molar absorption coefficient, the complex dielectric constant and the complex molar polarizability. The molar absorption coefficient and the imaginary dielectric constant and the imaginary molar polarizability have approximately the same accuracy as the imaginary refractive index, i.e. ±2-3%. The real dielectric constant and the real molar polarizability have approximately twice the error of the real refractive index, i.e. ±0.4%.

The optical constants and the molar absorption coefficient spectra of toluene and chlorobenzene measured in this work, together with those of liquid benzene and dichloromethane measured separately, were used to establish secondary infrared intensity standards for liquids. These standards have been published by the International Union of Pure and Applied Chemistry and can be used to calibrate other intensity measurements.

Molecular properties such as the dipole transition moment and the dipole moment derivative with respect to normal coordinate are more directly reflected in the imaginary molar polarizability spectrum than in the imaginary refractive index spectrum or the molar absorption coefficient spectrum. These properties are calculated from the integrated intensities of the bands. In order to obtain reliable integrated intensities, the imaginary molar polarizability spectrum had to be separated first into contributions from different transitions. The separation was achieved by curve fitting the imaginary molar polarizability spectra with bands of classical damped harmonic oscillator shape, then calculating the integrated intensities from the parameters of the fitted bands. In this work, an improved curve-fitting program was developed which allows a better fit to be obtained faster. The accuracy of the integrated intensities is estimated at 3-5% for strong bands and 5-10% for weak bands. The results of this work are corrected for liquid dielectric effects and agree usually within a factor of two with literature values for the gas obtained by experimental or by *ab initio* calculation. In these cases the agreement must mean that the vibrations in question have very similar intrinsic intensities in the liquid and gas phases.

The integrated intensities of the 30 fundamentals of liquid chlorobenzene and toluene were compared with each other because the two compounds have the same molecular skeleton with the exception of the chlorine atom and the methyl group. It was found for the two liquids that the integrated intensities of many of the fundamentals or of the sum of two fundamentals that result from the splitting of a degenerate fundamental in benzene, are usually within a factor of 2 and so do not change significantly upon substitution.

There are notable exceptions. In toluene the intensity of the CH stretching vibrations is stronger by a factor of 4.6 than that in chlorobenzene. It appears that the chlorine substitution shifts intensity from the CH stretching vibrations to other vibrations. This shift of intensity is compensated in ν_{26}, ν_7, ν_{10} and ν_{11}, in particular in ν_7 and ν_{10}, for which the integrated intensities in liquid chlorobenzene are significantly greater than those in toluene, by factors of 2.7, 62.1, 55.5 and 6.2, respectively. It is quite possible that the gain in intensity in these vibrations, is associated with the presence of the electronegative chlorine and with the loss of intensity of the CH stretching vibrations.

The procedure used to determine the optical constants of the liquid from transmission measurements is exact but computationally difficult. A simpler, approximate method was developed to obtain the optical constants of the liquids. In this method the apparent absorbance due to reflection losses is calculated by treating the liquid cell as a single slab of window material. This simplifies the computation and the method is useful for nearly all common liquids in cells with alkali halide windows. For all but the strongest absorption bands the approximate method gives imaginary refractive indices that are within ~1% of those obtained from the exact method. Larger deviations occur when the mismatch between the refractive indices of the sample and the window exceed 0.15

Finally, a method for data reduction and presentation is given. The data is reduced and incorporated into a format that we call Compact Table. The Compact

Table format allows a spectrum to be tabulated in about 1/10 of the space required for a traditional table. The format allows direct retrieval of specific values, and also the retrieval, through a recovery program, of the entire spectrum without loss of intensity and line shape information. Other quantities that are calculated from those recovered by the recovery program, are obtained with the same accuracy as if calculated from the original quantities.

References

1. D. Steele in *Advances in Infrared and Raman Spectroscopy*, R.J.H Clark and R.E. Hester, Ed. (Heyden & Son, London, 1975) Vol 1, p. 232.
2. IUPAC Commission on Molecular Structure and Spectroscopy, *Tables of Wavenumbers for the Calibration of Infra-red Spectrometers*. Butterworths, London, 1961.
3. A.R.H. Cole, Tables of Wavenumbers for the Calibration of Infra-red Spectrometers. 2nd ed. Pergamon Press, Oxford, 1977.
4. B. Crawford, Jr., in *Vibrational Intensities in Infrared and Raman Spectroscopy*. W.B. Person and G. Zerbi, Ed. (Elsevier, Amsterdam, 1982).
5. J.E. Bertie, R.N. Jones and V. Behnam, Appl. Spectrosc., **39**, 401 (1985).
6. J.E. Bertie, R.N. Jones and V. Behnam, Appl. Spectrosc., **40**, 427 (1986).
7. T.G. Goplen, D.G. Cameron and R.N. Jones, Appl. Spectrosc., **34**, 657 (1980).
8. J.E. Bertie, R.N. Jones and C.D. Keefe, Appl. Spectrosc., **47**, 891 (1993).
9. J.E. Bertie, R.N. Jones, Y. Apelblat and C.D. Keefe, Appl. Spectrosc., **48**, 127 (1994).
10. J.E. Bertie, R.N. Jones and Y. Apelblat, Appl. Spectrosc., **48**, 144 (1994).
11. J.E. Bertie, Z. Lan, R.N. Jones and Y. Apelblat, Appl. Spectrosc., **49**, 840 (1995).

12. International Union of Pure and Applied Chemistry, Physical Chemistry Division, Commission on Molecular Structure and Spectroscopy, *Tables of Intensities for the Calibration of Infrared Spectroscopic Measurements in the Liquid Phase*, prepared by J.E. Bertie, C.D. Keefe and R.N. Jones, Blackwell Science 1995.

13. E.B. Wilson, Jr., J.C. Decius and P.C. Cross, *Molecular vibrations: The Theory of Infrared and Raman Vibrational Spectra*. (McGraw-Hill book company, Inc., New York, 1955).

14. K.S. Pitzer and D.W. Scott, J. Am. Chem. Soc., **65**, 803 (1943).

15. J.K. Wilmshurst and H.J. Bernstein, Can. J. Chem., **35**, 911 (1957).

16. M.A. Kovner and B.N. Snegirev, Optics and Spectroscopy, 7, 309 (1959).

17. N. Fuson, C. Garrigou-Lagrange, M.L. Josien, Spectrochim. Acta, **16**, 106 (1960).

18. E.W. Schmid, J. Brandmuller and G. Nonnenmacher, Z. fur Elekrochem., **64**, 726 (1960).

19. C. La Lau and R.G. Snyder, Spectrochim. Acta, **27A**, 2073 (1971).

20. R.T.C. Brownlee, D.G. Cameron, R.D. Topsom, A.R. Katritzky and A.J. Sparrow, J. Mol. Struct., **16**, 365 (1973).

21. D.M. Haaland and G.C. Nieman, J. Chem. Phys., **59**, 4435 (1973).

22. L.M. Sverdlov, M.A. Kovner and E.P. Krainov, *Vibrational Spectra of Polyatomic Molecules*. (Halsted Press, 1974).

23. G. Varsanyi, *Assignments for Vibrational Spectra of Seven Hundred Benzene Derivatives*, (John Wiley & Sons, New York, 1974).

24. V.J. Morrison and J.D. Laposa, Spectrochim. Acta, **32A**, 443 (1976).

25. J.A. Draeger, Spectrochim. Acta, **41A**, 607 (1985).

26. Y. Xie and J.E. Boggs, J. Comput. Chem., 7, 158 (1986).

27. M. Tasumi, T. Urano and M. Nakata, J. Mol. Struct., **146**, 383 (1986).

28. Y. Guan and D.L. Thompson, J. Chem. Phys., **92**, 313 (1990).

29. B. Galabov, S. Ilieva, T. Gunev and D. Steele, J. Mol. Struct., **273**, 85 (1992).

30. W.J. Balfour and Y. Fried, Can. J. Phys., **72**, 1218 (1994).

31. W.J. Balfour and R.S. Ram, Can. J. Phys., **72**, 1225 (1994).

32. V.M. Grosev, H.W. Schrotter and J. Jonuscheit, J. Raman Spectrosc., **26**, 137 (1995).

33. T.S. Bican, H.W. Schrotter and V.M. Grosev, J. Raman Spectrosc., **26**, 787 (1995).

34. H.F. Hameka and J.O. Jensen, J. Mol. Struct. (Theochem), **331**, 203 (1995).

35. D.H. Whiffen, Spectrochim. Acta, **7**, 253 (1955).

36. R.R. Randle and D.H. Whiffen, Trans. Faraday Soc., **52**, 9 (1956).

37. D.H. Whiffen, J. Chem. Soc., 1350 (1956).

38. R. Mierzecki, Acta Physica Polonica, **25**, 797 (1964).

39. J.R. Scherer, Spectrochim. Acta, **20**, 345 (1964).

40. H.D. Bist, V.N. Sarin, A. Ohja and Y.S. Jain, Spectrochim. Acta, **26A**, 841 (1970).

41. D.G. Cameron, R.D. Topsom and A.R. Katritzky, J. Chem. Phys., **56**, 4717 (1972).

42. Y.S. Jain, H.D. Bist, J. Mol. Spectrosc., **47**, 126 (1973).

43. M. Horak and A. Vitek, Collection Czechoslov. Chem. Commun., **39**, 1107 (1974).

44. H.J.K. Koser, Spectrochim. Acta, **40A**, 117 (1984).

45. H.J.K. Koser, Spectrochim. Acta, **40A**, 547 (1984).

46. H.J.K. Koser, Ber. Bunsen-Ges. Phys. Chem., **88**, 24 (1984).

47. X. Zhou, G. Fogarasi, R. Liu and P. Pulay, Spectrochim. Acta, **49A**, 1499 (1993).

48. J.E. Bertie, S.L. Zhang and C.D. Keefe, J. Mol. Struct., **324**, 157 (1994).

49. J.P. Hawranek, P. Neelkantan, R.P. Young and R.N. Jones, Spectrochim. Acta, **32A**, 75 (1976).

50. J.P. Hawranek, P. Neelkantan, R.P. Young and R.N. Jones, Spectrochim. Acta, **32A**, 85 (1976).

51. J.P. Hawranek and R.N. Jones, Spectrochim. Acta, **32A**, 99 (1976).

52. J.P. Hawranek and R.N. Jones, Spectrochim. Acta, **32A**, 111 (1976).

53. D.G. Cameron, J.P. Hawranek, P. Neelkantan, R.P. Young and R.N. Jones, *Computer Programs for Infrared Spectrophotometry XLII to XLVII*, National

Research Council of Canada Bulletin 16 (National Research Council Canada, Ottawa, 1977).

54. J.E. Bertie, C.D. Keefe and R.N. Jones, Can. J. Chem., **69**, 1609 (1991).

55. A.C. Gilby, J. Burr, Jr., W. Krueger and B. Crawford, Jr., J. Phys. Chem., **70**, 1525 (1966).

56. C.E. Favelukes, A.A. Clifford and B. Crawford, Jr., J. Phys. Chem., **72**, 962 (1968).

57. G.R. Fowles, *Introduction to Modern Optics*, 2nd Ed. (Holt, Rinehart and Winston Inc., New York, 1975.

58. J. Fahrenfort, in *Infra-Red Spectroscopy and Molecular Structure*, M. Davies, Ed. (Elsevier, Amsterdam, 1963).

59. G.D. Christian and J.E. O'Reilly, *Instrumental Analysis*, 2nd Ed. (Allyn and Bacon Inc., Boston. 1986).

60. I. Mills, T. Cvitas, K. Homann, N. Kallay and K. Kuchitsu, *Quantities, Units and Symbols in Physical Chemistry*, 2nd Ed. (Blackwell Scientific Publications, Oxford, 1993).

61. C.P. Smyth, *Dielectric Behavior and Structure*, McGraw-Hill, New York, 1955.

62. M. Born and E. Wolf, *Principles of Optics: Electromagnetic Theory of Propagation and Diffraction of Light*, 6th Ed. (Pergamon Press, Oxford 1980).

63. J.W. Warner and M. Wolfsberg, J. Chem. Phys., **78**, 1722 (1983).

64. J. Overend, in *Infra-Red Spectroscopy and Molecular Structure: An Outline of the Principles*, M. Davies, Ed. (Elsevier, Amsterdam, 1963).

65. W.B. Person, in *Vibrational Intensities in Infrared and Raman Spectroscopy*. W.B. Person and G. Zerbi, Ed. (Elsevier, Amsterdam, 1982).

66. M.J. Dignam, Appl. Spectrosc. Rev., **24**, 99 (1988).

67. W.G. Harter, *Principles of Symmetry, Dynamics and Spectroscopy*, John Wiley & Sons, New York, 1993.

68. P.N. Schatz, Spectrochim. Acta, **21**, 617 (1965).

69. J.E. Bertie, H.H. Eysel, Appl. Spectrosc., **39**, 392 (1985).

70. J.E. Bertie, S.L. Zhang, H.H. Eysel, S. Baluja and M.K. Ahmed, Appl. Spectrosc., **47**, 1100 (1993).

71. E.B. Wilson, Jr., Phys. Rev., **45**, 706 (1934).

72. G. Herzberg, *Molecular Spectra and Molecular Spectra. II. Infrared and Raman Spectra of Polyatomic Molecules*, D. Van Nostrand Company, Inc., Princeton, 1945.

73. C.D. Keefe, Ph.D. Thesis, University of Alberta, 1994.

74. Report of the Joint Commission for Spectroscopy of the International Union and the International Union of Pure and Applied Physics, J. Chem. Phys., **23**, 1997 (1955).

75. F.A. Miller, J. Raman Spectroscopy, **19**, 219 (1988).

76. H.H. Nielsen, Phys. Rev., **38**, 1432 (1931).

77. S.L. Gerhard and D.M. Dennison, Phys. Rev., **43**, 197 (1933).

78. R.M. Badger and L.R. Zumwalt, J. Chem. Phys., **6**, 711 (1938).

79. T. Ueda and T. Shimanouchi, J. Mol. Spectrosc., **28**, 350 (1968).

80. X. Zhou, P. Pulay and G. Fogarasi, J. Mol. Struct. (theochem), **277**, 147 (1992).

81. R.L. Poynter, J. Chem. Phys., **39**, 1962 (1963).

82. G. Erlandsson, Arkiv for Fysik, **8(23)**, 341 (1954).

83. H.D. Rudolph, H Dreizler, A Jaeschke and P. Wendling, Z. Naturforschg., **22a**, 940 (1967).

84. J.E. Bertie and C.D. Keefe, J. Chem. Phys., **101**, 4610 (1994).

85. P.C. Painter and J.L. Koening, Spectrochim. Acta, **33A**, 1003 (1977).